UNIVERSITÀ
DEGLI STUDI
FIRENZE

DOTTORATO DI RICERCA IN SCIENZE CHIMICHE

CICLO XXX

COORDINATORE Prof. PIERO BAGLIONI

Synthesis of novel cancer selective theranostic nanodevices

Settore Scientifico Disciplinare CHIM/06

Dottoranda
Dott. Sara Piantini
(firma)

Tutore
Prof. Stefano Menichetti
(firma)

Coordinatore
Prof. Piero Baglioni
(firma)

Anni 2014/2017

Index

Preface

I was admitted to PhD as a supernumerary student. In the last three years I received three research grants on two different topics. In the first year of my PhD I dealt with the synthesis of model compounds for the study of Hydrogen Atom Transfer (HAT) mechanisms in energy-related processes, whose results are at a preliminary stage and are not reported in this thesis. The project was not founded for the second and the third PhD years, so I changed my PhD project in “Synthesis of novel cancer selective theranostic nano devices”. The project herein reported is thus relative to my second and third PhD years. It was funded by Istituto Toscana Tumori (ITT) and it was carried out in collaboration with Luisa Bracci’s research group from Department of Medical Biotechnologies at the University of Siena.

Abbreviations

Compounds numbering restart for each chapter; each compound number is preceded by the number of the chapter in which it is reported (*e.g.* compound 2.3 indicate compound number 3 of chapter 2). All numbers relative to the same compound, when it appears in different chapters, are reported in the experimental section.

DCM	Dichloromethane
DMF	Dimethylformamide
ET_2O	Diethyl ether
DMAP	4-dimethylaminopyridine
DIAD	Diisopropylazodicarboxylate
MeOH	Methanol
THF	Tetrahydrofuran
DMTrCl	4-4'-dimethoxytrityl chloride
DCC	N,N'-dicyclohexylcarbodiimide
EtOH	Ethanol
AcOEt	Ethyl acetate
EP	Petroleum ether
NMR	Nuclear magnetic resonance
IR	Infrared
DIC	N,N-diisopropylcarbodiimide
PTX	Paclitaxel
TOAB	tetraoctylamonium bromide
DIPEA	N,N-diisopropyl-N-ethyl amine
TEA	Tiethylamine
DMSO	Dimethylsulfoxide
ESI	Electrospray ionization
TEM	Transmission Electron Microscopy
QDs	Quantum Dots
AuNPs	gold nanoparticles
AuNPs-C5	penthantiol-capped gold nanoparticles
PCC	pyridinium chlorochromate

1. Introduction

1.1 Introduction to chemotherapy

Chemotherapy (often abbreviated to chemo) is the treatment of cancer with one or more cytotoxic antineoplastic drugs. The term "chemotherapy" has been coined by Paul Ehrlich in the early 1900s to describe a therapeutic approach which implies the use of chemicals to treat infectious diseases.[1] Although now the term "chemotherapy" is currently referred, in its common use, to cancer therapy, it originally indicated the use of drugs to cure diseases which were not caused by an endogenous organ dysfunction, rather induced by allogenous pathogens such as viruses, bacteria, parasites and so on. Cancerous cells, although deriving from sane human cells, are thus considered in the same manner as allogenous pathogens are: a strange sort of "enemy" cells which can be defeated by means of chemical agents, just like a bacterial infection can be eradicated by penicillin. Ehrlich was also the first to envisage a selective therapy aimed at eradicating pathogen-caused diseases; a therapy which could take advantage of the many differences existing between a human cell and the cell of the pathogen. He imagined a therapy armed with chemicals (which he called "magic bullets") that could specifically interfere with biochemical pathways exclusive to the infective micro-organism.

For instance, arsphenamine, marketed under the name of Salvarsan, was introduced at the beginning of the 1910s as the first effective treatment for syphilis. This organoarsenic compound steamed form Ehrlich's theory, that by screening many compounds, a drug could be discovered with antimicrobial activity without killing the human. Thus, it is nowadays considered the first modern chemotherapeutic agent. For sure, penicillin, inhibiting DD-transpeptidase, an enzyme which is involved in the synthesis of peptidoglican cell walls, not expressed by human cells, can be the perfect example of a "magic bullet", hitting a bacteria-specific target and avoiding mechanism-of-action related toxicity (*Figure 1.1*).

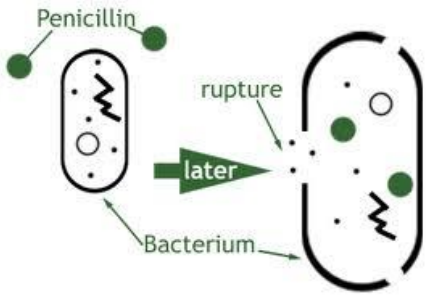

Figure 1.1 - Destruction of the peptidoglican cell wall operated by penicillin

Unfortunately, cancer cells, although distorted by a wild mutation process, are human cells and share the majority of biochemical pathways with the latter; as a consequence, a cytotoxic therapy aimed at killing the totality of cancer cells obviously implies a dramatic mechanism-of-action related toxicity. Although chemotherapy still remains one of the most controversial therapeutic approaches to cancer, research has the duty to persevere in its improvement, as it is one of the few approaches which can be adopted in the treatment of metastatic cancer. While surgical interventions are by far the most successful procedures in early cancer cure protocols (although ineffective in the treatment of advanced cancer), chemotherapy (in particular classic chemotherapy, as discussed above) attains satisfactory results in terms of survival and remissions number only in a restricted number of tumors (e.g. chronic myeloid leukemia) and it can often even worsen the clinical situation of the patient.

1.2 Classic versus targeted chemotherapeutics

The beginnings of the modern era of chemotherapy can be traced directly to the discovery of nitrogen mustard as an effective treatment for cancer.[2] In 1942, Goodman and Gilman, at Yale University, treated a patient with non-Hodgkin's lymphoma with nitrogen mustard, observing a remission, even if only temporary, of the tumorous masses.[3] Later on, in the earliest phases of the development of cancer chemotherapy, emphasis was on cell duplication rate, which constitutes a first discriminating factor between cancer cells and healthy cells. As a matter of fact, cancer cells proliferate several times faster than their "normal cell" homologues as a result of growth-promoting genes activation (oncogenes, such as *ras* genes) and mutation of growth-suppressing genes (oncosuppressors, such as *p53*). Thus, in the second post war period, every research effort was addressed to the development of drugs which could interfere with cells duplication, such as DNA alkylating agents, mitosis inhibitors, antimetabolites and every kind of toxin which could disrupt cellular cycle biochemical pathways, in order to kill high-rate duplication cells in which those processes were statistically more frequent.

Classic Chemotherapeutics: These first chemotherapeutic agents (commonly referred to as *classic chemotherapeutics*) show high toxicity and thus several side effects, below indicated:

i) Firstly, they act killing cells that divide rapidly, exerting their cytotoxic effect also on healthy cells with a high duplication rate in physiological conditions, such as epithelial, giving rise to a series of often intolerable side effects. In particular, hematopoietic precursors, gastrointestinal epithelial cells and hair follicles are hit, resulting in the typical side effects of chemotherapy: myelosuppression (decreased production of blood cells), mucositis (inflammation of the lining of the digestive tract) and alopecia (hair loss). These side effects lead many already compromised patients to give up therapy, as the latter are often more dangerous than the disease itself. It is, in fact, very difficult to find a compromise between

benefits and therapy-associated risk. Among others, frequent, heavy side effects are emesis and neuropathic pain, which necessarily require dedicated treatment, thus broadening the already wide number of drugs simultaneously administered to the patient, the risk of dangerous pharmacokinetic and pharmacodynamic interactions critically increases. Regarding neuropathic pain, for instance, platinum-based cancer chemotherapies induce a neurotoxicity characterized by a dose-dependent painful sensory neuropathy, presenting with symptoms in distal extremities that forced the patient to suspend the treatment in a early stage of the therapeutic protocol.

ii) Secondly, the most threatening risk associated to the use of classic chemotherapeutic agents is the possibility of the development of secondary cancers, provoked by drug-induced DNA damage. This occurs most frequently in patients treated with alkylating agents and recently the carcinogenicity of platinum complexes such as cisplatin has been anticipated by several studies.[4]

iii) Finally, classic cytotoxic agents have often unfavorable pharmacokinetic features which end up in a significant decrease of absorbed drug quantity, not to mention the high biodiversity of CYP 450 and other metabolic enzymes by which many chemotherapeutics are processed in vivo and which would require a personalized therapeutic protocol. Therefore, to reach minimum effective dose in blood stream, the administered drug dose has to be augmented, leading to a significant increase of the rise of the previously said side effects, which can be fatal in certain cases.

Targeted chemotherapeutics: In the case of targeted chemotherapy, instead, similar toxicological problems have not been observed thanks to the intrinsic specificity of these drugs mechanism of action. These drugs are indeed designed to attack only tumor-specific targets. During the last decades of the 20th century, consistent research efforts were made in order to develop targeted drugs that block the growth and spread of cancer by interfering with specific molecules involved in tumor growth and progression. Even though many breakthroughs have undoubtedly been made in this field and although many new, tumor-selective molecules have been successfully developed and tested, it has often been observed that these new drugs, though safer and more tolerable, can lose efficacy in a relatively short period of time due to the arising of specific resistance.[5] The most famous representative of this drug class is certainly *Imatinib*©, the lead compound in the tumor kinase inhibitor family. *Imatinib*© has been designed to inhibit BCR-ABL, a kimeric protein deriving only from Ph+ (Philadelphia gene-positive) cells, which are mutated cells common in chronic myeloid leukemia and other kind of rare tumors. Such kinase inhibition is fatal to cancer cells, while healthy cells are not affected. Nevertheless, such therapeutic approach has a significant limit. Because of their extraordinary duplication rate, tumor cells are subjected to develop mutation with a much higher frequency than healthy cells. Targeted drugs such as *Imatinib*© only exert their cytotoxic activity by means of a single, specific mechanism (such as the inhibition of a particular enzyme) and the continuative administration of such treatments can lead, in a relatively short period, to

the selection of a resistant generation of cancer cells. Cancer cells acquire this kind of specific resistance, for instance, by alteration of the active site of the target enzyme. Given their absolutely no specific mechanism of action, the activity of classic chemotherapeutic agents is not diminished in the least by this kind of mutation, but targeted chemotherapeutics result completely inactive once specific resistance has risen.

Nonetheless, both classic and target chemotherapy are limited by another kind of tumor cell resistance, namely multi-drug resistance (MDR). If specific resistance to a certain cytotoxic molecule is attained by tumor cells by modification of the molecule's target, multi-drug resistance is a condition enabling the tumor cells to resist distinct drugs or chemicals of a wide variety. Cancer cells explicate multi-drug resistance through various mechanisms, such as enzymatic deactivation of the anti-cancer drug, decreased cell wall permeability to cytotoxic drugs, altered active sites also in less specific enzymatic targets, increased mutation rate as a stress response, efflux mechanisms to remove drugs, *e.g.* glycoprotein P overexpression.

For all of these reasons, it is evidently necessary to maximize drug dose in proximity of the target, in order to increase the efficacy of the treatment and to minimize chemotherapy side effects. Therefore, the selective targeting of tumor cells is the goal of modern cancer therapy, aimed at overcoming this non-specific toxicity. This ambitious aim may be achieved by means of a targeted drug delivery system-involving therapy. Instead of focusing on a targeted pharmacodynamic activity, which may increase the probability of the development of specific resistance to targeted drugs, emphasis should be put on both selective pharmacodynamic and pharmacokinetic activity. This novel kind of therapeutic approach is very promising, for it may overcome the classical limits of chemotherapy, as reported in section 1.3.

1.3 Targeted drug delivery systems: the new frontier of chemotherapy

A targeted-drug delivery system strategy is aimed at conveying a bioactive molecule to its action site as specifically as possible, thus maximizing the in situ drug quantity without increasing administration dose and minimizing the side effects. The main target of all sophisticated drug delivery systems is to deploy medications intact to specifically targeted parts of the body through a medium that can control the therapy's administration (a process which is also known as drug vectorization) by means of either a physiological or chemical trigger. As a matter of fact, instead of exploiting tumor-specific pharmacodynamics targets, such as enzymes, in targeted drug delivery the specificity of action is ensured by interaction between the therapeutic agent and a tumor-specific pharmacokinetic target so that the distribution of the drug *in vivo* regards only the cancerous lesion. A similar pharmacokinetic target may be represented, for instance, by a receptor which is overexpressed by the tumor cell. The interaction with the specific target is not cytotoxic in itself, but the bond between the targeted drug delivery system and the receptor is exploited as a Trojan horse in order

to allow a highly focused distribution of the drug into the tumor cell. Drug delivery is often approached via a drug's chemical formulation, but it may also involve medical devices or drug-device combination products. The most common approach in the development of targeted drug delivery systems consists in conjugating the chemotherapeutic agent, which constitutes the cytotoxic portion of the system, to a carrier of various natures.

The carrier is the portion of the system which is expected to target the tumor cell, establishing a preferential interaction with the latter. Although the carrier may have an intrinsic cytotoxic activity (as shown in studies on metallic nanoparticles carriers),[6] it usually only works as a vehicle delivering the drug into the cancerous cell. It is thus evident that targeted drug delivery systems present numerous advantages. In detail:

i) Specific delivery of cytotoxic agents to tumor overexpressed receptors and subsequently a more selective killing of cancer cells. Moreover, the sparing of normal tissues from the harmful side effects of systemic therapy, allows lowering the administered dose in cure protocols. Such a decrease of the initial administered drug dose brings a series of major benefits, as a lowering in the incidence of chemotherapy side effects, not to mention the fact that this would postpone the necessity of dose escalation indicated whenever intrinsic resistance of some tumors to chemotherapeutic agents rises;

ii) Recycling of those classic, very cytotoxic chemotherapeutic agents which have been eliminated from cure protocols because of their critical toxicological profile. In fact, minimizing drug tissue distribution, dangerous but efficacious cytotoxins may be used (or re-used) in therapy and this could represent a certain benefit both from the therapeutic and the economical point of view.

iii) Very versatile entity which offers many modifiable sites on which the researcher can operate to improve the technological performance of the delivery system and the chemical stability of the conjugated pharmaceutical agent. A suitably modified carrier, in fact, may not function only as a mere drug vehicle, but (as in the case of liposomes, for instance) it could constitute a shield for a highly instable drug, protecting it e.g. from chemical or enzymatic hydrolysis in vivo or from degradation and aging during its shelf life.

It is for all these reasons that a rising interest on targeted drug delivery systems has been growing during the last three decades and nowadays, given the recent, impressive breakthroughs of nanomedicine, the possibilities offered by drug vectorization seem to be endless. This is also due to the very broad range of carriers which have been developed since the 1980s. In general, three main generations of vectors can be identified:

1) *First generation carriers*: these first vectors are constituted by organic polymer microcapsules or microspheres, which are injected intra arterially in the proximity of solid, primary tumors. Besides conveying the drugs directly to the tumor tissue, they also have a chemoembolization effect, which consists in causing a vascular disruption and the starving of the tumor, which undergoes ischemic necrosis. The obstruction in

tumor-lining blood vessels also prevents the drug from distributing in the systemic blood flow. This therapeutic strategy is not being applied in a very great number of cases; however, trans-arterial chemoembolization (TACE) has become standard treatment in selected patients affected by hepatocellular carcinoma.[7]

2) *Second generation carriers:* carriers such as liposomes[8] and nanoparticles[9] belong to this generation of vectors. They normally have colloidal dimensions (<1 μm) and are characterized by better intracellular permeation compared to first generation carriers. Liposomes are artificially-prepared vesicles composed of a lipid bilayer in which a drug may be encapsulated. Their surface offers many modifiable sites that can be functionalized with tumor receptor ligands (e.g. peptides, glycopeptides or even antibodies) to enhance the selectivity of its distribution. Besides working as specific carriers, they can protect the drug from *in vivo* degradation and slow drug metabolism and elimination down. For what concerns nanoparticles, a detailed analysis will be presented in the section 6.

3) *Third generation carriers:* antibodies,[10] especially monoclonal human or humanized antibodies (mAbs) against tumor antigens, are the most famous representatives of this generation of vectors, as they are undoubtedly the mainly used carriers of conjugated moieties for targeted tumor therapy or diagnosis.

In the1970s, the B-cell cancer myeloma was known, and it was understood that these cancerous B-cells all produce a single type of antigen. This was used to study the structure of antibodies, but it was not possible to produce identical antibodies specific to a given antigen. The process of producing monoclonal antibodies was invented by Georges Köhler and César Milstein in 1975.[11] Many antibodies-based pharmaceutical specialties have recently been approved by FDA, such as Herceptin (1998) for breast cancer, Erbitux (2004) and Avastin (2004) for metastatic colorectal cancer, with a subsequent revolution in chemotherapy. One possible treatment for cancer involves monoclonal antibodies that bind only to cancer cells specific antigens and induce immunological response on the target cancer cell (naked antibodies). Although unmodified mAbs may show some therapeutic potency, their effect tend to be various and ultimately not curative when not used in combination with classical chemotherapy. These antibodies would need to be administered to patients in massive doses to be effective, thus leading to serious side effects. As a result, mAbs have been armed with drugs, toxins, cytokines or radionuclides opening the door to the clinical use of targeted tumor therapy (*Figure 1.*2).

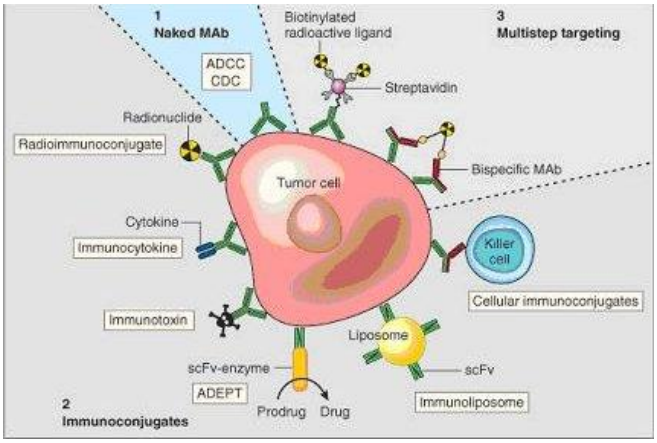

Figure 1.2 - Monoclonal antibodies for cancer. ADEPT, antibody directed enzyme prodrug therapy; ADCC, antibody dependent cell-mediated cytotoxicity; CDC, complement dependent cytotoxicity; mAb, monoclonal antibody; scFv, single-chain Fv fragment.

Antibodies-based drug delivery systems employ several mechanisms to damage cancer cells:

i) Making the cancer cells more visible to the immune system. The antibody marks the cancer cells as physiological B-cell produced antibodies normally mark pathogen cells during infections; as sometimes cancer cells are not recognized as enemies by the immune system, the antibody-mediated marking induces an immunological response addressed to the cancer cells;

ii) Blocking growth signals. Certain cancer cells overexpress growth factor receptors, whose interaction with their ligand makes them grow faster than healthy cells. Antibodies can also have an intrinsic antitumor activity, by binding to growth factor receptors. This synergistic combination of specific vectorization of pharmaceuticals to the cancer cell and selective cytotoxic activity, particularly increases the potency of this pharmaceutical specialties;

iii) Delivering radiation to cancer cells. By combining a radioactive particle with a monoclonal antibody, radiation can be delivered directly to the cancer cell;

iv) Delivering powerful drugs into cancer cells. Powerful anti-cancer drugs or toxins can be attached to monoclonal antibodies. Drugs remain inactive until they penetrate the target cells, lowering the chance of harming other cells.

This kind of drug delivery systems has raised great expectations among oncologists, so that many new antibodies-based targeted therapies have been approved by U.S. Food and Drug Administration (FDA) since 2010. Nonetheless, the use of immunoglobulins as targeting moieties has some drawbacks, such as the high costs of production, the difficulty in obtaining specific antibodies for every tumor type and, finally, toxicological issues. In fact, although antibodies can be disguised as human to evade the immune response, these delivery systems are xenobiotic substances and are soon recognized as such. This means there is only a short time when antibody therapy can be used before

it becomes ineffective, not to mention the fact that the xenobiotic moiety may trigger an abnormal immunologic response, which could give rise to severe side effects. More fundamentally, the number of tumor cells in patients with terminal disease overwhelms the therapy. Some cells express too little antigen to be targeted and cells in a large mass may escape attention altogether. Antibody therapy is most likely to be useful in the context of minimal, but disseminated disease; in fact just the situation that often occurs after conventional chemo-radiotherapy. Moreover, antibodies conjugates are characterized by suboptimal pharmacokinetics and biodistribution, as well as non-specific uptake by the liver and reticuloendothelial system (RES), which may result in a systemic diffusion of the drug, losing the targeting effect.[12] To overcome the limits of antibody-based therapeutic approach, another strategy has been recently developed, in which the targeting moiety of the drug delivery conjugate is a peptide (as discussed in section 1.4).

1.4 Drug-peptide conjugates as an evolution of antibodies-based drug delivery systems: the case of Neurotensin

The discovery that receptors for different endogenous regulatory peptides are overexpressed in several primary and metastatic human tumors led to their use as tumor antigens; this opened the door to peptide-based therapeutic and diagnostic approaches in oncology.[13] These receptors can be used as molecular targets by which radiolabeled peptides can localize cancers in vivo, a strategy which can be exploited both for therapeutic and diagnostic purposes. As tumor targeting agents, peptides have several advantages over antibodies,[14] including:

i) Better organ or tumor penetration and more efficient cellular internalization, because the antibody molecules are relatively large and might not reach the tumor easily;
ii) Greater stability (long storage at room temperature);
iii) Lower manufacturing costs (recombinant production takes approximately twice as much, in terms of time and costs than chemical synthesis) and more reproducible production performances;
iv) Batch-to-batch production parameters, due to the advances in solid-phase peptide synthesis;
v) Fewer and less expensive regulatory requirements (chemical synthesis versus recombinant production) and easier and quicker authority approval.

Peptides can serve as carriers for the local delivery of cytotoxic agents to the tumors, as demonstrated by the successful clinical use of radiolabeled somatostatin analog for the detection and treatment of some somatostatin receptor-positive tumors.[15] Thus, in recent years a series of cytotoxic peptide hormone conjugates were developed.
Moreover, an increasing number of tumors may be addressed by 'peptide-bullet' strategy: peptides can be conjugated with cytotoxic moieties or radionuclides and, provided that the receptor-ligand complex is internalized on binding, the functional moiety can be specifically delivered into the tumor cell.[16]

An excellent candidate for a drug-peptide conjugate therapy is, among many others, neurotensin, a regulatory peptide whose receptors are over-expressed by many types of tumors and on which our work has been focused.

Neurotensin

Neurotensin (NT) was first isolated in 1973 from extracts of bovine hypothalamus based on its ability to cause a visible vasodilatation in the exposed cutaneous regions of anesthetized rats.[17] NT is a 13-amino acids regulatory peptide, sharing significant similarity in its C-terminal portion of amino acids with several other neuropeptides (*Figure 1.3*). This region is responsible for the biological activity as neurotransmitter while the N-terminal portion has a modulator function.

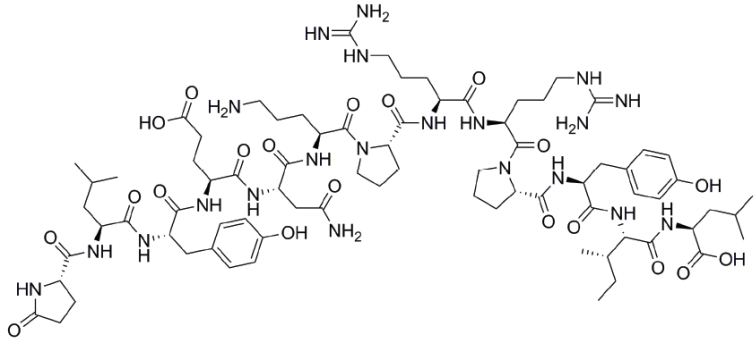

a.

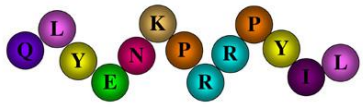

b.

Figure 1.3 - **a**. Neurotensin (NT), **b**. QLYENKPRRPYIL, schematic representation.

NT is distributed in discrete regions of the CNS of mammals, where this peptide likely plays an important role as a neurotransmitter or neuromodulator in neuronal signaling. It has also been shown to be present in the hypothalamus of a variety of species including rat, mouse, rabbit and man. In 1988, the rat NT gene was isolated and sequenced, finding out that the amino acids 8-13 of NT are essential for biologic activity.[18]

As many other neuropeptides, neurotensin works as both a neurotransmitter in the central nervous system (CNS) and as a local hormone in the peripheral tissues. In mammals, NT is widely distributed throughout the CNS (with highest levels in the hypothalamus, amygdala and nucleus accumbens) and digestive tract (enteroendocrine

cells of the small intestine), where it acts as a growth factor on a variety of normal or cancer cells.[19]

Neurotensin has various physiological functions; firstly it works as a vasodilation and hypotension inducer. In fact, it has been observed that central administration of neurotensin produces a marked dose-related decrease in body temperature of mice and rats at an ambient temperature of 25 °C. Other effects observed after central administration of neurotensin are decreases in locomotion and sedation. The effect is observed in both rats and mice, but only after central administration, neurotensin is, in fact, inactive after peripheral administration. This suggests that the tridecapeptide is not able to cross the blood-brain barrier in sufficient quantities to exert direct brain effects and also that the central nervous system locus of action of this compound lies within the confines of the blood-brain barrier. Thus, although neurotensin has been reported to induce several endocrine (increases in plasma concentrations of gonadotropins, ACTH, growth hormone, prolactin, corticosteroids, and glucagon) and hemodynamic (hypotension, vasodilatation, and cyanosis) changes after i.v. administration, it appears that the brain effects of this peptide are not mediated by such peripheral processes. Major peripheral functions of neurotensin include the stimulation of pancreatic exocrine secretion, inhibition of gastric acid secretion, and inhibition of gastroduodenal motility. Fat ingestion induces a dose-related increase in neurotensin plasma concentrations, whereas glucose and amino acids produce only minor or no effect.[20]

The actions of NT are mediated by the stimulation of several specific receptors, called NTR. Three specific membrane receptors have been described so far. NTR1 shows a high affinity for NT, whereas NTR2 exhibits a low affinity (*Figure 1.4*).

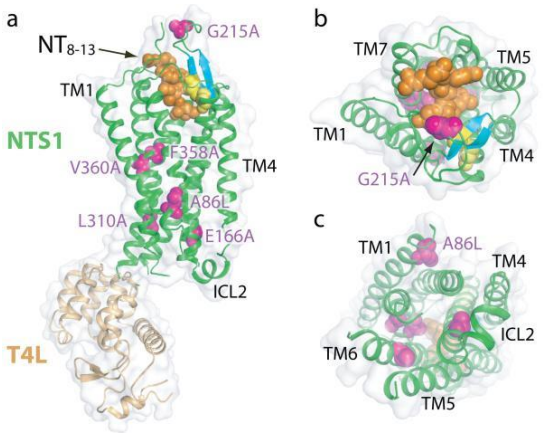

Figure 1.4 - Overview of agonist-bound NTR1[21]

NTR1 and NTR2 belong to the family of G protein-coupled receptors (GPCRs). NTR3, also named Sortilin (Sort1) is an entirely new type of neuropeptide receptor with a single transmembrane domain and it has been recently described as having an important role in pancreatic ductal adenocarcinoma cell migration. As previously

reported, NT receptors are overexpressed by certain tumor type. Reubi *et al*. found receptors expressed on many tumor cells, such as meningioma, pancreatic, prostatic, lung and colon carcinomas, in particular the high affinity NTR1. Over 75% of all ductal pancreatic carcinomas were reported to overexpress neurotensin receptors, whereas normal pancreas tissue, pancreatitis, and endocrine pancreas do not. Neurotensin receptors are observed more often in differentiated than in poorly differentiated tumors: indeed, as many as 83% of the differentiated adenocarcinomas are receptor positive; in particular, tumors with tubular differentiation are more often positive than solid tumors. Recently, it has been observed by Gui *et al.*[22] that NTR1 is commonly expressed in breast carcinomas; what is most interesting is that this overexpression is independent of ER/PR/Her2 profile, so a neurotensin based adjuvant therapy may be a breakthrough in the cure of "triple negative" breast carcinomas who cannot be treated with Herceptin and derivatives. Further and up-to-date elucidations about possible interactions between neurotensin and receptors or other membrane proteins are reported in below sections.

For all these reasons, neurotensin is considered an excellent lead compound for the design of a drug delivery system targeting moiety and, in particular, it seems to be the best possible candidate for peptide based therapy of exocrine pancreatic carcinomas, due to the high incidence and density of neurotensin receptors in these tumors, and of the whole gastrointestinal tract cancers in general. Unfortunately, the bottleneck for development of peptides as drugs has always been their extremely short half-life, due to physiological degradation by peptidases and proteases. High affinity ligands are also necessary, since unlike antibodies, monomeric peptides do not have the advantage of multimeric binding. To overcome this problem, various neurotensin analogues have been synthesized, including linear peptides, cyclic peptides, and non-peptide molecules (inserting D-amino acids, or pseudo amino acids), [38] but chemical modification of the native peptide may radically modify receptor affinity and specificity.

Prof. Luisa Bracci's group at the University of Siena, previously reported that synthesis in branched form increased the bio-stability of certain peptides, including neurotensin, obtaining promising results *in vitro* and *in vivo* both for diagnostic and therapeutic purposes.[23] The synthesis of bioactive peptides in Multiple Antigen Peptide (MAP) dendrimeric form turns out to be useful, leading to acquired resistance to protease and peptidase activity (*Figure 1.5*).

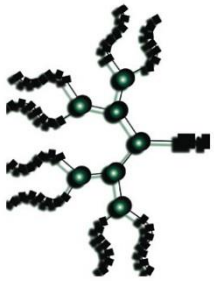

Figure 1.5 - Schematic MAP representation.

The greater *in vivo* stability to proteolytic enzymes of MAPs (Multiple Antigenic Peptides) compared to monomeric peptides is due to the greater complexity of their structure. The MAP system utilizes a peptidyl core of three or seven radially branched lysine residues, on to which the antigen sequences of interest (in this case a peptide) can be built using standard solid-phase chemistry (*Figure 1.6*).

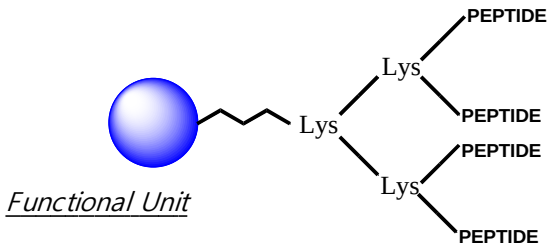

Figure 1.6 - Peptide tetramer with three-lysine branched core

Thanks to this lysine core, the MAP can bear four or eight copies of the peptide epitope (resulting in high molar ratio), depending on the inner core that generally accounts for less than 10% of total molecular weight. Moreover, the MAP system does not require a carrier protein for conjugation.

MAPs can be more efficient than monomeric peptides in diagnostic applications and also have the possibility to be conjugated to various Functional Units such as fluorophores, photosensitizes, cytotoxic groups or chelators for radioisotopes. As said before, the *in-vitro* and *in vivo* efficiency of dendrimeric peptides like MAPs is generally ascribed to their multimeric nature, which enables polyvalent interactions.

In order to demonstrate the longer half-life of MAPs derivate, Professor Luisa Bracci's research group (also thanks to AIRC funding) compared the stability of monomeric and tetrabranched neurotensin. Bioactivity of monomeric and MAP peptides was checked by testing the inhibition of nM [^{3}H]neurotensin-specific binding to membranes prepared from the human colon adenocarcinoma cell line HT 29.[24] Experiments were performed in the presence of protease inhibitors. MAP NT efficiently inhibited nM [^{3}H]neurotensin-specific binding, and its IC_{50} value was analogous to that of monomeric NT. The resistance to protease activity in human plasma and serum was tested for the two peptides. Monomeric and tetrabranched peptides were incubated with human plasma or serum for 2 or 24 h, and the mixture was analyzed by HPLC and mass spectrometry to follow the presence of uncleaved monomeric and MAP peptides. As a general rule, peptides that are cleaved in plasma in 2h are also cleaved in serum at the same time. Those resistant in serum after 24h are also resistant in plasma. It was found that the MAP form was more resistant than the monomeric form (*Table 1.1*).

Peptide	Plasma (2h)	Plasma (24h)	Serum (2h)	Serum (24h)
NT	+	-	+	-
MAP-NT	+	+	+	+

Table 1.1 - The absence (-) or presence (+) of peptide after the incubation times refers to the unproteolyzed peptide sequence as detected by HPLC and MS.

Moreover, in order to test the possible influence of peptide length, number of peptide copies, and steric hindrance on branched peptide stability to peptidases, the monomeric, two branched and tetra-branched forms of NT were synthesized and their stability, after incubation with human plasma and serum was compared. Prof. Bracci's research group found that the tetra-branched form of neurotensin was stable in both human plasma and serum for 24h, whereas the di-branched for 5h and the monomeric analogue was degraded in roughly 5h (*Table 1.2*).[16]

Peptide	Plasma *(2h)*	Plasma *(5h)*	Plasma *(24)*	Serum *(2h)*	Serum *(5h)*	Serum *(24h)*
Monomeric NT	+	-	-	+	-	-
Dibranched NT	+	+	-	+	+	-
Tetrabranched NT	+	+	+	+	+	+

Table 1.2 - Stability of the three peptides in plasma and serum.

As a result, steric hindrance may limit the access of such peptides to the cleavage site of proteolytic enzymes, increasing the peptide half-life, with obvious advantages for their use as drugs. The possibility to form supramolecular aggregates is another feature of branched peptides probably accounting for their increased stability. Tetrabranched peptides may arrange their four arms in parallel structures stabilized by intramolecular H-bonding of the backbone. This structure would resemble that of self-assembling β-sheet peptides. Prof. Bracci's results indicate that synthesis in dendrimeric form may be a general method to increase *in vivo* stability of bioactive peptides and so a step forward on the direction of the finding of new specifically targeted cytotoxic drugs.

1.5 Towards the synthesis of a MAP-NT based drug delivery system

MAP-NT does not present binding sites for bioactive molecules; therefore, in order to functionalize the dendrimer with the drug moiety, the synthesis of a non-peptidic linker able to bind the therapeutic moiety to the lysine core has been necessary. The C-terminal lysine side chain was functionalized with the chemotherapeutic agents spaced by an amino-terminal PEG (polyethylenglycol) moiety, chosen in consideration of synthetic and biological issues. Spacing is necessary, as the hindrance of the branched peptide might impair the access of the activated chemotherapeutic and therefore give poor reaction yields. Moreover the drug moiety, if closely linked to the branched peptide, might impair receptor recognition and, for slow realizing compounds, the closeness of branched peptide might compromise drug-target interaction inside the cell. A special care in choosing the suitable linker to insert between the functional unit and the tetrabranched peptide was taken, considering that in the case of cytotoxic molecules the link has to be broken preferably upon internalization into the tumor cell. In this sense the complex should be considered as a 'pro-drug', defined as a precursor of a drug that has to undergo chemical conversion by metabolic processes before becoming an active pharmacological agent. The final structure is then a lysine-core NT tetramer functionalized with an amino-terminal linker, which could constitute the binding sites for the therapeutic unit (*Figure 1.7*).

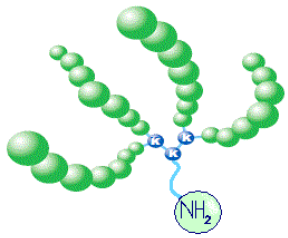

Figure 1.7 - Schematic representation of the amino-terminal linker functionalized MAP-NT.

As reported in previous works,[24] suitable derivatives of some of the most used chemotherapeutics, such as methotrexate or 5-Fluorouridin or Gemcitabine, were synthesized so that they could be linked to the amino-terminal MAP-NT moiety (*Figure 1.8*).

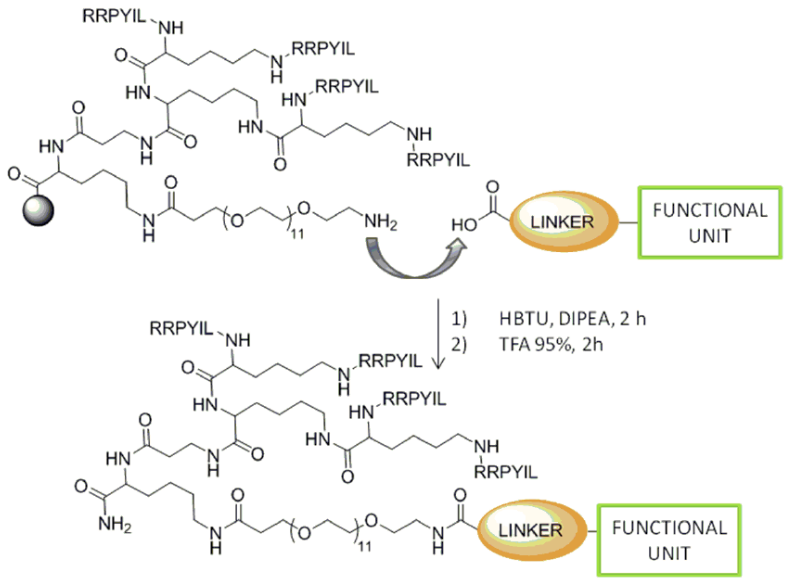

Figure 1.8 - Conjugation procedure.

These drugs have been coupled with aliphatic α-ω diacids. Such carboxylate-decorated drugs can be then coupled through an amidic bond with the amino-terminal MAP-NT moiety. The advantage of this final coupling is that the drug derivatives can be treated as an amino-acid and linked to the peptide exploiting the same procedure used for building up the primary sequence of MAP-NT on solid phase. It was decided to use ester linkage as covalent bonds suitable for safety delivering the drug inside the cell where the releasing of the anticancer agent occurs by hydrolysis (also mediated by ubiquitous esterases).

As for the achievement of the targeted drug delivery system, Bracci's group in Siena has set up a general method allowing conjugation by standard solid-phase peptide synthesis (*Figure 10*). Unfortunately this strategy couldn't be applied to all the chemically modified anticancer drug prepared. Indeed, in the last step peptide-functional unit conjugates are cleaved from the resin by treatment with concentrated trifluoroacetic acid (TFA). The drastic acid condition of the cleavage could, in some cases, partially or completely demolish the drugs integrity leading to an irreversible damage of the conjugate. Some antimetabolites, such as Gemcitabine and 5-fluoro-2'deoxyuridine, estrogens as estradiol and bioreductive agents as β-lapachone are not stable under the cleavage condition. To overcome this problem, we envisaged a 'post-cleavage coupling' strategy in which the peptide is cleaved from the resin prior to the coupling with the therapeutic unit, that is carried out in liquid phase. This preserves the conjugate from degradation.

To achieve this aim, it was exploited a 'click chemistry' strategy to properly decorate either the peptide and the drug. Among other strategies, we chose to insert a thiol group on MAP-NT, through a terminal cysteine residue, that could react with a

maleimide group bound on the anticancer agent (*Scheme 1.1*). This Michael reaction is highly selective and does not involve free groups on later chain of the amino acids that were deprotected with TFA during the cleavage of the peptide from the resin, allowing to lead it in solution phase without formation of side-products. In order to demonstrate the feasibility of the method, a MAP-NT-fluorophore (Alexa Fluor ®750) tagged complex has been synthesized exploiting thiol-maleimide coupling protocol and tested in xenografted mice with HT29 (colon adenocarcinoma).

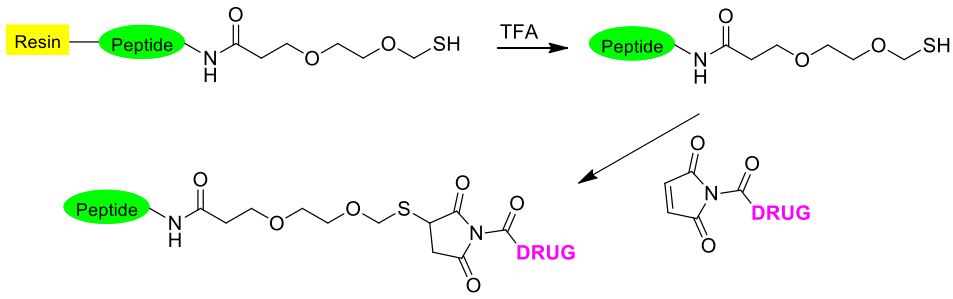

Scheme 1.1 - Click chemistry protocol for 'post-cleavage coupling' strategy. Step 1) simultaneous cleavage from the resin and deprotection of protecting groups on side-chain of the aminoacid. Step 2) coupling through a Michael reaction.

The injection of the conjugate in mice, primarily localized in proximity of the tumor mass, showed the effective and specific targeting of the conjugate to cancer cells.

Encouraged by these promising results, it was extended the strategy to drugs. Indeed, Paclitaxel, a mitotic inhibitor agent, is the perfect example of successful 'post-cleavage coupling' strategy.

1.6 Paclitaxel in targeted delivery systems

Taxanes, which include Paclitaxel, docetaxel and other analogues, are a class of potent chemotherapeutic drugs that act by binding microtubules and preventing their disassembly, thus blocking mitosis and eventually inducing apoptosis. Taxanes are highly effective against proliferating cancer and are an established option in the standard treatment of ovarian and breast cancer.[25]

Paclitaxel is one of the more used mitotic inhibitor used in cancer chemotherapy. It is a diterpenoid pseudoalkaloid, it has a tetracyclic 17-carbon (heptadecane) skeleton, with a total of 11 stereocenters. The active stereoisomer is (-)Paclitaxel. It was discovered in

a US National Cancer Institute program at the Research Triangle Institute in 1967 when Monroe E. Wall and Mansukh C. Wani isolated it from the bark of the Pacific yew tree, *Taxus brevifolia* and named it *taxol* (*Figure 1.9*).[26]

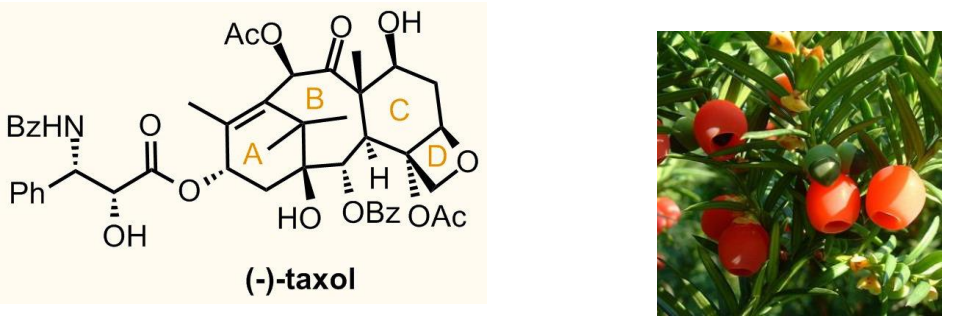

Figure 1.9 - (-)Paclitaxel (left) and *taxus brevifolia* (right).

In 1971 Paclitaxel was found to have cytotoxic effects on solid tumors and leukemic cells[27] and in early 1979 Dr. Horwitz Susan and her group delineated its main mechanism of action (since then unknown) involving the stabilization of microtubules.[28] After numerous *in vivo* studies, in 1992, Bristol-Myers Squibb marketed the drug as TAXOL® with the approval of the FDA where it was used for treatment of breast, ovary and AIDS-related Kaposi sarcoma.

Mechanism of action and current use

Taxanes are currently known to suppress and inhibit cell growth, differentiation and proliferation in indefinitely known cancer cell lines and are the most preferred anticancer drugs by physicians. They are commonly known as mitotic inhibitors or microtubule inhibitors as they cause a frozen mitosis; hence they are also sometimes called as mitotic poisons.[27] Paclitaxel, in spite of its excellent anti-tumor activity is still not cell specific and not all concentrations have similar effects on the microtubules; higher concentrations cause microtubule arrangement into bundles, while at lower concentrations, there is suppression and stabilization of microtubule dynamics without alteration of the polymer mass formed.[29] Moreover, taxanes have been found to be potential angiogenic inhibitors either as single agents, together with chemotherapeutic drugs or combination therapies, such as endogenous estrogens (2-methoxyestradiol)[30] and bevasizumab[31] which regulated VEGF (vascular endothelial growth factor) in an agonistic manner.

For the past two decades, Taxol has been undergoing infinite number of clinical studies in many cancer patients, in order to know about several factors regarding their usefulness as potential anti-neoplastic agents. Paclitaxel has neoplastic activity particularly against primary epithelial ovarian carcinoma breast cancer, colon, head, non-small cell lung cancer, and AIDS related Kaposi's sarcoma. This has led, in recent

time, to the approval of the drug in many countries for its use as second line treatment of ovarian and breast cancers.[32] Despite of the primary importance of several Paclitaxel-based monotherapies, conjoint therapy with platinum derivatives is, nowadays, a first line of treatment of ovarian cancer. In particular, Carboplatin-Paclitaxel combination is an emerging therapeutic protocol for advanced ovarian carcinoma, replacing the older and more toxic cisplatin-Paclitaxel one.[33] The same trend that envisages a more effective cancer management with combined therapies is found in treatments of breast cancer, for which, binary association with anthracyclines and triple with doxorubicin and Gemcitabine prolong patients' survival rates.[34] In general, thus, in order to achieve disease free survival taxol should be tried with several adjuvants to meet up to its expectancy.

Drawbacks of Paclitaxel therapy and alternative approaches for taxol formulation

There is no question that Paclitaxel is one of the more effective weapon we have in hands to treat a broad range of cancers that are generally considered to be refractory to conventional therapy. Unfortunately, its extended use has underlined several limitations, mainly related to: 1) availability, 2) solubility, 3) resistance.

1) Paclitaxel is extracted from the bark of Pacific Yew. Although the extraction has increased yields to 0.04% w/w, 4 trees have to be sacrificed to produce 2 g of the drug for the chemotherapy of one patient and this is not affordable from the environmental point of view.[14] Paclitaxel is currently formulated in a vehicle composed of 1:1 blend of Cremophor EL (polyethoxylated castor oil) and ethanol which is diluted with 5-20-fold in normal saline or dextrose solution (5%) for administration. Several problems employing this vehicle have been reported. For instance, Cremophor vehicle requires to be solubilized, it has a toxicity that includes hypersensitivity reactions, nephrotoxicity and neurotoxicity.[35] Moreover, the recommended concentration of the drug in the properly diluted clinical formulation is 0.3-1.2 mg ml^{-1} (0.35-14 mM) and has only short-term physical stability as some particles slowly tend to precipitate out of the aqueous media;
2) Paclitaxel is poorly soluble in an aqueous medium (approx. 0.6 mM), but can be dissolved in organic solvents. Its solutions can be prepared in a mM concentration in a variety of alcohols, such as methanol, ethanol, tertiary-butanol as well as in DMSO.
3) Acquired resistance to taxanes has become a serious clinical issue with increasing prescription. Though there have been a lot of successful outcomes with taxanes involved in the treatment of endless number of cancers, drug resistance remains a major obstacle which needs to be combated urgently. For years, profound researches have been going on just to understand the mechanisms related to MDR (multidrug resistance). Few of the mechanisms that have been highlighted includes P-glycoprotein which pumps out intracellular accumulation of respective drugs.[15]

Considering the above mentioned limitations, the main challenge of actual research is to develop alternative and safer strategies for an appropriate deliver of Paclitaxel.

Overall, 'carrier delivery systems', including liposomes, micelles and particulate drug delivery systems, seem to be the best possible approach towards the ideal dosage form.

Paclitaxel has also received extensive chemical studies during its development. Various chemical transformations have been carried out, which provided structure-activity relationships (SAR).

Kingston et al.[36] have studied the importance of the various hydroxyl groups of the taxane ring system on the activity of taxol (*Figure 1.10*). In these investigations it was shown that both the C-10 and C-7 positions could be deoxygenated without significant loss of activity, but that deoxygenation of the C-4 and C-2' positions did result in a significant activity loss. The use of esters as prodrugs has been extensively employed for modifying biologically active molecules containing either hydroxyl or carboxyl functionalities. For Paclitaxel, the simplicity of synthesis coupled with the facile enzymatic hydrolysis dictate esters as a first choice when considering prodrug strategies. Studies of 2'-taxol esters as prodrugs demonstrated that esters without α-substituents hydrolyzed only to the extent of 10% over a 24 h period, while those with electron-withdrawing substituents in the α-position showed remarkable enhancement in their rates of hydrolysis.[37] Among the most notable Paclitaxel derivatives synthesized so far are those in which the C-2 and C-7 hydroxyl groups of the molecule are engaged in a functional group that collapses, upon in vivo activation, releasing Paclitaxel.[38]

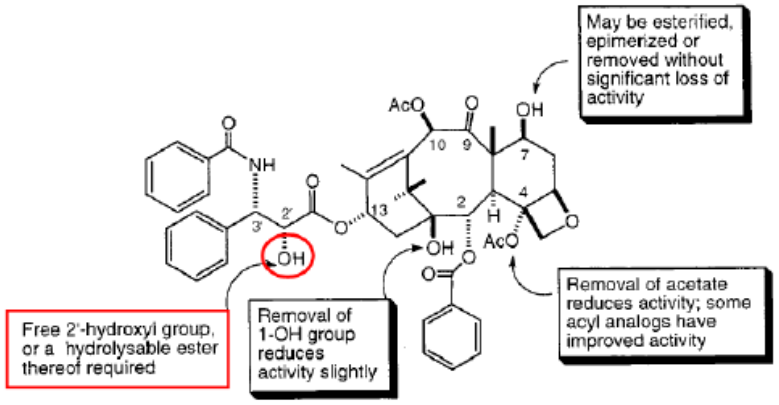

Figure 1.10 - Some structure-activity relationships of Paclitaxel.

In accordance with these considerations, first attempts of our research group were aimed to the achievement of a Paclitaxel-MAP-NT conjugate. The so obtained adduct should result in a "pro-drug" delivery system. Indeed, while the targeting activity of the peptide allows the selective accumulation of the drug in the tumor site, the presence of a linkage which can undergo *in vivo* chemical modification, ensures drug release form the adduct. To this purpose, we decided to exploit the more reactive OH function at position 2', to insert an orthogonal group able to react with the cysteine residue on the dendrimer. In detail, the thiol-maleimide click reaction was envisaged. Synthetically, the OH at position 2' was esterified with 3-maleimido propionic acid to both achieving

the maleimide-functionalization and ensure the presence of the ester bond. Maleimide group was, in turn, reacted with the thiol functionalized MAP-NT (*Scheme 1.2*).

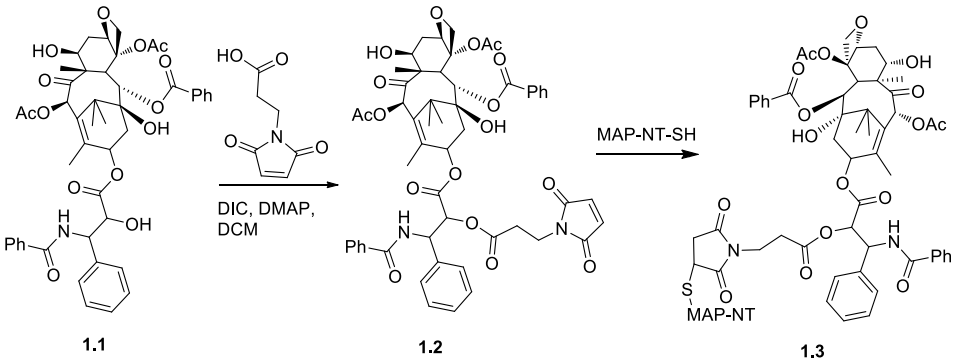

Scheme 1.2 – Synthesis of MAP-NT-PTX adduct.

In vitro cytotoxicity of the so obtained adduct was evaluated by using colon adenocarcinoma (HT-29) and pancreas carcinoma (PANC-1) cell lines, compared to that of the corresponding free drug (PTX) and to that of an unrelated conjugate (U4-PTX), which had been synthesized and conjugated with Paclitaxel by procedures identical to those used for synthesis and conjugation of NT4-PTX, though with a different, non-tumor-selective amino acid sequence. Results obtained with the control U4-PTX unrelated peptide conjugate showed that conjugation with a branched peptide that does not bind to cancer cells produces a reduction in Paclitaxel activity, thus confirming the cytotoxicity on NT4-PTX is due to its peptide-mediated transport into cancer cells.

NT4-PTX efficacy was tested *in vivo* in an orthotopic mouse model. Once mice attained palpable tumors, they were randomly divided into three groups and treated with NT4-PTX, free PTX and saline every 4 days by tail vein injection. Tumor growth was monitored by measuring volumes every 4 days with a caliber rule. At day 16, the average tumor volume of mice treated with NT4-PTX, as measured by caliber and imaging, had decreased by about 37% with respect to animals treated with free PTX and by 70% with respect to control animals (saline). NT4-Paclitaxel induced tumor regression, in the group of animals treated with it, while treatment with unconjugated Paclitaxel only produced a reduction in tumor growth with respect to controls, but not tumor regression. Mice treated with PTX and NT4-PTX were monitored for at least 2 weeks after the last drug injection. Among animals treated with NT4-PTX, regression was observed in each treated animal and 60% treated animals showed almost complete eradication of the disease with no recurrence during 3 weeks without treatment. Toxicity of NT4-PTX treatment was evaluated by monitoring animals daily. None of the treated animals showed any remarkable change in behavior or significant loss of body weight.[25]

2 Gold Nanoparticles

2.1 Metallic functionalized nanoparticles: an improvement of MAP-NT strategy

The previously described targeted drug delivery system (see the section 1 for details), composed by a targeting moiety (MAP-NT), an amidic (or thiolic) linker and a functional unit certainly represents an evolution of traditional targeted drug delivery systems, such as mAbs-drug conjugates. As already reported, peptides in such a dendrimeric form are particularly suitable for *in vivo* use, because they acquire a notable resistance to degradation by proteolytic enzymes, though maintaining or even increasing their natural biological activity. Moreover, neurotensin, synthesized as tetramer, offers accessible linking units for coupling of functional moieties. Nevertheless, one of the greatest drawbacks of peptide-based targeted therapy is the difficulty in multimeric drug binding, whereas, in the case of mAbs, each immunoglobulin is able to carry two (IgG) or five (IgM) drug units. This represents a great limit for this strategy, also considering, for example, the likelihood of premature hydrolysis of the drug-linker bond by means of plasmatic esterases or possible drug release problems, which would even decrease the quantity of drug per carrier molecule which would effectively reach the tumor cell. In order to maximize the poor drug/carrier molar ratio of MAP-NT-drug conjugates, then, our research group has oriented its synthetic efforts on the development of more complex drug delivery systems which could match the advantages of MAP-NT strategy with higher drug-binding capacity, *i.e.* the use of a nanocarrier. Several nanocarriers could be employed to this purpose, such as inorganic non-metallic nanomaterials (*e.g.* amorphous silica), carbon based nanomaterials (*e.g.* carbon nanotubes), organic macromolecular or polymeric nanomaterials (*e.g.* dendrimers) and metallic nanoparticles. Indeed, due to the highly functionalization of their surface, these nanosystems are currently investigated, for drug delivery.[39–43] However, most prominent nanomaterials in medical application are metallic nanoparticles (MNPs). The small size and the corresponding high surface-to volume ratio confers them properties which differ significantly from those of atoms as well as of those of the bulk materials. As a matter of fact, their specific and unique optical, electrical and magnetic properties make them excellent candidates for biomedical applications, such as imaging, hyperthermia, cell labelling, drug and gene delivery, especially in cancer therapy and diagnosis. High efficacy and improved safety of nanoparticles-based devices for cancer diagnosis and therapy are due firstly to the EPR (enhanced permeability and retention) effect, which ensure the targeting activity by a passive mechanism. As a matter of fact, nanoscale object, such as liposomes, nanoparticles, macromolecules, tend to be accumulated preferentially by tumor tissues rather than normal tissues, presumably because of the increased permeability of tumor blood vessels in combination with poor lymphatic drainage or transport. Despite this advantage, only 10 % of administered NPs reach the tumor because of the uptake by the reticuloendothelial system (RES) in which NPs are rapidly shuttled out of circulation to the liver or spleen, and nonspecific binding of NPs to non-targeted or non-diseased

areas. Concerns about NP toxicity often arise because of this RES accumulation. Aggregation can lead to NPs entrapment in the liver, lungs and other tissues due to capillary occlusion. [44] Thus, it may be profitable to further increase the targeting capacity of the MNPs switching from the passive vectorization mechanism to an active targeting mechanism. This can be achieved by conjugating NPs to an appropriate ligand, with a specific binding activity to the target cells. In addition, nanoparticles provide a platform to attach multiple copies of functional units (i.e. therapeutics or/and tracers) increasing the concentration of therapeutics or diagnostics at the pathological site. Thus, we focused on the synthesis of a MAP-NT-NPs-drugs conjugates (*Figure 2.1*) as an evolution of the previously synthesized MAP-NT-drug adduct.

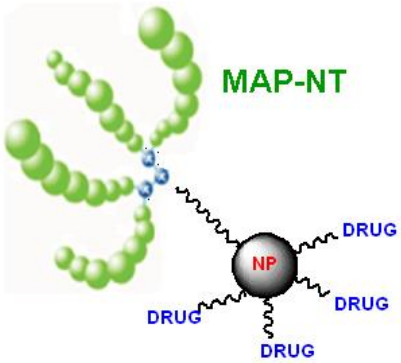

Figure 2.1 - Schematic representation of the MAP-NT -nanoparticle (NP) - drug conjugate.

Many different metallic nanoparticles have been recently investigated for their potential use as therapeutic, diagnostic as well as theranostic devices.

2.2 Paramagnetic metallic nanoparticles

Currently, the only clinically approved metallic nanoparticles are employed in diagnosis rather than in therapy. In particular, superparamagnetic iron oxide nanoparticles (SPIONs) have replaced gadolinium-based contrast agents in magnetic resonance imaging (MRI) for their slower renal clearance and higher relaxation values.[45] However, other paramagnetic NPs have a potential use in MRI. For instance, Cobalt nanoparticles (CoNPs) have been recently investigated as efficient contrast agent in this technique, due to their higher magnetic moment compare to SPIONs.[41] Furthermore, being the metal with the highest Curie point, cobalt firmly maintains its magnetic properties also in stress conditions thus allowing the development of nanosystems with a very prolonged shelf-life.[46] However, metallic nanoparticles have also great therapeutic

potential, as it is proved by the wide number of preclinical trials in which they are involved.[47]

Thanks to their elevated magnetic moment, SPIONs and most importantly CoNPs, could be the ideal candidates for tumor-focused hyperthermia. Indeed, when magnetically induced, such MNPs can conduct heat massively and selectively to the tumor cell in which they have been accumulated, causing tumor tissue shrinking and necrosis.[48]

When conjugating to a therapeutic agent, SPIONs and CoNPs could be applied for magnetic field assisted targeted drug delivery. As a matter of fact, through the application of a proper external magnetic field, the NP-drug conjugate can be selectively directed towards the tumor thus allowing a selective therapy.

For all these potential applications, paramagnetic NPs were selected in the past years from our research group for the development of selective theranostic devices. At this purpose, Combretastatin A4 (CA4) was chosen as therapeutic unit. It is a potent antimitotic agent and exhibits strong cytotoxicity against a broad spectrum of cancer cell lines, such as murine melanoma, human ovarian and colon cancer cells.[49] Since SPIONs are currently the only clinically approved MNPs, and CoNPs have shown interesting properties for a potential application in cancer theranostic, first attempts were directed to decorate SPIONs and CoNPs with C-A4. Thus, a proper functionalization was inserted on combretastatin A4 skeleton and C-A4-SPIONs and C-A4-CoNPs conjugates were prepared *(Figure 2.2)*. The synthesis of such drug delivery systems presented a certain complexity, also for the difficultly in handing, as well as their characterization, since superparamagnetic NPs cannot of course be analyzed by NMR analysis. However, so decorated NPs were characterized by IR spectroscopy, elemental and thermogravimetric analysis and are being in study for the evaluation of their potential application in cancer theranostic.

Figure 2.2 – CA4-capped SPIONs

Since difficulties encountered were ascribable to the paramagnetism of these MNPs, during my PhD, we decided to focus our research on the development of non-paramagnetic nanoparticles-based drug delivery system. As for SPIONs and CoNPs, also non-paramagnetic MNPs have a potential use for several biomedical applications; however they exhibit a more safety profile and ease in handle.

2.3 Gold Nanoparticles: Potential applications

Gold nanoparticles (AuNPs) are characterized by a chemical inertness, which render them more biocompatible and non-toxic compared to other metallic nanoparticles. AuNPs were widely studied for their prominent application in different fields of medicine and especially for their potential use in cancer diagnosis (*i.e.* bioimaging, biosensoring) and therapy (*i.e.* photothermal therapy and hyperthermia, drug delivery and targeted drug delivery): most prominent AuNPs applications are below briefly discussed.

Bioimaging: AuNPs have a potential use as contrast agents in X-ray technique; as a matter of fact, they could replace iodine-containing contrast agents (ICCA) since they showed better contrast with lower X-ray dose and permitting longer imaging times. [50,51] AuNPs have also a potential application for MRI and computed tomography (CT). [52,53] Furthermore, the feasibility to targeted AuNPs renders them more suitable as contrast agent compare to those currently available since allowing a selective diagnosis of the tumor.

Thermal therapy: Due to SPR, when AuNP are exposed to a proper energy source, electrons collectively coherently oscillate.[54] Excited electrons lose energy quickly as a phonon that heats the environment of the AuNP which in cancer treatments would be the cancerous cells. [55] Since SPR is strictly related to nanoparticles size and shape, these properties can be tuned to obtain AuNPs sensitive to wavelength in the range 700-1000 nm, because biological tissues are optically transparent at these wavelengths. [56,57]

Drug delivery and targeted drug delivery: AuNPs have the ability to firmly bind amines and thiols allowing surface modification. A wide variety of biomolecules, *e.g.* proteins, antibodies, genes, as well as smaller molecules, *e.g.* drugs, antioxidants etc., can be attached on the AuNP surface. As above mentioned, AuNPs passively accumulate at tumor sites due to the EPR effect, which can thus allow a selective drug deliver into the cancer cell. However, due to the uptake by the reticuloendothelial system (RES) and accumulation of nanoparticle aggregates mainly at the liver site, only a minor part of the administered dose can effectively reach the pathological site. Thus, an enhancement of the targeting ability of these nanosystems could enormously improve their efficacy in drug delivery. This can be achieved by conjugating the gold core with a targeting unit, thus increasing the drug dose at the tumor site.

2.4 Gold nanoparticles Synthetic methodologies

The synthesis of AuNPs with diameter ranging from a few to hundreds of nanometers is well-established in aqueous solution as well as in organic solvents. More common AuNPs synthetic methodologies envisage the reduction of a gold salt, typically $HAuCl_4$, by a reducing agent which leads to the nucleation of Au ions to NPs. Reductive reaction

usually occurs in the presence of a stabilizer, which both controls the growth of the gold cores, and prevents their agglomeration (*Figure 2.3*).

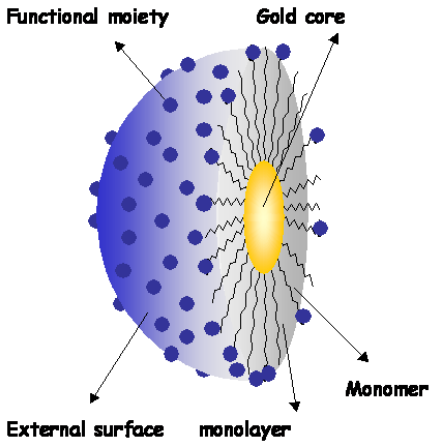

Figure 2.3 – Section of capped-gold nanoparticle.

Indeed, molecules with a certain affinity for the Au(0) atoms, spontaneously form a protective monolayer on the nanoparticle surface, called self-assembled monolayer (SAM). The chemical nature of the stabilizer, as well as the stabilizer-to-gold ratio, strongly influences the SAM formation rate, thus determining the gold clusters size. Since AuNPs properties strongly depend on their shape and size, the suitable synthetic methodology and the proper stabilizer, have to be chosen in order to achieve AuNPs with the size required for the specific use.

Turkevich et al,[58] in 1951, for the first time synthesized colloidal gold from gold salts by using citric acid as reducing agent. The method was refined by G. Frens,[59] in 1973, and Natan,[60] in 1995, to achieve NPs with better size distribution and size control in the 10-120 nm range. Currently, this synthetic methodology is used to produce modestly monodisperse spherical gold nanoparticles, suspended in water, of around 10–20 nm in diameter. Larger particles can be produced by varying the gold-to-citrate ratio, but this comes at the cost of mono-dispersity and shape. Synthetically, in the Turkevich method a hot aqueous solution of $HAuCl_4$ is reacted with aqueous sodium citrate. The colloidal gold will form because the citrate ions act as both a reducing agent, and a capping agent (*Scheme 2.1*).

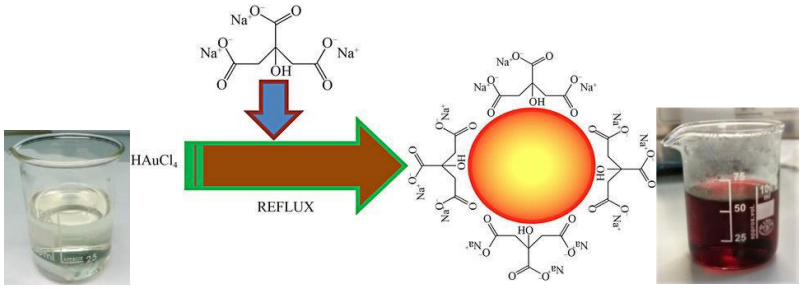

Scheme 2.1 - Turkevich AuNPs synthesis.

Considering the advantage in directly synthesizing water-soluble (*i.e.* biocompatible) AuNPs, recently, several research groups have focused their interest on the improvement of this synthetic procedure.[61,62] However, due to the weak gold-to-citrate interaction, these NPs are poor stable, since undergo desorption of citrate coating with a consequent coalescence and loss of the ability to form colloidal solutions. Thus, the citrate layer has to be replaced with a more stable ligand through a place-exchange reaction (see section 2.5 for details).

Both the poor stability and the modest monodispersity of citrate-capped AuNPs were overcome when, in 1994, Brust and Schiffrin reported a simple and versatile synthesis of alkylthiols-protected AuNPs ranging in diameter between 1-3 nm that has had a considerable impact on the overall field of NPs preparation.[63] They are soluble in organic solvents and have a narrow size distribution. A peculiar property of these materials is that they behave like large organic compounds; thus, they can be purified by precipitation, by repeated centrifugation, using size exclusion chromatography etc., without changing their properties.[64] Synthetically, an acqueous $HAuCl_4$ solution was stirred with a tetraoctylammonium bromide (TOAB) toluene solution. The latter acts as the phase-transfer reagent, and the $AuCl_4^-$ is transferred to the organic phase. Then, Au (III) was reduced with cold aqueous sodium borohydride, used in large excess, in the presence of a proper stabilizer, typically an alkyl thiol. On addition of the reducing agent, the organic phase changes color from orange to deep brown within a few seconds, indicating the successful of the reaction (*Scheme 2.2*).

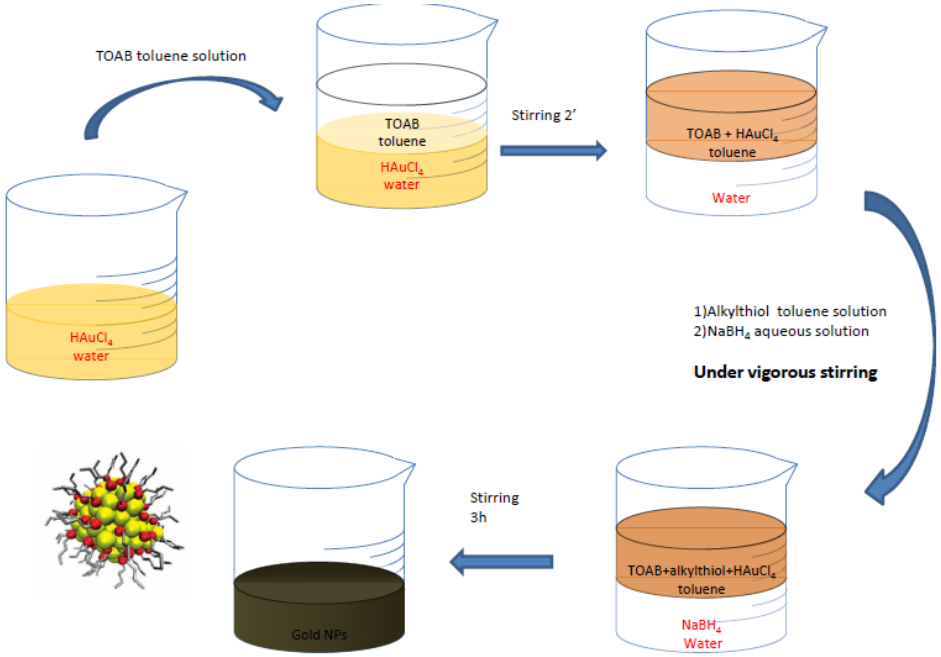

Scheme 2.2 – Schematic representation of Brust synthesis procedure.

The procedure, was firstly developed using dodecanethiol as capping agent, but it was then adapted to several thiols, such as pentanethiol, 10-mercaptoundecanoic acid etc., as well as to molecules fitted out with more than one sulfur atom, such as poly-thiols,[65–67] and disulfides.[68–74] A greater stability of the monolayer was shown when using poly-sulfurated ligands instead of monothiols. As a matter of fact, the polysulfide nature allows a polyvalent interaction of the ligand with the gold surface thus remarkably reducing the possibility of ligand desorption.
An evolution of the Brust procedure was achieved when Leff et al., in 1996,[75] used amines instead of thiols. Even if, due to the weaker Au(0)-N interaction compared to the Au(0)-S one, amino-capped NPs show a slightly lower stability, they behave very similar to their thiol-capped counterpart.
However, Brust synthesis provide NPs with a very good monodispersity in the range 2-5 nm. Afterwards, Murray and co-workers extensively investigated the possibility to tune the clusters size and their dispersion by changing *i)* Au : ligand molar ratio; *ii)* rate of reduction; *iii)* reduction temperature.[76,77] Briefly, large ligand-to-gold molar ratios produce small NPs; fast addition of reductant solution at low temperature leads to AuNPs with a narrow size distribution, in the 2-5 nm range.

2.5 Gold nanoparticles Functionalization

One of the most attractive features of monolayer-protected AuNPs is the possibility to introduce a wide variety of molecules into the ligand shell, obviously after a proper

functionalization *i.e.* with amine, thiol etc.. In addition, due to the AuNPs diamagnetism, NMR analysis can be exploited for the monitoring and characterization of the organic shell.
The three different available approaches for a suitable AuNPs decoration are below summarized:
i) Direct synthesis
When reducing Au(III) to Au(0) in the presence of a ligand (or a mixture of different ligands) with a certain gold affinity (*i.e.* thiols or amines), the latter is chemosorbed on the gold surface. Thus, performing the Au(III) reduction in the presence of a proper ligand(s), the desired functionalization of NPs can be achieved. This method can be adapted in both aqueous and organic media, depending on the chemical nature of the ligand involved. The main limitation is that ligands have to be compatible with reaction conditions, *i.e. a* reductive, basic environment. Furthermore, since the chemical nature of the ligand influences gold clusters growth, a good control in NPs size is not ensured (*Scheme 2.3*).

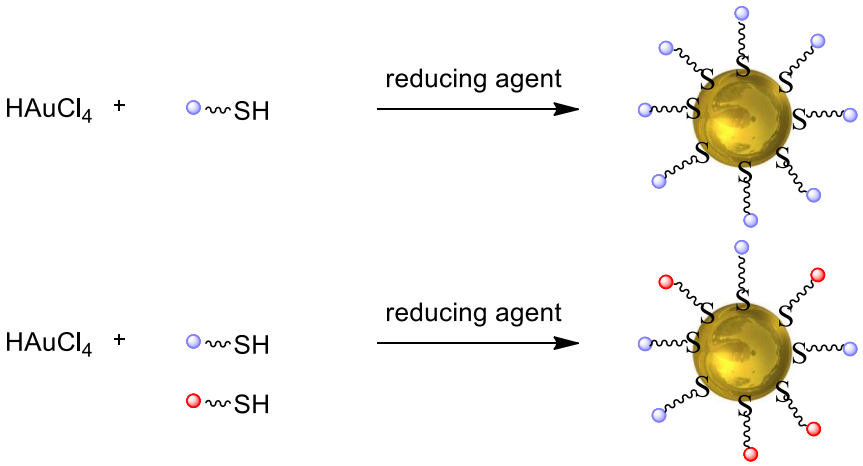

Scheme 2.3- Schematic Direct synthesis of functionalized gold nanoparticles.

ii) Ligand-exchange method
When capped AuNPs are placed in a solution containing a proper concentration of a ligand (or a mixture of different ligands) with a certain Au(0)- affinity, monolayer constituents are replaced by free ligands, preserving NPs size and shape. This process can be exploited for suitably decorate AuNPs, by choosing the proper incoming ligand(s). This represents the most used strategy for NPs functionalization, because, besides the great control in gold clusters size, it allows a wide variety of groups to be introduced in the monolayer, and to tune the composition of the protecting shell by changing the ratio of incoming ligands. The good control of gold nucleation is ensured by using classic Brust methodology for the synthesis of alkylthiol-capped NPs, as substrate for the place-exchange reaction, thus overcoming the drawback of "direct synthesis" protocol (*Scheme 2.4*).

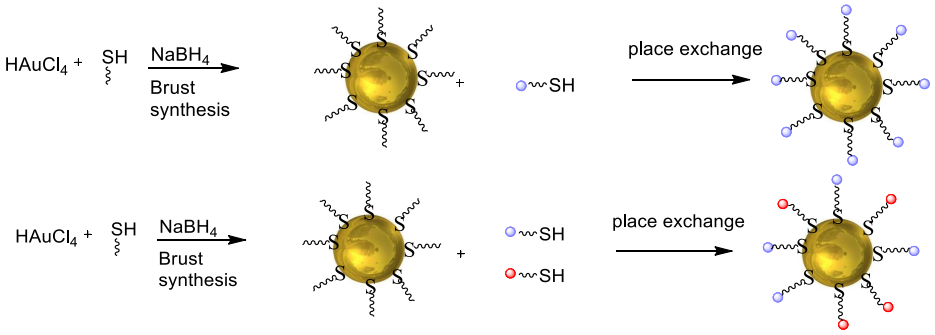

Scheme 2.4 –Place-exchange reaction.

This mild procedure occurs under neutral conditions and is particularly indicated for ligands bearing functional moieties that can be easily degradated under "direct synthesis" reaction conditions. Murray and co-workers reported several detailed studies of the kinetics and the factors determining enhancement or inhibition of this process.[78–82] These studies demonstrated that the place-exchange reaction is an equilibrium process between entering and incoming ligands and that steric hindrance and stoichiometry of ligands involved can deeply influence the rate and the efficacy of the place-exchange reaction. To improve the place-exchange reaction rate the different affinity of S and N to Au can be exploited. In particular, using amino-capped AuNPs as substrate in an exchange reaction with thiols, the rate of the place-exchange could be improved. The efficacy of this process can be further enhanced by using a polydentate molecule as entering ligand instead of the thiol one, thus allowing a polyvalent, *i.e.* more stable, interaction with gold surface.

iii) Post synthetic modification

Pendant functional groups inserted on the organic NPs shell can undergo many synthetic transformations. The post-synthetic modification requires reaction proceeding under mild conditions, compatible with the structure and the integrity of the self-assembled monolayer. The earlier examples reported (*Scheme 2.5*) are a) the esterification of phenolic-decorated AuNPs with propionic anhydride,[83] b)S_N2 reactions of bromoalkanethiolate AuNPs with primary amines,[84] c) amide- or ester-forming coupling reactions for the functionalization of carboxylic acid terminated-AuNPs.[85,86] Most recently, 'click chemistry' was reported as a simple and versatile approach for NPs modification. In particular, d) 1,3 dipolar cycloaddition, involving an alkyne and an azide to form a triazole ring in the presence of copper salts, [87] and e) maleimide-thiol Michael addition[88] were widely described. The latter is particularly attractive for peptide-AuNPs conjugation, since a thiol group is typically inserted on the peptide through a cysteine residue.

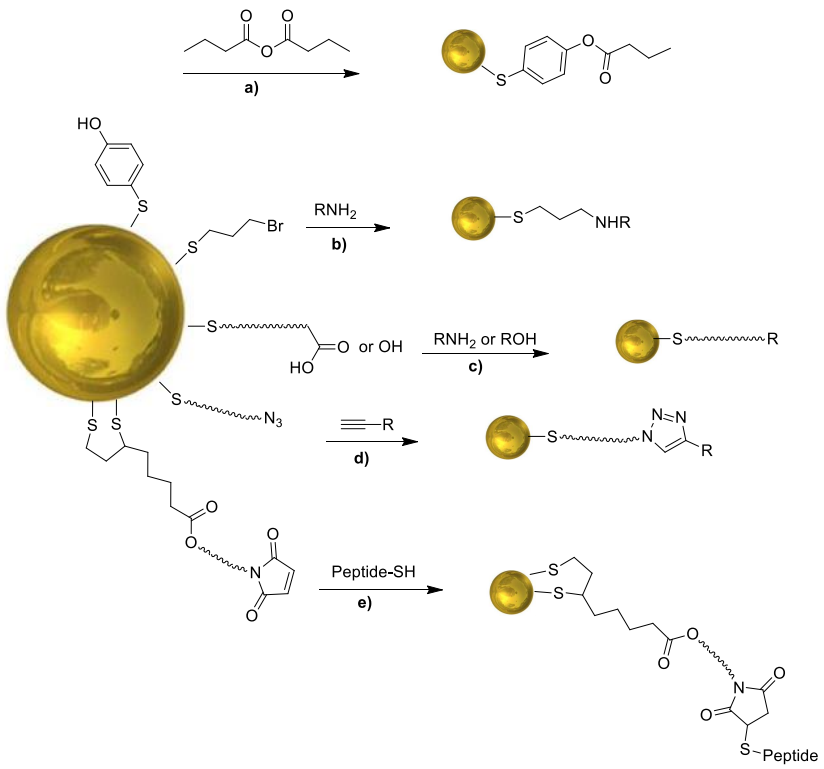

Scheme 2.5 - Examples of post-synthetic modifications: a) reaction of *p*-mercaptophenol with propionic anhydride; b) S_N2 reaction; c) amide and ester coupling reaction; d) azide-alkyne click reaction; e) maleimide-thiol click reaction.

2.6 Towards the development of targeted gold nanoparticles- based drug delivery systems:

The great variety of chemical modification to which AuNPs can undergo, together with their tunable optical and physical-chemical properties, make them ideal candidates for the development of a targeted drug delivery system.
As detailed in the *"introduction"*, Paclitaxel is one of the most effective cytotoxic drugs. It is active against several types of tumor, such as lung, ovarian and breast cancers. However, treatment with Paclitaxel is associated with severe side effects, due to its high hydrophobicity and its scarce selectivity towards cancer cells. Thus, it is evident how the development of a more safety pharmaceutical form of this therapeutic unit could revolutionize the treatment of such types of tumor. In our research group a more selective therapeutic form of Paclitaxel was synthesized by conjugating it with the targeting peptide, MAP-NT. The limit of this approach is the inability of the peptide to bind more than one therapeutic unit. In order to maximize its targeting ability we envisaged multi-drug decoration of MAP-NT through the introduction of a highly functionalized nanoparticle.

Some synthetic issues have to be considered:

i) A stable anchorage of both peptide and Paclitaxel on gold surface is required, thus avoiding undesirable ligand loss in the blood flow after the administration of the drug delivery system;

ii) The high steric hindrance of both peptide and drug moieties has to be considered, in order to enable the targeting ability of the peptide for the entire stay in the bloodstream and, on the other hand, ensure the therapeutic activity of Paclitaxel;

iii) A limited type of reactive groups can be inserted on the targeting unit. The thiol function is one of the available functionalizations, provided through the introduction of a cysteine residue.

To overcome these limitations, we envisaged the introduction of a properly designed bifunctional linker between the nanoparticle and both the therapeutic and targeting units. The suitable linker should possess, a polydentate sulfur moiety, providing a strong and stable interaction with the gold surface, [65–71] and a functional group able to easily react with both the peptide and the Paclitaxel. Considering the cysteine functionalization of the peptide and the ease of introduction of a thiol function on Paclitaxel, reasonably, we selected a double bond as binding site for functional units. As a matter of fact, alkenes can react with thiols in the thiol-ene click reaction, which was described as a convenient pathway for nanoparticles decoration.[67]
The designed tris thiol-alkene bifunctional linker **2.1** is reported in *Figure 2.4*.

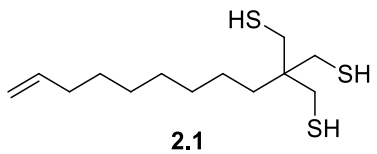

2.1

Figure 2.4 – Designed bifunctional linker.

The synthesis of the linker, reported in *Scheme 2.6*, started by reacting commercially available 10-undecenal **2.2** with 1 equiv. of KOH and 7 equiv. of 37% aqueous formaldehyde in water : ethanol = 50 : 50 as solvent at room temperature for 24 hours and at 50 °C for 4 hours. The tris-alcohol **2.3** was obtained as colorless oil after purification by column chromatography, in 60% yield. Afterwards, sulfur atoms were introduced by a Mitsunobu reaction with 4.5 equiv. of thiolacetic acid, in the presence of 4.5 equiv. of triphenylphosphine and 4.5 equiv. of DIAD (diisopropyl azodicarboxylate) in dry THF as solvent, overnight at room temperature and for 2 hours at reflux. The product **2.4** was obtained after purification by column chromatography in 29% yield. Thiolacetyl groups were, in turn, reduced to thiols in the presence of 7.5 equiv. of $LiAlH_4$ in dry diethyl ether as solvent, for 20 hours, to afford the final linker **2.1**, in quantitative yield.

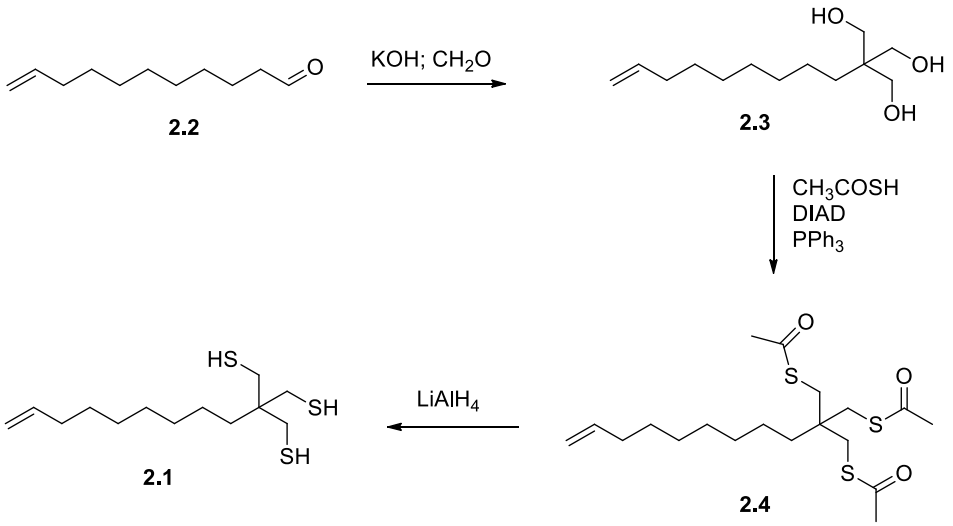

Scheme 2.6- Synthetic procedure for the achievement of the linker **2.1**.

With the linker in hand, we focused on the alkene-decoration of gold nanoparticles.
In this respect, two different approaches can be exploited. The selected ligand can be used directly as stabilizer in the Au(III) reduction step as well as incoming ligand in a place-exchange reaction with alkyl-capped AuNPs. Aimed to ensure a well-control in NPs size, penthanethiol-capped AuNPs (AuNPs-C5) were prepared following the Brust procedure, and were, in turn, employed in a place-exchange reaction with an excess of the linker **2.1.** The mixture was stirred in dry DCM at r.t.. After 3 days, the solution was concentrated under vacuum and methanol was added, to promote nanoparticles precipitation and thus facilitating removal of unbounded penthanethiol, and the excess of the ligand **2.1**. Unfortunately, after their precipitation, nanoparticles resulted in an agglomerate which cannot be redispersed. Analogous result was obtained when conducting the Brust synthesis using linker **2.1** instead of penthanethiol as stabilizer. Thus, we moved to consider the likelihood to provide both Paclitaxel and peptide with the tridentate moiety before the anchorage on gold, by performing the thiol-ene reaction in solution. Aimed to investigate the reactivity of our linker in a thiol-ene click coupling, a model reaction between the ester form of 10-mercaptoundecanoic acid and the acetylated form of the tris thiol derivative **2.4** was carried out (*Scheme 2.7)*. The thiol-ene reaction is a highly stereoselective reaction which proceeds under a variety of conditions, including radical pathway and *via* catalytic processes mediated by nucleophiles, acids, bases,[89] afforded the *anti*-Markovnikov addition product. A summary of the reactions performed is reported in *Table 2.1.*

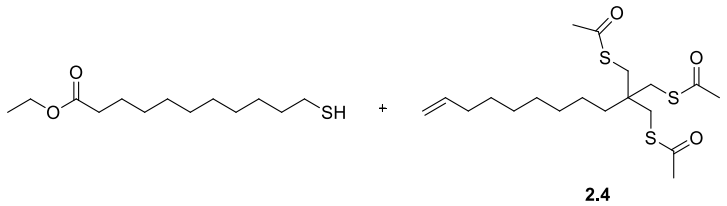

Scheme 2.7

Entry	*Ethyl 10-mercaptoundecanoate*	*Linker **2.4***	*Promoter*	*Reaction Conditions*	*Rif.*	*Yield*
1	1.1 equiv.	1 equiv.	UV-lamp	Dry DCM, 7 h, r.t.	[67,76]	-
2	1.1 equiv.	1 equiv.	BEt_3 1M solution in hexane	Dry THF, 48 h, r.t.	[90]	-
3	1.1 equiv.	1 equiv.	BEt_3 1M solution in hexane	Dry THF, 48 h, 50 °C	[90]	-
4	1.1 equiv.	1 equiv.	BEt_3 1M solution in hexane and O_2	Dry THF, 48 h, r.t., O	[91]	-
5	1 equiv.	1 equiv.	/	H_2O, r.t., 24 h	[92]	-
6	1.1 equiv.	1 equiv.	$CeCl_3 \cdot 7H_2O$	Neat, 24 h, r.t.	[93]	-

Table 2.1

Despite several attempts, neither under UV irradiation nor in the presence of chemical radical initiators, we achieved the desired product of coupling. We were not able to rationalize these unexpected results. However, we considered the replacement of the double bond with a functional group able to react in a more promising click reaction. The Huisgen reaction between a terminal alkyne and an azide derivative was selected as efficient alternative to the thiol-ene reaction; [94–96] thus, a new linker bearing a triple bond instead of the double one, was designed (*Figure 2.5*).

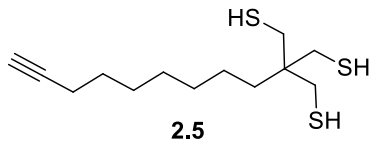

Figure 2.5 – Designed tris-thiol alkyne linker.

Reasonably, it was synthesized following the well-consolidated procedure used for the alkene analogous, obviously starting from a proper alkynil derivative (*Scheme 2.8*).

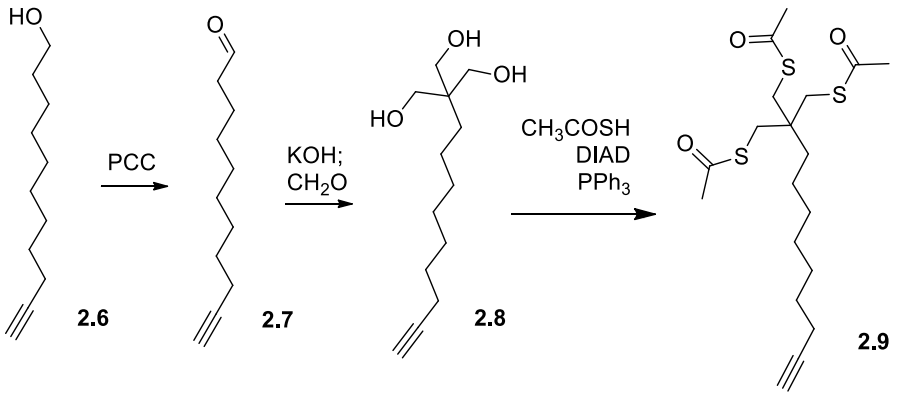

Scheme 2.8 – Synthetic procedure for the synthesis of tris-thiol-alkyne linker.

Thus, the commercially available 10-undecyn-1-ol **2.6** was oxidized by 1.5 equiv. of pyridinium chlorochromate (PCC) in dry DCM for 3 hours, to afford the corresponding aldehyde **2.7** which, in turn, underwent procedure described for alkene derivative **2**, to achieve the tris thioacetylate derivative **2.9**. Unfortunately, some synthetic complications occurred in the following reduction step, since the desired tris-thiol **2.5** was achieved just in trace. The ^{1}H-NMR analysis of the crude product showed broad peaks overlapping to expected signals of tris-thiol **2.5** derivative. This suggested that, perhaps, part of the final compound underwent a polymerization reaction, probably due to the formation of S-S intermolecular bridges and/or inter- or intra-molecular thiol-alkyne coupling reaction.[97] To circumvent this poor result, we move to consider an alternative strategy, aimed to avoid the employment of free thiol functions, which seemed to be the main cause of side reactions occurred in the reductive step. After a screening in literature, thanks to the high affinity of sulfur-to-gold, the feasibility of using disulfide compounds as stable NPs capping agents instead of thiols, has emerged. In particular, the use of lipoic acid as stable AuNPs capping agent is described. [72,73] Indeed, the presence of the 1,2-dithiolane ring allows the strong interaction with the gold surface. Lipoic acid was thus selected to introduce a polyvalent binding site for gold on the new designed linker. On the other hand, keeping the original idea of using a click reaction involving thiols for the coupling with the therapeutic and the targeting units, maleimide moiety was selected since it can react in the maleimide-thiol click reaction, already optimized for the synthesis of the MAP-NT-Paclitaxel adduct. Since ester bonds can be easily hydrolyzed *in vivo,* we considered an amido group for the maleimide-lipoic acid conjugation. The designed linker is depicted in *Figure 2.6* and the synthetic procedure we envisaged was an amidation reaction of activated lipoic acid with a proper bis-amine, since introducing both the amide bond and the pendant free

amino group required for the introduction of the maleimide residue, through the reaction with maleic anhydride.

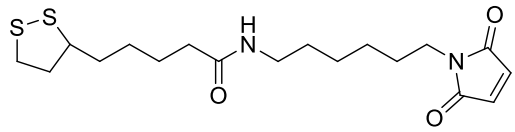

2.10

Figure 2.6-lipoc acid-maleimide designed linker

Thus, 1.0 equiv. of lipoic acid **2.11** was activated through a reaction with 1.0 equiv. of N-hydroxysuccinimide and 1.2 equiv. of DCC in dry DCM for 1 hour. Then, the mixture was kept at -5 °C overnight and the suspension was filtered to get rid of solid DCU. The filtrate was evaporated to achieve **2.12**, without further purification, in quantitative yield, that was, in turn, reacted with hexamethylenediamine **2.13**. Despite several attempts, we were unable to settle up suitable conditions for the selective mono-substitution of the activated acid, since the bis-coupling product was the only one recovered. To circumvent this problem, hexamethylene diamine **2.13**, was reacted with 0.15 equiv. of Boc_2O (di-tert-butyl-dicarbonate), in dry DCM, at 0 °C for 30 minutes and at r.t. overnight. The unreacted diamine was washed away with water and the desired final compound **2.14** was isolated in 95 % yield. Then, the activated lipoic acid **2.12** and mono N-Boc amine **2.14** were reacted in the presence of 2.0 equiv. of DIPEA as base in dry DCM, for 19 hours, at r.t.. The amide **2.15** was obtained, without purification, in 94% yield. The latter was, in turn, treated with a DCM : TFA 4 : 1 solution for 1 hour, giving a crude product whose ^{1}H-NMR spectrum showed characteristics signals of the expected amine **2.16**, overlapping to broader signals. Anyway, since the presence of the amino-functionalized lipoic acid **2.16** was confirmed by ESI-MS analysis, the crude product was reacted in the further step with 1 equiv. of maleic anhydride in dry DCM at r.t. for 6 hours. The solvent was removed, 1.1 equiv. of sodium acetate were added and the mixture was stirred in acetic anhydride at 140 °C for 6 hours.[98] Unfortunately, the ^{1}H-NMR analysis of the crude showed neither product nor starting material's protons characteristic peaks. A slightly better result was obtained reacting **2.16** with 1.0 equiv. of maleic anhydride in acetic acid, for 3 hours, at reflux. After purification by flash column chromatography, the final linker **2.10** was isolated in 5% yield, over two steps. The presence of the final linker **2.10** confirmed the presence of **2.16** in the crude product, even if the poor yield indicated that, probably, it was present in a very low amount (*Scheme 2.9*).

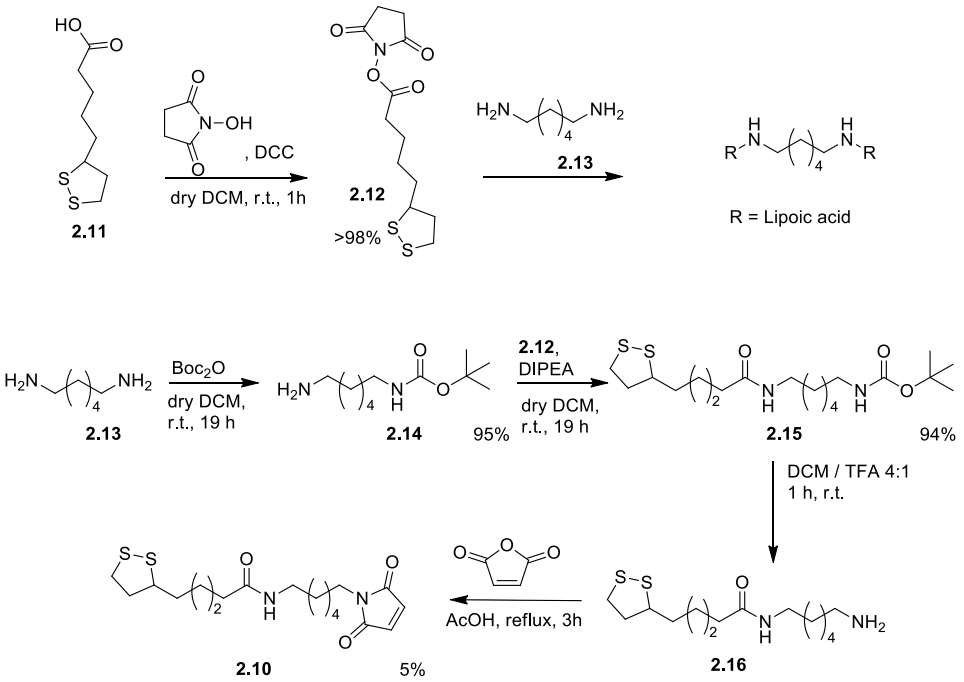

Scheme 2.9 – Synthetic procedure for the achievement of linker **2.10**.

We thus investigated the introduction of the maleimide residue as 3-maleimido propionic acid through an amidation reaction, since this synthetic pathway required milder conditions. The required activated form of 3-maleimido propionic acid **2.18** was synthesized by reacting 1 equiv. of β-alanine **2.17** with 1 equiv. of maleic anhydride, in acetic acid at reflux for 6 hours. The maleimide-acid derivative, obtained in 65 % yield, was, in turn, activated as NHS ester with 1.25 equiv. of N-hydroxysuccinimide in the presence of 1.5 equiv. of DIC in dry DMF overnight. Derivative **2.18** was achieved in 97 % yield, without purification. Hence, the amidation between the crude product **2.16** and the maleimide-derivative **2.18** was performed in the presence of 2.0 equiv. of DIPEA in dry DMF at r.t. overnight. The ^{1}H-NMR analysis of the crude recovered showed intense broad signals, ascribable to the presence of polymers, and characteristic proton peaks of the unreacted maleimide derivative **2.18**, while the desired final product was present just in traces. However, due to the great complexity of the crude, we were not able to isolate the compound **2.19** (*Scheme 2.10*).

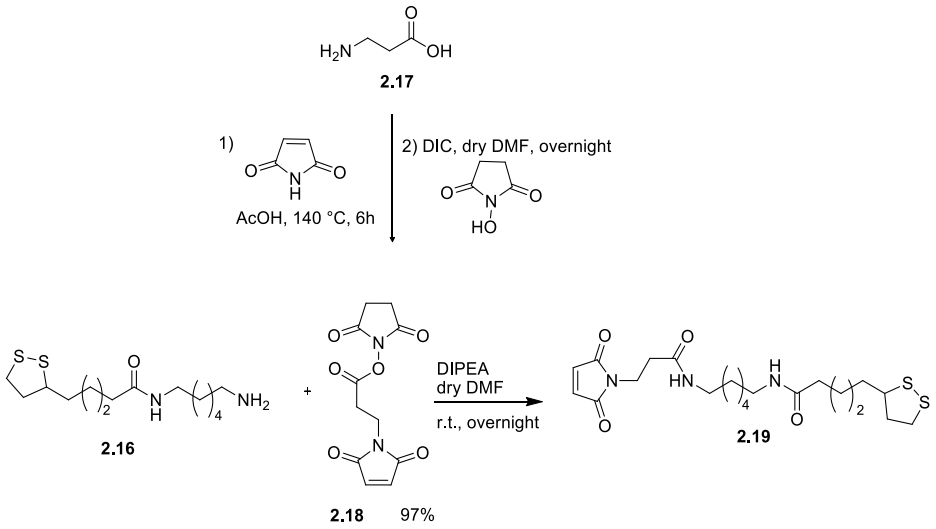

Scheme 2.10 – Synthetic effort for the synthesis of compound **2.19**.

We thus considered the insertion of lipoic acid residue as the last step of the procedure. The maleimide moiety was inserted on the N-Boc hexamethylene diamine **2.14**. Since treatment with maleic anhydride and acetic acid at 140 °C, did not allow the isolation of the expected derivative **2.20**, 1 equiv. of the mono-protected diamine **2.14** was reacted with 1 equiv. of maleic anhydride in DCM for 6 hours at r.t.. After the evaporation of the solvent, the crude product was suspended in acetic anhydride and reacted with 1.1 equiv. of sodium acetate for 6 hours at 110 °C, [4] to afford **2.20** after purification by flash column chromatography, in 50% yield (*Scheme 2.11*). Unfortunately, either using concentrated or diluted TFA : DCM solution, the desired Boc deprotection was not observed. Indeed, the characteristic signal of maleimide protons was not present in the ^{1}H-NMR spectrum, thus highlighting the instability of maleimide moiety to TFA treatment.

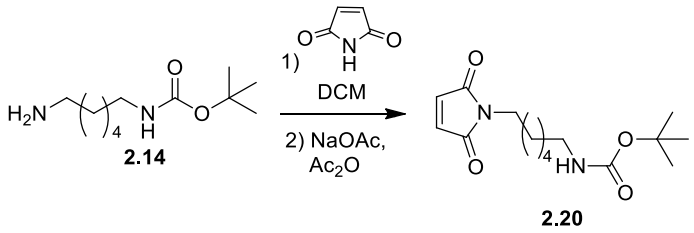

Scheme 2.11

Different amino protecting groups were tested to circumvent this obstacle. Unfortunately, neither when using Fmoc nor with Cbz we were able to afford the amino-maleimide derivative. Finally, chemical instability of maleimide moiety towards

TFA treatment was overcome when using an inorganic acid instead of the organic TFA. Indeed, the amino-maleimide derivative **2.22** was achieved, as ammonium chloride, by treating derivative **2.21** with a 3M HCl methanol solution for 1 hour at r.t., in 70 % yield. Derivative **2.22** was, in turn, conjugated with 1.1 equiv. of NHS ester activated lipoic acid **2.12**, in the presence of 2 equiv. of DIPEA in dry DMF. After 20 hours at r.t. the desired linker **2.19** was isolated in 20 % yield and the structure was confirmed by NMR, IR and ESI-MS spectroscopy (*Scheme 2.12*).

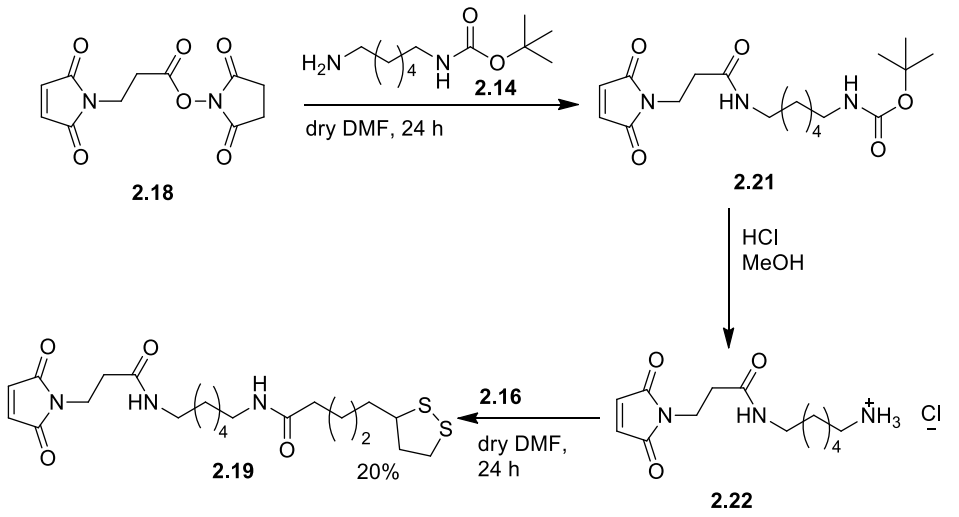

Scheme 2.12 – Synthesis of the linker **2.19**.

The so prepared linker was designed to serve as binding site for the peptide as well as for the drug. While the targeting unit is already provided with the thiol function required, due to the presence of the cysteine residue, the thiol functionalization of Paclitaxel has to be carried out. Keeping in mind the need of an *in vivo* hydrolysable bond on the drug proximity to ensure the *in vivo* drug release and thus maintaining the cytotoxic activity against the cancer cells, we esterified the OH on the 2' position of Paclitaxel **2.23** with 1.2 equiv. of commercially available 10-mercaptoundecanoic acid **2.24** in the presence of 0.2 equiv. of DMAP and 1.2 equiv. of DCC. The product **2.25** was isolated after 16 hours at r.t., by flash column chromatography, in 73% yield (*Scheme 2.13*).

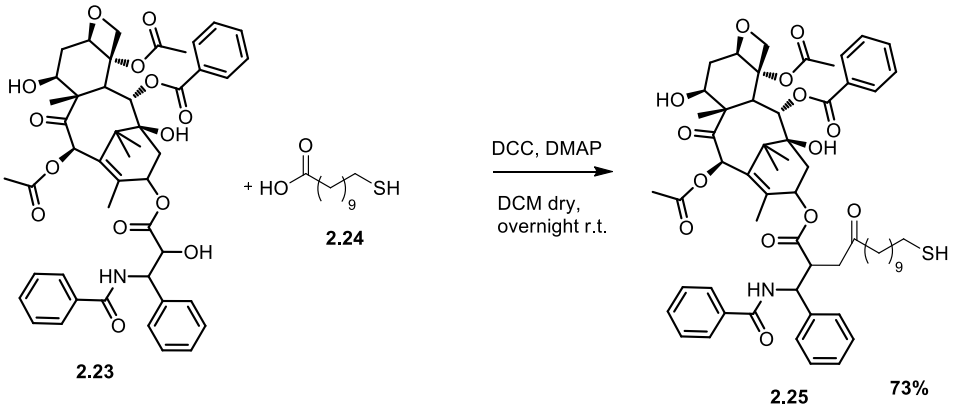

Scheme 2.13 – Synthesis of thiol-functionalized Paclitaxel.

In order to find out suitable click reaction conditions for anchoring thiol-Paclitaxel on maleimide-decorated AuNPs, a model reaction between 1 equiv. of Paclitaxel derivative **2.25** and 1 equiv. of maleimide linker **2.19** in the presence of 1 equiv. of TEA as base in dry DMF, was performed. After 3 hours at r.t., the final adduct **2.26** was isolated in 50 % yield (*Scheme 2.14).*

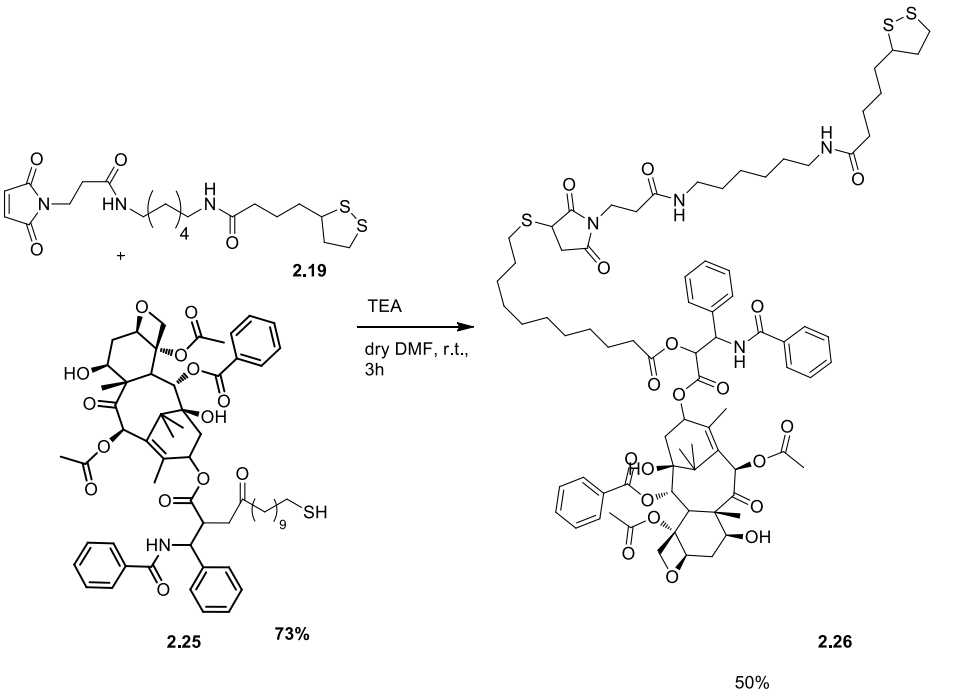

Scheme 2.14 – Synthesis of linker-Paclitaxel adduct *via* Michael addition.

The ^{1}H-NMR analysis showed typical peaks of Paclitaxel moiety (blue circle) together with characteristic peaks of lipoic acid (yellow square) whose integrals are in accordance with derivative **2.26**. Morover, the success of the coupling was demonstrated by the presence of charachteristic succinimide protons peaks, whose CH_2 showed a multiplet at around 3.8 ppm (red arrow) while the CH proton appears as a multiplet at around 3.7 ppm (green arrow) (*Figure 2.7*). ESI-MS analysis showed $[M+Na]^+$ peak thus confirming the success of the coupling.

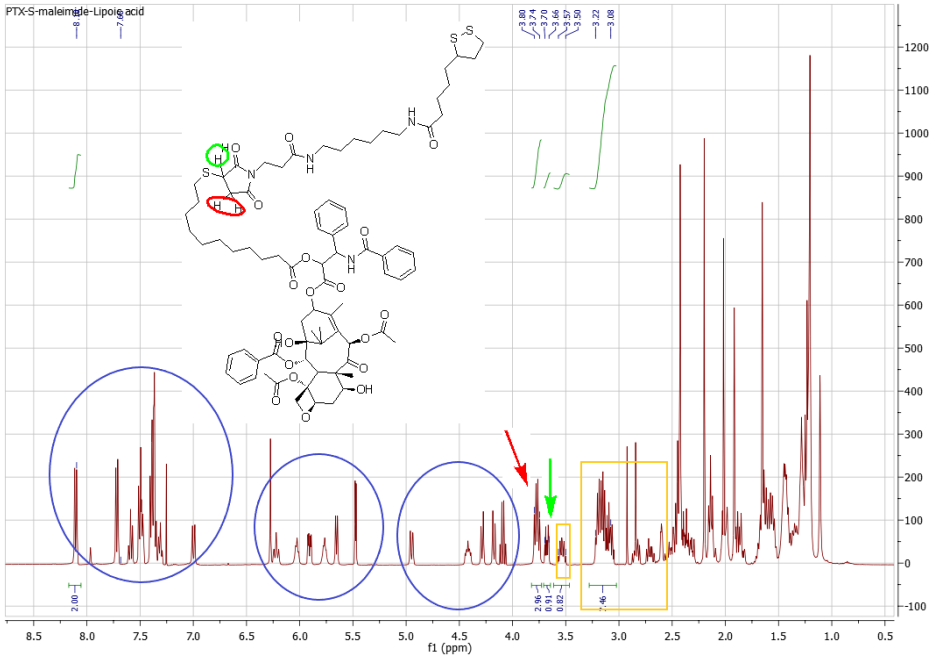

Figure 2.7

2.7 Decoration of Gold Nanoparticles

Our first goal was the maleimide decoration of AuNPs by anchoring ligand **2.19** on gold surface. To achieve a properly decorated AuNPs with a good gold core size distribution in the range 2-5 nm, the place-exchange protocol seemed the most convenient way. The process can be facilitated by involving an incoming ligand with a greater affinity for gold compared to the leaving one. In detail, amino coated NPs can easily undergo place-exchange reaction with sulfurated ligands present in the NPs external environment. The greater affinity of Au-to-S compare to Au-to-N, on one hand, enhances the place-exchange rate and, on the other hand, avoids incoming ligand displacement from amino-ligands, once place-exchange is occurred.

Thus, oleylamine-capped AuNPs in a size distribution of 2 - 5 nm, were prepared by using the Brust procedure, and were characterized by TEM analysis, to establish the average size of gold clusters, and by ^{1}H-NMR, to characterize the organic monolayer (*Figure 2.8*).

a)

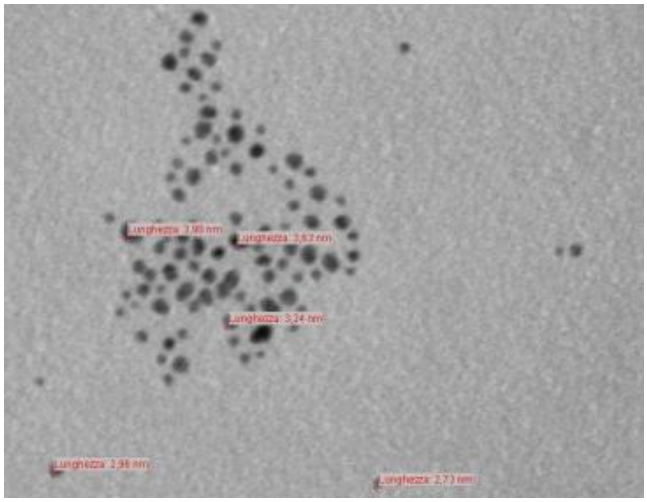

b)

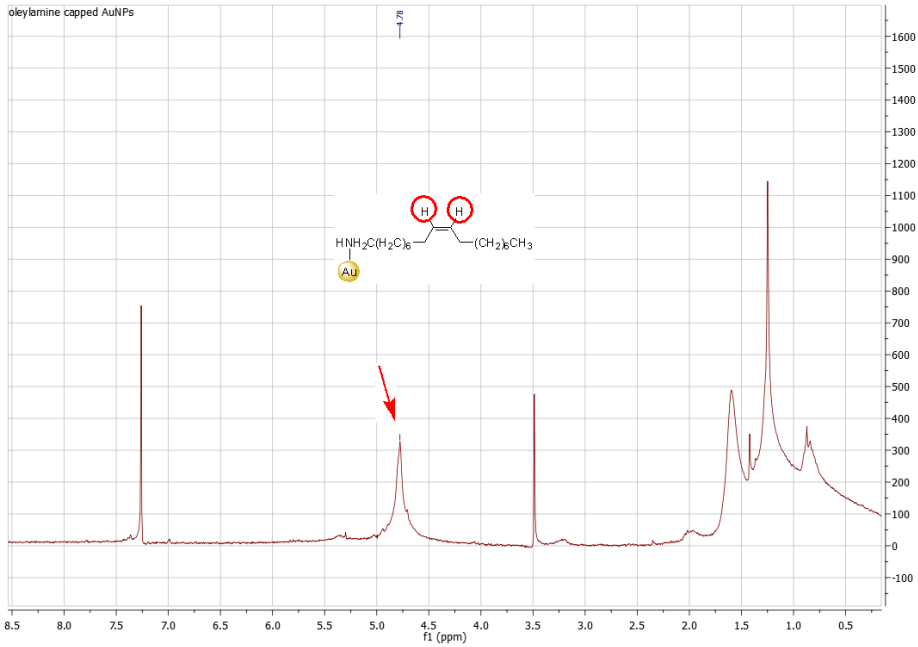

Figure 2.8 – a) TEM analysys and *b)* ^{1}H-NMR spectrum of oleylamine-capped AuNPs. The broad peak at around 5.0 ppm is characteristic of the vinylic protons of oleylamine anchored on gold.

Oleylamine-AuNPs were then placed in a dry DCM solution, containing an excess of the maleimide-ligand **2.19**, and the mixture was stirred in inert atmosphere. Unfortunately, after 16 hours, nanoparticles resulted in a black agglomerate insoluble in many types of solvents. The feasibility in exploiting the different affinity of gold to heteroatoms in this process was further investigated, by employing TOAB as both phase transferreagent and stabilizer.[73] The ligand **2.19** was added directly in the mixture, after gold clusters formation, and the mixture was stirred overnight. Also in this case, gold clusters underwent agglomeration. We thus decided to investigate the use of alkylthiol-capped AuNPs as substrate for the place-exchange step. Even if the more stable thiolate monolayer might decrease the place-exchange rate, the stronger S-Au bond should ensure a better stability of the so coated NPs, thus avoiding agglomeration during this crucial step.

Hence, penthanethiol-capped AuNPs (AuNPs-C5) were synthesized and characterized by TEM (*Figure 2.9*-a) and ^{1}H-NMR analysis (*Figure 2.9-b*). A well monodispersity of NPs size in the range 2-5 nm was showed and residual unbounded pentanethiol was not present.

a)

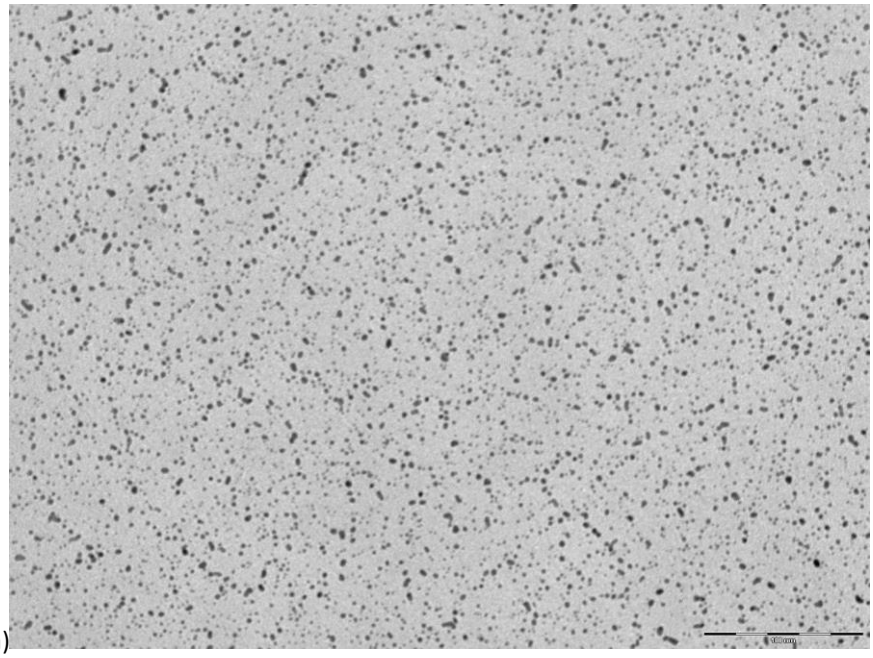

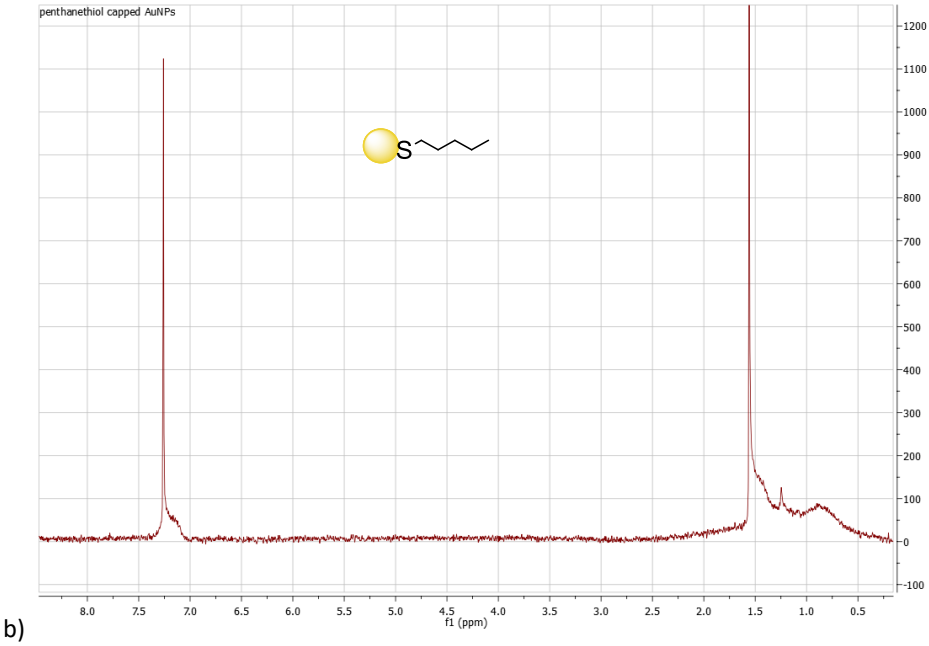

b)

Figure 2.9-a) TEM image b) ^{1}H-NMR spectrum of AuNPs-C5.

The place-exchange reaction, between AuNPs-C5 and ligand **2.19**, was carried on in dry DCM for 3 days, then the solution was concentrated under vacuum and methanol was added in order to promote NPs precipitation and purification. Even if a precipitate was observed, the colored supernatant indicated that not all nanoparticles were able to precipitate, preventing their efficient purification. Indeed, we were able to collect only a minor part of NPs. ^{1}H-NMR analysis , besides to several broad peaks in the lower part of the spectrum, ascribable to gold-bounded penthanethiol, showed typical peaks of the linker (red arrows) together with the maleimide singlet at 6.7 ppm (green arrow) (*Figure 2.10*).

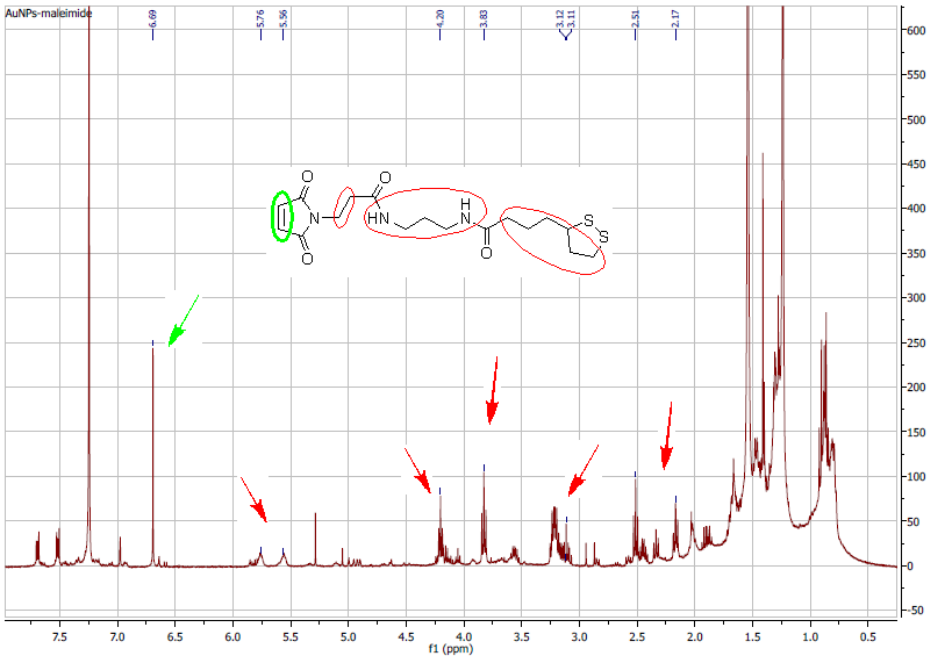

Figure 2.10 – ^{1}H-NMR collected AuNPs sample which underwent place-exchange with the linker.

Anyway, due to the improper purification, we could not certainly affirm that maleimide signal detected by NMR derived only from linker anchored on gold, since some unbounded ligand could be present in the mixture. We decided however to perform the maleimide-thiol click reaction with thiol-functionalized Paclitaxel **2.25**, to verify the real success of the ligand-exchange step. Thus, collected AuNPs were solubilized in dry DMF and stirred in the presence of an excess of both Paclitaxel derivative **2.25** and TEA for 3 hours. Unfortunately, AuNPs purification resulted not trivial and expected signals of Paclitaxel moiety were not showed by ^{1}H-NMR analysis of recovered NPs. As possible cause of these failures, we reasonably hypothesized that the thiol-maleimide click reaction between free penthanethiol desorbed from gold in the exchange step and maleimide could take place in both the exchange step and in the second step, since, due to the ineffective purification, residual free thiols are present in the mixture. In order to validate this hypothesis, place-exchange condition were simulated by stirring ligand **2.19** in the presence of penthanethiol for 3 days in DCM; then TEA was added, thus mimicking click reaction conditions, and the mixture stirred for 3 hours. The product of the click reaction was detected in a very few amount after the place-exchange-like reaction, while it was present as predominant product after TEA addition. These results were supported by ^{1}H-NMR and ESI-MS analysis. On these evidences and considering difficulties emerged in NPs handle, we decided to modify the stoichiometry ratio AuNPs : ligand. Hence, the toluene : DCM 4 : 1 solution of AuNPs-C5 and an excess of derivative **2.26** was stirred for three days. Also in this case the purification step gave some problems. The ^{1}H-NMR spectrum of collected NPs showed characteristic proton compound **2.26** signals despite some differences, in term of chemical shifts, compared

to the unbounded ligand. This result suggested that, perhaps, the place-exchange reaction took place. Unfortunately such AuNPs, resulted unstable, since after one day a change in the solution color from brown to dark red was displayed, indicating NPs coalescence. We reasonably hypothesized that the different final NPs solubility, due to the entire replacement of the native monolayer, was the main cause of both difficult purification and no lasting stability. To overcome these drawbacks, we investigated the feasibility of a partial ligand-exchange, aimed to keep part of the original organic layer, thus maintaining the initial AuNPs solubility and stability. Unfortunately, we were not able to partially replace penthanethiol with the selected ligand.

We thus concluded that the replacement of inert capping agent with the only maleimide-linker **2.19**, as well as the Paclitaxel-linker **2.26**, is not the convenient way for the development of nanosystems with appropriate properties. In particular, a greater stability and a more easy and efficient methodology for removing excess of ligands, were required. For this purpose, after a screening in literature,[72,73,99–102] we found out that the introduction of a water soluble stabilizer as a constituent of the monolayer, could provide water solubility and, as a consequence, providing access to convenient purification techniques, such as dialysis.[103–105] Several ligands with a pendant polar group were described in literature for this purpose, including lipoic acid.[72,73] When using carboxylic acid terminal thiols or disulfides, the water solubility is pH-dependent. Thus, a special care in choosing external environment conditions has to be taken. For the achievement of pH-indipendent water soluble AuNPs, poly(ethylene glycol) (PEG) chain can be used as part of the external shell. The PEG chain can be inserted as central part of the ligand as well as pendant unit directly anchored on the gold core. Besides the ability to provide pH-indipendent water solubility, the affinity of PEG chain for both organic solvent and water render them a very versatile compound. Considering that a proper maleimide linker, as well as the Paclitaxel one, had been already synthesized and keeping in mind the need in a disulfide function as binding site for the gold core, a proper disulfide-PEGylated ligand was prepared through the esterification of 1.2 equiv. of lipoic acid **2.11** with 1 equiv. of poly(ethylene glycol) methyl ether average MW 750 (mPEG 750) **2.27**, in the presence of a catalytic amount of DMAP and 1.2 equiv. of DCC. After 16 hours in dry DCM, the expected product **2.28** was achieved in 97 % yield, without purification (*Scheme 2.15*).

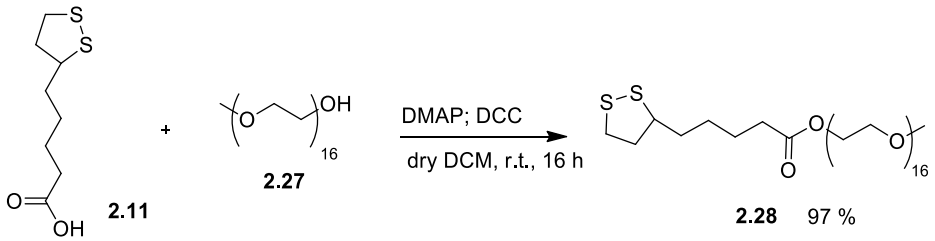

Scheme 2.15 – Synthesis of PEGylated lipoic acid.

In order to verify the ability of this PEG chain length of water solubilizing and stabilizing NPs, AuNPs-C5 were reacted in a place-exchange reaction with an excess of the PEGylated stabilizer **2.28** for 5 days in dry DCM. After removal of the organic solvent,

NPs were solubilized in mQ water, centrifugated to get rid of water non-soluble compounds, and dialyzed (MWCO membrane 3.5 kDa) against 5 L of mQ water for 3 days.[1]H- NMR analysis and FT-IR spectrum showed characteristic peaks of PEGylated ligand, while UV-vis spectrum did not showed differences compare to the one of AuNPs-C5, thus highlighting that gold cores maintained their size during the place-exchange process.

Encouraged by this good result, we focused on the introduction of ligand **2.28** as main component of the AuNPs organic shell, to provide the nanosystem with the required water solubility and stability. Several attempts aimed to find out the suitable PEGylated lipoic acid **2.28**/maleimide-ligand **2.19**/lipoic acid-Paclitaxel **2.26** ratio for the place-exchange reaction were performed (*Table 2.2)*.

Entry	mPEG-lipoic acid **2.28**	Maleimide-lipoic acid linker **2.19**	PTX-lipoic acid **2.26**	Water solubility	DCM solubility
1	100%			X	X
2	75%	25%	-	-	X
3	85%	15%	-	-	X
4	95%	5%	-	partial	X
5	95%	2%	3%	X	X

Table2

While using 75% and 85% of PEGylated ligand **2.28** (**entry 2** and **3** respectively) we were not able to obtain water soluble AuNPs, ligands ratio used in **entry 4** provided NPs with water solubility but no long lasting stability. Indeed, water soluble AuNPs precipitated during the dialysis step. However none agglomeration was displayed and the precipitate can be re-dispersed simply by shaking the sample, thus confirming the good stabilizing ability of the PEGylated ligand. The good result was obtained with ratio reported in **entry 5**. Such AuNPs resulted well soluble and long lasting stable in both organic (*e.g.* DMF, DCM) and aqueous media. AuNPs were dyalized for 4 days against mQ water (MWCO membrane 14kDa) and characterized by NMR analysis, FT-IR, TEM and UV-vis spectroscopy. The ^{1}H-NMR analysis of recovered NPs displayed characteristic protons signals of the three ligands thus confirming the success of the place-exchange. In detail, in blue circles are highlighted typical proton signals of Paclitaxel; the singlet at 6.7 ppm, highlighted in green, is the characteristic peak of maleimide protons while the intense peak at 3.6 ppm and the triplet at 3.8 ppm, indicated by red arrows, showed the presence of the PEG chain. Integral values of each characteristic peak allowed a rough determination of the ligands content ratio. PEGylated lipoic acid **2.28**/maleimide-ligand **2.19**/lipoic acid-Paclitaxel **2.26** resulted in a 81%, 1% and 18% respectively (*Figure 2.11*).

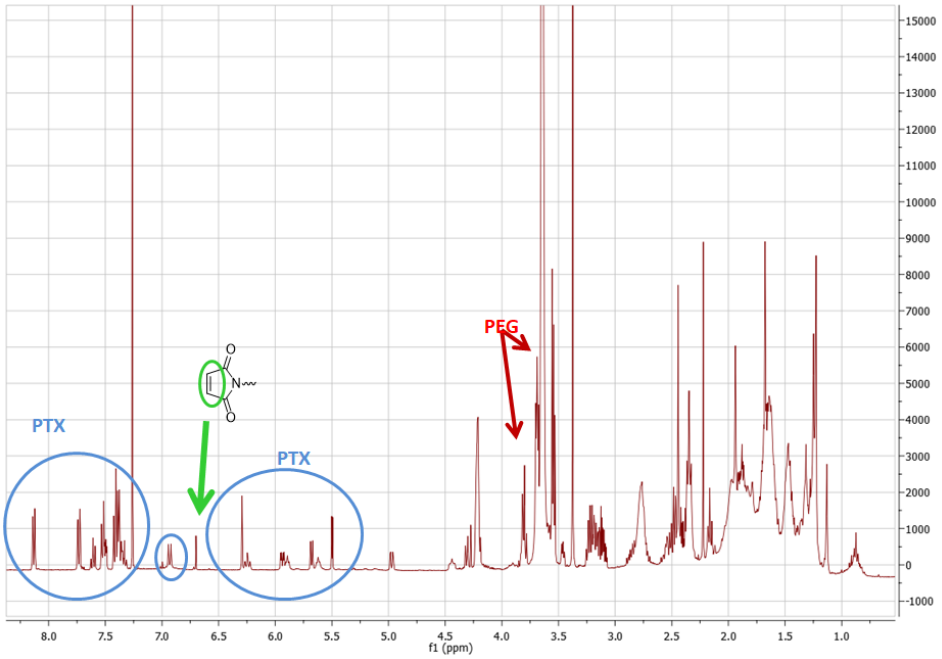

Figure 2.11 – H-NMR analysis of AuNPs capped with mPEG-750 ligand, maleimide-ligand and Paclitaxel ligand.

FT-IR spectrum clearly showed typical peaks of PEGylated ligand, while signal ascribable to other ligands are not very intense.

Gold cores were characterized by TEM analysis and UV-vis spectroscopy, which demonstrated the well preserved size of gold clusters. Indeed, none difference between TEM and UV analysis of AuNPs-C5 and the final nanosystem was highlighted (*Figure 2.12*).

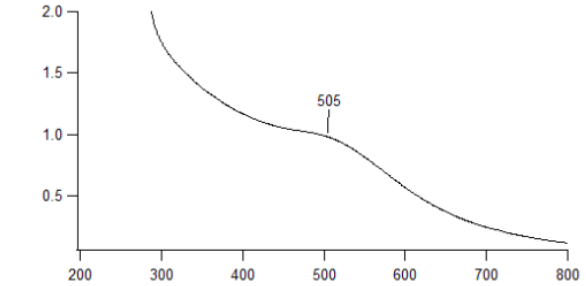

a)

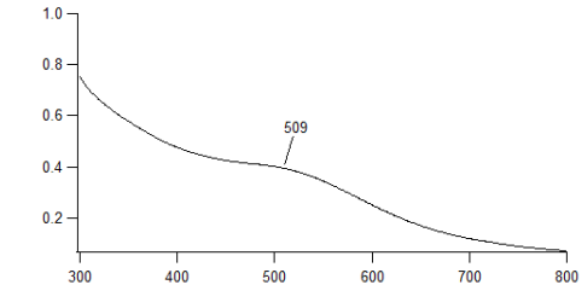

b)

c)

Figure 2.12– a) UV-vis spectrum of AuNPs-C5 compare to *b)* UV-vis spectrum of AuNPs capped with mPEG-lipoic acid : Paclitaxel-lipoic acid : maleimide-lipoic acid in 95 : 3 : 2 ratio; *c)* TEM imagine of final nanoparticles.

2.8 NT4 conjugation of maleimide-AuNPs-PTX

Decorated AuNPs were conjugated to the NT4 peptide in the Luisa Bracci's research group, at the University of Siena. The general thiol-maleimide procedure, previously optimized for the Paclitaxel-NT4 conjugation, was adapted to the gold nanosystems. Thus, AuNPs were dissolved in acetonitrile:phosphate buffered saline (PBS) 1:3 and then reacted with NT4. The mixture was stirred for 1 hour at r.t., then acetonitrile was evaporated and the AuNPs PBS solution was dialyzed for 72 hours, at 4 °C to afford purified NT4-AuNPs-PTX.

2.9 In vitro binding activity of NT4-AuNPs-PTX

Binding activity of NT4-AuNPs-PTX was evaluated on human colon adenocarcinoma cell lines (HT-29) and monitored by TEM. AuNPs-PTX, not decorated with the peptide, were used as reference.

AuNPs were diluted in the culture medium and incubated with the HT-29 cells at 37 °C. The binding activity was evaluated after 30 minutes of incubation. Thus, samples were washed and TEM images were recorded (*Figure 2.13)*.

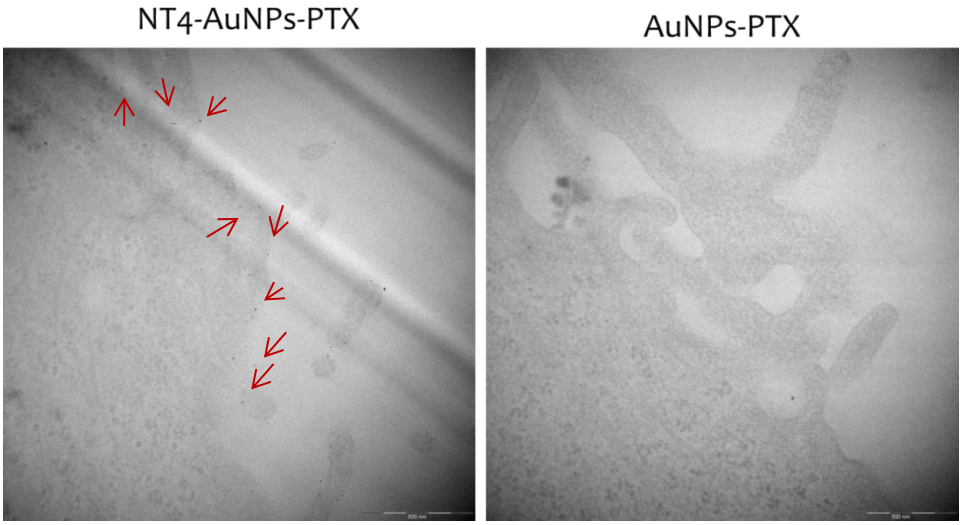

Figure 2.13- Binding assay on a) NT4-AuNPs-PTX and b) AuNPs-PTX, not decorated with the peptide. Red arrows highlighted some AuNPs on the cell membrane and intracellularly.

AuNPs localization on cell membrane was not detected for AuNPs-PTX, not decorated with NT4. Otherwise, NT4-AuNPs-PTX showed a preferential accumulation either on cell

membrane and intracellularly. This result, even if preliminarily, demonstrated the targeting ability of NT4 when bounded to AuNPs, and a tendency of such system to be internalized within the cell. This likely depends not only on the good targeting activity of the NT4, but also to the suitable size of the nanosystem, which could facilitate the process of cellular internalization. However, further investigations will be carried out to confirm this outcome. *In vitro* cytotoxicity will be evaluated and i*n vivo* binding ability and cytotoxicity will be performed, compare to AuNPs-PTX not conjugated with the peptide.

In conclusion, after several unsuccessful attempts, we developed a convenient method for the preparation of water soluble AuNPs, with an average gold core size in the range 2-5 nm and with a good monodispersity. Gold cores characteristics were well preserved during the surface modification of NPs, as have been demonstrated by TEM and UV analysis of both AuNPs-C5 and maleimide-AuNPs-PTX. The final monolayer inserted on gold surface contains a certain amount of PEGylated ligand, maleimide and Paclitaxel and the nanosystem resulted stable in several different type of solvent (*e.g.* organic and aqueous solvents). Decorated AuNPs were targeted with the NT4 peptide and a preliminary evaluation of the binding activity was *in vitro* performed. TEM images recorded showed a good binding activity besides to the tendency of targeted nanosystems to be internalized within the cell. In order to validate this prominent outcome, further binding assays, *i.e. in vivo* binding tests, will be carried out and the cytotoxicity will be *in vitro* and *in vivo* evaluated.

3. Targeted Multi-Paclitaxel Delivery Systems

3.1 Synthesis of multi-valent linkers

The feasibility of providing the targeting peptide NT4 with a great number of drug molecules, through the conjugation with a highly drug-functionalized nanoparticle, (AuNPs as well as QDs) certainly represents an important evolution of the targeted pro-drug able to bear only one therapeutic unit since it could allow to maximise the targeting potential of the peptide. However, the exactly quantification of drug (*i.e.* Paclitaxel) loaded on the nanoparticle is not trivial. This represents a limit, considering the importance of understanding the relationship of drug delivery system cytotoxicity with different stoichiometry of vectoring peptide / vectored drug.

Aimed to face this issue, we decided to develop different targeted systems, able to bear a defined number of Paclitaxel molecules to thus evaluate the role of vectored drug stoichiometry. In order to avoid differences caused by the chemical nature of the linker, a common spacer, obviously provided with a variable (1-3) number of drugs' binding sites, was designed. Additionally, we decided to exploit orthogonal reactions for the coupling with the targeting and the therapeutic units. The thiol-maleimide Michael reaction, between the thiol group of the cysteine residue on MAP-NT and a maleimide moiety, was selected for the coupling of the linker with the targeting unit. Hence, a maleimide residue has to be introduced on the linker moiety. At the same time, the highly efficient Huisgen click reaction, involving a terminal alkyne and an azide, was chosen as suitable process for the coupling (or multi-coupling) of the linker with the therapeutic unit(s). The Huisgen reaction, *i.e*. Copper(I)-catalyzed Azide-Alkyne Cycloaddition (CuAAC), is a regioselective 1,3-dipolar cycloaddition requiring a copper(I) salt as catalyst. The latter can be generated *in situ* by reduction of a copper(II) salt with a proper reducing agent. The 1,2,3-triazole derivatives formed by click reactions are commonly very stable to both metabolic and chemical degradations thus perfectly suitable for *in vivo* applications.[106]

The choice of a thiol-maleimide reaction together with the CuAAC procedure required the synthesis of a maleimide linker bearing 1, 2 or 3 terminal alkyne residues while, reasonably, a single azido function had to be installed on the skeleton of Paclitaxel. The designed linkers are schematized in *Figure 3.1*.

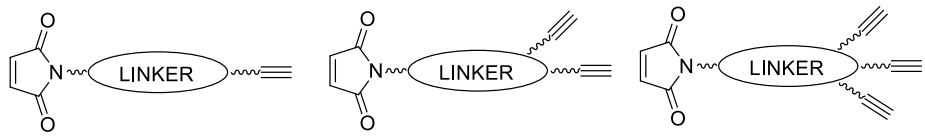

Figure 3.1 - Designed linkers for MAP-NT delivering of 1, 2 or 3 drug units.

A special care in the Paclitaxel functionalization has to be taken, in consideration of the need of an *in vivo* hydrolysable ester bond in the drug proximity. Thus, 1.0 equiv. of commercial 6-bromo hexanoic **3.1** acid was reacted with 3 .0 equiv. of NaN_3 in dry DMF for 6 hours at 85 °C. [107] After purification, the corresponding azido derivative **3.2,** obtained in 47% yield was esterified with the OH on the 2' position of Paclitaxel **3.3** in the presence of 0.2 equiv. of DMAP and 1.2 equiv. of DCC in dry DCM for 24 hours at reflux.[108] The azido functionalized Paclitaxel **3.4** was obtained after purification by column chromatography in 85 % yield (*Scheme* 3.*1*).

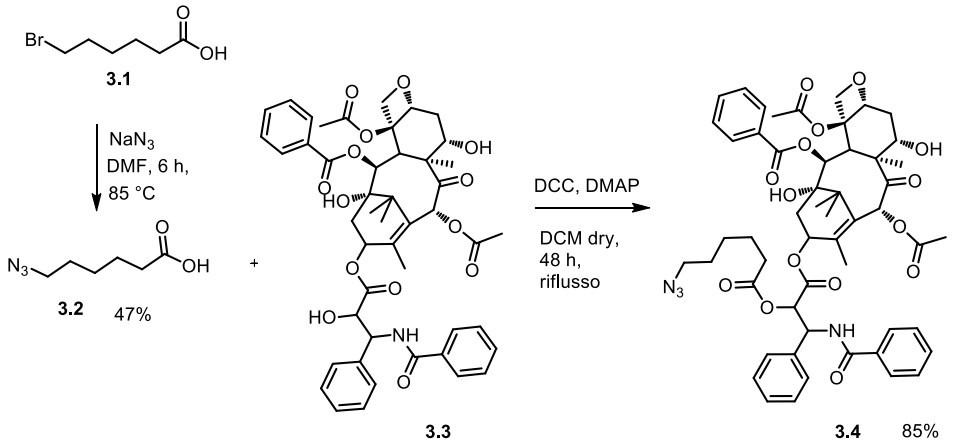

Scheme 3.1 – Azido –functionalization of Paclitaxel.

The product was characterized by ^{1}H-NMR analysis. The success of the coupling was demonstrated by i) the deshielding of the doublet relative to the H on the 2' position, from 4.8 to 5.6 ppm (highlighted in red); ii) the integral ratio 1:2 between this proton signal and the triplet relative to the methylene in α position to the azide group (highlighted in green) (*Figure 3.2*).

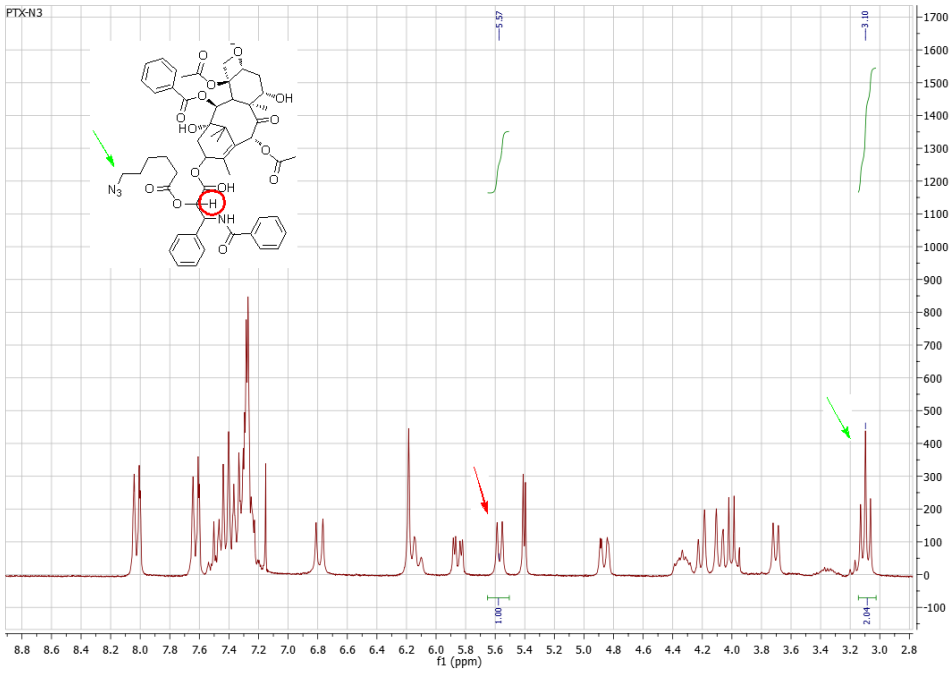

Figure 3.2

With the azido-Paclitaxel in hand, we focused on the development of a general procedure for the achievement of the three designed linkers. Attempts of linkers synthesis started with the oxidation of commercially available 11-bromo-1-undecanol **3.5**. The reaction was performed with 1.5 equiv. of pyridinium chlorochromate (PCC) in dry DCM, under a N_2 atmosphere, for 6 hours at r.t., to give the corresponding aldehyde **3.6**, in 89% yield, used in the next step without purification. The aldehyde **3.6** was reacted with 7.5 equiv. of 37% aqueous formaldehyde and 1 equiv. of KOH in 50% aqueous EtOH, initially for 24 hours at r.t., then for 4 hours at 50 °C. Under these conditions, triol **3.7** was obtained, after purification by flash column chromatography, in 44% yield (*Scheme 3.2*).[109]

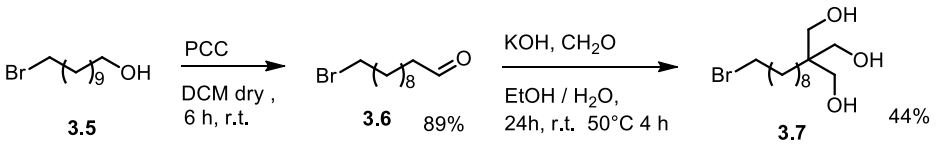

Scheme 3.2- Synthesis of the derivative **7**.

Primary bromide of **3.7** was then reacted with 1.1 equiv. of potassium phthalimide in dry DMF for 19 hours at 90 °C. The corresponding N-alkylphthalimide **3.8** was obtained without purification in 64% yield[110] (*Scheme 3.3*).

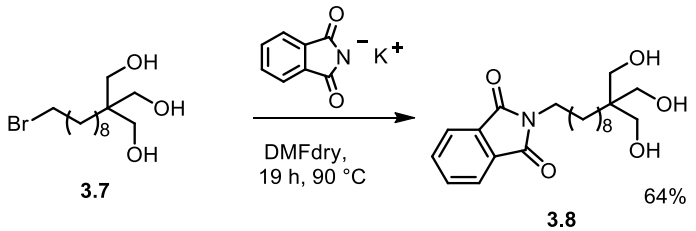

Scheme 3.3- Introduction of phthalimide moiety.

In the next step a selective mono-, bis- and tris- propargylation was attempted under different propargyl bromide/base/**3.8** ratio and reaction conditions. Initially, we tried to isolate the tris-propargyl derivative, but independently upon the amount of propargyl bromide, and the base used (sodium carbonate or NaOH), we were able to obtain the desired O-alkylation.

Better results were obtained using 5.0 equiv. of NaH as base and 5.0 equiv. of propargyl bromide in dry DMF for 24 hours, at 90 °C. Under these conditions, after purification by column chromatography, the bis-propargyl derivative **3.9** was isolated as the major product (25% yield) while the tris- substituted derivative **3.10** was obtained in traces (*Scheme 3.4*).

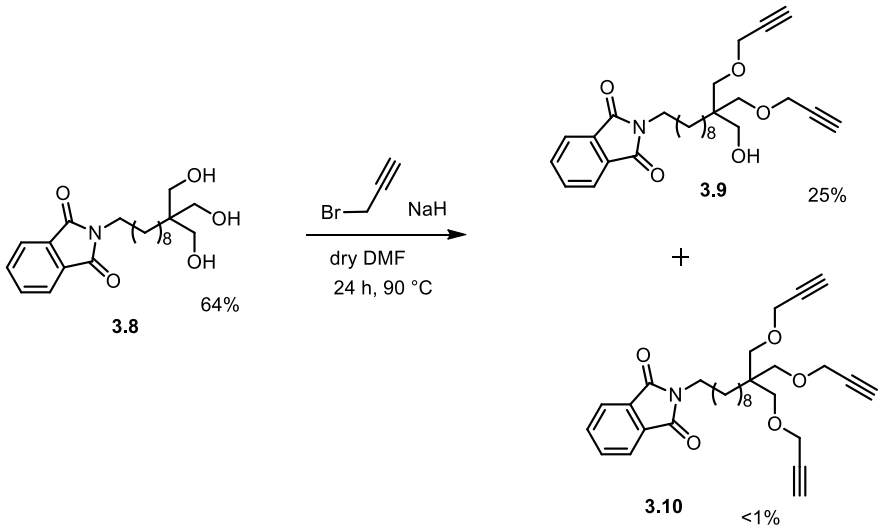

Scheme 3.4

These poor results suggested to modify the structure of the linker since to have a more nucleophilic hydroxy derivative. Thus we selected commercial ethyl gallate **3.11** as new starting material for the preparation of the linker(s). Also in this case, we tried to achieve a selective mono-, bis-, or tris- propargylation reaction by simply modulating the reaction condition of propargylation (*Scheme 3.5*).

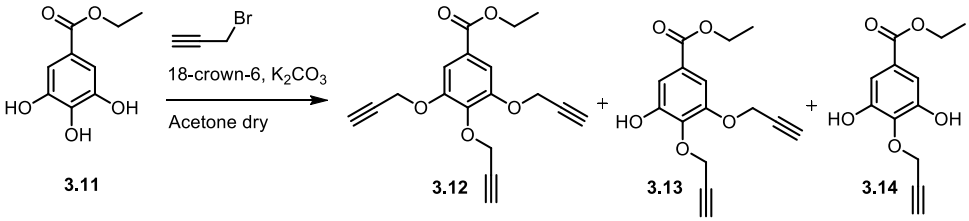

Scheme 3.5 – Possible propargylation products.

According to literature,[111] **3.11** was reacted with propargyl bromide in the presence of K_2CO_3 as base and 18-crown-6. A summary of the reactions performed is reported in *Table 3.1*.

Entry	Propargyl bromide (equiv.)	K_2CO_3 (equiv.)	18-cown-6 (equiv.)	Conditions	**3.12** (yield)	**3.13** (yield)	**3.14** (yield)
1	0.9	0.43	0.002	7h, reflux	trace	trace	26%
2	3.1	0.43	0.004	24h, reflux	-	trace	42%
3	0.9	0.9	0.001	19h, reflux	trace	3%	19%
4	6.0	6.0	0.004	18h, reflux	quant.	-	-

Table 3.1- Attempts of S_N2 reaction on ethyl gallate.

Mono-derivative **3.14** was obtained in acceptable yield when using 0.43 equiv. of K_2CO_3 (**Entry 2-3**). The selective alkylation of the 4-OH group was easily demonstrated by ^{1}H-NMR based on the symmetry of the isolated mono-propargyl derivative. Despite the several attempts we were unable to settle up suitable condition for the selective preparation of **3.12-3.14** that, moreover, are very difficultly separated by chromatography. Thus, we moved to consider three different starting materials ensuring a very similar structure for the final linker. In particular, commercial hydroxy esters or acid **3.11**, **3.15** and **3.16** showed in *Figure 3.3* were considered.

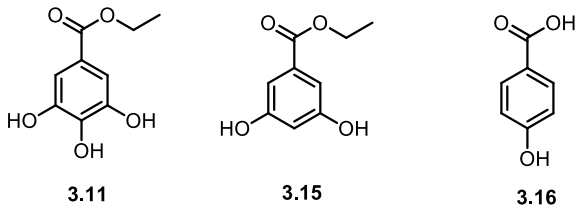

Figure 3.3- Starting materials selected for achievement of propargyl-linkers.

In the first attempt, the synthesis of the tris-propargyl derivative **3.12** was carried out. According to the literature,[111] 1.0 equiv. of ethyl gallate **3.11** was reacted with 6.0 equiv. of propargyl bromide, 6.0 equiv. of K_2CO_3 and 0.004 equiv. of 18-cown-6 in dry acetone at reflux for 18 hours. The desired derivative **3.12** was obtained without purification in quantitative yield.
The same procedure was also applied to bis-phenol **3.15** to give derivative **3.17** in 96% yield (*Schema 3.6*).

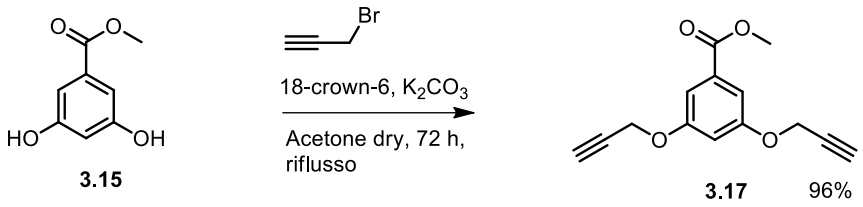

Scheme 3.6- Synthesis of bis-propargylate derivative **3.17**.

Regarding the synthesis of the mono-propargyl derivative, commercial available 4-hydroxybenzoic acid **3.16** was esterified under classical Fisher conditions, to give quantitative yield of ester **3.18** that, in turn, was reacted under the above reported conditions allowing the isolation of propargyl ether **3.19**, in quantitative yield (*Scheme 3.7*).

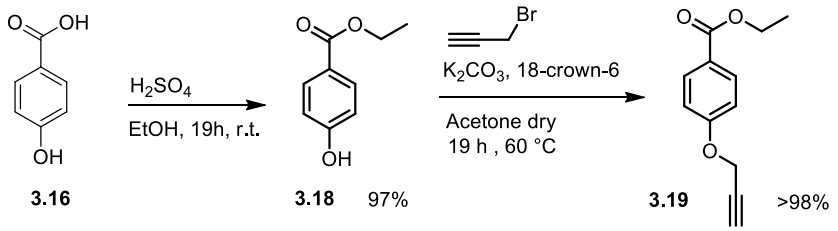

Scheme 3.7- Synthesis of mono-propargyl derivative **3.19**.

The further step was the introduction of the maleimide moiety. The synthetic methodology was optimized using the tris-propargyl derivative **3.12** as a model. The first procedure we envisaged was a nucleophilic substitution using maleimide as nucleophile and transforming benzylic position of **3.12** in a suitable electrophile. So, ester **3.12** was reduced with 5.0 equiv. of $LiAlH_4$ for 19 hours in dry THF to give the corresponding primary alcohol **3.20**, in 95% yield. Alcohol **3.20** was transformed in primary chloro derivative **3.21** using 1.2 equiv. of PPh_3 and 10.0 equiv. of CCl_4 in refluxing dry THF for 40 hours.[3] Under these conditions, chloride **3.21** was obtained, after purification by flash column chromatography, in 32% yield (*Scheme 3.8-method a*). An excellent improvement in the yield of **3.21** (91 %) was achieved carrying out the

chlorination reaction with 2.4 equiv. of $SOCl_2$ and 0.1 equiv. of pyridine in dry Et_2O for 3 hours at reflux (*Scheme 3.8-method b*).

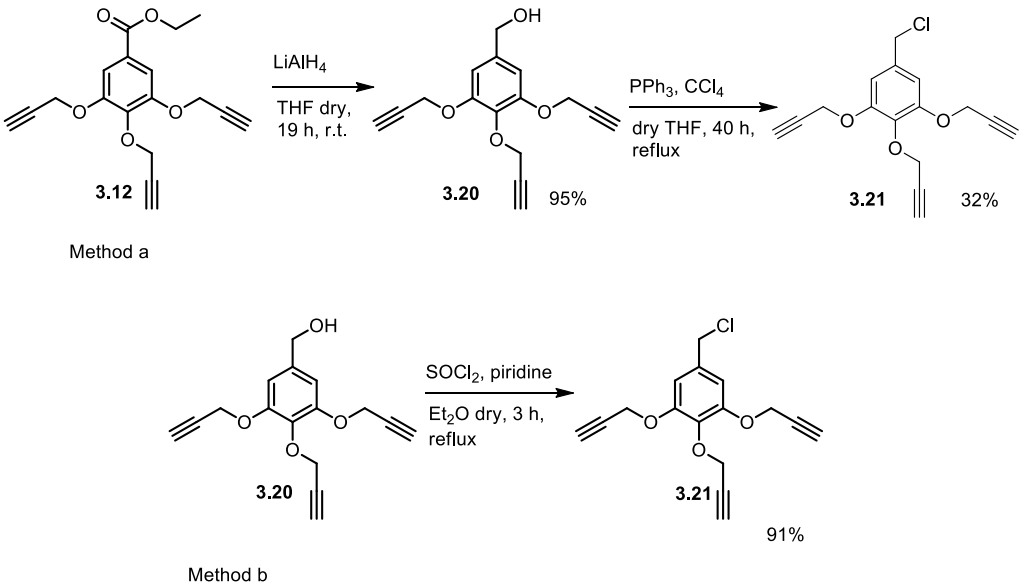

Scheme 3.8

The nucleophilic substitution between chloride **3.21** and maleimide was performed under several different conditions, without any success as summarized in *Table 3.2.*

Entry	**3.21** (equiv.)	Maleimide (equiv.)	Base (equiv.)	Solvent	Additive (equiv.)	Conditions	Results
1	2.0	1.0	K_2CO_3	Acetone	-	3 days, reflux	-
2	2.0	1.0	K_2CO_3	Acetone	-	24h, 50 °C	-
3	2.0	1.0	K_2CO_3	CH_3CN	-	24h, 50 °C	-
4	3.0	1.0		DMF	-	r.t.	-
5	3.0	1.0		DMF	-	24h, 30 °C	-
6	1.0	1.3	K_2CO_3	DMF	-	80 °C	-
7	1.0	2.0	K_2CO_3	Dry CH_3CN	-	7days, reflux	-

8	2.0	3.0	K_2CO_3	Dry CH_3CN	-	4days, 50 °C	-
9	2.0	1.0	K_2CO_3	Acetone	KI 1.2 equiv.	18h reflux	-
10	2.0	1.0	K_2CO_3	CH_3CN	KI 1.2 equiv.	18h 55°C	-
11	1.0	2.0	K_2CO_3	Acetone	KI 2.0 equiv.	18h reflux	-
12	1.0	2.0	K_2CO_3	CH_3CN	KI 2.0 equiv.	18h 55°C	-

Table 3.2- summary of attempts for nucleophilic substitution.

Despite these disappointing results, we kept the original idea of using chloride **3.21** as a suitable electrophile that was reacted with 1.2 equiv. of potassium phthalimide and 0.1 equiv. of 18-crown-6 in dry toluene, for 18 hours, at 100 °C.[112] The good reactivity showed by potassium phthalimide under nucleophilic substitution conditions with the benzylchloride **3.21**, is a peculiar result considering the ineffective of the same reaction when using maleimide. The N-alkyl phthalimide derivative **3.22** was isolated in 74% yield, after purification by flash column chromatography. In the next step, **3.22** was reacted with 2.0 equiv. of N_2H_4 in EtOH for 2 hours, at 60 °C to liberate primary amine **3.23** which, in turn, was reacted with 1.0 equiv. of maleic anhydride in AcOH at 140 °C. After 6 hours the expected maleimide derivative **3.24** was isolated after purification by flash column chromatography, in 12% yield over two steps[110,113] (*Scheme 3.9*).

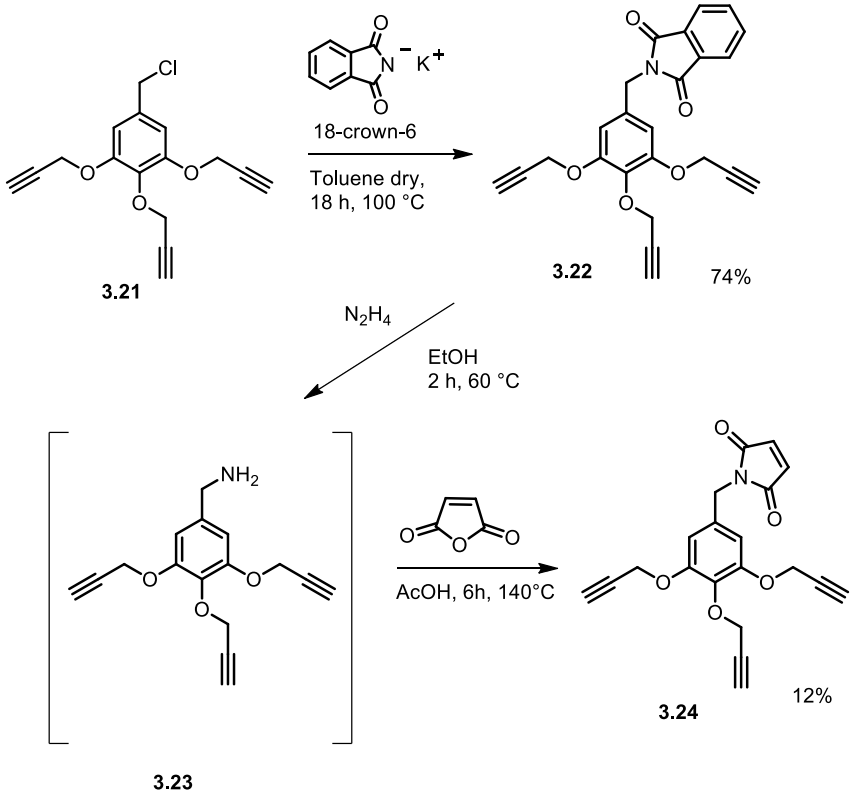

*Scheme 3.9- L*inker synthesis procedure involving Gabriel's reaction.

Considering the low yield and the number of steps required to get **3.24**, we decided to consider other synthetic strategies like, for example, the possibility of directly using benzyl alcohol **3.20** in a Mitsunobu reaction with maleimide, thus avoiding all the steps required for the synthesis of chloride **3.21** and amine **3.23**.
Thus, alcohol **3.20** was reacted under classic Mitsunobu condition: 1.0 equiv. of PPh_3 and 1.0 equiv. of DIAD with 1.0 equiv. of maleimide in dry THF, for 48 hours at reflux, to give desired product **3.24** in 12% yield (*Scheme 3.10*).

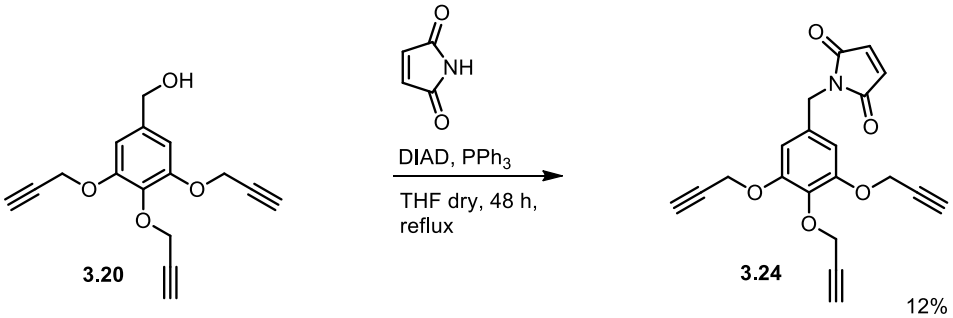

Scheme 3.10- Mitsunobu step.

Several reaction conditions were tested to improve the Mitsunobu step, without any success (*Table 3.*3).

Entry	**3.20** (equiv.)	Maleimide (equiv.)	PPH_3 (equiv.)	DIAD (equiv.)	Conditions	**3.24** (yield)
1	1.1	1.0	1.0	1.0	dry THF, 72 h, r.t.	6%
3	1.1	1.0	1.0	1.0	dry THF, 16 h, reflux	5%
2	1.0	1.5	1.5	1.5	dry THF, 19 h at r.t., then 28 h at 50 °C	3%

Table 3.3 – Attempt of Mitsunobu reaction optimization.

A significant further improvement of the procedure was obtained performing the Mitsunobu reaction in a microwave reactor, at 110 °C for 1.5 hours. Under these conditions linker **3.24** was isolated in comparable yield (22%) but in very shorter reaction times.
The same procedure was applied to the mono- and bis- propargyl derivatives **3.19** and **3.17**, to achieve the corresponding maleimide propargyl compounds **3.25** and **3.26** in 21% and 29% yield respectively as reported in *Scheme 3.11*.

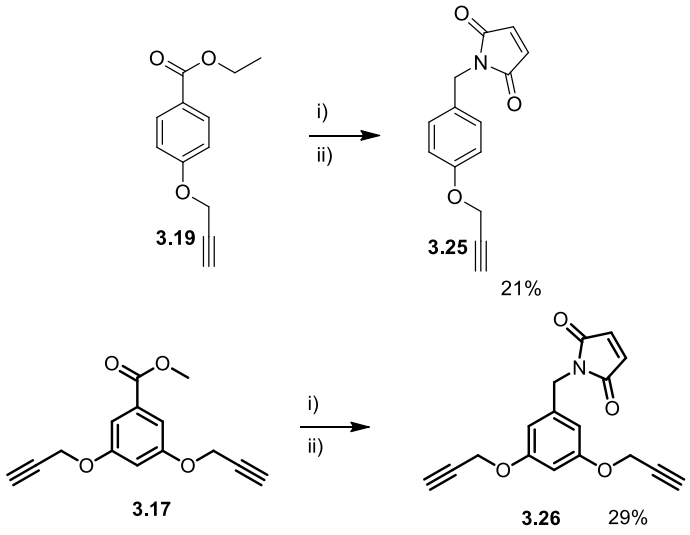

Scheme 3.11- i) $LiAlH_4$, dry THF, 19-24h, r.t.: ii) DIAD, PPh_3, dry THF, MW 45-80 min., 120 °C

3.2 Click reaction: Synthesis of maleimide-Paclitaxel adducts

The final step towards the synthesis of Paclitaxel-maleimide conjugates required the Huisgen click reaction between propargyl derivatives **3.24**-**3.26** and the azido-functionalized Paclitaxel **3.4**. The Huisgen reaction could be performed in different type of solvents using commercially available Cu(I) salts as catalyst, but the reaction works better using a mixture of a Cu(II) salt together with a reducing agent. [108,114,115] We decided to use catalytic amount of $CuSO_4$ and sodium ascorbate as the source of Cu(I) and a 4:1 mixture of DMF : water as solvent. These conditions were investigated in a model reaction between 2.0 equiv. of alkyne **3.19** and 1.0 equiv. of Paclitaxel-2'-6-azido-hexanoate **3.4** which were reacted at r.t. After 30 hours, the corresponding 1,2,3-triazole conjugate **3.27** was isolated in 48% yield, after chromatography purification (*Scheme 3.12*).

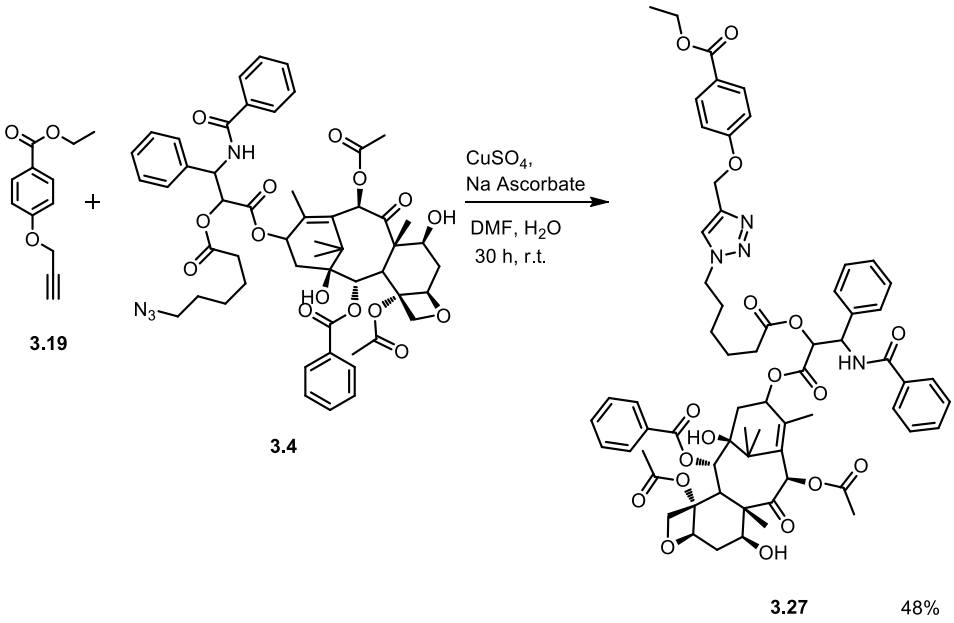

3.19 **3.4** **3.27** 48%

Scheme 3.12- Model click reaction.

With this result in hand, we repeated the click reaction using alkyne linker **3.25** and, satisfactorily, the mono-Paclitaxel-maleimide adduct **3.28** was isolated in 42% yield (*Scheme 3.13*).

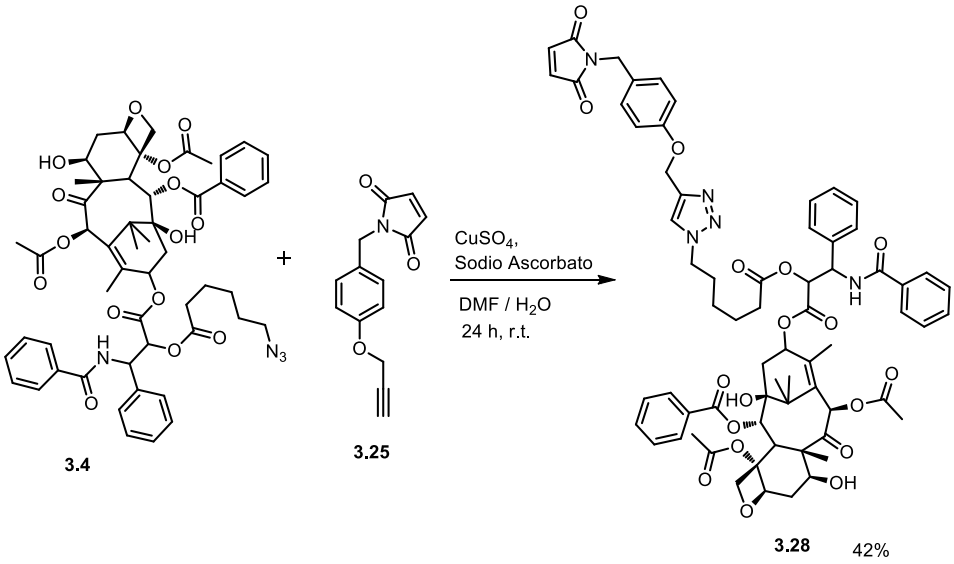

Scheme 3.13- Synthesis of maleimide-Paclitaxel conjugate **3.28**.

The structure of the expected product was confirmed by ^{1}H-NMR analysis (*Figure 3.4-a*) which showed: i) the characteristic peak of the methylene group in α position to 1,2,3-triazole ring (around 4.3 ppm; highlighted in red) deshielded compare to the methylene-azido protons signal of the starting derivative **3.4** (3.21 ppm), with an integral value for two protons; ii) the singlet at 6.7 ppm , relative to maleimide protons, with an integral value for two protons (highlighted in green); iii) The integral ratio between aforementioned peaks and other signal's integrals is coherent with the structure of **3.28**. ESI-MS analysis supported this data since the peak corresponding to $[M + Na^{+}]^{+}$ was showed (*Figure 3.4-b*).

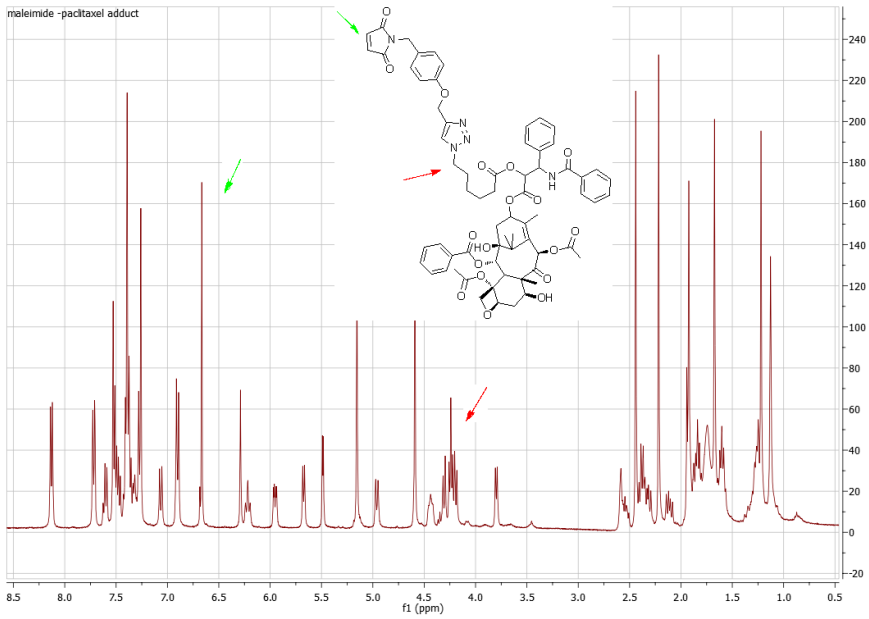

a)

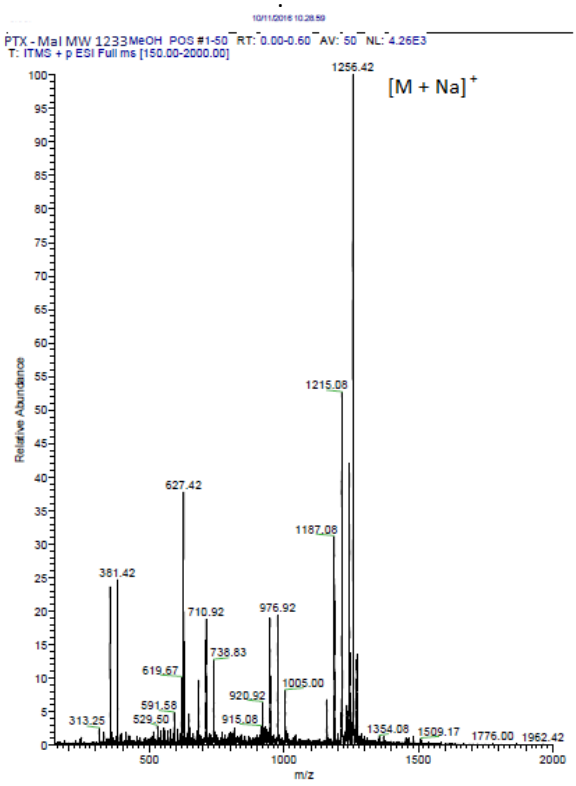

b)

Figure 3.4 –a) ^{1}H-NMR spectrum and b) ESI-MS of maleimide-mono Paclitaxel derivative **3.28**.

Unexpectedly, the reaction failed when repeated identically on alkyne linker **3.26** that allowed the isolation of expected bis-Paclitaxel-maleimide adduct **3.29** in roughly 5% yield, while the products of the mono-click were isolated as major product (*Scheme 3.14*).

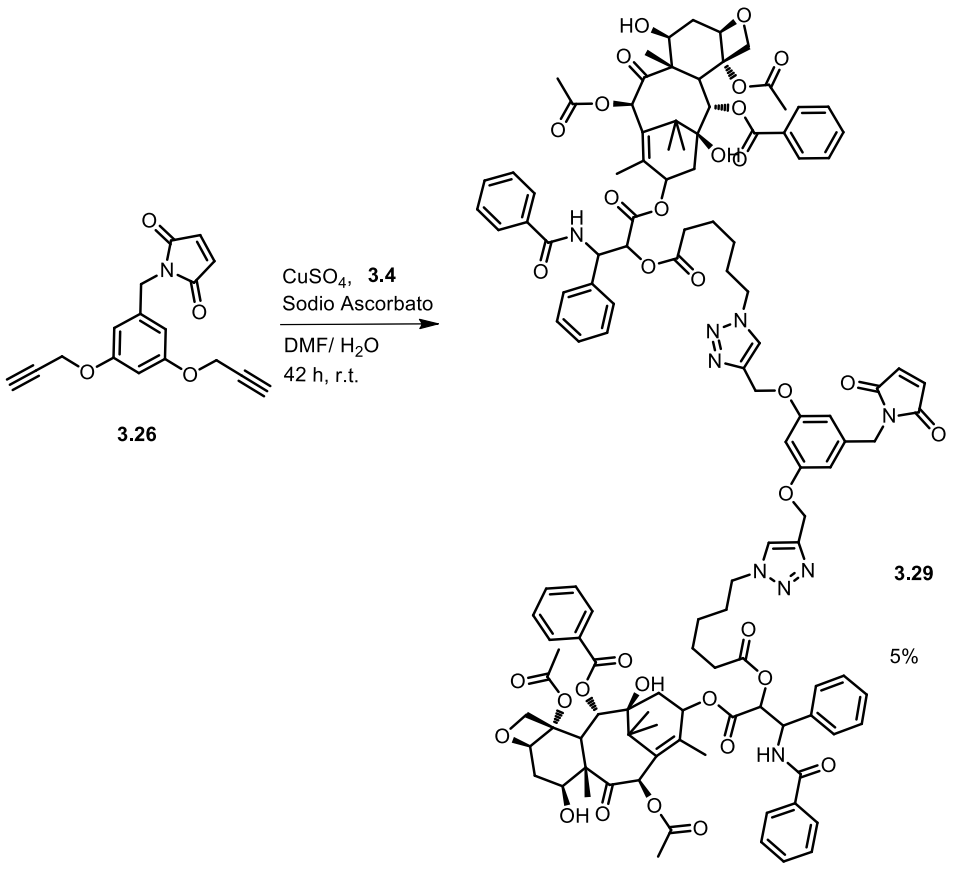

*Scheme 3.14- B*is-alkyne-Paclitaxel conjugation.

We considered that, possibly, the remarkable steric hindrance of Paclitaxel-2'-6-azido-hexanoate **3.4** prevented its double insertion on the linker skeleton. Thus we tested the reactivity of derivative **3.26** with the 'steric non-demanding' azido derivative **3.2**. However, despite the different attempts carried out, even under forced reaction conditions, also in this case we were unable to detect the formation of any CuAAC triazole product (*Scheme 3.15*), while the unreacted starting materials were recovered.

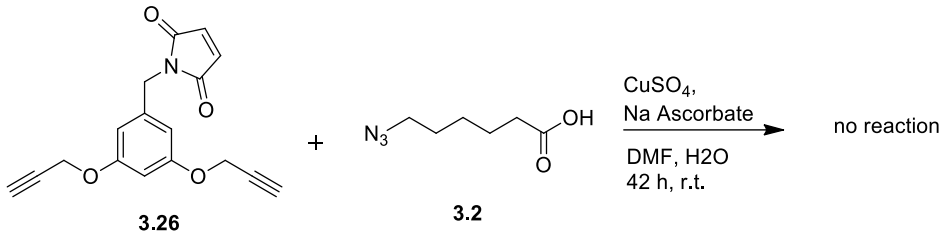

3.26 3.2

Scheme 3.15- Model bis-click reaction on derivative **3.26**.

The lack of reactivity of 1,2,3 tri-substitutes derivative **3.26** under CuAAC conditions is a peculiar result with no evident rationals. In the hope to overcome this problem we decided to prepare a bis-alkyne with a different substitution pattern on the ring. Thus, commercial available ethyl 3,4-dihydroxy-benzoate **3.30** was propargylated under the previous reported conditions to give the bis-alkyne **3.31** in quantitative yield.
Bis-alkyne derivative **3.31** was then used in a model CuAAC test with ethyl 6-azido hexanoate **3.32** under the reaction conditions that failed using **3.25.** Indeed, bis-triazole derivative **3.33**, deriving from the coupling of alkyne **3.31** with azide **3.32**, was isolated in 48% yield (*Scheme 3.16*).

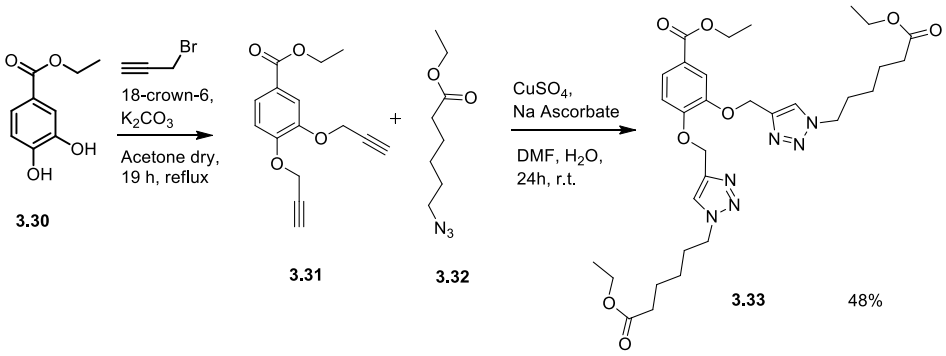

3.30 3.31 3.32 3.33

Scheme 3.16.

Encouraged by this result, the bis-linker maleimide derivative **3.34** was synthesized by reduction of the ester moiety of **3.31** followed by Mitsunobu reaction with maleimide, as reported in *Scheme 3.17*.

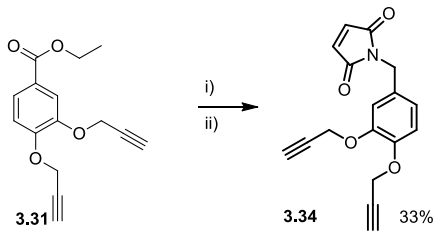

3.31 3.34

Scheme 3.17- i) $LiAlH_4$, dry THF, 19-24h, r.t.: ii) DIAD, PPh_3, dry THF, MW 45-80 min., 120 °C

Satisfactorily, 3,4-bispropargyl ether **3.34** reacted with 2.0 equiv. of azido-Paclitaxel **3.4** under the previous described CuAAC condition and after stirring for 19 hours at 50 °C bis-adduct **3.35** was isolated by flash column chromatography in 23% yield (*Scheme 3.18*).

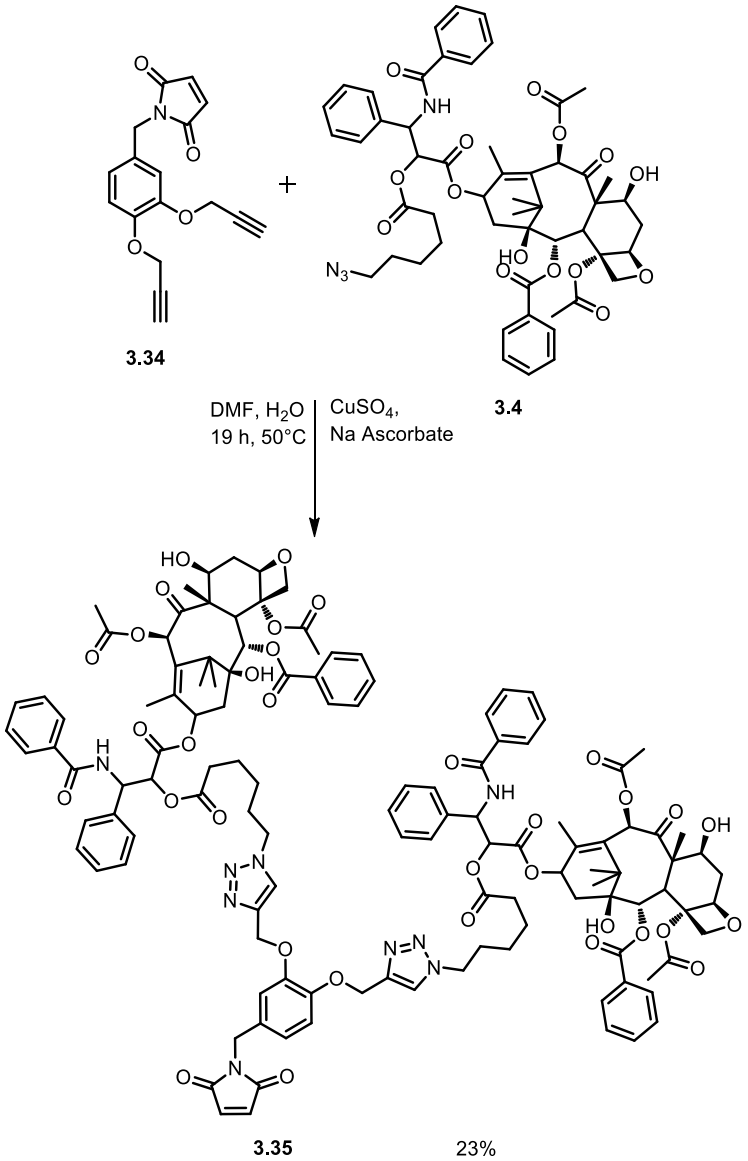

Scheme 3.18-Synthesis of maleimide-bis-Paclitaxel adduct.

The bis-adduct was characterized by ^{1}H-NMR and ESI-MS analysis. The NMR spectrum showed similar peaks to that observed for the derivative **3.28**, with integral values

coherent with the bis-functionalization. The result was confirmed by mass spectroscopy whose spectrum displayed the peak corresponding to $[M + Na^+]^+$ and $[M + H^+]^+$. The molecular formula extrapolated from the HR ESI-MS analysis, $C_{123}H_{135}O_{34}N_9$, is in accordance to the theoretical one (*Figure 3.5*).

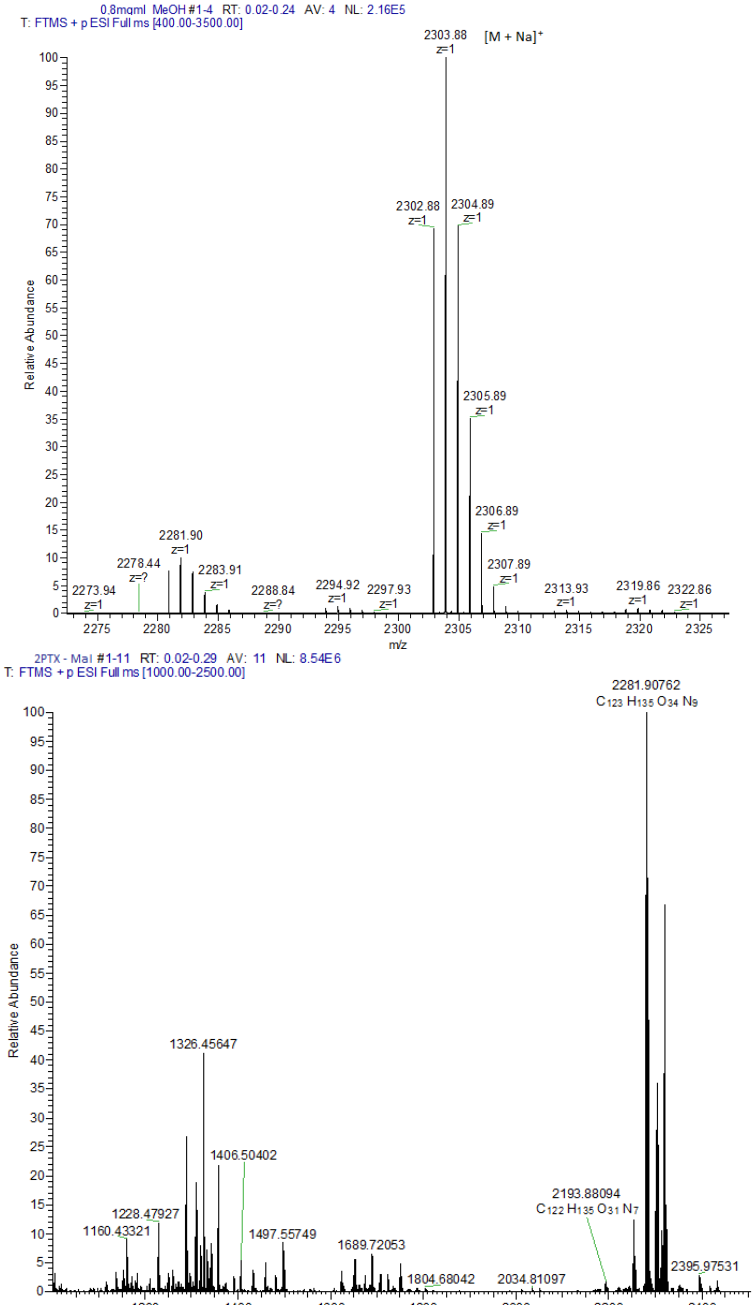

Figure 3.5- ESI-MS and HR ESI-MS spectra of derivative **3.35**.

As for mono- and bis- derivatives **3.25** and **3.34**, the click reaction was performed for tris-alkyne-maleimide linker **3.24**. The corresponding tris-Paclitaxel adduct **3.36** was isolated, after purification by flash column chromatography, in 16% yield (*Scheme 3.19*).

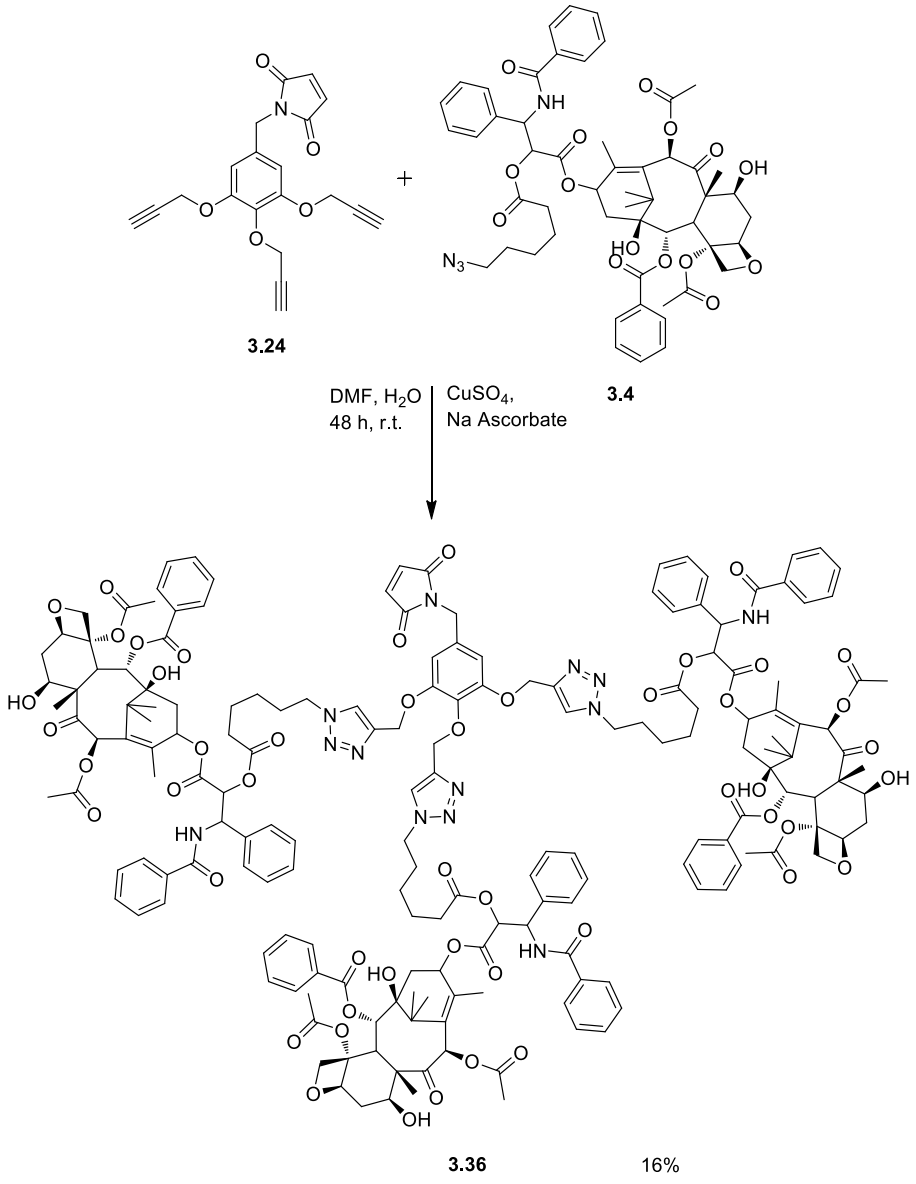

Scheme 3.19- Synthesis of tris-Paclitaxel maleimide conjuagate.

^{1}H-NMR analysis confirmed the tris substitution of linker **3.24**, since characteristic peaks of maleimide-Paclitaxel adducts, whose integrals are in agreement with the tri-functionalization, were showed. The HR ESI-MS spectroscopy showed peaks corresponding to $[M + 2H^{+}]^{2+}$, $[M + Na^{+} + H^{+}]^{2+}$, $[M + 2Na^{+}]^{2+}$, and values of mass recorded were consistent with the theoretical molecular formula, $C_{179}H_{197}O_{50}N_{13}$ (*Figure 3.6*).

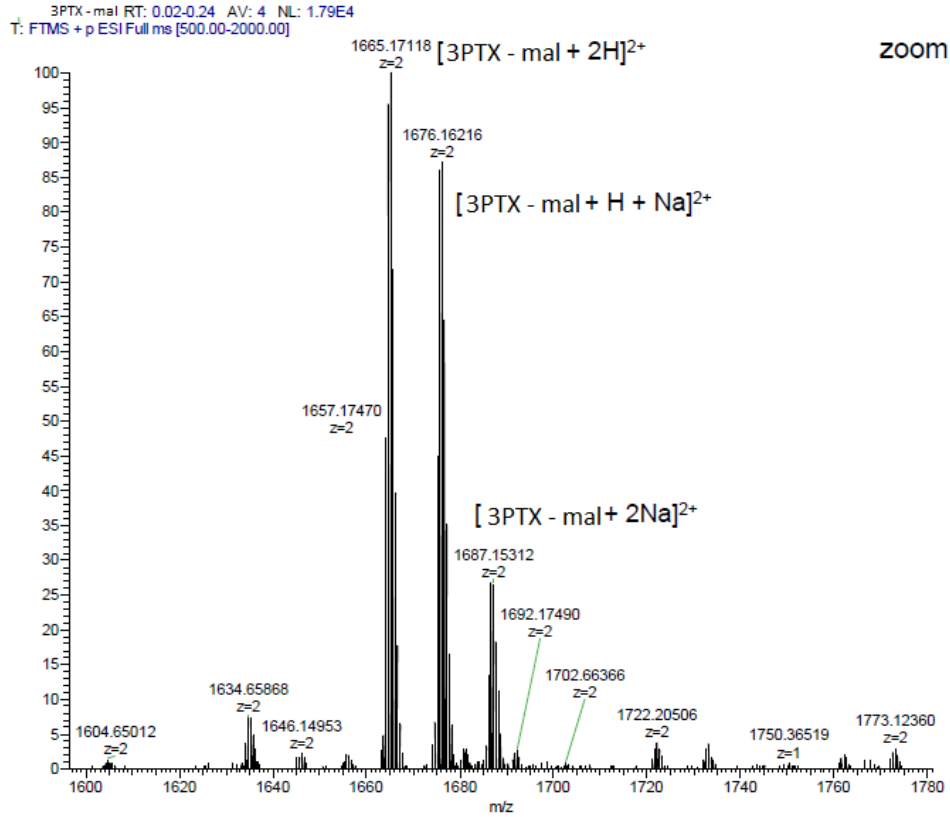

Figure 3.6– HR-ESI-MS analysis of tris Paclitaxel-maleimide adduct.

3.3 NT4-Paclitaxel adducts conjugation

The three Paclitaxel adducts **3.28**, **3.35** and **3.36** properly functionalized with the maleimide moiety, were conjugated with NT4 to achieve targeted drug delivery systems with a different drug / peptide stoichiometry. In Luisa Bracci's research group, at the University of Siena, a general thiol-maleimide procedure has been already developed at this purpose. [25] In detail, 1.0 equiv. of NT4-Cys and 3.0 equiv. of maleimide derivative were reacted in the presence of 1.0 equiv. of DIPEA in DMF (*Scheme 3.20*). The reaction was monitored through analytical HPLC at different times: 1 h, 3 h, 20 h and 48 h. The final adducts were characterized by MALDI analysis and their *in vitro* cytotoxicity was evaluated.

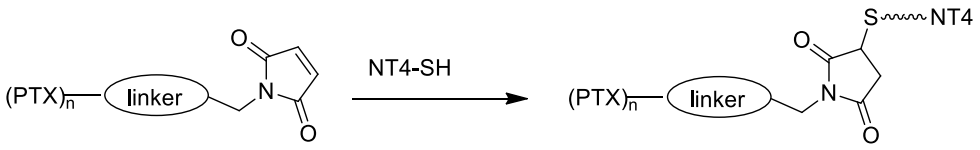

n=1 **NT4-3.28**
n=2 **NT4-3.35**
n=3 **NT4-3.36**

Scheme 3.20- Synthesis of targeted drug delivery systems.

3.4 Cytotoxicity assay

Cytotoxic potency of the targeted pro-drug forms of Paclitaxel was evaluated by incubating human breast adenocarcinoma cell lines (MDA-MB 231) with different concentrations (range: 10^{-9}-10^{-5} M) of the delivery systems **NT4-3.28**, **NT4-3.35** and **NT4-3.36**. EC50 of the previously developed[11] NT4-PTX adduct **3.37** (*Figure 3.7*), was employed as reference value. Operatively, MDA-MB 231 were plated at a density of 5 × 103 per well in 96-well microplates. Different concentrations of NT4 conjugates were added 24 h after plating. Cells were washed after 1 h incubation and then left 6 days at 37 °C with the same medium. Growth inhibition was assessed by 3-(4,5-dimethylthiazol-2-yl)-2,5-diphenyltetrazolium bromide (MTT). Experiments were performed in triplicate. The level of significance is $p < 0.05$ for two-sided testing.

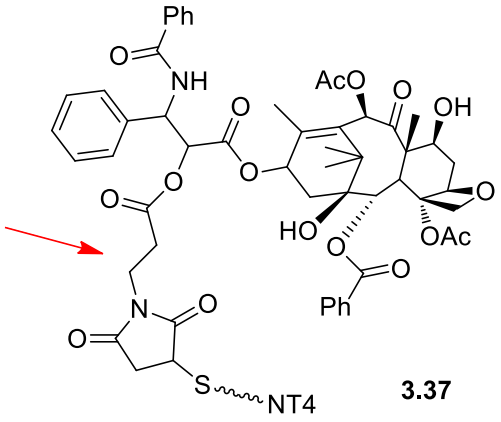

3.37

Figure 3.7 – Previously developed[25] NT4-PTX **3.37**

In *Figure 3.*8 the percentage of surviving cells is plotted against the logarithm of the concentration of each tested substance.

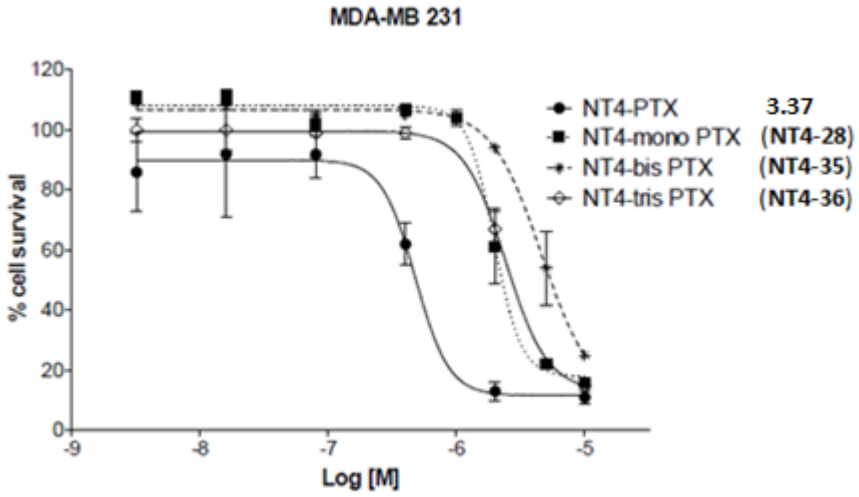

Figure 3.8 – Cytotoxic activity of the four NT4-*x*PTX (**3.37**, **NT4-3.28**, **NT4-3.35** and **NT4-3.36**) tested.

From the analysis of the data reported in *Figure 3.8* two important outcomes emerged:

i) Derivatives **NT4-3.28**, **NT4-3.35** and **NT4-3.36** were administered to the cell cultures in equimolar amount, in order to compare different Paclitaxel doses delivered from the same amount of the targeting peptide. Thus, increasing the stoichiometry ratio NT4/Paclitaxel from 1:1 (**NT4-3.28**) to 1:3 (**NT4-3.36**), no significant enhancement in cellular mortality was observed. Indeed, cytotoxicity curves relative to **NT4-3.28**, **NT4-3.35** and **NT4-3.36** administrations appeared almost superimposable. This result actually strongly confirmed the targeting ability of the NT4 peptide that is able to transfer inside cancer cells a killing dose of PTX even with a 1:1 stoichiometry. Despite this peculiar cytotoxicity result should be confirmed and validate in other experiments and, of course, *in vivo,* nevertheless it opens the way to better designed NT4 multi-drugs adducts more than NT4 poly-drugs conjugates;

ii) A slightly different cytotoxicity was shown by equimolar amounts of derivatives **3.37** and **NT4-3.28**, both carrying a single PTX unit. In particular, drug delivery system **3.37** showed a better cytotoxicity. Such difference can be ascribed to the different chemical nature of the spacer inserted on the two conjugates to link the NT4 and the PTX unit. A simple alkylic junction is present in adduct **3.37** (*Figure 3.7*; red arrow), while an aromatic spacer was used in **NT4-3.28**. The correlation between the spacer structure and the cytotoxicity probably deserves to be considered but not yet been studied in detail. Once the *in vivo* tests of derivatives **NT4-3.28**, **NT4-3.35** and **NT4-3.36** will confirm the lack of relationship

between stoichiometry and toxicity, the role of the linker chemical structure on the whole therapeutic activity will be re-considered since to maximize the therapeutic ability of this NT4-PTX adduct.

On the other hands, the cytotoxic evidences previously reported suggested two reasonable developments of the research:

i) *In vivo* environment can differently influence drug delivery and release in comparison to the *in vitro* conditions. Indeed, some pharmacodynamic and pharmacokinetic factors, which differs to that present in the culture medium, can influence the *in vivo* pharmacological activity. For instance, the presence of plasmatic esterases could affect the drug delivery towards the tumor site, through an early hydrolysis of the drug-carrier bond altering the anticancer activity. Moreover, these and other enzymes could differently interact with the delivery ability of NT4-drug conjugates due to their structure (i.e. 1, 2 or 3 drug moieties). Theoretically, due to the trivalent nature, derivative **NT4-3.36** should be able to maintain a certain therapeutic activity even if one or two Paclitaxel moieties are hydrolyzed from the carrier. Analogous behavior is reasonably expected for derivative **NT4-3.35**, while the **NT4-3.28** toxicity might show a higher sensitivity to these physiological processes. For this reason, a different activity of **NT4-3.28**, **NT4-3.35** and **NT4-3.36** against cancer cells could be expected shifting from *in vitro* to *in vivo* conditions. Thus, in order to validate our data and hypothesis all the drug delivery systems prepared will be used for *in vivo* pharmacological tests;

ii) Data reported in *Figure 3.8* demonstrated the remarkable anticancer potency of the prepared drug delivery systems and corroborated the targeting ability of NT4 peptide. Keeping in mind the (*in vitro*) relative importance of the NT4:drug stoichiometry, we moved to the design and synthesis of multi-drug targeting system where a NT4 peptide is conjugated with two or more different anticancer drugs. In other word, we imagined to use a NT4 peptide to transfer in the same cancer cell two or more different therapeutic agents typically used in the combination therapy. In the next chapter are reported the preliminary results obtained in the synthesis of one of this system targeted synergetic NT4-combination conjugates.

4. Targeted combination therapy

4.1 Combination therapy: an evolution of the monotherapy

Chemotherapeutics are the most efficient weapon against cancer developed up to now. However, they are associated with some drawbacks. In particular, due to their aspecificity, high doses are required for an efficient cancer treatment, leading to side effects and drug resistance in the target organism. Different strategies were recently developed to overcome these problems. One of the most prominent is the combination therapy. It is defined as a treatment modality that combines two or more different therapies, such as chemotherapy, hormone therapy, immunotherapy and radiotherapy, to treat a single type of cancer. The co-delivery of different drugs is the most common combination therapeutic modality in cancer treatment. The enhanced anticancer activity exhibited by this therapeutic approach is due to the synergistic action of drugs. This allows a reduction of the administered dose of the single drug, compared to the monotherapy, allowing a reduction of side effects, and, most importantly, decreases the likelihood of cancer cell mutation that commonly leads to drug resistance.[116,117] In *Figure 4.1* advantages related to combination therapy are reported.

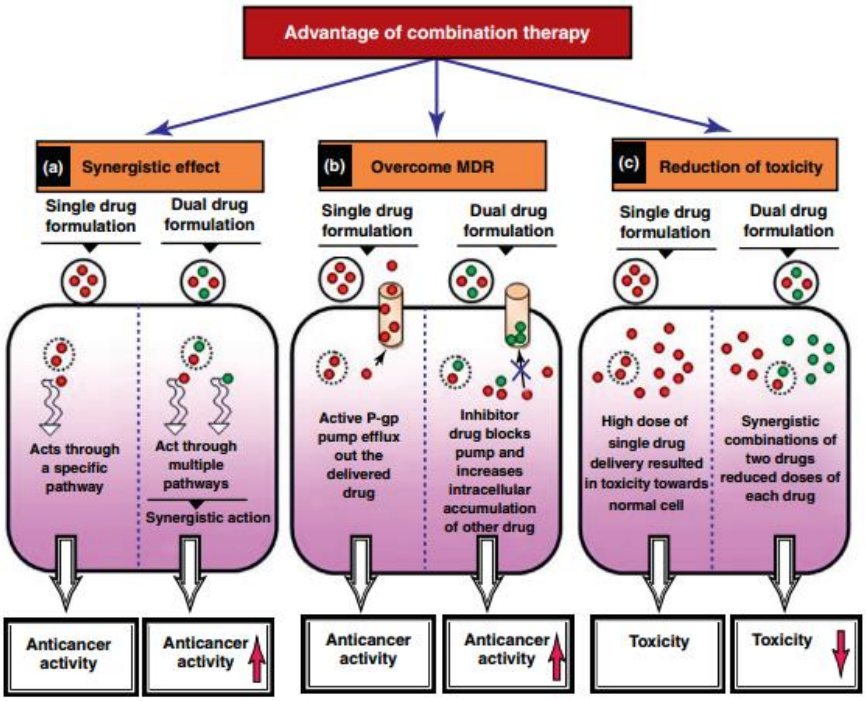

Figure 4.1-Schematic representation depicting various advantages shown by combination drug delivery for cancer therapy. (**a**) Single drug acts through a particular pathway, whereas multiple drugs can show enhanced anticancer activity by acting through several pathways. (**b**) In the case of single drug treatment, MDR proteins such as P-gp efflux drug out of the cell, whereas for dual formulations P-gp inhibitor blocks the role of MDR proteins and increases the intracellular concentration of other co-administered drugs resulting in higher efficacy by overcoming the MDR phenotype. (**c**) High dose is needed for single drug treatment and consequently results in toxicity to the normal cells, whereas treatment with different drug combinations by synergistic action can reduce the dose of each single drug and thereby decrease the toxicity.

Several combinations of two or more drugs were recently approved by FDA for the treatment of many types of cancers, as an efficient alternative to the monotherapy. For instance, Paclitaxel in association with cis-platin is the first-line treatment for ovarian cancer, Gemcitabine and cis-platin are used against biliary tract tumor, Gemcitabine and Nab-Paclitaxel or Gemcitabine, Paclitaxel and carboplatin are effective in metastatic breast cancer as well as in pancreatic adenocarcinoma treatment.[118,119] However, the effectiveness of these therapies is limited by the inability of such drugs to strongly distinguish between healthy and pathological cells. In this respect, the approach of conjugating therapeutic unit(s) to a residue with a certain affinity for a

target on the cancer cell, *e.g.* the targeting peptide NT4, could be extended to the combination therapy thus achieving a selective multi-drug treatment.

Among the endless combinations Gemcitabine and Paclitaxel together was the therapeutic approach we considered most attractive for the development of a targeted combination therapy.

Gemcitabine

Gemcitabine (or 2',2'-difluorodeoxycytidine: dFdC) **4.1** is classified as antimetabolite. Structurally, it is a deoxycytidine analog in which hydrogen atoms on the 2' carbon are replaced by fluorine atoms. It is marketed as Gemzar® (*Figure 4.2*).

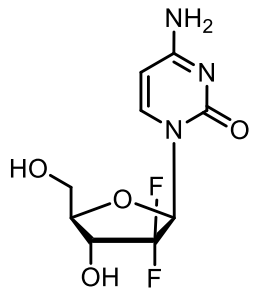

4.1

Figure 4.2- Gemcitabine.

Gemcitabine is used to treat certain types of breast, pancreatic, ovarian, and lung cancer and it is being studied in the treatment of other types of cancer. It has a good safety profile with a low incidence of toxicities (diarrhea, weakness, hair loss, mouth sores, difficulty sleeping, shortness of breath) that occurs in 10-29% of patients.

Gemcitabine is a pro-drug since it must be activated by cellular enzymes through phosphorylation. Di- and tri-phosphorylated form of Gemcitabine, marked as dFdCDP and dFdCTP respectively, inhibit processes required for DNA synthesis. Indeed, after incorporation of Gemcitabine nucleotide, dFdCTP, on the end of the elongating DNA strand, the DNA polymerases are unable to proceed thus causing DNA damage and induction of apoptosis. This action ("masked termination") apparently locks the drug into DNA as the proofreading enzymes are unable to remove dFdCTP from this position.[120]

4.2 Towards the development of a targeted combination therapy

Aimed to develop a targeted combination therapy, we envisaged the anchorage of both Paclitaxel and Gemcitabine on the peptide NT4, through a properly designed spacer. The first purpose was the conjugation of an equimolar amount of the two drugs and the peptide. Thus, we considered a trivalent spacer, depicted in *Figure 4.3*, provided with two binding sites for the drug units and with a maleimide residue, able to react with the thiol function installed on the peptide.

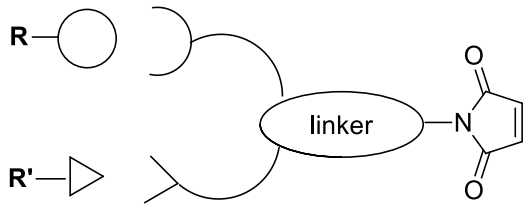

Figure 4.3 - **R** = Gemcitabine binding site; **R'** = Paclitaxel binding site

In order to ensure NT4/Gemcitabine/Paclitaxel equimolarity in the final device, and contemporary guarantee the *in situ* therapeutic activity of both drugs, some synthetic issues had to be considered:

i) Orthogonal reactions for the conjugation with Gemcitabine and Paclitaxel were reasonably envisaged. As a matter of fact, selective coupling reactions ensure drugs equimolarity. On the other hand, proper functions had to be inserted on drug units;

ii) An *in vivo* hydrolysable linkage has to be inserted on drugs proximity since ensuring their release from their pro-drug form in the tumor surrounding. As drugs should act synergistically, the same type of hydrolysable bond was required on both therapeutic units, thus permitting their simultaneously release from the delivery system;

iii) *In vivo* hydrolysable bonds cannot be exploited for drugs-spacer conjugation since preventing multiple labile sites and a consequent lower control in drug release process.

It is evident that the introduction of an equimolar amount of NT4, Gemcitabine and Paclitaxel on the same skeleton, is not a trivial task. We envisaged a Multi Component Reaction (MCR) for this purpose, *i.e.* a chemical reaction where three or more components react in a sequential manner to give selectively a single product that retains the majority of the starting material atoms. Several types of

MCR are reported. Among the several MCR procedures nowadays available we focused our attention on the Ugi reaction, a four-component MCR involving a carboxylic acid, a primary amine, a carbonyl compound and an isocyanide derivative that react one-pot to form a bis-amide (*Scheme 4.1*).

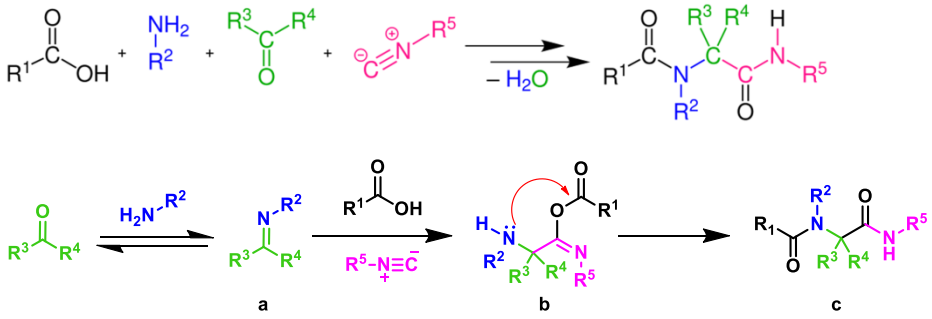

Scheme 4.1 - Mechanism of the Ugi reaction

After a screening in literature, we found out that cyclohexyl isocyanide, benzylamine, benzaldehyde and alkyl carboxylic acid derivatives exhibited a good reactivity under Ugi reaction conditions. Thus, 1.0 equiv. of 6-bromo-hexanoic acid **4.2**, 1.0 equiv. of cyclohexyl isocyanide **4.3**, 0.7 equiv. of benzyl amine **4.4** and 3.3 equiv. of 4-bromo benzaldehyde **4.5**, all commercially available, were reacted in a model Ugi reaction. Reagents were stirred in methanol for 1 hour at r.t. to afford bis-amide **4.6** isolated after flash column chromatography, in 58% yield.[121] (*Scheme 4.2*)

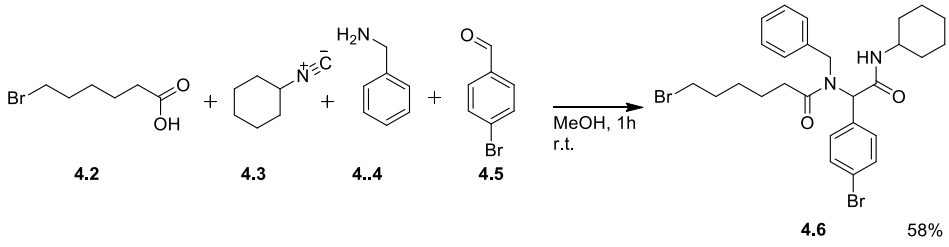

Scheme 4.2 – Model of Ugi reaction.

Structure of adduct **4.6** was confirmed by ^{1}H-NMR and ESI-MS analysis (*Figure 4.4-a* and *4.4-b* respectively).

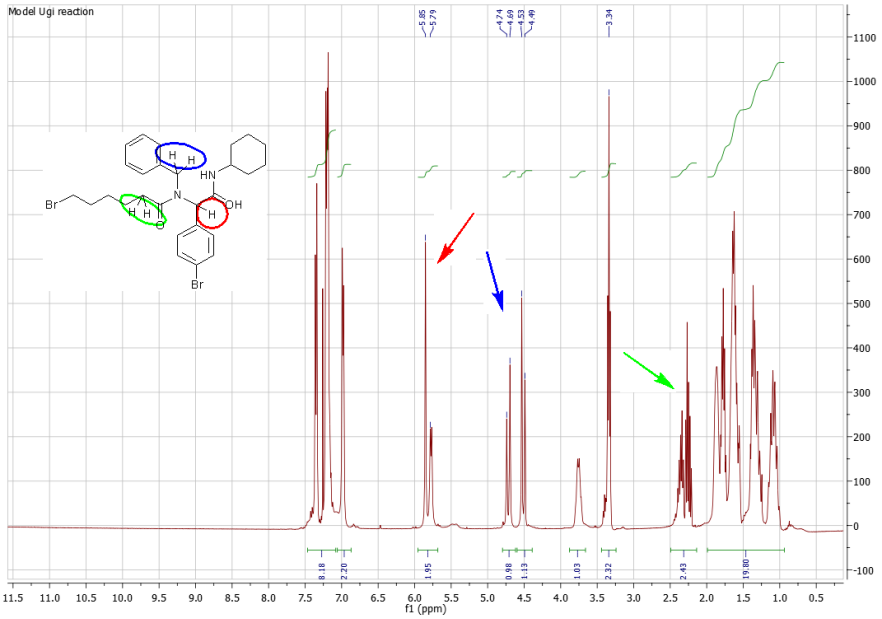

a)

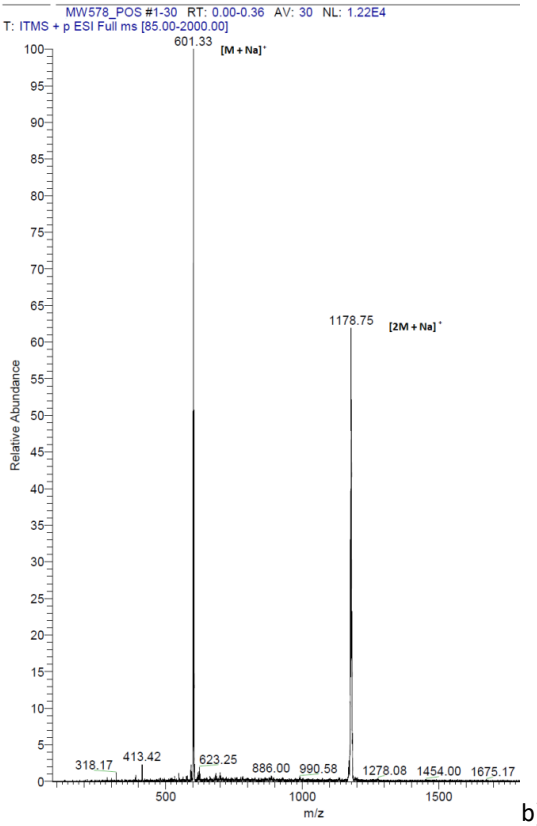

b)

Figure 4.4- a) ^{1}H-NMR and b) ESI-MS spectra of derivative **4.6**.

Once the good reactivity of selected derivatives was demonstrated, we decided to insert benzaldehyde and amine on Paclitaxel and Gemcitabine moieties, respectively, while cyclohexyl isocyanide was kept as "inert branch" of the final compound. Maleimide residue was inserted as 3-maleimido propionic acid **4.9** which was prepared reacting 1.0 equiv. of β-alanine **4.8** with 1.0 equiv. of maleic anhydride **4.7** in acetic acid at reflux for 5 hours .[113] Reactivity of derivative **4.9** under Ugi reaction conditions was tested. After 1 hour and 30 minutes at r.t. final adduct **4.10** was isolated in 60% yield (*Scheme 4.3*).

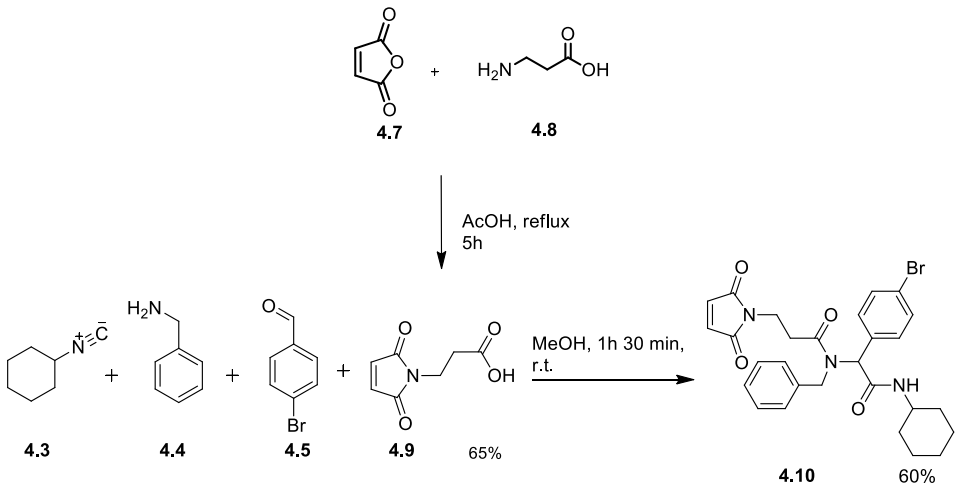

Scheme 4.3

The latter was characterized by ^{1}H-NMR analysis which reasonably showed peaks analogous to that described for derivative **4.6** (*Figure 4.5-a*; highlighted in green, red and blue), since the same skeleton is present in both adducts **4.6** and **4.10**. The characteristic singlet of maleimide moiety, displayed at 6.7 ppm with an integral value for two protons in respect to other peaks, indicated that derivative **4.9** is part of the final compound. The ESI-MS analysis confirmed this data showing the peak corresponding to $[M+Na^{+}]^{+}$ and $[2M+Na^{+}]^{+}$ (*Figure 4.5-b*).

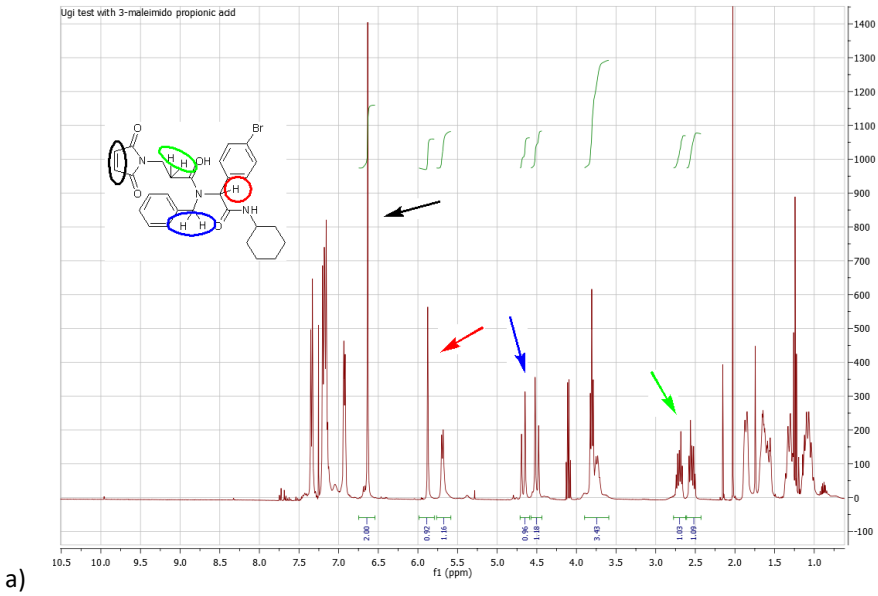

a)

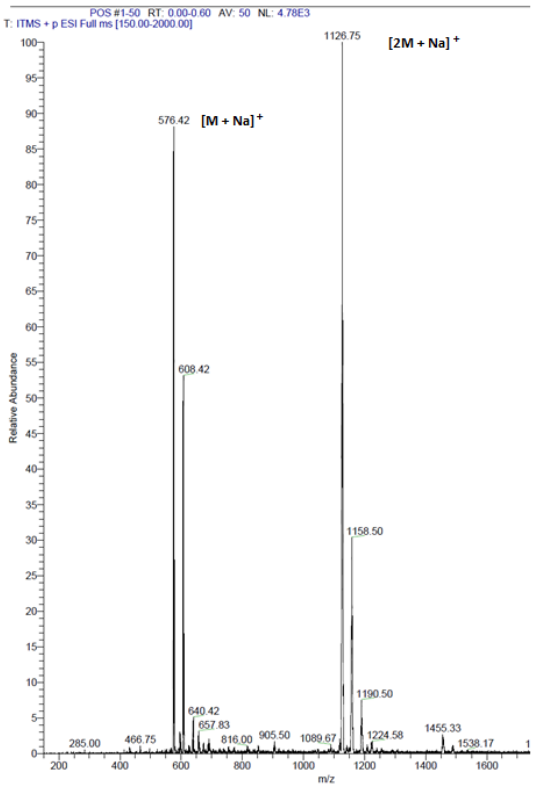

b)

Figure 4.5-a) ^{1}H-NMR and b) ESI-MS spectra of derivative **4.10**.

Aldehyde functionalization of Paclitaxel

The efficient Huisgen click reaction involving azido-functionalized Paclitaxel, was envisaged for the insertion of a benzaldehyde moiety on the Paclitaxel skeleton. Thus, commercial 4-hydroxy benzaldehyde **4.11** was provided with a terminal alkyne through the reaction with 4.0 equiv. of propargyl bromide and a catalytic amount of 18-crown-6. The mixture was stirred in dry acetone for 24 hours at reflux and the alkyne derivative **4.12** was isolated in 46% yield. The latter was, in turn, coupled with 1.3 equiv. of azido Paclitaxel **4.13**, in the presence of 0.1 equiv. of $CuSO_4$ and 0.2 equiv. of sodium ascorbate in DMF/H_2O 4:1 for 24 h, at r.t. The corresponding 1,2,3-triazole derivative **4.14** was obtained, after flash chromatography purification, in 20% yield (*Scheme 4.5*). The synthesis of azido-functionalized Paclitaxel is reported in section 3.1.

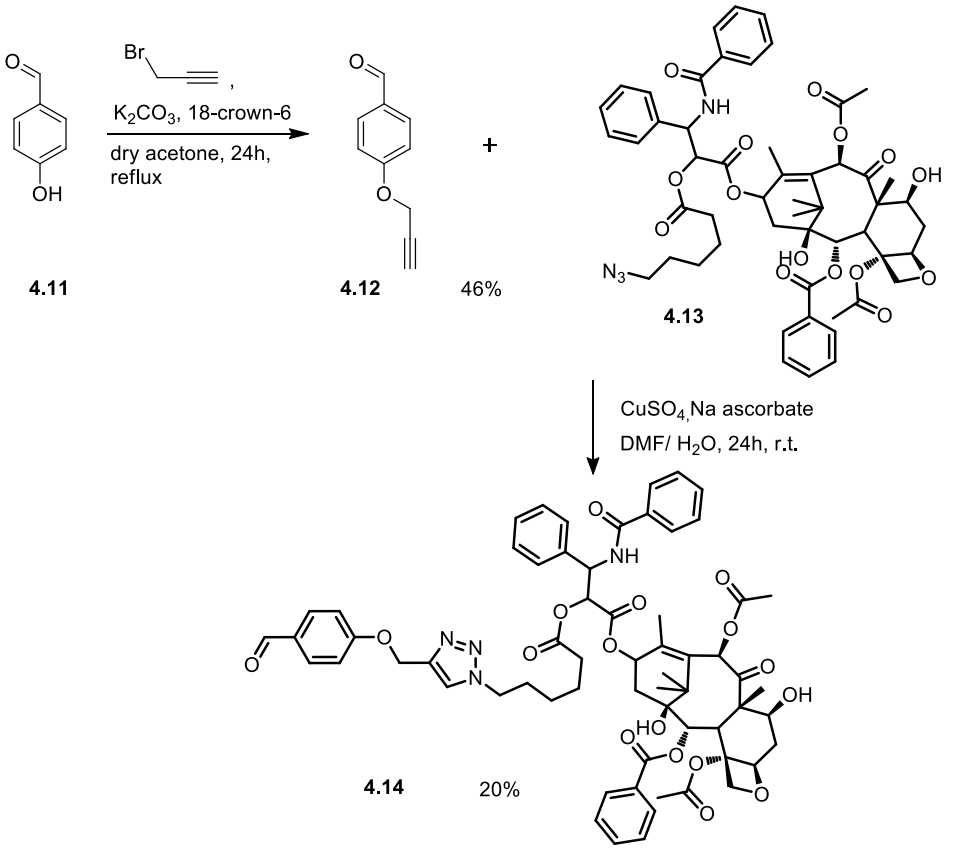

Scheme 4.5- Insertion of a benzaldehyde residue on the Paclitaxel skeleton.

Amino functionalization of Gemcitabine

The OH on the 3' position was selected for the selective insertion of a primary amine residue on the Gemcitabine skeleton. Thus, the protection of the primary alcohol on modified ribose ring and the primary amine on the cytosine ring were performed by reacting commercial Gemcitabine **4.1** with 2.2 equiv. of 4,4'-dimethoxytritylchloride in the presence of 0.1 equiv. of DMAP and 2.2 equiv. of DIPEA in dry DCM. After 19 hours at r.t. derivative **4.15** was isolated in 43% yield. The free hydroxyl group on the 3' position was, in turn, esterified with 1.1 equiv. of 6-azido hexanoic acid **4.16** in the presence of 1.0 equiv. of DMAP and 1.1 equiv. of DIC in dry DCM at r.t.. The esterification ensured the presence of the *in* vivo hydrolysable bond needed for the drug release. The azido-derivative **4.17** was isolated, after 19 hours, in 46% yield. The latter was then reacted with 2.2 equiv. of triphenylphosphine to promote reduction of azide group into the corresponding amine[122] (*Scheme 4.6*). Due to the difficulties encountered in the reduction of the azido to the required primary amino group, we decided to use N_3 residue in a CuAAC reaction with propargyl derivative **4.19**.

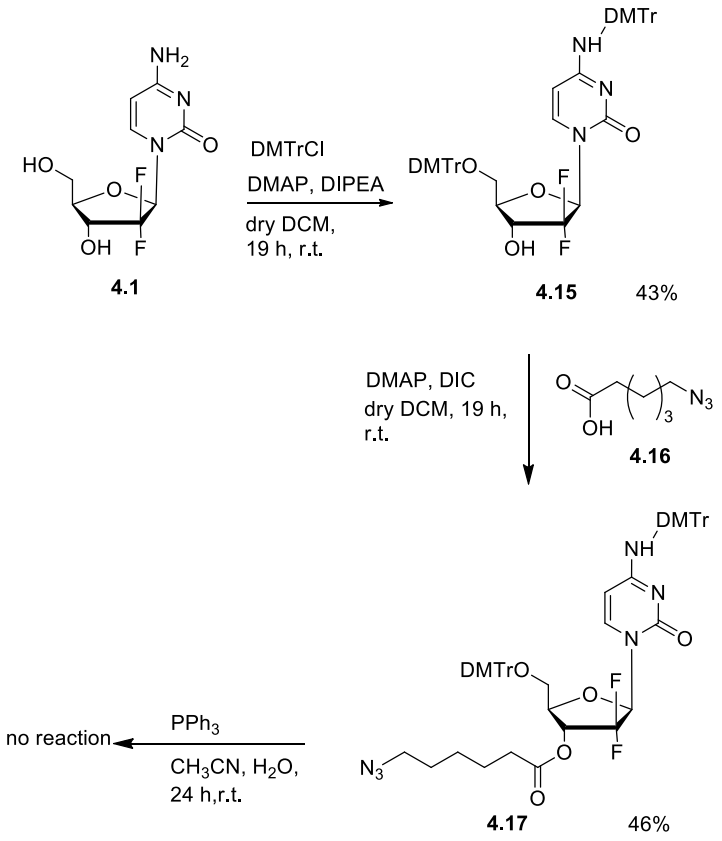

Scheme 4.6

The latter was prepared by reacting commercial 4-hydroxy benzylamine **4.18** with 1 equiv. of propargyl bromide, 0.1 equiv. of 18-crown-6 and 1 equiv. of potassium tertbutoxide in dry THF at -70 °C for 2 hours and at 0 °C for 2 hours. The low temperature led to the selective hydroxyl propargyl-substitution, preventing the undesired amino-propargylation. The desired final product **4.19** was obtained in 67% yield without purification (*Scheme 4.7*).[123]

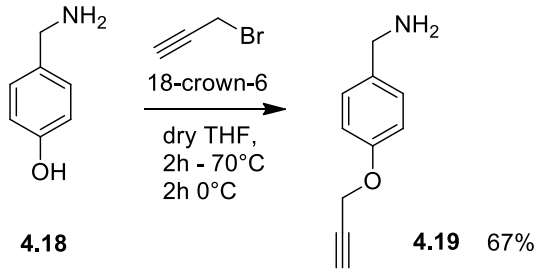

4.18 **4.19** 67%

Scheme 4.7

In the further step, alkyne **4.19** will be reacted in a Huisgen reaction with azido-Gemcitabine **4.17** and the amino-Gemcitabine derivative will be involved in a Ugi reaction with aldehyde-paclitaxel, maleimide-acid and cyclohexylisocyanide. Final adduct will contain the two drug units and the maleimide residue required for the NT4 coupling. Indeed, the targeted multi-drugs device will be synthesized and involved in *in vitro* and *in vivo* tested in order to both verify its anticancer ability and evaluated advantages or disadvantages of the targeted combination therapy in comparison to the targeted monotherapy.

5. Chelating agents: DOTA analogues

Current interest in the clinical use of chelating agents as vehicles for metals in biological systems has led to the synthesis and study of a large number of new cyclic polioxa or polyaza ligands. One class that has shown great promise for clinical applications is the polyazamacrocyclic polycarboxilate ligands.[124] Particularly, 1,4,7,10-tetraazacyclodecane-N,N',N'',N'''-tetracetic acid (DOTA) (*Figure 5.1*) and its analogues became a subject of universal interest because they form stable complexes with a wide variety of metal ions. Furthermore metal-DOTA complexes have been shown to be kinetically inert under physiological conditions.[125]

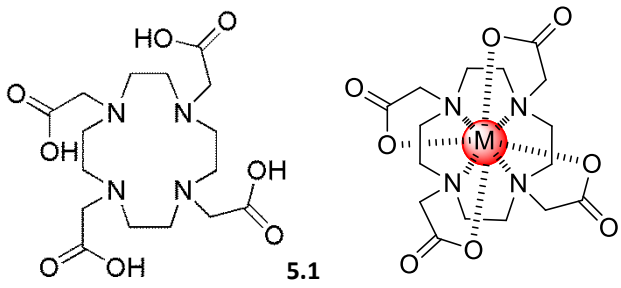

Figure 5.1- DOTA and octa-coordination around a metal

Among metal ions which can be strongly encapsulated by DOTA, radionuclides such as ^{111}In(III), ^{67}Ga(III) and ^{99m}Tc(IV) have suitable physical properties for tumor imaging, while ^{90}Y(III), ^{67}Cu(II), ^{186}Re(VII) and ^{177}Lu(III) have cytotoxic proprieties which can be exploited for therapy.

Paramagnetic ions, as Gd(III), are instead generally exploited for Magnetic Resonance Imaging (MRI), which provides a potent diagnostic alternative to light microscopy and radiopharmaceutical methods.[126–129] The image is based upon the NMR signal of the water's proton, where the signal intensity is a function of the water concentration and relaxation times (T_1 and T_2). Gadolinium contrast mediums enhance and improve the quality of the MRI images by increasing the relaxation rate ($1/T_1$) of water protons and are widely used in clinical diagnostics.[130] One of the major problems in conventional contrast agents and radiopharmaceuticals is that they are primarily extracellular with an aspecific biodistribution.

For these reasons, the next generation of contrast agents will include systems able to recognize specific targets on the cellular surface that act as early reporters of a given pathology. Targeting of over-expressed membrane receptors with specific radiopharmaceuticals is already a well-established diagnostic method in nuclear medicine for several types of tumors. A somatostatin radioligand, DOTA-[D-Phe1-Tyr3]-octreotide (DOTATOC), has been the first synthesized for therapeutic purposes, because of its stable and easy labelling with ^{90}Y. Starting from this successful compound, the number of peptide-metal chelate based molecular sensors, diagnostic or therapeutic agents is rapidly increasing and is becoming one of the most challenging areas of research.[131,132]

Considering our perspectives in peptide targeted tumor therapy we decided to conjugate a chelating agent to our carrier and exploit its efficacy on detecting or killing tumors, once complexed with an appropriate metal. For this purpose we selected, as a suitable chelating agent, DOTA because of the promising results obtained and the opportunity of direct coupling between the peptide's free amine and its carboxylic functionalities.

In literature is reported that DOTA-peptide conjugates are generally synthesized either in solution[133] or on solid support[134,135] through a coupling reaction involving the free amino group inserted on the peptide residue. DOTA or a derivative can be directly attached to the peptide or a spacer may be inserted between the peptide chain and the chelator. Based on this, we designed DOTA derivatives **5.2** and **5.3** (*Figure* 5.2) functionalized with a single pending free carboxylic acid moiety, to permit their coupling with an amino group of the dendrimeric peptide using standard solid phase peptide synthesis. The carboxylic acids not involved in the coupling, were protected as *t*-Bu esters, to avoid side reactions and poli DOTA functionalization. Tert-butyl esters are easily deprotected in the final acid cleavage of the modified peptide from the solid support with trifluoacetic acid (TFA).

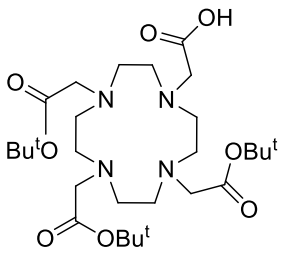

5.2

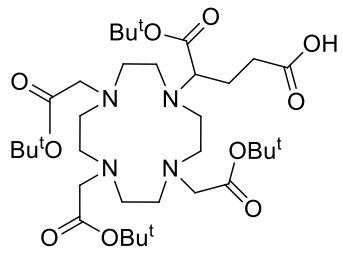

5.3

Figure 5.2

As a suitable common starting material, 1,4,7,10-tetraazacyclododecane-1,4,7-tris(*tert*-butylacetate) **5.5**, was prepared, as shown in Scheme 2.46, reacting in dimethylacetamide (DMA) *tert*-butylbromoacetate (3.0 equiv.) with a solution of tetraazacyclododecane **5.4** (1 equiv.), commercially available as cyclen, and Na(CH_3COO) (3.0 equiv.). The *tert*-butyl ester of DOTA (1,4,7,10-tetraazacyclododecane-1,4,7-triacetic acid) **5.5** was obtained by precipitation after 20 days under stirring in 55% yield. (*Scheme 5.1*)

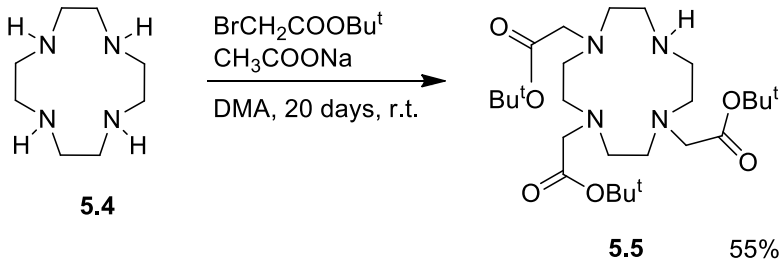

Scheme 5.1

The derivative **5.6** was obtained by adding 1.2 equiv. of benzylbromoacetate to compound **5.5** in DMF in the presence of NaH. [133] The reaction mixture was stirred for 24 hours at r.t., then the product was isolated by flash chromatography, to yield *N*-(benzylcarboxymethyl)-1,4,7,10-tetraazacyclododecane-N',N'',N'''-triacetic acid tri-*tert*-butyl ester **5.6** in 67% yield.

A mixture of this compound and 10% Pd/C was hydrogenated in methanol under H_2 atmosphere for 6 hours to yield the modified DOTA macrocycle **5.2** in 50% yield (*Scheme* 5.2).

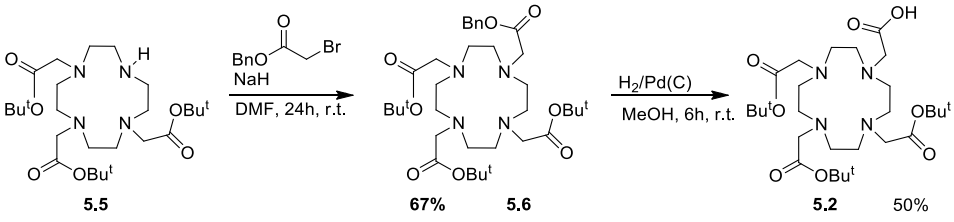

Scheme 5.2

Structure of compound **5.2** ensures a selective and efficient coupling with the dendrimeric peptide, through the formation of a single amide linkage. However this will cause a lower ability of encapsulating metals due to the lack of one carboxylic acid group when compared with unmodified DOTA. (*Figure 5.3*)

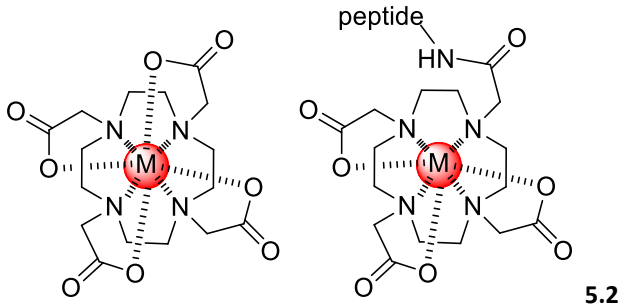

5.2

Figure 5.3

Therefore we planned to synthesize the DOTA derivative **5.3**, by modification of previous methods,[136] which contemporarily ensures the possibility of an active coupling, using the standard solid phase peptide chemistry, and an octa-coordination around the selected metal once the *t*-butyl esters have been hydrolysed.

Operatively, starting from the commercially available L-glutamic acid-5-benzylester **5.7** using a method analogous to Holmberg,[134,137] a suspension with 3.0 equiv. of sodium bromide in a cooled 1N solution of bromidric acid was made and 2.0 equiv. of sodium nitrite were added portionwise. The yellow solution was stirred for 2 h and finally 560 µL of 98% sulfuric acid were added, followed by diethylether. The product **5.8** was obtained in 82% yield.

The protection of the free carboxylic group was obtained adding dropwise a solution of 2.0 equiv. of *tert*-butyltrichloroacetimidate (TBTA) in cyclohexane to a solution of 1.0 equiv. of **5.8** in $CHCl_3$. During the addition a white precipitate formed, which was dissolved by the addition of DMA before adding a catalytic amount of boron trifluoridiethyl etherate. The reaction mixture was stirred for three days at r.t. and bromoester **5.9** was isolated, after purification, in 50% yield.

The following coupling with the macrocyclic ring was performed as usual, in mild basic conditions. A mixture of 1.0 equiv. of **5.5** and 3.0 equiv. of K_2CO_3 was stirred in dry acetonitrile at 60°C for 10 min before adding dropwise, over a period of 40 min, a solution of 2.0 equiv. of **5.9** in dry acetonitrile. After 42 h under stirring at 60°C, benzyl ester **5.10** was isolated in 59% yield. Finally **5.10** was dissolved in absolute ethanol and

hydrogenated over 10% Pd/C under a H_2 atmosphere for 48 hours to give the desired product **5.3** in 79% yield without purification. (*Scheme 5.3*)

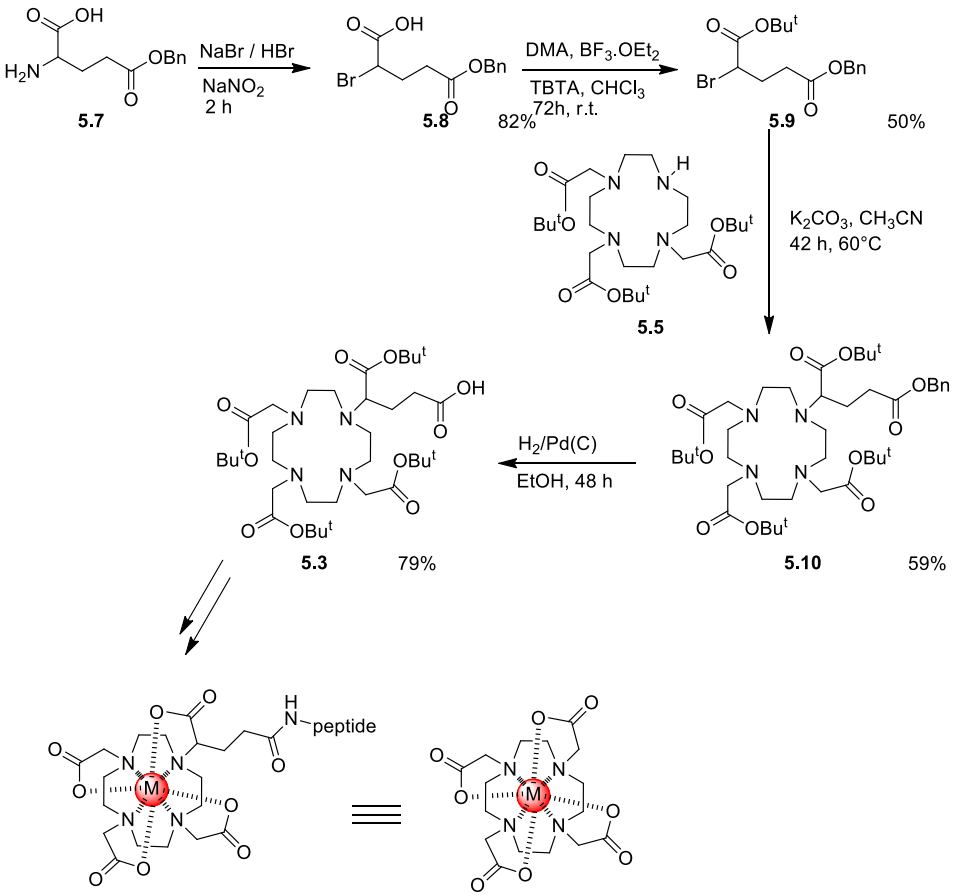

Scheme 5.3

As it is shown in Scheme 5.3 this derivative can be conjugated to the dendrimeric peptide without affecting its complexation ability, because, like for DOTA, an octa-coordination around the metal, resulting in a compact square-antiprism involving four nitrogen atoms in one plane and the four oxygen atoms in a second plane, is perfectly available.

Thus, Luisa Bracci's research group at University of Siena, will deal with the coupling of such derivatives with the targeting peptide NT4, properly provided with an amino terminal non-peptidic PEGylated branch. The amidation coupling can be performed directly on solid support, since the chelating derivative can be treated as an amino acid. The cleavage step, involving concentrated TFA, besides the release of the peptide from the solid support, allow the tertbutylated acids deprotection on DOTA derivative, thus rendering acid groups available for chelating the selected metal ion. Indeed, it will be octa-coordinated within the DOTA structure as the last step of the procedure, before *in vivo* testing of the new targeting imaging tool.

6. Quantum Dots

QDs manipulations and in vitro and in vivo tests were performed by Prof. Luisa Bracci's research group at the University of Siena.

6.1 Characteristics of QDs

Quantum Dots (QDs) are semiconductor nanocrystals with a core-shell structure and a diameter that typically ranges from 2 to 10 nm.[138] Recently, they have been explored for a wide range of applications, such as solar cells, transistors, LEDs as well as medical application with best regard for both *in-vitro* and *in-vivo* imaging and cancer therapy and theranostic. QDs exhibit a wide range of unique and excellent optical properties, such as a broad absorption spectra coupled with a narrow emission spectrum bands. Furthermore, QDs display long-lasting and more stable photoluminescence compared to conventional organic fluorophore (*e.g.* rhodamine), which render them particularly attractive for the *in-vivo* imaging application. The frequency of the light emitted by a specific quantum dot is related directly to its size; smaller particles tend to emit higher-energy radiation. (*Figure 6.1*) Thus QDs size is strongly related to their application.

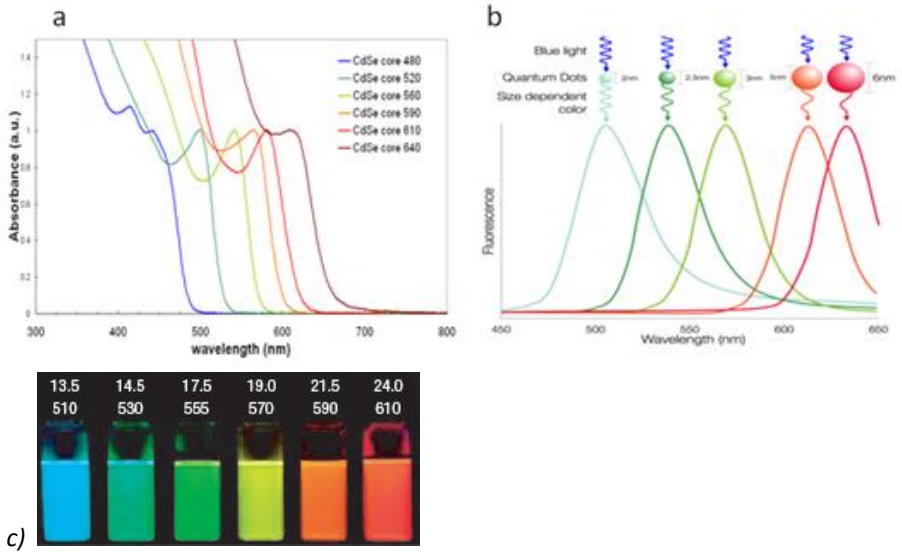

Figure 6.1 – a) absorption spectra and *b)* fluorescence spectra of CdSe QDs in different size. *c)* QDs colours related to their size.

6.2 Structure of QDs

QDs are usually composed by a core of a semiconducting material enclosed within a shell of another semiconductor. The core of QDs is usually composed of compounds from groups II–VI such as CdSe, CdS or CdTe, groups III–V such as InP or InAs, or groups IV–VI such as PbSe. The shell is usually composed of ZnS[139,140] (CdSe/ZnS QDs are the most widely used for biomedical research).
The ZnS shell protects the core from oxidation, increases photostability and improves its quantum yield up to 80% when compared with that of the core alone, which is usually less than 10%.[141,142] On the other hand, since *in*-vivo oxidative environment lead to a release of heavy metal ions from the QD, the protective shell increases QDs human safety. The inorganic core-shell is, in turn, coated by an organic layer responsible for QDs physical-chemical properties, *e.g.* solubility (*Figure 6.2*). In addition, several different molecules, ranging from small molecules to peptides or polymers, can be conjugated with QDs making them a very versatile tools for different research areas.[143] (see below for details).

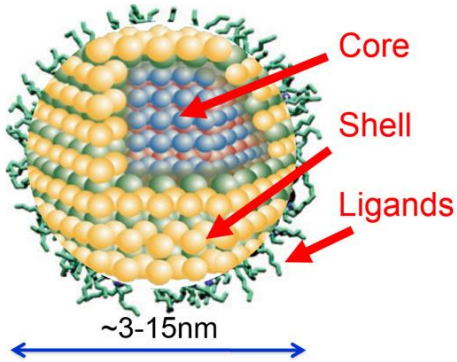

Figure 6.2 - Schematic structure of QDs.

6.3 QDs synthesis and functionalization

As for AuNPs, several synthetic methodologies, in both organic and aqueous solvents, were developed for the synthesis of well monodisperse QDs with well-tuned optical properties by varying the NPs size.[142,144] The most used synthetic procedure involves organometallic precursors, which are reacted, in the presence of a stabilizer, at high temperature (300 °C). QDs with different selected sizes can be prepared by setting the reaction time. Analogously to AuNPs, the high affinity of thiols towards the ZnS shell can be exploited for a suitable decoration of the QDs surface.

In particular, the thiolate ligand can be introduced directly during the synthetic step (*Figure 6.3-a*) as well as capped QDs can undergo place-exchange reaction with ligand properly provided with a thiol function (*Figure 6.3-b*).

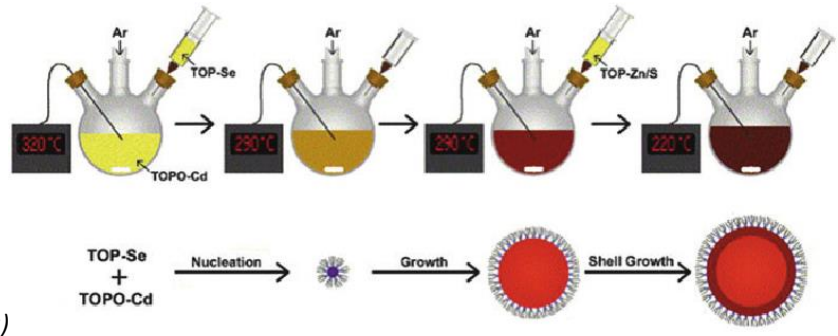

a)

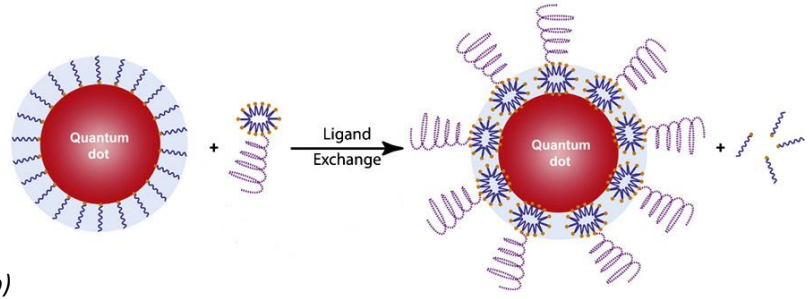

b)

Figure 6.3- a) Direct synthesis of coated CdSe/ZnS quantum dots; *b)* place-exchange reaction.

However, the more widely used approach is the "post synthetic modification". Commonly, the well-defined amidation reaction, involving carboxylated QDs, is used. Synthetically, external carboxyl groups are activated by N-(3-dimethylaminopropyl)-ethylcarbodiimide (EDC) or sulfo-N-hydroxysuccinimide (s-NHS) and, in turn, reacted with an amino-functionalized unit. This strategy was then adapted to amino coated QDs, achieving the carboxylated-ligands conjugation.[145]

When the amidation reaction cannot be used for the direct coupling, it however can be exploited to insert on the QDs surface, through a bifunctional linker, a suitable reactive group, such as maleimide moiety or a terminal alkyne or an azide etc., in order to adapt the synthetic procedure to this limit. The properly functionalized QDs and biomolecules can thus be linked through a click chemistry reaction.[145]

So, the great versatility of the post-synthetic functionalization approach, allows the anchorage of a wide variety of molecules and biomolecules on QDs surface.
In F*igure 6.4*, an overview of different bioconjugation (left side, BOI = biomolecule of interest) and surface coating (right side) strategies for QDs is reported. Two surface coating strategies are presented: encapsulation with amphiphilic polymers (i, ii) and cap exchange with hydrophilic ligands exploiting the thiol-affinity of the ZnS shell of the QD (iii–v).[146]

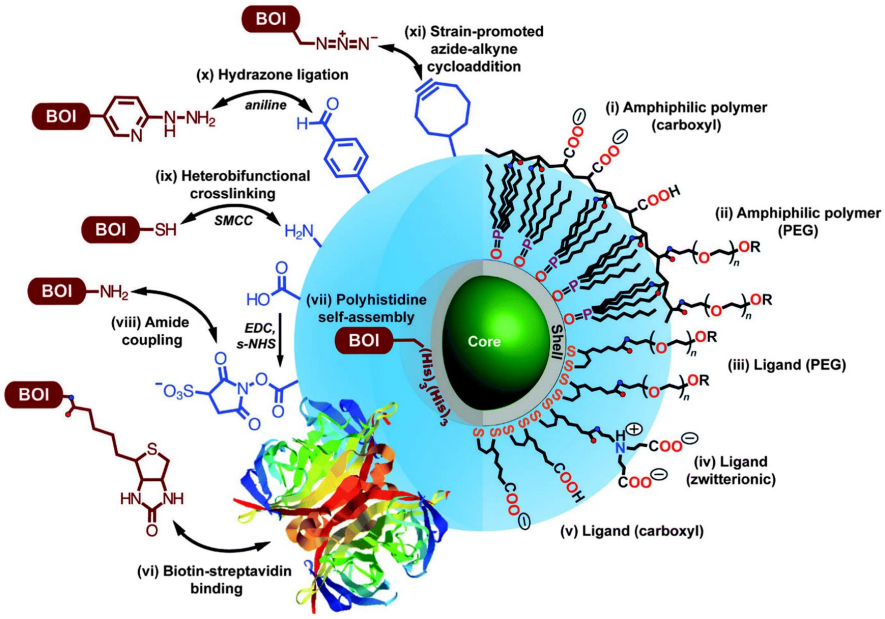

***F**igure 6.4* – Different strategies for QDs decoration.

6.4 QDs for targeted theranostic

As above said, QDs are being intensively studied with a focus on their application as contrast agents. As all metallic NPs, also QDs passively accumulate in the tumour site, due to the EPR effect. Nevertheless, it would be convenient increasing their targeting ability by conjugating their surface with a molecule with a certain affinity for a target unit on the tumour, thus enhancing the effectiveness for imaging application. However, the ability of NPs to bind a great number of molecules on their surface has to be considered. Indeed, the likelihood to decorate the QDs surface with several therapeutic units, allows extending the QDs potential application from diagnostic to theranostic. As a matter of fact, the peculiar features of the inorganic core render the nanosystem suitable as tumour tracer, while the multi-functionalization with both targeting and therapeutic units allows a selective therapy. Thus, the development of targeted multi

drugs-QDs could represent a breakthrough in medical research. On these considerations, our work was focused on the NT4-QDs-drugs conjugation as an evolution of the previously described NT4-AuNPs-drugs devices.

6.5 Construction of NT4-QDs

Qdot® 705 ITK™ amino (PEG) quantum dots (maxima emission at 705 nm) were selected as substrate for the development of targeted QDs. The organic monolayer of these nanoparticles is composed of an amino-derivatized PEG, which prevents non-specific interactions and provides a convenient handle for conjugation. In particular, amino-QDs efficiently react with activated acid. Thus, the latter ones were reacted with an activated acid-maleimide bifunctional linker, sulfo-SMCC **6.1**, for 1 hour in phosphate buffer saline (PBS) at pH = 4.
Maleimide moieties so inserted were, in turn, reacted with the targeting peptide in the well-tuned maleimide-thiol reaction (*Scheme 6.1*). The bifunctional linker was used in defect, ensuring the presence of free amino groups in the successive step, in view of their drug-decoration (see section 6.6 for details).

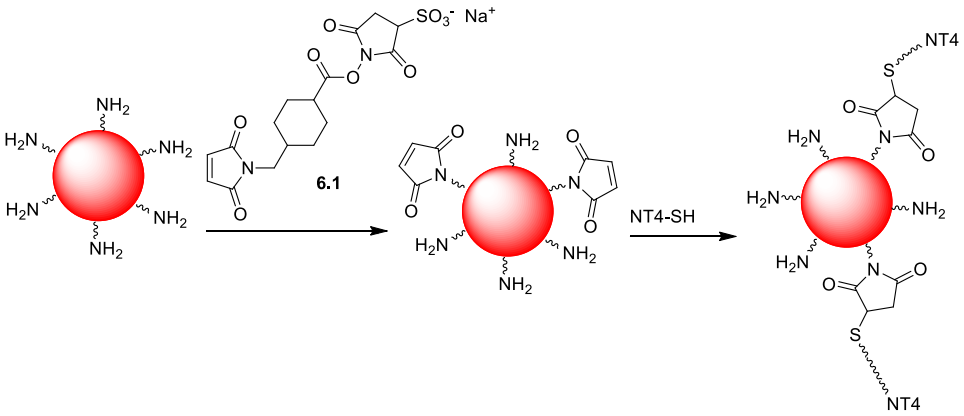

Scheme 6.1 - Schematic illustration of the preparative procedures of NT4-QDs 705.
NT4-QDs were purified using superdex 200 by size exclusion chromatography. The concentration of purified NT4-QDs in the eluate was calculated to be 250 nM, according to the extinction coefficient at 532 nm of 2.1×10^6 (mol/L)−1 cm−1 provided by the manual.

6.5.1 Stability assays of NT4-QDs:

NT4-QDs were characterized by TEM analysis, which showed a well-dispersity of the system without any aggregation, thus demonstrating that the NT4-conjugation did not affect NPs morphology and stability and hence their potential use for our purpose (*Figure 6.5-a*).

A previous evaluation of cytotoxicity of QDs has to be carried out in view of their application in cellular and in vivo study. Thus, human adenocarcinoma cell lines (HT-29) were incubated for 24 hours with NT4-QDs and unconjugated QDs in concentrations ranging from 0.5 to 20 nM. No significant cytotoxic activity was showed in each sample (*Figure 6.5-b*).

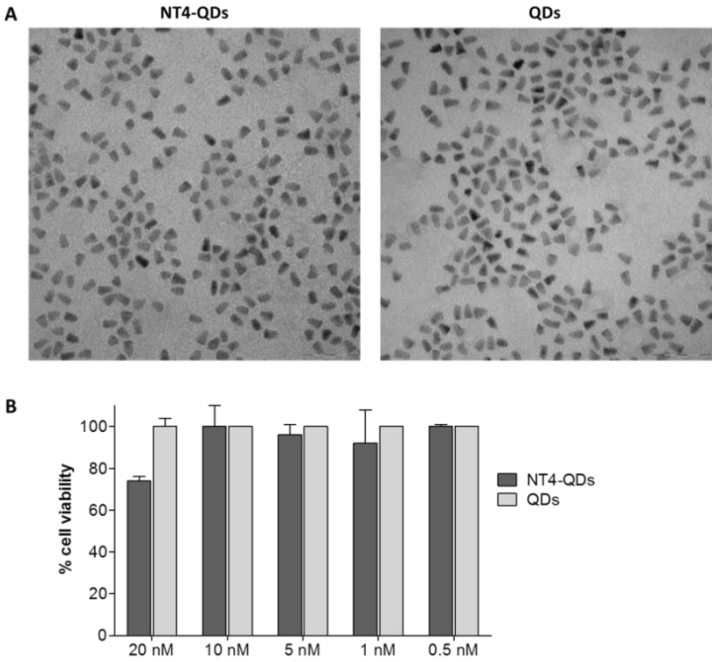

Figure 6.5- Characterization of NT4-QDs. A) TEM image of monodispersed NT4-functionalized NIR QDs. The average size of the particles is around 10 nm. B) Cytotoxicity of NT4-QDs and free QDs in HT-29 human colon adenocarcinoma cell line after 24 hours incubation.

6.5.2 In vitro binding and internalization of NT4-QDs

Binding ability of targeted QDs was evaluated in comparison of unconjugated QDs, by immunofluorescence assay on human adenocarcinoma cell line (HT-29).
Nuclei were stained with DAPI (blue), plasma membrane was stained with Wheat Germ Agglutinin-Alexa Fluor 488 (green) while the red signal indicated QDs accumulation. NT4-QDs binding on cancer cell membrane was revealed after 30 minutes of incubation (T0). After 1 hour of incubation, NT4-QDs were localized into the cell membrane while, at following incubation times, NT4-QDs were clearly visualized intracellularly. On the other hand, no signal was detected either on the cell membrane or intracellularly, with undecorated QDs (F*igure 6.6*), thus demonstrating that the binding ability is related to the NT4 peptide conjugation.

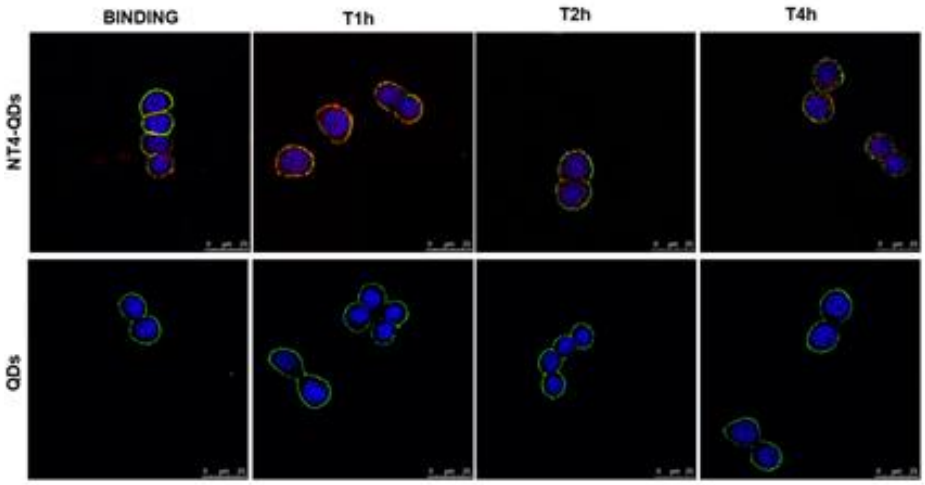

F*igure 6.6*- Binding and internalization (T 1h, 2h, and 4h) of NT4-QDs (red) on HT-29 by immunofluorescence.

Once the stability and the targeting ability of NT4-QDs was demonstrated, we focused on providing such system with a proper number of drug units, in order to combine the demonstrated targeted diagnostic activity with the therapeutic potential of Paclitaxel.

6.6 Construction of NT4-QDs-PTX

Aimed to exploit the well-defined amidation protocol involving NHS ester derivative (see section 6.5 for details*)* for the achievement of PTX-QDs conjugation, a proper function has to be inserted on the drug unit. Keeping in mind the need of an ester bond for ensuring the in vivo drug release, Paclitaxel was reacted with 1.6 equiv. of succinic anhydride in the presence of 0.3 equiv. of DMAP, in dry pyridine, for 24 hours at r.t., to

afford the corresponding derivative **6.3** selectively esterified on the 2' OH, in quantitative yield (*Scheme 6.2*).

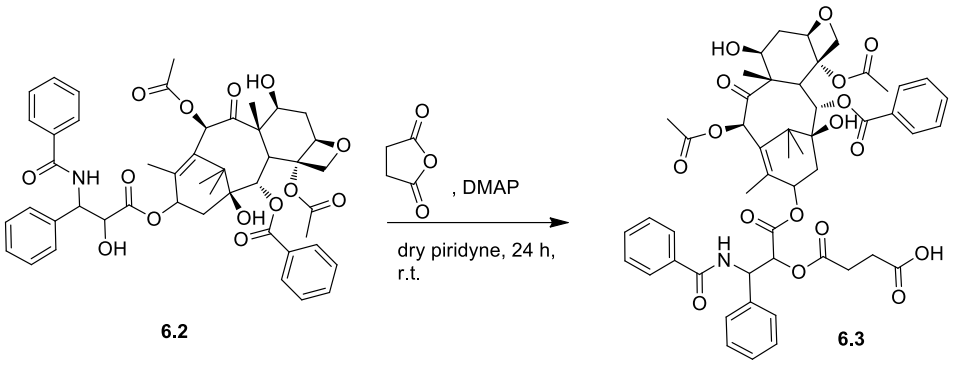

Scheme 6.2 – Acid functionalization of Paclitaxel.

To activate the acid moiety as NHS ester, N-succinimydil diphenylphosphonate (SDPP) **6.6** was required. It was prepared by reacting N-hydroxysuccinimide **6.5** with an equimolar amount of diphenyl phosphoryl chloride **6.4** in the presence of 1.4 equiv. of TEA in dry DCM for 6 hours at r.t.. SDPP **6.6** was used without purification in the further reaction with Paclitaxel derivative **6.3,** in the presence of 1.4 equiv. of TEA as base. After 6 hours in acetonitrile at r.t. the NSH ester form of Paclitaxel **6.7** was isolated in 51% yield (*Scheme 6.3*).

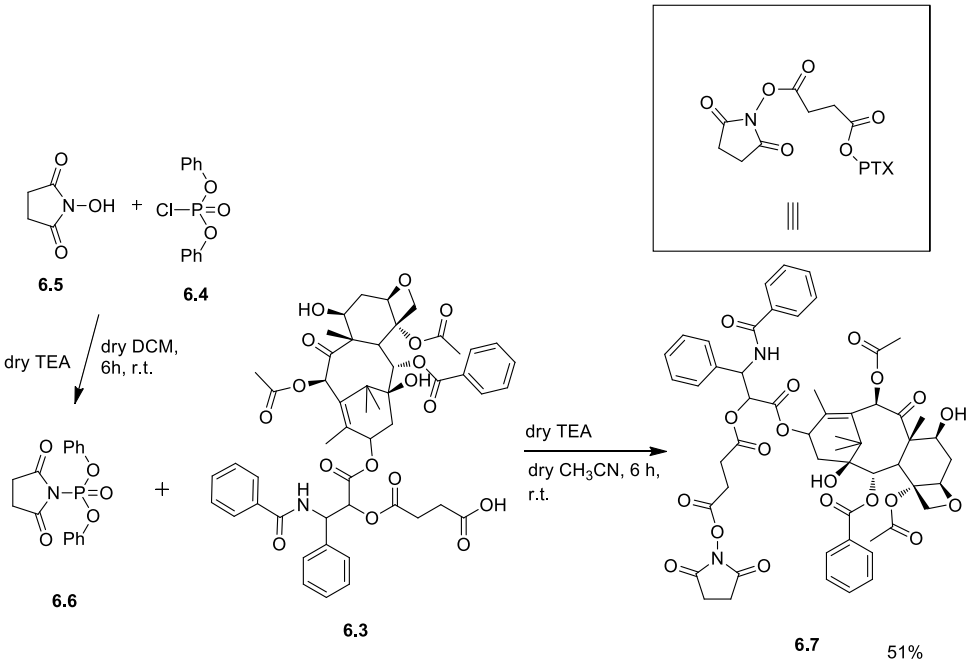

Scheme 6.3- Synthesis of NHS ester Paclitaxel.

Maleimide residues were inserted on QDs surface by reacting the bifunctional linker **6.1**, sulfo-SMCC, with amino QDs in an amidation reaction. The linker **6.1** was used in substechiometric amount thus ensuring the presence of unreacted amino groups which were, in turn, reacted under the same amidation conditions with NHS ester Paclitaxel **6.7.** After 1 hour in acetonitrile at r.t. in the dark, the mixture was purified by NAP5 Sephadex G-25 column, eluting with PBS. Collected QDs were incubated with a PBS solution of MAP-NT and, after 1 hour, 2-mercapto ethanol was added in order to saturate unreacted maleimide residues. The synthetic protocol is reported in *Scheme 6.*4.

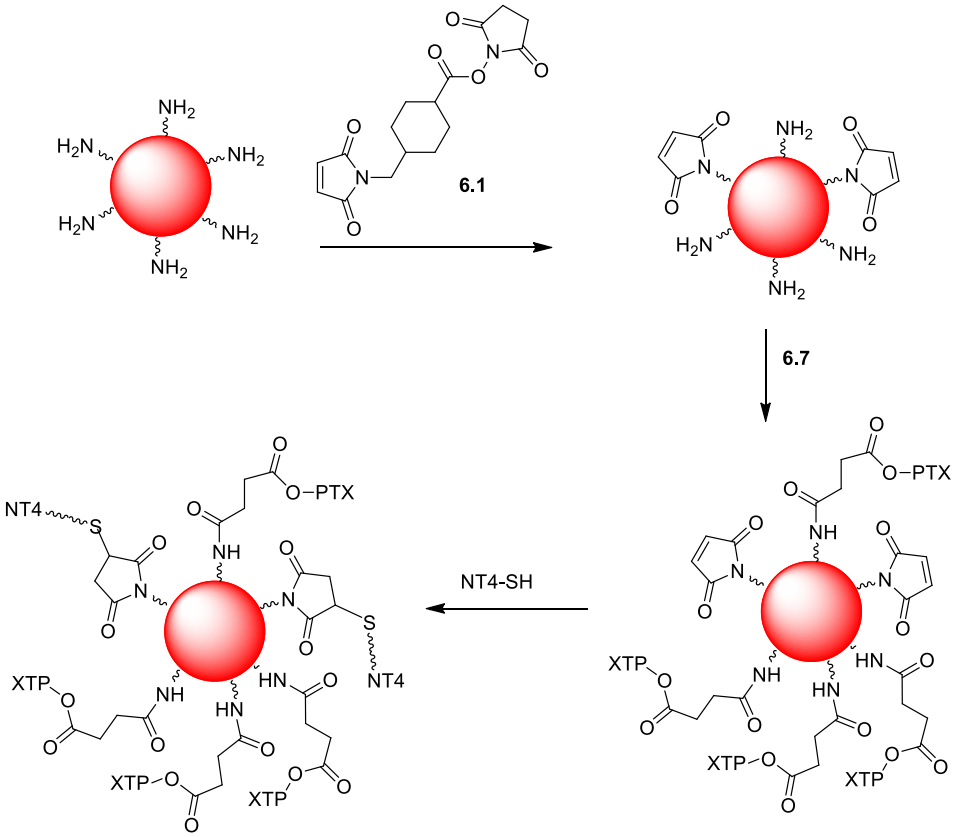

Scheme 6.4 – Synthesis of NT4-QDs-PTX.

The quantization was performed through spectrophotometric analysis at 532 nm in which $\varepsilon = 2.1 \times 10^{6}\ (mol/L)^{-1}cm^{-1}$.

6.6.1 Binding and cytotoxicity experiments of NT4-QDs-PTX

Human colon adenocarcinoma cell lines (HT-29) were incubated with a 20 nM solution of NT4-QDs-PTX. QDs-PTX, not decorated with the peptide, were used in the same concentration as reference. After 30 minutes, the binding ability of the two systems was evaluated. In the figure, nuclei were stained with DAPI (blue signal), while the red signal indicated the NT4-QDs-PTX accumulation.
Analyzing immunofluorescence images, a localization of NT4-QDs-PTX on cell membrane was showed (red line), while no QDs signal was detected in the cell surrounding when QDs-PTX are not decorated with the targeting peptide. This data confirmed the well-demonstrated targeting ability of the peptide and its capacity to efficiently deliver the QDs-PTX conjugate on the tumor site.

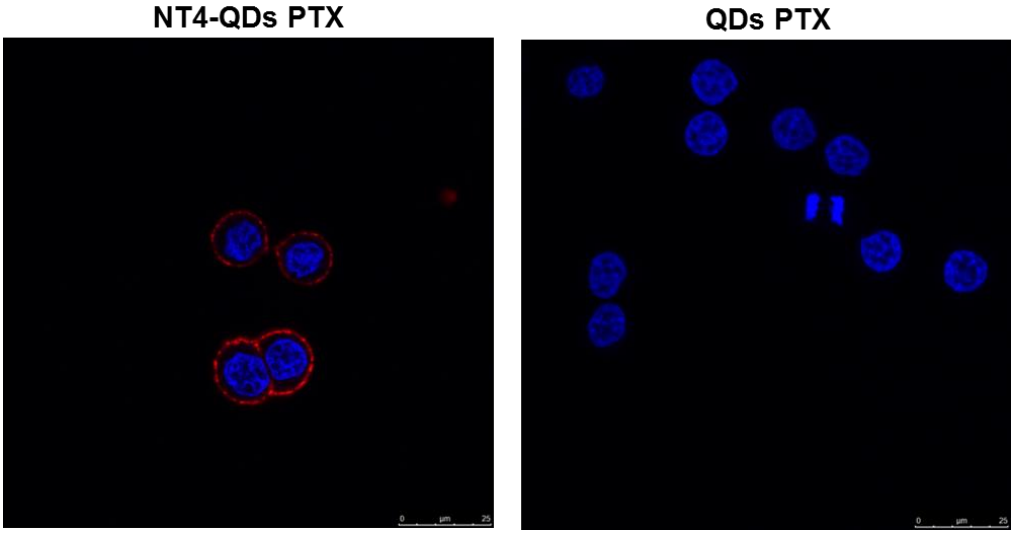

Figure 6.7 - Binding assay for NT4-QDs-PTX and QDs-PTX on HT-29 cell line.

6.6.2 Cytotoxicity assays

Cytotoxicity of both NT4-QDs-PTX and QDs-PTX was evaluated through test on human colon adenocarcinoma cell lines (HT29), by using different concentrations of QDs (40 nM, 20 nM, and 10 nM). Each sample was incubated for 1 h at 37 °C, then, cells were washed with medium and were allowed to grow for 6 days, at 37 °C. Cells viability was evaluated with 3-(4,5-dimethylthiazol-2-yl)-2,5-diphenyltetrazolium bromide (MTT) (*Figure 6.8*). A greater cytotoxicity of the targeted QDs-PTX was highlighted, in particular when using a 20 nM concentration of the nanosystem.

Indeed, while almost no toxic effect was shown for QDs-PTX, the targeted system was able to kill the 80% of involved cells.

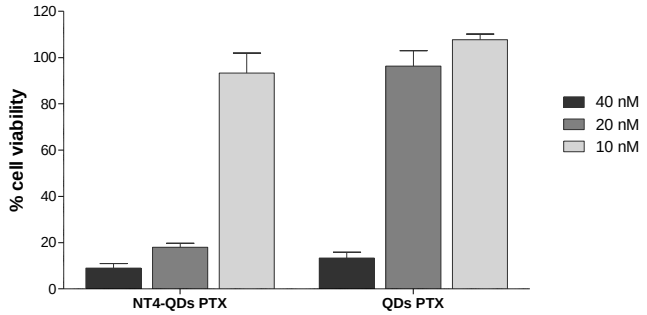

Figure 6.8- Cytotoxicity of NT4-QDs-PTX and QDs-PTX in different concentrations.

In conclusion, an efficient protocol for NT4 decoration of commercial amino-QDs was developed as well as for their decoration with both NT4 and Paclitaxel. Once the stability and the efficient targeting ability of peptide-decorated QDs was established, we developed a targeted theranostic system whose targeting potential together with its therapeutic activity was demonstrated. In the next steps, we will focus on the in vivo binding and cytotoxicity evaluation of the theranostic QDs-based drug delivery system.

7. Conclusions and future prospective

As already said in "Preface", I was admitted to PhD as a supernumerary student. In the last three years I received three research grants on two different topics. In the first year of my PhD I worked on the development of model compounds for the study of Hydrogen Atom Transfer (HAT) mechanisms in energy-related processes, whose preliminary results are not reported in this thesis. The work herein reported was carried out in my second and third PhD years, thanks to a research grant financed by Istituto Toscana Tumori (ITT) and in collaboration with Luisa Bracci's research group from the Department of Medical Biotechnologies at the University of Siena.

My PhD project was focused on the development of targeted multivalent drug delivery systems, as an evolution of the targeted drug delivery system (NT4-PTX) previously developed in our research group. Targeted delivery systems bearing a variable and defined number of Paclitaxel units (1-3) were synthesized. Their *in vitro* cytotoxicity assays demonstrated their great activity as anticancer agents and clirified, even if preliminarly, the role of vectored drug on their toxic potency.

Targeted devices bearing a higher number of therapeutic units were developed by conjugating the targeting unit to a highly functionalized nanoparticles (QDs or AuNPs), with the aim to maximize the targeting ability of NT4. Preliminary *in vitro* assays demonstrated a good binding and anticancer activity of QDs-based delivery systems, while AuNPs-based targeted carriers are currently being studied. Besides that, we designed a polyvalent NT4-based device able to carry into the tumor synergistically acting drugs, for the development of a targeted combination therapy.

Conclusions and ongoing investigation are reported in detail for each chapter.

Experimental section

Materials and methods

All the reactions were monitored by TLC on commercially available precoated plates silica gel 60 F 254) and the products were visualized with acidic vanillin solution. Silica gel 60, 230–400 mesh, was used for column chromatography. ^{1}H and ^{13}C NMR spectra were recorded with Varian Gemini 200 or Varian Mercury Plus 400 using as solvent:
- $CDCl_3$ using the reference at 7.26 ppm of the residue of chloroform in ^{1}H NMR spectra and at 77.0 ppm in the ^{13}C NMR spectra. Melting points were measured on a Stuart SMP50 Automatic Melting Point. FT-IR spectra were recorded in CDCl3 solutions with FT Infrared Spectromer 1600 Perkin-Elmer. GC – MS spectra were recorded with a QMD 100 Carlo Erba. ESI - MS spectra were measured with *J*EOL MStation *J*MS700. Commercial available reagents, catalysts and ligands were used as obtained, unless otherwise stated, from freshly opened container without further purifications. Dry dichloromethane, diethyl ether, tetrahydrofuran and dimethylformamide were obtained by Pure Solv Micro device. Acetone was distilled over calcium chloride.

Synthesis of 2'-maleimido-paclitaxel (1.2)

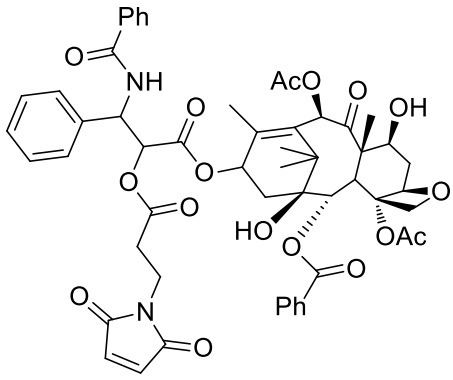

To a solution of Paclitaxel (0.050g, 0.06 mmol) in 8 mL of dry DCM, DMAP (0.0007 g, 0.006 mmol) was added, under a N_2 atmosphere. The colourless solution was cooled at 0°C, then 3-maleimidopropionic acid (0.01 g, 0.06 mmol) was added, followed by DIC (9 µL, 0.06 mmol). The reaction mixture was stirred for 18 h at r.t. to give a reddish solution, then poured onto 20 mL of DCM and washed with a saturated solution of NH_4Cl (3x40 mL), then a saturated solution of $NaHCO_3$ (2x40 mL) followed by a saturated solution of NH_4Cl (5x40 mL). The recollected organic layer was dried over Na_2SO_4, filtered and evaporated to obtain a reddish oil (48 mg). The crude was purified

by flash chromatography using EtP : AcoEt 2 : 3 as eluent to obtain the final pure product (**54**) as white powder in 52% yield.

^{1}H NMR (400MHz, $CDCl_3$) reported in literature.[147]

^{13}C-NMR (100 MHz, $CDCl_3$) δ 9.59; 14.77; 20.80; 22.14; 22.67; 26.77; 32.47; 33.29; 35.48; 43.13; 45.54; 52.36; 58.49; 71.74; 72.09; 74.47; 75.12; 75.60; 79.14; 81.02; 84.45 (24C, $C_{aliph.}$) 126.52; 127.43; 128.27; 128.50; 128.72; 129.01; 129.22; 130.26; 131.87; 132.67; 133.64; 134.03; 136.87; 142.86 (22C); 167.04; 167.24; 167.68; 169.36; 169.88; 171.24 (7C, C=O); 203.83 (1C).

FT-IR ($CDCl_3$) 3607.75, 3517.24 (m, OH stretch. free and bonded); 3387.93 (m, NH stretch. bonded); 3060.96 (w, CH_{arom} stretch.); 2948.27, 2896.55 (w, $CH_{aliph.}$ stretch.); 1737.63 (s, $C{=}O_{ester}$ stretch.); 1711.82 (s, $C{=}O_{ketone}$ stretch.); 1664.51 (s, $C{=}O_{amide}$ stretch.) cm^{-1}.

ESI -MS: *m/z* = 1027.33 $[M+Na]^+$; 1039.67 $[M+Cl]^-$.

Synthesis of 2-(hydroxymethyl)-2-(non-8-en-1-iy)propan-1,3-diol (2.3)

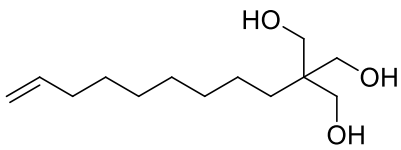

To a solution of 10-undecenal (454 mg; 2.69 mmol) and CH_2O (1.6 mL 37% aqueous solution) in H_2O/EtOH 50/50 (7 mL) a solution of KOH (151 mg; 2.69 mmol) in H_2O/EtOH 50/50 (7mL) was added at 0 °C. the mixture was stirred for 20 hours at room temperature and at 50 °C for 4 hours. Then, EtOH was evaporated under reduce pressure and the aqueous phase was extracted with diethyl eter (3x). The organic phase was dried over Na_2SO_4, filtered and evaporated under reduce pressure. The crude was purified by flash column chromatography using DCM : MeOH 9: 1 as eluent to obtain the product as colourless oil (410 mg) in 66% yield. Spectroscopic data were previously reported.[148]

^{1}H NMR (200MHz, $CDCl_3$) δ 5.90-5.70 (m, 1H); 5.03-4.90 (m, 2H); 3.67 (s, 6H); 3.46 (bs, 3H, OH); 2.07-1.97 (m, 2H); 1.26 (bs, 8H); 1.17(bs, 4H), ppm.

Synthesis of S, S'-(2-((acetylthio)methyl)-2-(non-8-en-1-yl)propan-1,3-dyil)diethanthiolate (2.4)

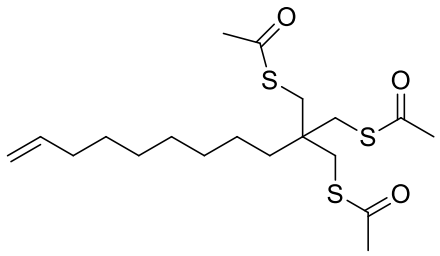

To a solution of PPh_3 (2762 mg; 10.53 mmol) in dry THF (35 mL) DIAD (2129 mg; 10.53 mmol) was added dropwise at 0 °C under nitrogen atmosphere. The mixture was heated at room temperature and a solution of 2-(hydroxymethyl)-2-(non-8-en-1-iy)propan-1,3-diol **2.3** (540 mg; 2.34 mmol) and thioacetic acid (802 mg; 10.53 mmol) in dry THF (12 mL) was added. The mixture was stirred under nitrogen overnight at room temperature and at reflux for 1 hour, then EtOH (12 mL) was added and the mixture was stirred at reflux 1 hour more. Volatile components were evaporated under reduce pressure then the residue was extracted with hexane (20 mL) to obtain a yellow oil that was purified by flash column chromatography using DCM as eluent to obtain the pure product as yellow oil (270 mg) in 29 %.

Spectroscopic data were previously reported[149].

^{1}H NMR (200 MHz, CDCl3) δ 5.90-5.70 (m, 1H), 5.03-4.85 (m, 2H), 2.97 (s, 6H), 2.33 (m, 9H), 2.07-1.93 (m, 2H), 1.30-1.10 (m, 12H) ppm.

Synthesis of 2-(mercaptomethyl)-2-(non-8-en-1-yl)propane-1,3-dithiol (2.1)

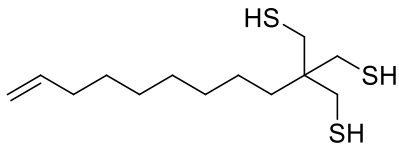

To a suspension of $LiAlH_4$ (21 mg; 0.55 mmol) in dry THF (1.5 mL) a solution of S, S'-(2-((acetylthio)methyl)-2-(non-8-en-1-yl)propan-1,3-dyil)diethanthiolate **2.4** (30 mg; 0.074 mmol) in dry THF (1.5 mL) **w**as added portionwise at 0 °C in inert atmosphere. The mixture was stirred at room temperature overnight then added to a mixture of 3M HCl and ice. The aqueous phase was extracted with DCM. The organic phase was dried over Na_2SO_4 , filtered and evaporated under reduce pressure to obtain a yellow oil (30 mg) in quantitative yield.

Spectroscopic data were previously reported[149]

^{1}H NMR (200 MHz, CDCl3) δ 5.91-5.71 (m, 1H), 5.04-4.88 (m, 2H), 2.58 (d, *J* = 10 Hz, 6H), 2.05-1.99 (m, 2H), 1.42-1.10 (m, 15H) ppm.

FT-IR (CDCl3) cm^{-1}: 2583 ($SH_{stretch.}$).

ESI - MS: *m/z* = 277 $[M-H]^-$.

Synthesis of undec-10-ynal (2.7)

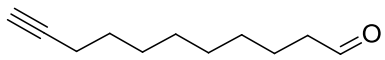

To a solution of PCC (320 mg, 1.49 mmol) in 2 mL of dry DCM, 10-undecyn-1-ol (167 mg, 0.99 mmol) was added dropwise under nitrogen. After 3 hours the mixture was quenched with water (10 mL) and washed with a saturated aqueous solution of NaCl (3x10 mL). The organic phase was dried over Na_2SO_4, filtered and evaporated under reduce pressure to afford a brownish oil (150 mg) in 91 % yield. The crude product was used without purification. Spectroscopic data were previously reported[150]

Synthesis of 2-(hydroxymethyl)-2-(non-8-yn-1-yl)propane-1,3-diol (2.8)

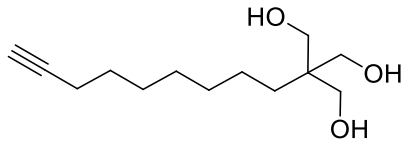

To a solution of undec-10-ynal **2.7** (480 mg, 2.86 mmol) and CH_2O (13 mL 37% aqueous solution) in 8 mL of H_2O/EtOH 50/50 a solution of KOH (151mg; 2.69 mmol) in 7 mL of H_2O/EtOH 50/50 was added at 0 °C. The mixture was stirred for 20 hours at room temperature and at 50 °C for 4 hours. Then, EtOH was evaporated under reduce pressure and the aqueous phase was extracted with diethyl eter (3x20 mL). The organic phase was dried over Na_2SO_4, filtered and evaporated under reduce pressure. The crude was purified by flash column chromatography using DCM : MeOH 10: 1 as eluent to obtain a colourless oil (320 mg) in 49% yield.

^{1}H NMR (400MHz, $CDCl_3$) δ 3.72 (bs, 3H, OH), 3.65 (s, 6H), 2.16 (td, *J* = 6.8 Hz, *J* = 2.6 Hz, 2H), 1.94 (t, *J* = 2.6 Hz, 1 H), 1.5 (quint., *J* = 6.8 Hz, 2H), 1.37-1.16 (m, 10H) ppm.

^{13}C NMR (400MHz, $CDCl_3$) δ 127.7, 84.7, 68.2, 66.1, 42.8, 30.4, 29.0, 28.6, 28.4, 22.9, 18.3 ppm. 11 found of 13 real.

Synthesis of S,S'-(2-((acetylthio)methyl)-2-(non-8-yn-1-yl)propane-1,3-diyl) diethanethioate (2.9)

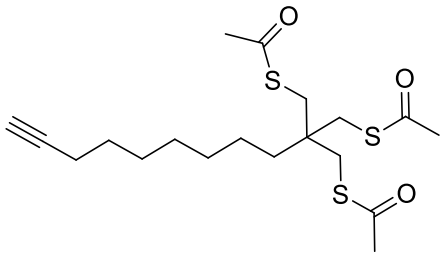

To a solution of PPh_3 (932 mg; 3.55 mmol) in 12 mL of dry THF, DIAD (718 mg; 3.55 mmol) was added dropwise at 0 °C under nitrogen atmosphere. The mixture was heated at room temperature and a solution of 2-(hydroxymethyl)-2-(non-8-yn-1-yl)propane-1,3-diol **2.8** (180 mg; 0.789 mmol) and thioacetic acid (270 mg; 3.55 mmol) in 4 mL of dry THF was added. The mixture was stirred under nitrogen overnight at

room temperature and at reflux for 1 hour, then EtOH (4 mL) was added and the mixture was stirred at reflux 1 hour more. Volatile components were evaporated under reduce pressure then the residue was extracted with hexane (9 mL) to obtain a yellow oil that was purified by flash column chromatography using DCM as eluent to obtain the pure product as yellow oil (180 mg) in 57% yield

^{1}H NMR (400MHz, $CDCl_3$) δ 2.97 (s, 1H), 2.33 (s, 9H), 2.17 (td, *J* = 6.8 Hz, *J* = 2.4 Hz, 2H), 1.93 (t, *J* = 2.4 Hz, 1H), 1.51 (quint., *J* = 6.8 Hz, 2H), 1.40-1.22 (m, 10H) ppm.

^{13}C NMR (400MHz, $CDCl_3$) δ 194.7, 68.4, 67.8, 41.0, 36.0, 35.2, 30.9, 30.4, 29.8, 28.8, 28.6, 28.4, 32.3 ppm. 13 found of 19 real.

FT-IR ($CDCl_3$) 3307, 2934, 2116, 1691 cm^{-1}.

Synthesis of 2,5-dioxopyrrolidin-1-yl 5-(1,2-dithiolan-3-yl)pentanoate (2.12)

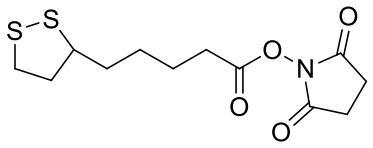

To a solution of commercial lipoic acid (200 mg, 0.97 mmol) and N-hydroxysuccinimide (112 mg, 0.97 mmol) in dry DCM (2 mL) a solution of dicyclohexylcarbodiimide (DCC) (250 mg, 1.21 mmol) in dry DCM (1.5 mL) was added dropwise at 0 °C. The mixture was stirring at 0 °C for 10 minutes and then at r.t. for 1 h. Then, the white suspension was kept at -20 °C overnight to fully precipitate DCU. The suspension was filtered under vacuum to get rid of the precipitate and the filtered solution was evaporated to afford 2,5-dioxopyrrolidin-1-yl 5-(1,2-dithiolan-3-yl)pentanoate as a yellow solid in a quantitative yield without further purification. Spectroscopic data were previously reported. [151]

^{1}H NMR (400 MHz, CDCl3) δ 3.61-3.54 (m, 1H), 3.21-3.08 (m, 2H), 2.83 (s, 4H), 2.62 (t, *J* = 7.3 Hz, 2H) 2.50-2.42 (m, 1H), 1.96-1.88 (m, 1H), 1.82-1.75 (m, 2H), 1.74 (m, 2H), 1.60-1.51 (m, 2H) ppm.
^{13}C NMR (100 MHz, CDCl3) δ 169.1, 168.4, 56.1, 40.1, 38.5, 34.4, 30.7, 28.3, 25.6, 24.4 ppm.

Synthesis of *tert*-butyl(6-aminohexyl)carbamate (2.14)

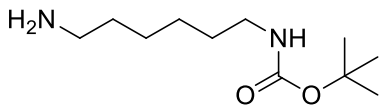

To a solution of hexamethylen diamine (1300 mg, 11.18 mmol) in 49 mL of dry DCM, a solution of di-tert-butyl-dicarbonate (488 mg, 2.24 mmol) in 6.5 mL of dry DCM was added dropwise in 20 minutes at -10 °C. The mixture was left in the ice-bath and was left to warm at room temperature. The reaction mixture was stirred overnight. Then, the white precipitate was filtered out and the filtrate was evaporated. The so obtain white solid was dissolved in 50 mL of AcOEt and the organic layer was washed with brine (3 x 50 mL). The organic layer was dried over Na_2SO_4, filtered and evaporated under vacuum to obtain a white solid (460 mg) in 95% yield. The product was used without further purification. Spectroscopic data were previously reported.[152]

^{1}H NMR ($CDCl_3$, 400 MHz) δ 4.54 (br. s, 1H), 3.08-3.10 (m, 2H), 2.68 (t, *J* = 7.0 Hz, 2H), 1.89 (s, 2H), 1.43-1.50 (m, 13H), 1.31-1.34 (m, 4H) ppm.

Synthesis of *tert*-butyl-(6-(5-(1,2-dithiolan-3-yl)pentanamido)hexyl)carbamate (2.15)

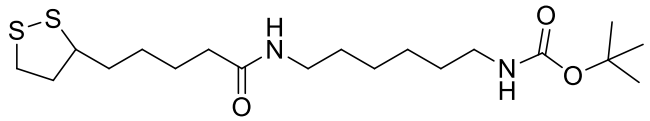

To a solution of *tert*-butyl(6-aminohexyl)carbamate **2.14** (197 mg, 0.912 mmol) and DIPEA (147 mg, 1.14 mmol) in dry DCM (5 mL), a solution of 2,5-dioxopyrrolidin-1-yl 5-(1,2-dithiolan-3-yl)pentanoate **2.12** (231 mg, 0.76 mmol) in dry DCM (5mL) was added under nitrogen atmosphere. The mixture was stirred overnight, than diluted with DCM (30 mL). The organic layer was washed with a saturated aqueous solution of $NaHCO_3$ (30 mL) and with water (4x30 mL). The organic layer was dried over Na_2SO_4, filtered and evaporated under vacuum to obtain the amide as white solid (290 mg) in 94% yield. The product was used without further purification.

^{1}H NMR (400 MHz, CDCl3) δ 5.67 (bs, 1H, NH), 4.54 (s, 1H, NH), 3.63-3.49 (m, 1H), 3.27-3.05 (m, 6H), 2.53-2.37 (m, 1H), 2.17 (t, *J* = 7Hz, 1H), 1.98-1.28 (m, 25 H) ppm.

^{13}C NMR (100MHz, CDCl3) δ 172.6, 156.1, 56.4, 40.2, 39.1, 38.4, 36.5, 34.9, 34.6, 30.0, 29.5, 28.9, 28.4, 25.4 ppm. 14 found of 19 real.

Synthesis of N-(6-(2,5-dioxo-2,5-dihydro-1H-pyrrol-1-yl)hexyl)-5-(1,2-dithiolan-3-yl)pentanamide (2.10)

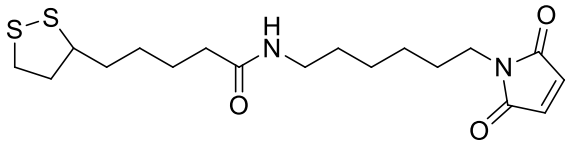

To a solution of *tert*-butyl-(6-(5-(1,2-dithiolan-3-yl)pentanamido)hexyl)carbamate **2.15** (130 mg, 0.32 mmol) in DCM (5 mL) trifluoroacetic acid (1 mL) was added dropwise at 0 °C. The mixture was stirred at r.t. for 4 hours, then a saturated aqueous solution of Na_2CO_3 was added until pH = 7-8. The aqueous phase was extracted with DCM (3x 10 mL). The organic layer was dried over Na_2SO_4, filtered and evaporated under vacuum to obtain a yellowish oil. The crude product was suspended in acetic acid (1.2 mL) and maleic anhydride (42 mg, 0.43 mmol) was added. The mixture was stirred at 140 °C for 3 hours. The solution was then evaporated under vacuum and residual acetic acid was removed by azeotroping with toluene (2 x 5 mL).). The yellowish oil was purified by flash column chromatography to affors the final product as white solid (7 mg) in 5% yield.

^{1}H NMR (400 MHz, CDCl3) δ 6.69 (s, 2H), 5.51 (br. s, NH, 1H), 3.66-3.47 (m, 3H), 3.27-3.04 (m, 4H), 2.55-2.38 (m, 1H) 2.38-1.82 (m, 3H), 1.82-1.76 (m, 14 H) ppm.

ESI - MS: *m/z* = 407.42 $[M+Na]^+$.

Syntesis of 2,5-dioxopyrrolidin-1-yl 3-(2,5-dioxo-2,5-dihydro-1H-pyrrol-1-yl)propanoate (2.18)

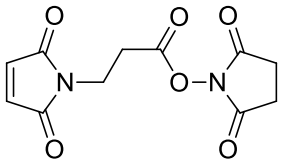

To a solution of N-hydroxysuccinimide (98 mg, 0.85 mmol) and 3-(2,5-dioxo-2,5-dihydro-1*H*-pyrrol-1-yl)propanoic acid (115 mg, 0.68 mmol) in dry DMF (4 mL), DIC (172 mg, 1.36 mmol) was added dropwise at 0 °C. After 15 min. the solution was left to warm at room temperature and the mixture was stirred under nitrogen overnight. The

mixture was diluted with DCM (40 mL) and washed with water (7 x 30 mL). The organic layer was dried over Na_2SO_4, filtered and evaporated under vacuum to obtain a white solid (110 mg) in 61% yield. The product was used without further purification.[153]

^{1}H NMR ($CDCl_3$, 400 MHz) δ 6.71 (s, 2H), 3.94 (t, J=7.0 Hz, 2H), 3.02 (t, J=7.0 Hz, 2H), 2.82 (s, 4H) ppm.

Synthesis of *tert*-butyl(6-(3-(2,5-dioxo-2,5-dihydro-1*H*-pyrrol-1-yl)propanamido)hexyl)carbamate (2.20)

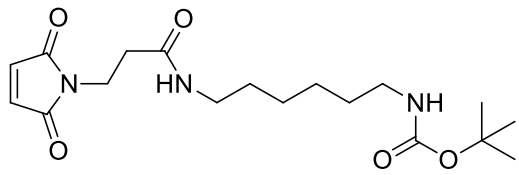

To a solution of 2,5-dioxopyrrolidin-1-yl 3-(2,5-dioxo-2,5-dihydro-1*H*-pyrrol-1-yl)propanoate **2.18** (200 mg, 0.75 mmol) in 7 mL of dry DMF a solution of *tert*-butyl(6-aminohexyl)carbamate **2.14** (175 mg, 0.80) in 7 mL of dry DMF was added slowly under nitrogen atmosphere. The reaction mixture was stirred for 22 hours, than diluted with AcOEt and washed with a saturated aqueous solution of $NaHCO_3$ (30 mL) and with water (6 x 30 mL). The organic layer was dried over Na_2SO_4, filtered and evaporated under vacuum to obtain a white solid (200 mg) in 73% yield, which was used without purification in the next step.

^{1}H NMR (400 MHz, CDCl3) δ 6.69 (s, 2H), 5.91 (br.s, 1H, NH), 4.58 (br.s, 1H, NH), 3.82 (t, *J* = 7.2, 2H), 3.21-3.16 (m, 2H), 3.11-3.06 (m, 2H), 2.50 (t, , *J* = 7.2, 2H), 1.41 (s, 9H), 1.33-1.28(m, 8H) ppm.

^{13}C NMR (100MHz, CDCl3) δ 170.5, 169.5, 110.5, 34.7, 34.3, 29.9, 29.2, 28.4, 26.3, 26.09, 26.07, 26.0, 25.5 13 found of 18 real.

Synthesis of 6-(3-(2,5-dioxo-2,5-dihydro-1*H*-pyrrol-1-yl)propanamido)hexan-1-aminium chloride (2.22)

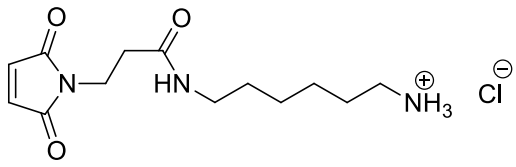

A solution of *tert*-butyl(6-(3-(2,5-dioxo-2,5-dihydro-1*H*-pyrrol-1-yl)propanamido)hexyl)carbamate **2.20** (179 mg, 0.49 mmol) in 1 mL a 3 M solution of HCl in methanol was stirred at room temperature for 1 hour; then the mixture was dried under vacuum to give a colorless oil (154 mg) in 70% yield. The product was used without purification.

^{1}H NMR (400 MHz, CDCl3) δ 6.82 (s, 2H),3.77 (t, *J* = 6.8 Hz, 2H), 3.30 (quint., J = 1.6 Hz, 2H), 3.13 (t, *J* = 6.8 Hz, 2H), 2.47 (t, *J* = 6.8 Hz, 2H), 1.70-1.63 (m 4 H), 1.53-1.35 (m, 8H) ppm.

ESI - MS: *m/z* = 268 $[M+1]^+$, 290.33 $[M+Na]^+$, 557.17 $[2M+Na]^+$

Synthesis of N-(6-(3-(2,5-dioxo-2,5-dihydro-1H-pyrrol-1-yl)propanamido)hexyl)-5-(1,2-dithiolan-3-yl)pentanamide (2.19)

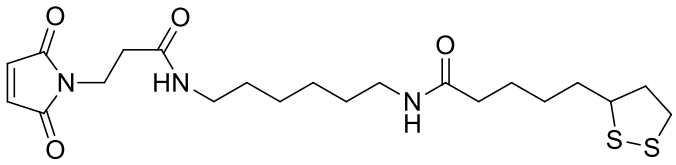

To a solution of 6-(3-(2,5-dioxo-2,5-dihydro-1*H*-pyrrol-1-yl)propanamido)hexan-1-aminium chloride **2.22** (335 mg, 0.953 mmol) in 7 mL of dry DMF, DIPEA (224 mg, 1.73 mmol) and a solution of 2,5-dioxopyrrolidin-1-yl 5-(1,2-dithiolan-3-yl)pentanoate **2.12** (263 mg, 0.87 mmol) in 7 mL of dry DMF were added. The solution was stirred under nitrogen for 20 hours. The mixture was then diluted with ethyl acetate (30 mL) and washed with a saturated aqueous solution of $NaHCO_3$ (30 mL) and with water (6 x 30

mL). The organic layer was dried over Na_2SO_4, filtered and evaporated under vacuum. The crude was purified on silica gel to obtain a white solid (62 mg) in 20% yield.

^{1}H NMR (400 MHz, CDCl3) δ 6.70 (s, 2H), 5.80 (bs, 1H, NH), 5.59 (bs, 1H, NH), 3.83 (t, *J*= 7.2 Hz, 2H), 3.60-3.53 (m, 1H), 3.26-3.07 (m, 6H), 2.51 (t, *J* = 7.2 Hz, 2H), 2.49-2.13 (m, 1H), 1.94-1.86 (m, 1H), 1.73-1.61(m, 6H), 1.51-1.43 (m, 6H), 1.34-1.29 (m, 4H) ppm.

^{13}C NMR (100MHz, CDCl3) δ 172.8, 170.5, 169.5,134.2, 56.5, 40.2, 39.0, 38.7, 38.5, 36.5, 34.7, 34.6, 34.3, 29.4, 29.2, 28.9, 25.8, 25.4 ppm. 18 found of 19 real.

ESI - MS: *m/z* = 478.42 $[M+Na]^+$.

Synthesis of (2aR,4S,4aS,6R,11S,12S,12bS)-9-((3-benzamido-2-((11-mercaptoundecanoyl)oxy)-3-phenylpropanoyl)oxy)-12-(benzoyloxy)-4,11-dihydroxy-4a,8,13,13-tetramethyl-5-oxo-2a,3,4,4a,5,6,9,10,11,12,12a,12b-dodecahydro-1H-7,11-methanocyclodeca[3,4]benzo[1,2-b]oxete-6,12b-diyl diacetate (2.25)

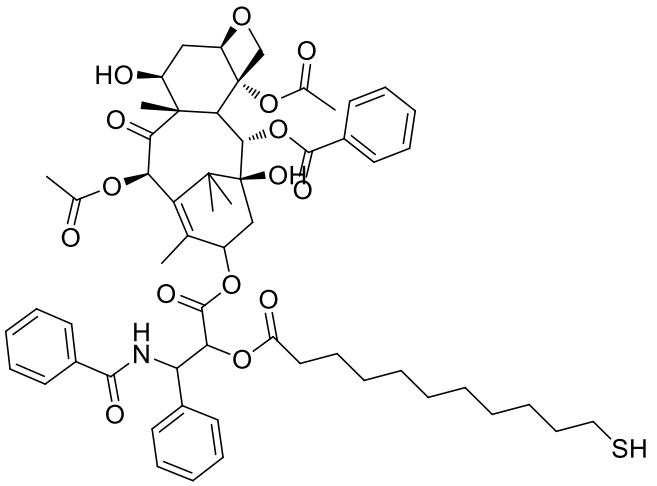

In a schlenk tube, to a solution of Taxol (145 mg, 0.17 mmol) and DMAP (4.4 mg, 0.036 mmol) in 7 mL of dry DCM, the solution of 11-mercaptoundecanoic acid (44.5 mg, 0.2 mmol) and DCC (41 mg, 0.2 mmol) in 7 mL of dry DCM were slowly added at 0 °C under nitrogen. The mixture was warmed at r.t. and stirred overnight. Then, the solution was diluted with DCM (30 mL) and washed with an aqueous saturated solution of NH_4Cl (2x30 mL), a saturated aqueous solution of $NaHCO_3$ (3x30 mL) and with an aqueous

saturated solution of NH_4Cl (2x30 mL). The organic layer was dried over Na_2SO_4, filtered and evaporated under vacuum. The crude was purified by column chromatography on silica gel to afford the final product as a white solid (130 mg, 0.123 mmol) in a 73 % yield.

^{1}H NMR (400 MHz, CDCl3) δ 8.12 (d, *J* = 7.2 Hz, 2H), 7.73 (d, *J* = 6.8Hz, 2H), 7.58 (t, *J* = 8 Hz, 1H), 7.53-7.48 (m, 3H), 7.43-7.31 (m, 7H), 6.91 (d, *J* = 8.8 Hz, 1H), 6.29 (s, 1H), 6.25 (t, *J* =8.8 Hz, 1H), 5.94 (dd, *J* = 3.2 Hz, *J* =8.8 Hz, 1H), 5.67 (d, *J* = 6.8 Hz, 1H), 5.50 (d, *J* = 3.6 Hz, 1H), 4.96 (d, *J* = 9.6 Hz, 1H), 4.47-4.41 (m, 1H), 4.30 (d, *J* = 8.4 Hz, 1H), 4.19 (d, *J* = 8.4 Hz, 1H), 3.80 (d, *J* = 6.8 Hz, 1H), 2.58-2.32 (m, 11H), 2.21-2.12 (m, 4H), 1.94-1.84 (m, 7H), 1.63-1.53 (m, 5H), 1.37-1.22 (m, 18H) ppm.

^{13}C NMR (100MHz, CDCl3) δ 203.7, 172.7, 171.2, 169.7, 168.0, 167.0, 142.7, 136.9, 133.6, 132.7, 131.9, 130.1, 29.1, 128.9, 128.7, 128.6, 128.4, 84.4, 80.9, 79.1, 76.3, 75.5, 75.0, 73.7, 72.1, 71.6, 58.4, 52.8, 45.5, 43.1, 35.5, 35.4, 33.9, 33.7, 29.3, 29.2, 29.1, 28.9, 28.8, 28.3, 26.7, 24.6, 24.5, 22.6, 22.1, 20.8, 14.8, 9.5 ppm

ESI - MS: *m/z* = 1075.83 $[M+Na]^+$.

Synthesis of (2a*R,4aS*, *6*R, 11*S*, 12*S*, 12b*S*)-9-((2-((11-((1-(3-((6-(5-(1,2-dithiolan-3-yl)-3-oxopropul)2,5-dioxopyrrolidin-3-yl)thio)undecanoyl)oxy)-3-benzamido-3-phenylpropanoyl)-12-(benzoyloxy)-4,11-dihydroxy-4a, 8, 13, 13-tetramethyl-5-oxo-2a, 3, 4, 4a, 5, 6, 9, 10, 11, 12, 12a, 12b-dodecahydro-1*H*-7, 11-methanocyclodeca[3,4]benzo[1,2-*b*]oxete-6, 12b-diyl diacetate (2.26)

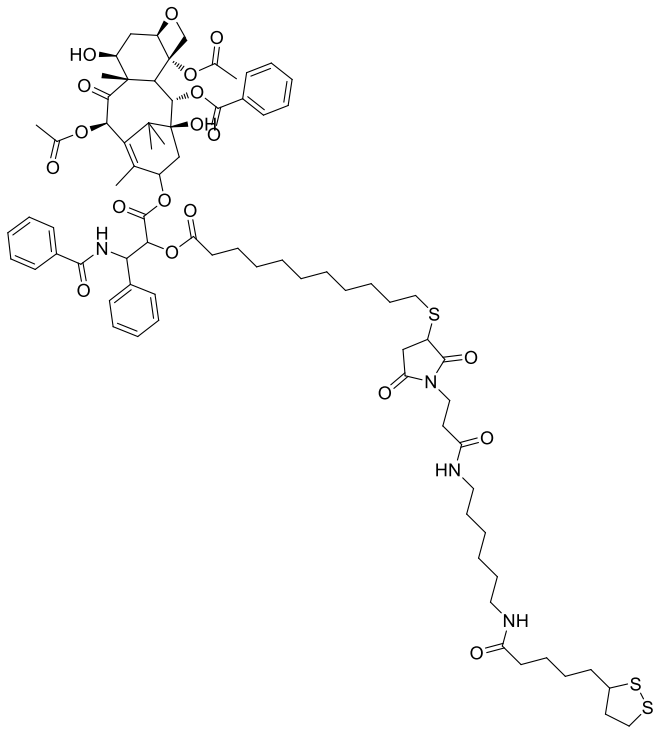

In a schlenk tube to a solution of **2.25** (118 mg, 0.112 mmol) in dry DMF (10 mL) a solution of **2.19** (51 mg, 0.112 mmol) in dry DMF (20 mL) and triethylamine (11 mg, 0.112 mmol) were added at room temperature under nitrogen atmosphere. The solution was stirred for 5 hours then quenched with water. The aqueous phase was extracted with DCM (3x30 mL). the organic phase was washed with water (6x30 mL) and a satured solution of NH_4Cl (2x30 mL). The organic layer was dried over Na_2SO_4 , filtered and evaporated under vacuum to obtain a white solid (170 mg) which was purified by flash column chromatography (eluent: ethyl acetate then DCM:methanol 15:1) to obtain the product as a white solid (85 mg, 50% yield).

^{1}H NMR (400 MHz, CDCl3) δ 8.11 (d, *J* = 7.2 Hz, 2H), 7.73 (d, *J* = 7.2 Hz, 2H), 7.57 (t, *J* =.6 Hz, 1H), 7.52-7.47 (m, 3H), 7.41-7.30 (m, 7H), 7.00 (d, *J* =9.2 Hz, 1H), 6.28 (s, 1H), 6.23 (t, *J* =8.8 Hz, 1H), 6.05-6.02 (m, 1H), 5.91 (dd, J_1 = 9.2 Hz, J_2 = 3.6 Hz, 1H), 5.79-5.76 (m, 1H), 5.66 (d, *J* = 7.2 Hz, 1H), 5.47 (d, *J* = 3.6 Hz, 1H), 4.95 (d, *J* = 9.6 Hz, 1H), 4.45-4.39 (m, 1H), 4.29 (d, *J* = 8.8 Hz, 1H), 4.18 (d, *J* = 8.4 Hz, 1H), 3.80-3.75 (*m*, 3H), 3.70-3.66 (m,

1H), 3.57-3.50 (m, 1H), 3.23-3.06 (m, 7H), 2.88-2.80 (m, 1H), 2.75-2.68 (m, 1H), 2.60-2.30 (m, 12H), 2.14 (t, *J* = 7.2 Hz, 3H), 2.03-1.98 (m, 4H), 1.92-1.82 (m, 5H), 1.69- 1.11 (m, 39H) ppm.

^{13}C NMR (100MHz, CDCl3) δ 203.8, 176.5, 174.7, 172.9, 172.8, 171.2, 169.8, 169.5, 168.2, 167.1, 166.9, 142.7, 137.0, 133.7, 133.6, 132.7, 132.0, 130.2, 129.2, 129.0, 128.7, 128.4, 127.1, 126.6, 110.5, 108.5, 84.4, 81.0, 79.0, 75.6, 75.1, 73.8, 72.1, 71.7, 58.4, 56.5, 52.9, 45.6, 43.1, 40.2, 39.03, 39.02, 38.9, 38.4, 36.5, 36.1, 35.5, 35.4, 34.6, 33.71, 33.67, 31.7, 29.4, 29.3, 29.2, 29.1, 29.0, 28.92, 28.87, 28.8, 28.7, 26.8, 25.90, 25.88, 25.4, 24.7, 22.7, 22.1, 20.8, 14.8, 9.6 ppm. (71 found of real 79)

ESI - MS: *m/z* = 1531.50 $[M+Na]^+$.

Synthesis of Thioctic acid-mPEG750 (2.28)

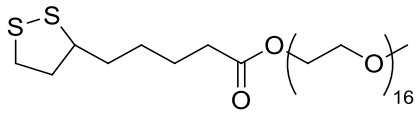

In a schlenk tube to a solution of mPEG 750 (1.21 mmol) and DMAP in dry DCM (4 mL) a suspension of DCC and thioctic acid in dry DCM (6 mL) was added dropwise at 0 °C. the mixture was left warmed at rt and stirred under nitrogen overnight. Then the white precipitate was filtered off and the filtrate was evaporated. The crude was dissolved in ethyl acetate (40 mL) and washed with water (2x15mL). The organic phase was dried over Na_2SO_4, filtered and evaporated under vacuum to obtain the final product (1.1 g; 1.17 mmol), without further purification, in a 97% yield.

^{1}H NMR (400 MHz, CDCl3) δ 4.2 (t, *J* = 8 Hz, 2H), 3.69-3.51 (m, 66H), 3.36 (s, 3H), 3.19-3.06 (m, 2H), 2.45-2.38 (m, 1H), 2.33 (t, *J* = 8 Hz, 2H), 1.93-1.85 (m, 2H), 1.71-1.60 (m, 5H), 1.52-1.39 (m, 2H) ppm.

Brust synthesis for gold nanoparticles

$HAuCl_4$ x 3 H2O (40 mg, 0.10 mmol) in 20 mL H2O were transferred in 10 mL of toluene using TOAB (137 mg, 0.25 mmol) as phase transfer. A solution of pentanethiol (10.4 mg, 0.10 mmol) or oleylamine (294 mg, 1.10 mmol) in 5 mL of toluene was added under stirring, then a cold solution of NaBH4 (54 mg, 1.43 mmol) in 3 mL of H2O was added under vigorous stirring. The solution became dark brown in 20 seconds. The solution

was stirred at room temperature for 3 hours, then water was removed and the organic phase was concentrate under reduce pressure until 2 mL. Methanol was added and the suspension was centrifugated for 15 minutes at 6000 rpm/min. The procedure was repeated for three times. Capped gold nanoparticles were stored in a toluene solution.

Synthesis of 6-Azido-hexanoic acid (3.2 and 4.16)

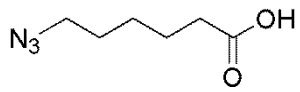

To a solution of 6-Bromo-hexanoic acid (600 mg, 3.08 mmol) in DMF (3 mL), NaN_3 (601 mg, 9.25 mmol) was added. The mixture was stirred at 85 °C for 24 h, then DCM (15 mL) was added, and the mixture was washed with HCl 0.1 M (15 mL) followed by water (6x50 mL). The organic phase was dried over Na_2SO_4, filtered and evaporated to give 210 mg the azido derivative, as a yellow oil, in 43% yield.

^{1}H NMR (400 MHz, $CDCl_3$) δ 1.35-1.51 (m, 2H), 1.56-1.75 (m, 4H), 2.38 (t, *J* = 7.4 Hz, 2H), 3.28 (t, *J* = 6.6 Hz, 2H) ppm.

Synthesis of Taxol-2'-6-azide-hexanoate (3.4 and 4.13)

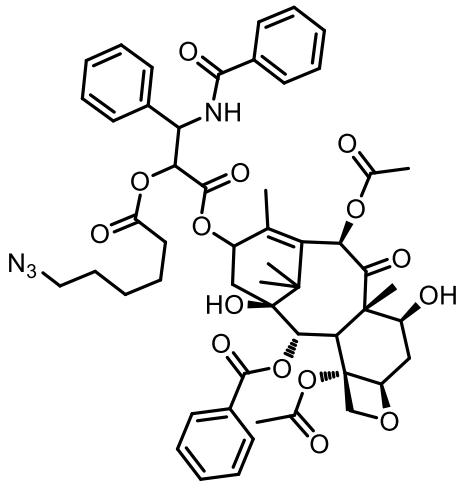

To a solution of Paclitaxel (200 mg, 0.23 mmol) in dry DCM (8 mL), DMAP (6 mg, 0.05

mmol) was added, in a N_2 atmosphere. The colourless solution was cooled at 0 °C, then 6-azido-hexanoic acid **3.2** (44 mg, 0.28 mmol) was added, followed by DCC (58 mg, 0.28 mmol). The reaction mixture was stirred for 24 h, at reflux, under a N_2 atmosphere, then poured onto DCM (15 mL) and washed with a saturated solution of NH_4Cl (3x40 mL), then a saturated solution of $NaHCO_3$ (3x40 mL) followed by a saturated solution of NH_4Cl (3x40 mL). The recollected organic layer was dried over Na_2SO_4, filtered and evaporated to obtain a white solid (270 mg). The crude was purified by flash column chromatography (EP/AcOEt 1:1) to obtain 195 mg of **3.4 (4.13)**, as white powder, in 85% yield.

^{1}H NMR (400MHz, $CDCl_3$) δ 1.14 (s, 3H), 1.23 (s, 3H), 1.31-1.38 (m, 4H), 1.52-1.63 (m, 3H), 1.68 (s, 3H), 1.94 (s, 3H), 2.17 (s, 1H), 2.23 (s, 3H), 2.33-2.42 (m, 2H), 2.46 (s, 3H), 2.48-2.60 (m, 2H), 3.21 (t, *J* = 6.8 Hz, 2H), 3.82 (d, *J* = 7.2 Hz, 1H), 4.20 (d, *J* = 8.8 Hz, 1H), 4.31 (d, *J* = 8.8 Hz, 1H), 4.42-4.47 (m, 1H), 4.97 (d, *J* = 9.6 Hz, 1H), 5.51 (d, *J* = 3.6 Hz, 1H), 5.68 (d, *J* = 7.2 Hz, 1H), 5.96 (dd, *J* = 12.0 Hz, *J* = 2.8 Hz, 1H), 6.25 (t, *J* = 10.0 Hz, 1H), 6.29 (s, 1H), 6.88 (d, *J* = 9.2 Hz, 1H), 7.34-7.63 (m, 11H), 7.74 (d, *J* = 8.4 Hz, 2H), 8.13 (d, *J* = 8.4 Hz, 2H) ppm.

Synthesis of 11-bromo undecenal (3.6)

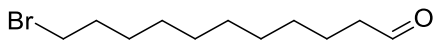

To a suspension of PCC (1280 mg; 5.98 mmol) in dry DCM (4 mL) a solution of 11-bromo undecanol (1000mg; 3.98 mmol) in dry DCM (4 mL) was added under nitrogen atmosphere. After 4 hours the solution was diluted with H_2O (20 mL) and the aqueous phase was extracted with diethyl eter (3x20 mL). The organic phase was washed with H_2O (20 mL) and a saturated solution of NaCl (3x20 mL). The organic phase was dried over Na_2SO_4, filtered and evaporated under reduce pressure to obtain a brown solid (810 mg) in 89% yield. The product was used without further purification. Spectroscopic data are previously reported.[154]

^{1}H-NMR (200MHz, $CDCl_3$) δ 9.75 (t, *J* = 1.8 Hz, 1H; CHO); 3.39 (t, *J* = 6.8 Hz, 2H); 2.41 (td, *J* = 7.4 Hz, *J* = 1.8 Hz, 2H); 1.84 (quint., 2H); 1.54-1.41 (m, 2H); 1.27 (bs, 12H) ppm.

Synthesis of 2-(9-bromononyl)-2-(hydroxymethyl) propane-1,3-diol (3.7)

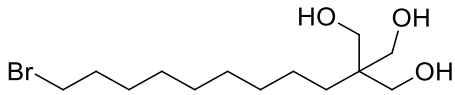

To a solution of 11-bromoundecanal **3.6** (160 mg; 0.642 mmol) and CH_2O (0.385 mL 37% aqueous solution) in H_2O/EtOH 50/50 (2 mL) a solution of KOH (36mg; 0.642 mmol) in H2O/EtOH 50/50 (2mL) was added at 0 °C. The mixture was stirred at room temperature for 20 hours and at 50 °C for 4 hours. Then, EtOH was evaporated under reduce pressure and the aqueous phase was extracted with diethyl eter (3x). The organic phase was dried over Na_2SO_4, filtered and evaporated under reduce pressure. The crude was purified by flash column chromatography using DCM : MeOH 9: 1 as eluent to obtain a colorless oil (100 mg) in 50%.

^{1}H NMR (400MHz, $CDCl_3$) δ 3.66 (s, 6H); 3.58 (bs; 3H, OH); 3.39 (t, *J* = 6.8 Hz, 2H); 1.83 c(quint., 2H); 1.42-1.36 (m, 2H); 1.26- 1.15 (m, 12H) ppm.

^{13}C NMR (400MHz, $CDCl_3$) δ 66.4; 42.8; 34.1; 30.7; 30.5; 29.4 (2C); 28.7; 28.1; 22.9 ppm.

ESI - MS: *m/z* = 333.05 $[M+Na]^+$.

Synthesis of 2-(11-Hydroxy-10,10-bis-hydroxymethyl-undecyl)-isoindole-1,3-dione (3.8)

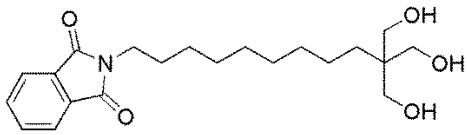

To a solution of 11-Bromo-2,2-bis-hydroxymethyl-undecan-1-o **3.7** (730 mg, 2.35 mmol) in DMF dry (15 mL), potassium phthalimide (479 mg, 2.58 mmol) was added. The yellow reaction mixture was stirred at 90 °C for 19 h, under a N_2 atmosphere. The reaction mixture was quenched with water (25 mL) and it was extracted with DCM (3x35 mL). The organic phase was washed with water (7x25 mL), dried over Na_2SO_4, filtered and evaporated to give 570 mg of compound **8**, as a white solid, in 64% yield.

Melting point: 94 °C.

^{1}H NMR (400 MHz, $CDCl_3$) δ 1.16-1.30 (m, 14H), 1.64 (t, *J* = 7.2 Hz, 2H), 3.13 (s, 3H), 3.65 (t, *J* = 7.2 Hz, 2H), 3.71 (s, 6H), 7.69-7.71 (m, 2H), 7.82-7.84 (m, 2H) ppm.

^{13}C NMR (100 MHz, $CDCl_3$) δ 1.0, 22.8, 26.7, 28.5, 29.0, 29.3, 30.4, 30.7, 38.0, 42.8, 66.9, 123.1, 132.1, 133.9, 168.5 ppm.

FT-IR ($CDCl_3$) 3630, 3551, 2931, 2857, 1711 cm^{-1}.

Synthesis of 2-(11-Prop-2-ynyloxy-10,10-bis-prop-2-ynyloxymethyl-undecyl)-isoindole-1,3-dione (3.10)

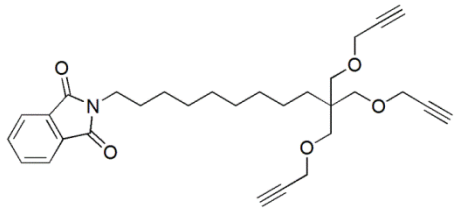

A solution of 2-(11-Hydroxy-10,10-bis-hydroxymethyl-undecyl)-isoindole-1,3-dione **3.8** (50 mg, 0.13 mmol) in DMF dry (1 mL) was cooled at 0 °C, under a N_2 atmosphere, and NaH (60% in oil, 16 mg, 0.65 mmol) was added. After 15 min, propargyl bromide (72 µL, 0.65 mmol) was added at 0 °C, dropwise. The yellow-brown solution was stirred at 0 °C for 45 min, then it was stirred at r.t. and then at 90 °C, under a N_2 atmosphere, for 48 h. The reaction mixture was cooled at 0 °C, it was acidified with HCl 0.1 M (10 mL) and it was extracted with DCM (3x20 mL). The organic layers were collected together, washed with water (6x40 mL), dried over Na_2SO_4, filtered and evaporated to give compound **3.10**, as a yellow oil, in trace. The bis-substituted derivative **3.9** (2-(10-Hydroxymethyl-11-prop-2-ynyloxy-10-prop-2-ynyloxymethyl-undecyl)-isoindole-1,3-dione) was isolated in 25% yield and characterized.

Characterization of **3.9**:

^{1}H NMR (400 MHz, $CDCl_3$) δ 1.25-1.31 (m, 12H), 1.63-1.67 (m, 4H), 2.43 (t, *J* = 2.4 Hz, 2H), 2.47 (t, *J* = 6.0 Hz, 1H), 3.48 (d, *J* = 9.0 Hz, 2H), 3.52 (d, *J* = 9.0 Hz, 2H), 3.57 (d, *J* = 6.0 Hz, 2H), 3.66 (t, *J* = 7.2 Hz, 2H), 4.13 (at, *J* = 2.0 Hz, 4H), 7.69-7.71 (m, 2H), 7.82-7.84 (m, 2H) ppm.

^{13}C NMR (100 MHz, $CDCl_3$) δ 22.8, 26.8, 28.6, 29.1, 29.4, 30.3, 30.5, 38.1, 42.7, 58.7, 66.9, 72.4, 74.4, 79.7, 123.1, 132.1, 133.8, 168.5 ppm.

FT-IR ($CDCl_3$) 3692, 3308, 2931, 2857, 1711 cm^{-1}.

Characterization of **3.10**:

^1H NMR (400 MHz, $CDCl_3$) δ 1.25-1.35 (m, 14H), 1.62-1.70 (m, 2H), 2.39-2.41 (m, 2H), 3.40 (s, 6H), 3.48 (d, *J* = 9.0 Hz, 2H), 3.67 (t, *J* = 7.2 Hz, 2H), 4.11 (d, *J* = 2.0 Hz, 6H), 7.69-7.72 (m, 2H), 7.83-7.85 (m, 2H) ppm.

^{13}C NMR (100 MHz, $CDCl_3$) δ 22.8, 26.9, 28.6, 29.2, 29.5, 30.4, 38.1, 42.7, 58.6, 70.1, 70.8, 74.0, 80.2, 123.1, 132.1, 133.8, 168.5 ppm.

FT-IR ($CDCl_3$) 3322, 2933, 2856, 1712 cm^{-1}.

Synthesis of 3,4,5-Tris-prop-2-ynyloxy-benzoic acid ethyl ester (3.12)

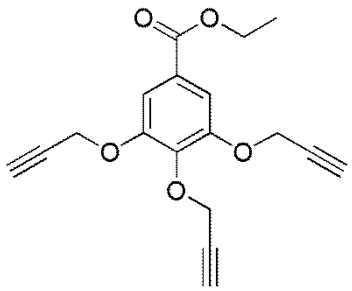

To a solution of ethyl gallate (500 mg, 2.52 mmol) in acetone dry (5 mL), K_2CO_3 (1.57 g, 11.36 mmol), 18-crown-6 (3 mg, 0.01 mmol) and propargyl bromide (1.26 mL, 11.34 mmol) were added, under a N_2 atmosphere. The suspension was stirred at reflux for 72 h. Acetone was evaporated, water (40 mL) was added and the mixture was extracted with DCM (3x30 mL). The organic phase was dried over Na_2SO_4, filtered and evaporated to give 830 mg of compound **3.12** in quantitative yield.

^1H NMR (400 MHz, CD_3OD) δ 1.38 (t, *J* = 7.2 Hz, 3H), 2.86 (t, *J* = 2.4 Hz, 1H), 3.00 (t, *J* = 2.4 Hz, 2H), 4.36 (q, *J* = 7.2 Hz, 2H), 4.78 (d, *J* = 2.4 Hz, 2H), 4.83 (d, *J* = 2.4 Hz, 4H), 7.47 (s, 2H) ppm.

Synthesis of 3,5-Dihydroxy-4-prop-2-ynyloxy-ethyl benzoate (3.13)

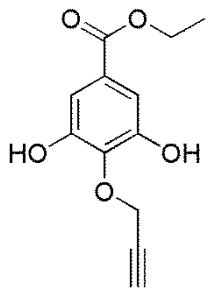

To a solution of ethyl gallate (100 mg, 0.5 mmol) in acetone dry (1 mL), K_2CO_3 (30 mg, 0.21 mmol), 18-crown-6 (1 mg, 0.004 mmol) and propargyl bromide (173 µL, 1.55 mmol) were added, under a N_2 atmosphere. The suspension was stirred at reflux for 24 h. Acetone was evaporated, water (15 mL) was added and the mixture was extracted with DCM (3x20 mL). The organic phase was dried over Na_2SO_4, filtered and evaporated to give 100 mg of crude. This was purified by flash column chromatography ($CHCl_3$/AcOEt 2:1) to give 50 mg of **3.13**, as a colorless solid, in 42% yield.

Melting point: 139 °C.

^{1}H NMR (400 MHz, CD_3OD) δ 1.35 (t, *J* = 7.2 Hz, 3H), 2.82 (t, *J* = 2.4 Hz, 1H), 4.29 (q, *J* = 7.2 Hz, 2H), 4.84 (d, *J* = 2.4Hz, 2H), 4.90 (s, 2H), 7.02 (s, 2H) ppm.

^{13}C NMR (100 MHz, $CDCl_3$) δ 14.6, 60.0, 62.0, 76.7, 80.1, 109.9, 127.4, 138.3, 152.1, 168.0 ppm.

FT-IR ($CDCl_3$) 1713, 2985, 3305, 3542, 3743 cm^{-1}.

Synthesis of 3,5-Bis-prop-2-ynyloxy-benzoic acid methyl ester (3.17)

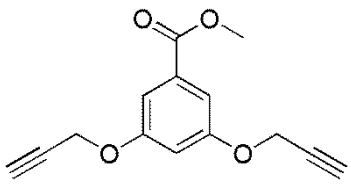

To a solution of 3,5-Dihydroxy-benzoic acid methyl ester (412 mg, 2.38 mmol) in acetone dry (4 mL), K_2CO_3 (1.316 g, 9.52 mmol), 18-crown-6 (3 mg, 0.009 mmol) and propargyl bromide (1.06 mL, 9.52 mmol) were added, under a N_2 atmosphere. The suspension was stirred at reflux for 24 h. Acetone was evaporated, water (15 mL) was added and the mixture was extracted with DCM (3x30 mL). The organic phase was dried over Na_2SO_4, filtered and evaporated to give 470 mg of pure product **3.17**, as a pale yellow powder, in 81% yield.

^{1}H NMR (400 MHz, $CDCl_3$) δ 2.55 (t, *J* = 2.4 Hz, 2H), 3.90 (s, 3H), 4.71 (d, *J* = 2.4 Hz, 4H), 6.80 (t, *J* = 2.4 Hz, 1H), 7.29 (d, *J* = 2.4 Hz, 2H) ppm.

Synthesis of 4-Hydroxy-benzoic acid ethyl ester (3.18)

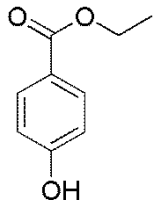

To a solution of 4-hydroxy-benzoic acid (1.5 g, 10.86 mmol) in EtOH (10 mL), concentrated H_2SO_4 (1 mL) was added. The reaction mixture was stirred for 24 h at r.t., and then was stirred at reflux for 2 h. The solution was quenched with water (25 mL) and was extracted with Et_2O (3x30 mL). The organic phase was dried over Na_2SO_4, filtered and evaporated to obtain 1.75 g of pure product **3.18**, in quantitative yield.

^{1}H NMR (200 MHz, $CDCl_3$) δ 1.38 (t, *J* = 7.0 Hz, 3H), 4.36 (q, *J* = 7.0 Hz, 2H), 6.35 (s, 1H), 6.84-6.91 (m, 2H), 7.92-8.00 (m, 2H) ppm.

Synthesis of 4-Prop-2-ynyloxy-ethyl benzoate (3.19)

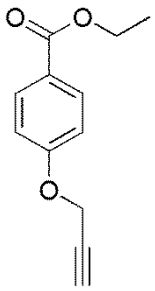

To a solution of 4-Hydroxy-benzoic acid ethyl ester **3.18** (500 mg, 3.01 mmol) in acetone dry (6 mL), K_2CO_3 (832 mg, 6.02 mmol), 18-crown-6 (3 mg, 0.01 mmol) and propargyl bromide (671 µL, 6.02 mmol) were added, under a N_2 atmosphere. The suspension was stirred at reflux for 24 h. Acetone was evaporated, water (30 mL) was added and the mixture was extracted with DCM (3x30 mL).

The organic phase was dried over Na_2SO_4, filtered and evaporated to give 600 mg of compound **3.19**, as a brown oil, in quantitative yield.

^{1}H NMR (200 MHz, $CDCl_3$) δ 1.38 (t, *J* = 7.6 Hz, 3H), 2.55 (t, *J* = 2.4Hz, 1H), 4.35 (q, *J* = 7.6 Hz, 2H), 4.75 (d, *J* = 2.4Hz, 2H), 6.99 (m, 2H), 8.02 (m, 2H) ppm.

Synthesis of (3,4,5-Tris-prop-2-ynyloxy-phenyl)-methanol (3.20)

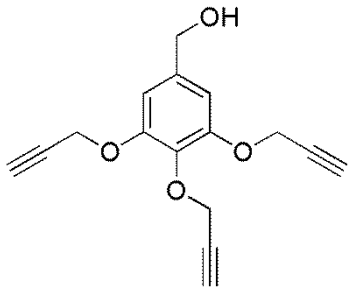

A suspension of $LiAlH_4$ (581 mg, 22.4 mmol) in THF dry (7.5 mL) was cooled at 0 °C and a solution of 3,4,5-Tris-prop-2-ynyloxy-benzoic acid ethyl ester (1.4 g, 4.48 mmol) in THF dry (7.5 mL) was added, dropwise. The reaction mixture was stirred at r.t. overnight, under a N_2 atmosphere. Then the mixture was cooled at 0 °C and a saturated solution of NH_4Cl (30 mL) was added. Then it was acidified to pH=2 with HCl 10%. The mixture was extracted with DCM (3x40 mL), dried over Na_2SO_4, filtered and evaporated to give 1.15 g of compound **3.20** in 95% yield.

^{1}H NMR (200 MHz, $CDCl_3$) δ 2.45 (t, *J* = 2.4 Hz, 1H), 2.51 (t, *J* = 2.4 Hz, 2H), 4.64 (s, 1H, OH), 4.72 (d, *J* = 2.4 Hz, 2H), 4.76 (d, *J* = 2.4 Hz, 4H), 6.77 (s, 2H) ppm.

Synthesis of 5-Chloromethyl-1,2,3-tris-prop-2-ynyloxy-benzene (3.21)

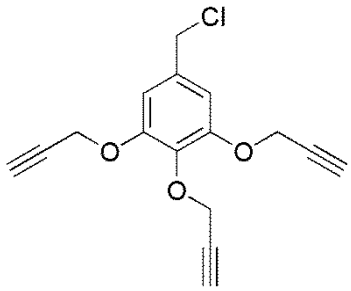

To a suspension of (3,4,5-Tris-prop-2-ynyloxy-phenyl)-methanol **3.20** (400 mg, 1.48 mmol) in Et_2O dry (1 mL), a solution of pyridine (5 µL, 0.07 mmol) and $SOCl_2$ (129 µL, 1.78 mmol) in Et_2O dry (0.5 mL) was added, dropwise. The reaction mixture was stirred

at reflux for 1 h, and then a solution of pyridine (5 µL, 0.07 mmol) and $SOCl_2$ (129 µL, 1.78 mmol) in Et_2O dry (0.5 mL) was added, dropwise. The reaction mixture was stirred at reflux for 3 h and then it was poured onto water (15 mL) and was extracted with Et_2O (3x25 mL). The organic phase was washed with water (20 mL), dried over Na_2SO_4, filtered and evaporated to gain 390 mg of **3.21,** as a brown oil in 91% yield.

^{1}H NMR (200 MHz, $CDCl_3$) δ 2.47 (t, *J* = 2.4 Hz, 1H), 2.53 (t, *J* = 2.4 Hz, 2H), 4.54 (s, 2H), 4.73 (d, *J* = 2.4 Hz, 2H), 4.77 (d, *J* = 2.4 Hz, 4H), 6.80 (s, 2H) ppm.

Synthesis of 1-(3,4,5-Tris-prop-2-ynyloxy-benzyl)-pyrrole-2,5-dione (3.24)

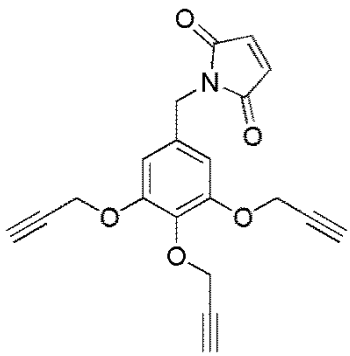

A solution of PPh_3 (89 mg, 0.34 mmol) in THF dry (2 mL) was cooled at 0 °C and DIAD (67 µL 0.34 mmol) was added dropwise. After 5 minutes a solution of (3,4,5-Tris-prop-2-ynyloxy-phenyl)-methanol **3.20** (100 mg, 0.37 mmol) in THF dry (1 mL) was added, followed by the addition of a solution of maleimide (33 mg, 0.34 mmol) in THF dry (2 mL), after 10 minutes. The flask was placed in microwave reactor. Microwave irradiation was performed at 80 °C for 30 min and then at 100 °C for 1 h. THF was evaporated obtaining 330 mg of a brown oil. The crude was purified by flash column chromatography (DCM/AcOEt 30:1) to obtain 27 mg of **3.24**, a colorless solid as pure product, in 22% yield.

Melting point: 120 °C.

^{1}H NMR (400 MHz, $CDCl_3$) δ 2.45 (t, *J* = 2.4 Hz, 1H), 2.51 (t, *J* = 2.4 Hz, 2H), 4.60 (s, 2H), 4.68 (d, *J* = 2.4 Hz, 2H), 4.73 (d, *J* = 2.4 Hz, 4H), 6.72 (s, 2H), 6.75 (s, 2H) ppm.

^{13}C NMR (100 MHz, $CDCl_3$) δ 41.4, 57.0, 60.3, 75.2, 76.0, 78.2, 79.1, 108.8, 132.3, 134.2, 136.7, 151.5, 170.2 ppm.

FT-IR ($CDCl_3$) 1711, 3308 cm^{-1}.

ESI - MS: *m/z* = 372.17 $[M+Na]^+$.

Synthesis of 1-(4-Prop-2-ynyloxy-benzyl)-pyrrole-2,5-dione (3.25)

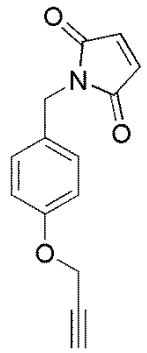

A suspension of $LiAlH_4$ (344 mg, 9.05 mmol) in THF dry (2 mL) was cooled at 0 °C and a solution of 4-Prop-2-ynyloxy- ethyl benzoate **3.19** (369 mg, 1.81 mmol) in THF dry (2 mL) was added, dropwise. The reaction mixture was stirred at r.t. overnight, under a N_2 atmosphere. Then the mixture was cooled at 0 °C and a saturated solution of NH_4Cl (15mL) was added. Then it was acidified to pH=2 with HCl 10% and was extracted with DCM (3x20 mL), dried over Na_2SO_4, filtered and evaporated to give 280 mg of the corresponding alcohol derivative ((4-Prop-2-ynyloxy-phenyl)-methanol) in 95% yield.

^1H NMR (200 MHz, $CDCl_3$) δ 2.52 (t, *J* = 2.4 Hz, 1H), 4.64 (s, 1H), 4.70 (d, *J* = 2.4 Hz, 2H), 6.95-7.02 (m, 2H), 7.30-7.35 (m, 2H) ppm.

A solution of PPh_3 (267 mg, 1.02 mmol) in THF dry (2 mL) was cooled at 0 °C and DIAD (200 µL, 1.02 mmol) was added, dropwise. After 5 min a solution of (4-Prop-2-ynyloxy-phenyl)-methanol (153 mg, 0.94 mmol) in THF dry (1 mL) was added, followed by the addition of a solution of maleimide (82 mg, 0.85 mmol) in THF dry (2 mL) after 10 min. The flask was placed in microwave reactor. Microwave irradiation was performed at 100 °C for 1 h and then at 120 °C for 45 min. THF was evaporated obtaining 730 mg of a brown oil. The crude was purified by flash column chromatography (DCM) to obtain 43 mg of **3.25,** a colorless solid as pure product in 21% yield.

Melting point: 109 °C.

^{1}H NMR (400 MHz, $CDCl_3$) δ 2.50 (t, *J* = 2.0 Hz, 1H), 4.61 (s, 2H), 4.66 (d, *J* = 2.0 Hz, 2H), 6.69 (s, 2H), 6.91 (d, *J* = 8.8 Hz, 2H), 7.30 (d, *J* = 8.8 Hz, 2H) ppm.

^{13}C NMR (100 MHz, $CDCl_3$) δ 40.7, 55.7, 75.6, 78.4, 114.9, 129.3, 129.8, 134.1, 157.1, 170.4 ppm.

FT-IR ($CDCl_3$) 1711, 1732, 2258, 3308 cm^{-1}.

Synthesis of 1-(3,5-Bis-prop-2-ynyloxy-benzyl)-pyrrole-2,5-dione (3.26)

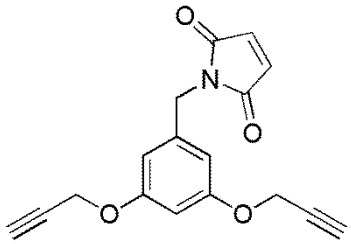

A suspension of $LiAlH_4$ (250 mg, 6.55 mmol) in THF dry (2 mL) was cooled at 0 °C and a solution of 3,5-Bis-prop-2-ynyloxy-benzoic acid methyl ester **3.17** (320 mg, 1.31 mmol) in THF dry (3 mL) was added, dropwise. The reaction mixture was stirred at r.t. overnight, under a N_2 atmosphere. Then the mixture was cooled at 0 °C and a saturated solution of NH_4Cl (15 mL) was added. Then it was acidified to pH=2 with HCl 10%. The mixture was extracted with DCM (3x20 mL), dried over Na_2SO_4, filtered and evaporated to give 280 mg of crude. This was purified by flash column chromatography (DCM/Et_2O 10:1) to give 250 mg of the corresponding alcohol (1-(3,5-Bis-prop-2-ynyloxy-benzyl)-pyrrole-2,5-dione) in 88% yield.

^{1}H NMR (200 MHz, $CDCl_3$) δ 2.53 (t, *J* = 2.4 Hz, 2H), 4.63 (s, 2H), 4.67 (d, *J* = 2.4 Hz, 4H), 6.53 (t, *J* = 2.4 Hz, 1H), 6.62 (d, *J* = 2.4 Hz, 2H) ppm.

A solution of PPh_3 (115 mg, 0.55 mmol) in THF dry (2 mL) was cooled at 0 °C and DIAD (108 µL, 0.55 mmol) was added, dropwise. After 5 min a solution of (3,5-Bis-prop-2-ynyloxy-phenyl)-methanol (110 mg, 0.51 mmol) in THF dry (1 mL) was added, followed by the addition of the solution of maleimide (45 mg, 0.46 mmol) in THF dry (2 mL) after 10 min. The flask was placed in microwave reactor. Microwave irradiation was performed at 120 °C for 1h and then at 120 °C for 20 min. THF was evaporated

obtaining 420 mg of crude. This was purified by flash column chromatography (DCM) to obtain 39 mg of **3.26** as pure product in 29% yield.

Melting point: 127 °C.

^{1}H NMR (400 MHz, $CDCl_3$) δ 2.52 (t, *J* = 2.4 Hz, 2H), 4.61 (s, 2H), 4.65 (d, *J* = 2.4 Hz, 4H), 6.52 (t, *J* = 2.0 Hz, 1H), 6.58 (d, *J* = 2.0 Hz, 2H), 6.71 (s, 2H) ppm.

^{13}C NMR (100 MHz, $CDCl_3$) δ 41.2, 55.9, 75.8, 78.1, 101.4, 107.8, 134.2, 138.4, 158.7, 170.2 ppm.

FT-IR ($CDCl_3$) 1713, 2254, 3155, 3308 cm^{-1}.

ESI - MS: *m/z* = 318.25 $[M+Na]^+$.

Synthesis of Taxol-ethyl benzoate-adduct (3.27)

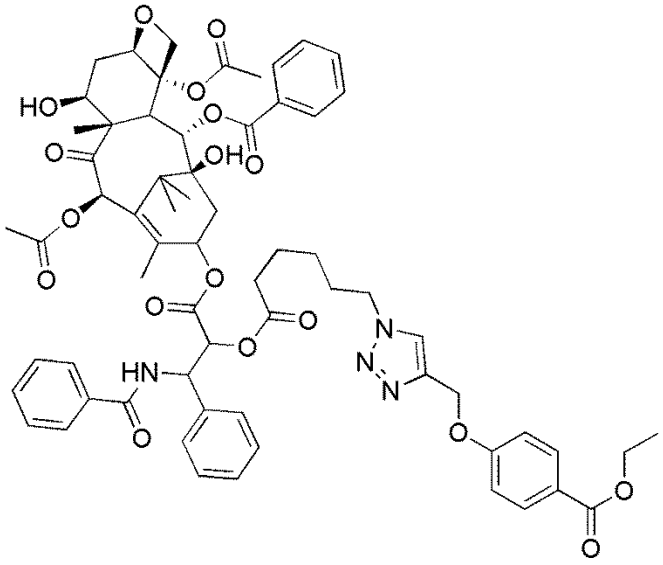

To a solution of 4-Prop-2-ynyloxy-ethyl benzoate **3.19** (134 mg, 0.07 mmol) in DMF (1 mL), $CuSO_4$ (0.5 mg, 0.003 mmol) and sodium ascorbate (1 mg, 0.006 mmol) were added. After 5 min, a solution of taxol-2'-6-azide-hexanoate **3.4** (33 mg, 0.03 mmol) in DMF dry (1 mL) was added. The solution was stirred for 24 h. Then water (0.5 mL), $CuSO_4$ (0.5 mg, 0.003 mmol) and sodium ascorbate (1 mg, 0.006 mmol) were added.

After 7 h, the reaction mixture was poured onto water (25 mL) and was extracted with DCM (3x30 mL). The organic phase was washed with water (7x25 mL), dried over Na_2SO_4, filtered and evaporated to give 30 mg of crude. The crude was purified by flash column chromatography (AcOEt/EP 1:1) to obtain 20 mg of pure product **3.27** as a white solid in 48% yield.

Melting point: 201 °C.

^{1}H NMR (400 MHz, $CDCl_3$) δ 1.13 (s, 3H), 1.23 (s, 3H), 1.25-1.31 (m, 2H), 1.36 (t, *J* = 6.8 Hz, 2H), 1.57-1.64 (m, 2H), 1.68 (s, 3H), 1.82-1.89 (m, 2H), 1.93 (s, 3H), 2.08-2.14 (m, 3H), 2.22 (s, 3H), 2.29-2.41 (m, 3H), 2.44 (s, 3H), 2.51-2.59 (m, 3H), 3.80 (d, *J* = 6.8 Hz, 1H), 4.19-4.21 (m, 1H), 4.25-4.35 (m, 4H), 4.41-4.47 (m, 1H), 4.96 (d, *J* = 8.8 Hz, 1H), 5.24 (s, 2H), 5.49 (d, *J* = 4.0 Hz, 1H), 5.68 (d, *J* = 7.2 Hz, 1H), 5.96 (dd, *J* = 9.6 Hz, *J* = 4.0 Hz, 1H), 6.22 (t, *J* = 8.0 Hz, 1H), 6.29 (s, 1H), 6.99 (d, *J* = 8.8 Hz, 2H), 7.05 (d, *J* = 9.2 Hz, 1H), 7.31-7.62 (m, 10H), 7.72 (d, *J* = 7.2 Hz, 2H), 7.98 (d, *J* = 8.8 Hz, 2H), 8.13 (d, *J* = 6.8 Hz, 2H) ppm.

^{13}C NMR (100 MHz, $CDCl_3$) δ 9.6, 14.3, 14.7, 20.8, 22.1, 22.6, 23.8, 25.5, 26.7, 29.6, 33.3, 35.5, 43.1, 45.5, 49.9, 52.8, 58.4, 60.7, 62.0, 71.8, 72.0, 74.0, 75.0, 75.5, 76.4, 79.1, 81.0, 84.4, 114.3, 122.6, 123.5, 126.5, 127.0, 128.4, 128.6, 129.0, 129.2, 130.2, 131.5, 131.9, 132.8, 133.6, 136.9, 142.6, 143.5, 161.7, 166.2, 166.9, 167.1, 168.1, 169.8, 171.1, 172.2, 203.7 ppm.

FT-IR ($CDCl_3$) 1715, 2947, 3447 cm^{-1}.

ESI - MS: *m/z* = 1219.42 $[M+Na]^+$.

Synthesis of Mono-Taxol-Maleimide adduct (29)

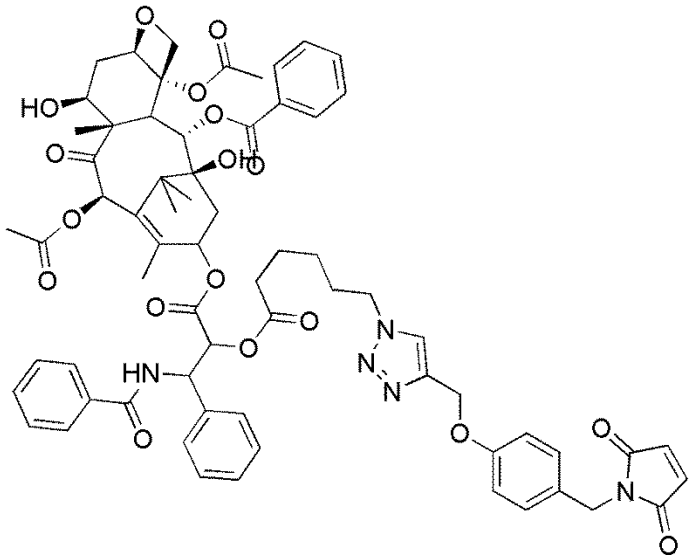

To a solution of 1-(4-Prop-2-ynyloxy-benzyl)-pyrrole-2,5-dione **3.25** (10 mg, 0.04 mmol) in DMF (2 mL) $CuSO_4$ (1 mg, 0.006 mmol) and sodium ascorbate (2 mg, 0.01 mmol) were added. After 5 min, a solution of taxol-2'-6-azide-hexanoate **3.4** (49 mg, 0.05 mmol) in DMF (2 mL) and water (1.5 mL) were added. The solution was stirred at r.t. for 24 h. The reaction mixture was poured onto water (25 mL) and was extracted with DCM (3x30 mL). The organic phase was washed with water (7x25 mL), dried over Na_2SO_4, filtered and evaporated to give 50 mg of crude. The crude was purified by flash column chromatography (AcOEt/EP 5:1) to obtain 21 mg of pure product (**3.28**) as a white solid in 42% yield.

^{1}H NMR (400 MHz, $CDCl_3$) δ 1.13 (s, 3H), 1.23 (s, 3H), 1.25-1.31 (m, 3H), 1.57-1.64 (m, 2H), 1.68 (s, 3H), 1.82-1.89 (m, 3H), 1.93 (s, 3H), 2.08-2.14 (m, 1H), 2.22 (s, 3H), 2.29-2.41 (m, 3H), 2.44 (s, 3H), 2.51-2.59 (m, 2H), 3.80 (d, *J* = 6.8 Hz, 1H), 4.18-4.32 (m, 4H), 4.41-4.47 (m, 1H), 4.60 (s, 2H), 4.96 (d, *J* = 8.8 Hz, 1H), 5.16 (s, 2H), 5.49 (d, *J* = 4.0 Hz, 1H), 5.68 (d, *J* = 7.2 Hz, 1H), 5.96 (dd, *J* = 9.6 Hz, *J* = 4.0 Hz, 1H), 6.22 (t, *J* = 8.0 Hz, 1H), 6.29 (s, 1H), 6.67 (s, 2H), 6.90 (d, *J* = 8.8 Hz, 2H), 7.07 (d, *J* = 9.2 Hz, 1H), 7.28-7.63 (m, 12H), 7.72 (d, *J* = 7.2 Hz, 2H), 8.13 (d, *J* = 7.2 Hz, 2H) ppm.

^{13}C NMR (100 MHz, $CDCl_3$) δ 9.5, 14.7, 20.8, 22.1, 22.6, 23.8, 25.5, 26.7, 29.6, 33.3, 35.50, 35.52, 40.7, 43.1, 45.5, 49.8, 52.8, 58.4, 62.0, 71.7, 72.0, 74.0, 75.0, 75.5, 76.4, 79.0, 81.0, 84.4, 114.8, 122.5, 126.5, 127.0, 128.4, 128.6, 129.04, 129.08, 129.1, 129.8,

130.1, 131.9, 132.7, 133.64, 133.67, 134.1, 136.8, 142.6, 144.1, 157.7, 166.9, 167.1, 168.1, 169.8, 170.4, 171.1, 172.2, 203.7 ppm.

ESI - MS: *m/z* = 1256.42 $[M+Na]^+$.

Synthesis of 3,4-Bis-prop-2-ynyloxy-benzoic acid ethyl ester (3.31)

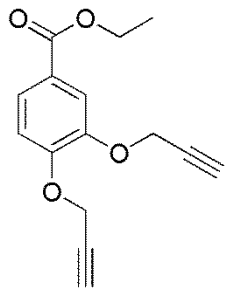

To a solution of 3,4-Dihydroxy-benzoic acid ethyl ester (258 mg, 1.42 mmol) in acetone dry (4 mL), K_2CO_3 (782 mg, 5.66 mmol), 18-crown-6 (2 mg, 0.007 mmol) and propargyl bromide (630 µL, 5.66 mmol) were added, under a N_2 atmosphere. The suspension was stirred at reflux for 24 h. Acetone was evaporated, water (15 mL) was added and the mixture was extracted with DCM (3x30 mL). The organic phase was dried over Na_2SO_4, filtered and evaporated to give 380 mg of crude. This was purified by flash column chromatography (ACOEt/EP 1:1) to gain 297 mg of pure product (**3.31**) in 81% yield.

^{1}H NMR (400 MHz, $CDCl_3$) δ 1.37 (t, *J* = 7.2 Hz, 3H), 2.53 (t, *J* = 2.4 Hz, 2H), 4.35 (q, *J* = 7.2 Hz, 2H), 4.80 (d, *J* = 2.4 Hz, 2H), 4.81 (d, *J* = 2.4 Hz, 2H), 7.06 (d, *J* = 9.2 Hz, 1H), 7.71-7.73 (m, 2H) ppm.

^{13}C NMR (100 MHz, $CDCl_3$) δ 14.3, 56.6, 56.9, 60.9, 76.2, 76.4, 77.7, 77.9, 113.1, 115.4, 124.0, 124.2, 146.8, 151.2, 166.0 ppm.

FT-IR ($CDCl_3$) 1718, 2857, 2935, 3437 cm^{-1}.

ESI - MS: *m/z* = 208.08 $[M+Na]^+$.

Synthesis of 6-Azido-hexanoic acid ethyl ester (3.32)

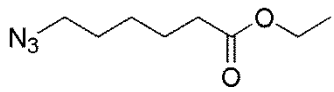

To a solution of 6-Azido-hexanoic acid (93 mg, 0.59 mmol) in EtOH (2 mL), concentrated H_2SO_4 (2 drops) was added. The reaction mixture was stirred for 24 h at r.t. The solution was quenched with water (15 mL) and was extracted with DCM (2x25 mL). The organic phase was dried over Na_2SO_4, filtered and evaporated to obtain 81 mg of pure product (**33**), as a colorless oil in 75% yield.

^{1}H NMR (400 MHz, $CDCl_3$) δ 1.25 (t, *J* = 7.2 Hz, 3H), 1.36-1.44 (m, 2H), 1.57-1.69 (m, 4H), 2.30 (t, *J* = 7.6 Hz, 2H), 3.26 (t, *J* = 7.2 Hz, 2H), 4.12 (q, *J* = 7.2 Hz, 2H) ppm.

^{13}C NMR (100 MHz, $CDCl_3$) δ 14.2, 24.4, 26.2, 28.5, 34.1, 51.2, 60.2, 173.4 ppm.

FT-IR ($CDCl_3$) 1727, 2100, 2868, 2942, 2983 cm^{-1}.

Synthesis of 3,4-Bis-[1-(5-ethoxycarbonyl-pentyl)-1H-[1,2,3]triazol-4-ylmethoxy]-benzoic acid ethyl ester (3.33)

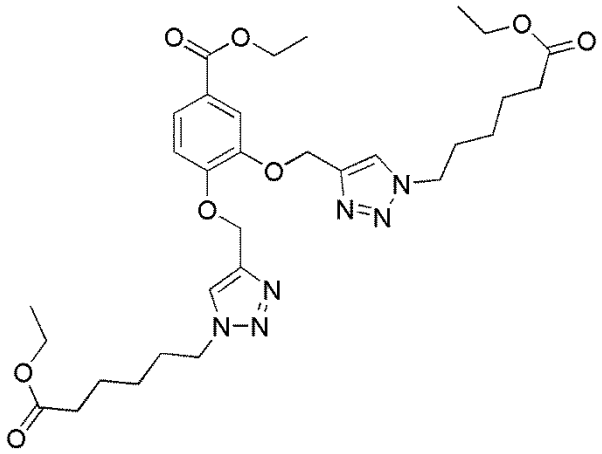

To a solution of 3,4-Bis-prop-2-ynyloxy-benzoic acid ethyl ester **3.31** (30 mg, 0.12 mmol) in DMF (3 mL) $CuSO_4$ (4 mg, 0.024 mmol) and sodium ascorbate (9 mg, 0.05 mmol) were added. After 5 min, a solution of 6-Azido-hexanoic acid ethyl ester **3.32** (56 mg, 0.30 mmol) in DMF (3 mL) and water (1 mL) were added. The solution was stirred

at r.t. for 24 h. The reaction mixture was poured onto water (15 mL) and was extracted with DCM (3x25 mL). The organic phase was washed with water (7x25 mL), dried over Na_2SO_4, filtered and evaporated to give 47 mg of crude. The crude was purified by flash column chromatography (AcOEt/EP 2:1) to obtain 36 mg of pure product (**3.33**), as a white solid, in 48% yield.

^{1}H NMR (400 MHz, $CDCl_3$) δ 1.22 (2t, *J* = 7.2 Hz, 6H), 1.30-1.35 (m, 4H), 1.36 (t, *J* = 7.2 Hz, 3H), 1.60-1.69 (m, 4H), 1.84-1.95 (m, 4H), 2.27 (2d, *J* = 7.2 Hz, 4H), 4.09 (2q, *J* = 7.2 Hz, 4H), 4.30-4.36 (m, 6H), 5.26 (s, 2H), 5.30 (s, 2H), 7.06 (d, *J* = 8.4 Hz, 1H), 7.66-7.69 (m, 4H) ppm.

^{13}C NMR (100 MHz, $CDCl_3$) δ 14.2, 14.3, 24.2, 25.9, 29.90, 29.94, 33.9, 50.09, 50.14, 60.3, 60.9, 63.2, 63.6, 113.7, 116.2, 122.9, 123.0, 123.9, 124.5, 143.5, 143.6, 147.8, 152.4, 166.0, 173.3 ppm.

FT-IR ($CDCl_3$) 1724, 2248, 2871, 2942, 2983 cm^{-1}.

ESI - MS: *m/z* = 651.33 $[M+Na]^+$.

Synthesis of 1-(3,4-Bis-prop-2-ynyloxy-benzyl)-pyrrole-2,5-dione (3.34)

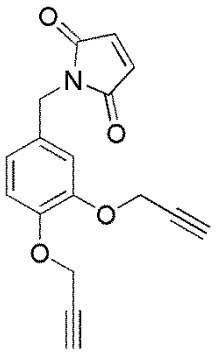

A suspension of $LiAlH_4$ (160 mg, 4.21 mmol) in THF dry (4 mL) was cooled at 0 °C and a solution of 3,4-Bis-prop-2-ynyloxy-benzoic acid ethyl ester (140 mg, 0.54 mmol) in THF dry (4 mL) was added, dropwise. The reaction mixture was stirred at r.t. overnight, under a N_2 atmosphere. Then the mixture was cooled at 0 °C and a saturated solution of NH_4Cl (15 mL) was added. Then it was acidified to pH=2 with HCl 10%. The mixture was extracted with DCM (3x20 mL), dried over Na_2SO_4, filtered and evaporated to give

130 mg of crude. The crude was purified by flash column chromatography (DCM/MeOH 20:1) to gain 70 mg of the corresponding alcohol ((3,4-Bis-prop-2-ynyloxy-phenyl)-methanol), as a white solid, in 42% yield.

^{1}H NMR (200 MHz, $CDCl_3$) δ 2.49-2.52 (m, 2H), 4.63 (d, *J* = 5.0 Hz, 2H), 4.76 (at, *J* = 2.2 Hz, 4H), 6.97-7.09 (m, 3H) ppm.

A solution of PPh_3 (92 mg, 0.35 mmol) in THF dry (1 mL) was cooled at 0 °C and DIAD (70 µL, 0.35 mmol) was added dropwise. After 5 min, a solution of (3,5-Bis-prop-2-ynyloxy-phenyl)-methanol (70 mg, 0.32 mmol) in THF dry (2 mL) was added, followed by the addition of the solution of maleimide (29 mg, 0.29 mmol) in THF dry (2 mL) after 10 min. The flask was placed in microwave reactor. Microwave irradiation was performed at 120 °C for 1 h and then at 120 °C for 20 min. THF was evaporated obtaining 280 mg of crude. This was purified by flash column chromatography (DCM/Et_2O 10:1) to obtain 28 mg of a yellow solid as pure product (**3.34**) in 33% yield.

^{1}H NMR (400 MHz, $CDCl_3$) δ 2.49 (t, *J* = 2.4 Hz, 1H), 2.51 (t, *J* = 2.4 Hz, 1H), 4.61 (s, 2H), 4.72 (d, *J* = 2.4 Hz, 2H), 4.73 (d, *J* = 2.4 Hz, 2H), 6.69 (s, 2H), 6.96-6.97 (m ,2H), 7.06 (d, *J* = 1.2 Hz, 1H) ppm.

^{13}C NMR (100 MHz, $CDCl_3$) δ 41.0, 56.8, 56.9, 75.9, 76.0, 78.2, 78.4, 114.7, 115.3, 122.2, 130.1, 134.2, 147.1, 147.4, 170.3 ppm.

FT-IR ($CDCl_3$) 1711, 1732, 3307 cm^{-1}.

ESI - MS: *m/z* = 318.17 $[M+Na]^+$.

Synthesis of Bis-Taxol-Maleimide adduct (3.35)

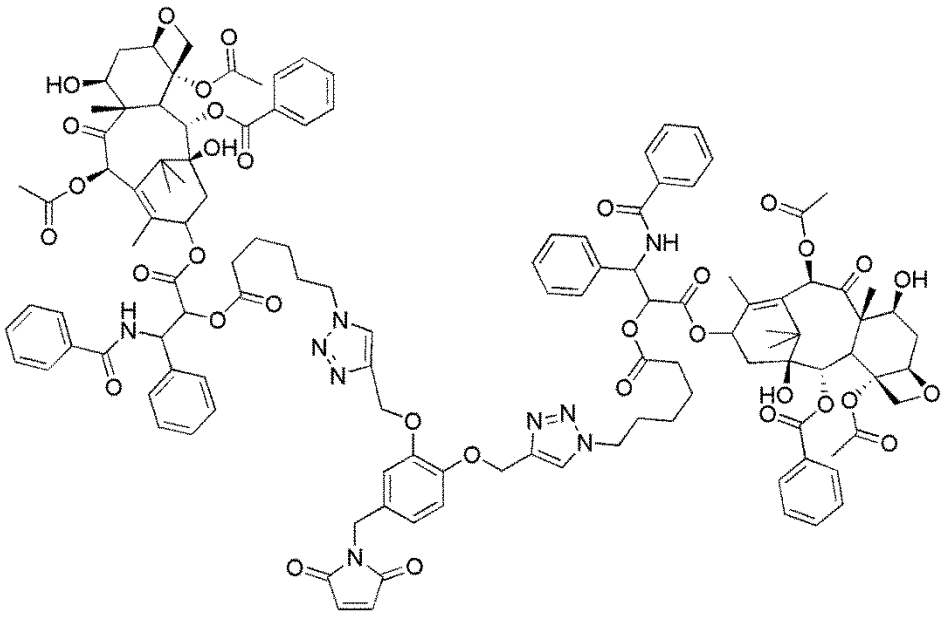

To a solution of 1-(3,4-Bis-prop-2-ynyloxy-benzyl)-pyrrole-2,5-dione **3.34** (15 mg, 0.05 mmol) in DMF (1.5 mL), $CuSO_4$ (1 mg, 0.007 mmol) and sodium ascorbate (4 mg, 0.02 mmol) were added. After 5 min, a solution of taxol-2'-6-azide-hexanoate **3.4** (97 mg, 0.10 mmol) in DMF (1.5 mL) and water (1 mL) were added. The solution was stirred at r.t. for 24 h. The reaction mixture was poured onto water (20 mL) and was extracted with DCM (3x20 mL). The organic phase was washed with water (7x25 mL), dried over Na_2SO_4, filtered and evaporated to give 90 mg of crude. The crude was purified by flash column chromatography (AcOEt/EP 5:1 → AcOEt), to obtain 27 mg of pure product (**3.35**) as a brown solid in 23% yield.

^{1}H NMR (400 MHz, $CDCl_3$) δ 1.12-1.25 (m, 18H), 1.56-1.75 (m, 10H), 1.75 -1.92 (m, 16H), 2.04-2.10 (m, 4H), 2.20 (s, 6H), 2.26- 2.37 (m, 6H), 2.43 (s, 6H), 2.49-2.62 (m, 4H), 3.79 (d, *J* = 7.2 Hz, 2H), 4.18 (d, *J* = 7.6 Hz, 2H), 4.29 (d, *J* = 8.4 Hz, 2H), 4.41-4.46 (m, 2H), 4.55 (s, 2H), 4.95 (d, *J* = 9.6 Hz, 2H), 5.17 (s, 1H), 5.19 (s, 1H), 5.50 (d, *J* = 4.0 Hz, 2H), 5.66 (d, *J* = 6.8 Hz, 2H), 5.94 (dd, *J* = 4.0 Hz, *J* = 9.2 Hz, 2H), 6.20 (t, *J* = 8.0 Hz, 2H), 6.29 (s, 2H), 6.66 (s, 2H), 6.93-6.95 (m, 1H), 7.15-7.18 (m, 2H), 7.29-7.63 (m, 24H), 7.71 (d, *J* = 7.6 Hz, 4H), 8.12 (d, *J* = 7.2 Hz, 4H) ppm.

^{13}C NMR (100 MHz, $CDCl_3$) δ 9.6, 14.8, 20.8, 22.1, 22.7, 23.8, 25.5, 26.8, 29.6, 33.3, 35.4, 35.6, 43.1, 45.6, 49.8, 53.0, 58.4, 71.7, 72.0, 74.1, 75.0, 75.6, 79.1, 81.0, 84.4, 126.7, 127.1, 128.5, 128.6, 128.7, 129.0, 129.2, 130.2, 131.9, 132.8, 133.6, 133.7, 134.2, 137.0, 142.7, 167.0, 167.1, 168.2, 169.8, 170.4, 171.1, 172.3, 203.7 ppm.

Ft-IR ($CDCl_3$) 1713, 2248, 2258, 2944, 3447, 3524, 3567 cm^{-1}.

ESI - MS: *m/z* = 2303.88 $[M+Na]^+$.

Synthesis of Tri-Taxol-Maleimide adduct (3.36)

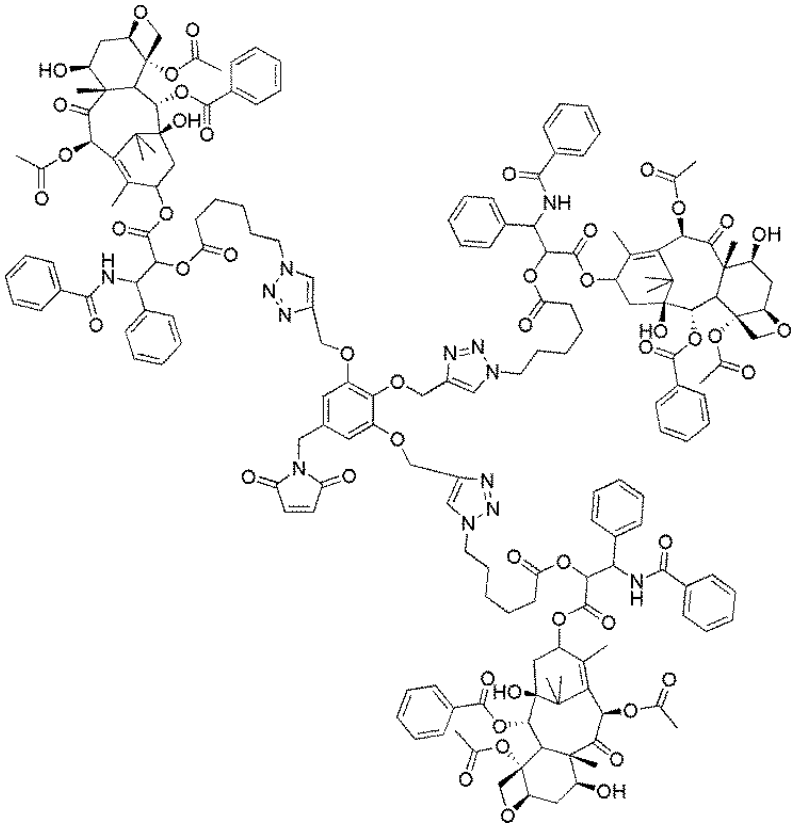

To a solution of 1-(3,4,5-Tris-prop-2-ynyloxy-benzyl)-pyrrole-2,5-dione **3.24** (8 mg, 0.02 mmol) in DMF (3 mL), $CuSO_4$ (1 mg, 0.007 mmol) and sodium ascorbate (3 mg, 0.01 mmol) were added. After 5 min, a solution of taxol-2'-6-azide-hexanoate **3.4** (90 mg, 0.09 mmol) in DMF (3 mL) and water (1.5 mL) were added. The solution was stirred at r.t. for 48 h. The reaction mixture was poured onto water (25 mL) and was extracted with DCM (3x30 mL). The organic phase was washed with water (7x25 mL), dried over Na_2SO_4, filtered and evaporated to give 40 mg of crude. The crude was purified by flash column chromatography (DCM/MeOH 10:1), to obtain 12 mg of pure product as a white solid in 16% yield.

^{1}H NMR (400 MHz, $CDCl_3$) δ 1.12 (s, 9H), 1.25 (s, 9H), 1.25-1.40 (m, 6H), 1.54-1.62 (m, 6H), 1.66-1.96 (m, 12H), 1.79-1.87 (m, 4H), 1.91 (s, 9H), 2.05-2.11 (m, 3H), 2.20 (s, 9H), 2.25-2.36 (m, 9H), 2.42 (s, 9H), 2.49-2.66 (m, 6H), 3.42-3.50 (m, 3H), 3.78 (d, *J* = 7.2 Hz, 3H), 4.09-4.31 (m, 15H), 4.40-4.53 (m, 3H), 4.95 (d, *J* = 9.6 Hz, 3H), 5.07-5.15 (m, 4H), 5.48 (d, *J* = 4.0 Hz, 3H), 5.66 (d, *J* = 6.8 Hz, 3H), 5.93 (dd, *J* = 6.8 Hz, *J* = 4.4 Hz, 3H), 6.17-

6.23 (m, 3H), 6.29 (s, 3H), 6.66 (s, 2H), 6.69 (s, 2H), 7.31-7.53 (m, 27H), 7.59-7.73 (m, 12H), 8.12 (d, *J* = 8.4 Hz, 6H) ppm.

^{13}C (100 MHz, $CDCl_3$) δ 9.6, 14.8, 20.8, 22.05, 22.08, 22.7, 23.8, 24.9, 25.5, 26.7, 29.60, 29.64, 29.68, 33.2, 33.9, 43.1, 49.1, 49.8, 58.4, 75.5, 79.0, 80.9, 84.3, 84.4, 126.7, 127.1, 128.64, 128.69, 129.0, 129.1, 130.1, 133.6, 136.9, 166.9, 167.1, 168.2, 169.8, 170.3, 171.1, 172.3, 203.7

Ft-IR ($CDCl_3$) 1713, 2801, 2860, 3308, 3435 cm^{-1}.

ESI - MS: *m/z* = 1665.17 $[(M+2H)/2]^+$.

Synthesis of 6-Bromo-hexanoic acid benzyl-[(4-bromo-phenyl)-cyclohexylcarbamoyl-methyl]-amide (4.6)

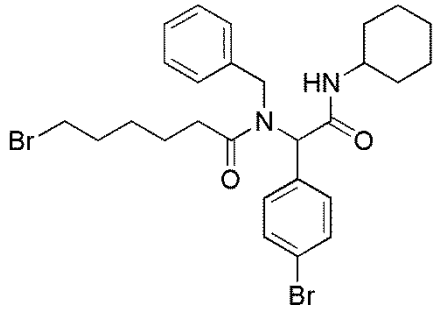

To a solution of cyclohexyl isocyanide (20 mg, 0.18 mmol), 4-Bromo-benzaldehyde (113 mg, 0.61 mmol), 6-Bromo-hexanoic acid (37 mg, 0.19 mmol) in MeOH (1 mL), benzylamine (13 µL, 0.12 mmol) was added, dropwise. The reaction mixture was stirred at r.t. for 1h. MeOH was evaporated to obtain 150 mg of crude. The crude was purified by flash column chromatography (EP/AcOEt 3:1 → 2:1) to gain 40 mg of **4.6**, as a pink solid, in 58% yield.

Melting point: 127 °C.

^{1}H NMR (400 MHz, $CDCl_3$) δ 1.01-1.15 (m, 3H), 1.24-1.40 (m, 4H), 1.56-1.86 (m, 9H), 2.32-2.40 (m, 1H), 2.21-2.29 (m, 1H), 3.34 (t, *J* = 6.8 Hz, 2H), 3.72-3.79 (m, 1H), 4.51 (d, *J* = 17.6 Hz, 1H), 4.72 (d, *J* = 17.6 Hz, 1H), 5.78 (d, *J* = 7.6 Hz, 1H), 5.85 (s, 1H), 6.98 (d, *J* = 8 Hz, 2H), 7.18-7.22 (m, 5H), 7.36 (d, *J* = 8 Hz, 2H) ppm.

^{13}C NMR (100 MHz, $CDCl_3$) δ 24.2, 24.65, 24.71, 25.4, 27.7, 32.4, 32.68, 32.74, 33.6, 33.7, 48.6, 50.1, 62.2, 108.5, 110.4, 122.6, 126.0, 127.1, 128.4, 131.2, 131.7, 134.2, 137.3, 168.2, 174.6 ppm.

ESI - MS: *m/z* = 577.42 $[M-H]^-$.

Synthesis of N-Benzyl-N-[(4-bromo-phenyl)-cyclohexylcarbamoyl-methyl]-3-(2,5-dioxo-2,5-dihydro-pyrrol-1-yl)-propionamide (4.10)

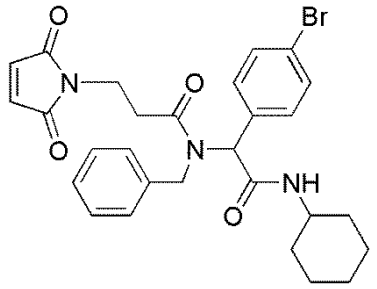

To a solution of cyclohexyl isocyanide (20 mg, 0.18 mmol), 4-Bromo-benzaldehyde (113 mg, 0.61 mmol), 3-(2,5-Dioxo-2,5-dihydro-pyrrol-1-yl)-propionic acid **4.9** (32 mg, 0.19 mmol) in MeOH (1 mL), benzylamine (13 µL, 0.12 mmol) was added, dropwise. The reaction mixture was stirred at r.t. for 1h. MeOH was evaporated to obtain 170 mg of crude. The crude was purified by flash column chromatography (EP/AcOEt 1:1) to gain 40 mg of **4.10**, as a white solid, in 60% yield.

Melting point: 190 °C

^{1}H NMR (400 MHz, $CDCl_3$) δ 1.01-1.16 (m, 3H), 1.27-1.37 (m, 2H), 1.56-1.69 (m, 4H), 1.85-1.88 (m, 2H), 2.51-2.59 (m, 1H), 2.67-2.75 (m, 1H), 3.70-3.77 (m, 1H), 3.81 (t, *J* = 7.2 Hz, 1H), 4.50 (d, *J* = 17.6 Hz, 1H), 4.68 (d, *J* = 17.6 Hz, 1H), 5.70 (d, *J* = 8 Hz, 1H), 5.88 (s, 1H), 6.64 (s, 2H), 6.93 (d, *J* = 6.8 Hz, 2H), 7.16-7.21 (m, 5H), 7.35 (d, *J* = 8.4 Hz, 2H) ppm.

^{13}C NMR (100 MHz, $CDCl_3$) δ 24.7, 24.8, 25.4, 32.1, 32.69, 32.72, 34.1, 28.7, 49.9, 61.7, 122.7, 125.9, 127.1, 128.5, 131.3, 131.7, 134.0, 134.1, 136.8, 167.9, 170.4, 171.9 ppm.

FT-IR ($CDCl_3$) 1711, 2248, 2857, 2936, 3424 cm^{-1}.

ESI - MS: *m/z* = 1126.75 $[2M+Na]^+$.

Synthesis of 3-(2,5-dioxo-2,5-dihydro-1*H*-pyrrol-1-yl)propanoic acid (4.9)

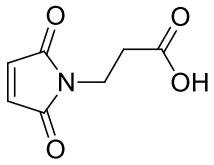

A suspension of maleic anhydride (1.50 g, 16.84 mmol) and β-alanine (1.65 g, 16.84 mmol) in 45 mL of acetic acid was heated at reflux (bath temperature: 140 °C) for 90 min., then stirred at r.t. for 16 h. The solution was refluxed again for 4h. The solution was then evaporated under vacuum and residual AcOH was removed by azeotroping with toluene (2 x 50 mL). The yellowish oil was dissolved in 50 mL of water and extracted with AcOEt (4 x 50 mL). The combined organic layers were dried over Na_2SO_4, filtered and evaporated to obtain a yellow powder. The crude residue was crystallized (AcOEt, 50 mL, 7° C) and washed with cold AcOEt (2 x 5 mL) to give desired compound as white solid in 50 % yield, without purification.

^1H and ^{13}C NMR spectra are reported in literature[155]

^1H NMR (500 MHz, CDCl3) δ 6.72 (s, 2 H), 3.83 (t, J =7.2 Hz, 2 H), 2.70 (t, J = 7.2 Hz, 2 H) ppm.

Synthesis of 4-Prop-2-ynyloxy-benzaldehyde (4.12)

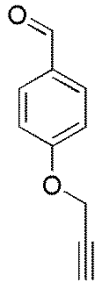

To a solution of 4-Hydroxy-benzaldehyde (250 mg, 2.05 mmol) in acetone dry (20 mL), K_2CO_3 (1.133 g, 8.2 mmol), 18-crown-6 (2 mg, 0.008 mmol) and propargyl bromide (913 µL, 8.2 mmol) were added, under a N_2 atmosphere. The suspension was stirred at reflux

for 24h. Acetone was evaporated, water (40 mL) was added and the mixture was extracted with DCM (3x30 mL). The organic phase was dried over Na_2SO_4, filtered and evaporated to give 340 mg of crude. This was purified by flash column chromatography (DCM) to gain 150 mg of **48** as a white solid in 46% yield.

^{1}H NMR (200 MHz, $CDCl_3$) δ 2.57 (t, *J* = 2.2 Hz, 1H), 4.78 (d, *J* = 2.2 Hz, 2H), 7.06-7.11 (m, 2H), 7.83-7.87 (m, 2H), 9.90 (s, 1H) ppm.

Synthesis of Taxol-Benzaldehyde adduct (4.14)

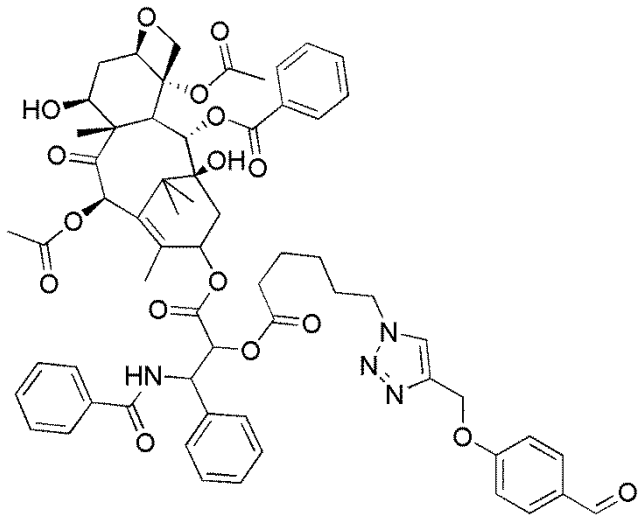

To a solution of 4-Prop-2-ynyloxy-benzaldehyde **4.12** (7 mg, 0.04 mmol) in DMF (1 mL), $CuSO_4$ (1 mg, 0.007 mmol) and sodium ascorbate (3 mg, 0.01 mmol) were added. After 5 min, a solution of taxol-2'-6-azide-hexanoate **4.13** (60 mg, 0.06 mmol) in DMF (1 mL) and water (1 mL) were added. The solution was stirred at r.t. for 48 h. The reaction mixture was poured onto water (15 mL) and was extracted with DCM (3x15 mL). The organic phase was washed with water (7x25 mL), dried over Na_2SO_4, filtered and evaporated to give 70mg of crude. The crude was purified by flash column chromatography (DCM/MeOH 20:1), to obtain 10 mg of pure product (**4.14**) as a white solid in 20% yield.

^{1}H NMR (400MHz, $CDCl_3$) δ 1.04-1.40 (m, 11H), 1.58-1.76 (m, 7H), 1.82 -1.95 (m, 5H), 2.22 (s, 3H), 2.29- 2.41 (m, 3H), 2.45 (s, 3H),3.43-3.52 (m, 2H), 3.81 (d, *J* = 7.2 Hz, 1H),

4.20 (d, *J* = 7.6 Hz, 1H), 4.27 (d, *J* = 7.6 Hz, 1H), 4.42-4.47 (m, 1H), 4.97 (d, *J* = 9.2 Hz, 1H), 5.29 (s, 2H), 5.50 (d, *J* = 3.6 Hz, 1H), 5.68 (d, *J* = 7.2 Hz, 1H), 5.97 (dd, *J* = 3.6 Hz, *J* = 9.2 Hz, 1H), 6.23 (t, *J* = 9.2 Hz, 1H), 6.29 (s, 1H), 7.09 (d, *J* = 8.8 Hz, 2H), 7.31-7.63 (m, 12H), 7.74 (d, *J* = 7.6 Hz, 2H), 7.83 (d, *J* = 8.8 Hz , 2H), 8.14 (d, *J* = 7.2 Hz, 2H), 9.86 (s, 1H) ppm.

^{13}C NMR (100MHz, $CDCl_3$) δ 9.6, 14.8, 20.8, 22.1, 22.7, 23.8, 24.9, 25.6, 26.8, 29.7, 33.3, 33.9, 35.5, 43.2, 45.6, 49.1, 50.0, 52.8, 58.5, 62.1, 71.8, 72.1, 74.0, 75.0, 75.6, 77.0, 79.1, 81.0, 84.4, 108.5, 110.5, 115.1, 122.8, 126.6, 127.1, 128.5, 128.7, 129.0, 130.2, 130.3, 132.0, 132.8, 133.7, 136.9, 142.7, 143.3, 156.7, 163.0, 167.0, 168.1, 169.8, 171.2, 172.3, 190.8, 203.8 ppm.

FT-IR ($CDCl_3$) 1718, 2857, 2935, 3437 cm^{-1}.

ESI - MS: *m/z* = 1174.83 $[M+Na]^+$.

Synthesis of (4-(prop-2-yn-1-yloxy)phenyl)methanamine 4.19

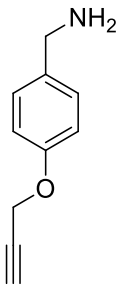

To a suspension of 4 hydroxybenzylamine (400mg, 3.23 mmol), potassium tert-butoxide (362 mg, 3.23 mmol) and 18-crown-6 (87 mg, 0.33 mmol) in dry THF (14 mL) propargyl bromide (384 mg, 3.23 mmol) was added at -70°C under N_2. The reaction mixture was stirred at -65°C for 1 hour and for 2,5 hours at 0°C. Then, the mixture was quenched with 100 mL of water and the organic phase was extracted with AcOEt (2X100ml). The combined organic layers were washed with H_2O (100ml) and a saturated solution of NaCl (2x80ml), dried over Na_2SO_4, filtered and concentrated under vacuum to afford the final product in 65% yield wwithout purification.
^{1}H NMR (400 MHz; $CDCl_3$): δ 1.69 (br s, 2H), 2.51 (t, $^4J_{CH,CH2}$ = 2.4 Hz, 1H), 3.81 (s, 2H), 4.67 (d, $^4J_{CH2,CH}$ = 2.4 Hz, 2H), 6.94 and 7.24 (AA'BB', 4H) ppm.

^{13}C NMR (100 MHz; $CDCl_3$): δ 45.8, 55.8, 75.4, 78.6, 114.9, 128.2, 136.4, 156.4.

Synthesis of DMTr-Gemcitabine (4.15)

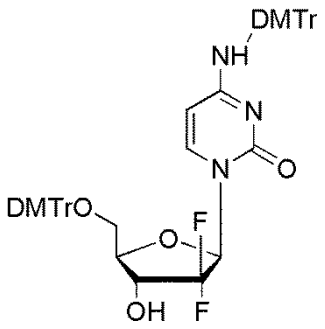

Gemcitabine (50 mg, 0.19 mmol) was dissolved in dry DCM (1 mL) and DIPEA (54 mg, 0.42 mmol) and DMAP (2 mg, 0.02 mmol) were added, under a N_2 atmosphere. DMTrCl (141 mg, 0.42 mmol) was dissolved in dry DCM (0.5 mL) and it was added to the above described solution, at 0°C, dropwise. The solution turns yellow. The solution was stirred at r.t., for 20 h and then DCM (20 mL) was added and it was extracted with water (3x20 mL). The organic layer was dried over Na_2SO_4, filtered and evaporated to give 150 mg of crude. It was purified by flash column chromatography (DCM/MeOH 30:1) to gain 70 mg of product **4.15** in 43% yield.

^{1}H NMR (200 MHz, CDCl3) δ 3.38-3.52 (m, 2H,), 3.69-3.73 (m, 12 H), 4.02-4.06 (m, 1 H), 4.40-4.45 (m, 1 H), 4.88 (d, 1 H, *J* = 6.8), 6.30-6.42 (m, 1 H), 6.70-6.81 (m, 8 H), 7.01-7.32 (m, 20 H), 7.57 (d, 1 H, *J* = 6.8) ppm.

^{13}C NMR (100 MHz, CDCl3) δ 55.3, 61.2, 70.4, 80.4, 84.5, 86.7, 95.5, 113.2, 113.6, 127.4, 127.8, 128.3, 128.4, 129.9, 130.2, 135.0, 135.1, 135.7, 136.1, 141.0, 144.2, 144.8, 155.1, 158.4, 158.5, 165.3 ppm.

Synthesis of DMTr-Gemcitabine-2'-6-azide-hexanoate (4.17)

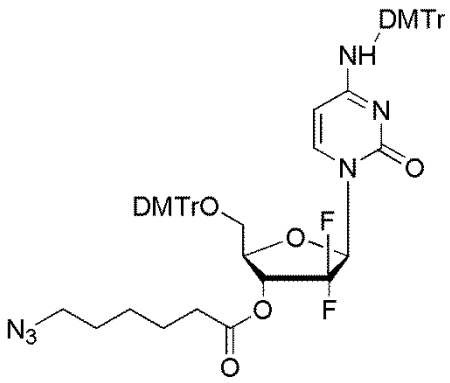

To a solution of bis-DMTr-Gemcitabine **4.15** (56 mg, 0.06 mmol) in dry DCM (1 mL), DMAP (8 mg, 0.06 mmol) was added. The solution was cooled at 0 °C, then DIC (9 mg, 0.07 mmol) and 6-azido-hexanoic acid (11 mg, 0.07 mmol) were added, under a N_2 atmosphere. The yellow solution was stirred at r.t. overnight, then poured onto Et_2O (15 mL) and washed with a saturated solution of NH_4Cl (2x20 mL), then a saturated solution of $NaHCO_3$ (2x20 mL) followed by a saturated solution of NH_4Cl (2x20 mL). The recollected organic layer was dried over Na_2SO_4, filtered and evaporated to obtain 50 mg of crude. This was purified by flash column chromatography (DCM/MeOH 30:1) to obtain 30 mg of **4.17** in 46% yield.

^{1}H NMR (400 MHz, $CDCl_3$) δ 1.37-1.43 (m, 2H), 1.56-1.69 (m, 4H), 2.32-2.45 (m, 2H), 3.26 (t, *J* = 6.8 Hz, 2H), 3.29-3.31 (m, 1H), 3.38-3.42 (m, 1H), 3.74-3.76 (m, 12H), 4.06-4.09 (m, 1H), 4.94 (d, *J* = 7.2 Hz, 1H), 5.42-5.48 (m, 1H), 6.42 (t, *J* = 8.4 Hz, 1H), 6.73-6.82 (m, 8H), 7.08-7.21 (m, 14H), 7.26-7.28 (m, 4H), 7.38 (d, *J* = 7.2 Hz, 1H) ppm.

^{13}C NMR (100 MHz, $CDCl_3$) δ 24.1, 26.0, 28.4, 33.4, 51.0, 55.0, 55.1, 61.2, 70.1, 86.7, 95.2, 108.4, 109.9, 113.1, 113.5, 126.8, 127.4, 127.7, 127.8, 128.3, 128.4, 129.7, 129.8, 130.0, 134.9, 134.9, 135.8, 136.0, 144.2, 144.3, 158.5, 158.58, 158.64, 165.4, 171.5 ppm.

FT-IR ($CDCl_3$) 1755, 2110, 2245, 2839, 2936, 3393 cm^{-1}.

ESI - MS: *m/z* = 1029.33 $[M+Na]^+$.

Synthesis of 1,4,7,10-tetraazacyclododecane-1,4,7-triacetic acid (5.5)

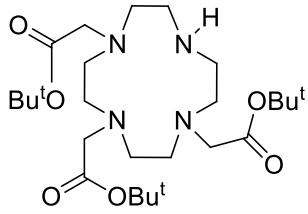

To a solution of tetraazacyclododecane (1.50 g, 8.72 mmol) and Na(CH_3COO) (2.14 g, 26.13 mmol) in dimethylacetamide (31 mL), *tert*-butylbromoacetate (5.10 g, 26.13 mmol) was added. The white suspension was stirred for 20 days, then the precipitate was filtered and dried to give **4** as a white solid in 55% yield.

^{1}H NMR (200 MHz, $CDCl_3$) δ 1.44 (s, 9H, tBu); 1.45 (s, 18H, tBu); 2.82-2.96 (m, 12H, CH_2); 3.03-3.12 (m, 4H, CH_2); 3.28 (s, 2H, CH_2); 3.36 (s, 4H, CH_2); 10.00 (s, 1H, NH) ppm

^{13}C NMR (50 MHz, $CDCl_3$) δ 28.1 (6C, CH_3); 28.2 (3C, CH_3); 47.5, 49.2, 51.3, 58.2 (2C, CH_2); 81.6 (1C, N-CH_2); 81.8 (2C, N-CH_2); 169.6 (1C, CO); 170.5 (2C, CO) ppm.

Synthesisi of N-(benzylcarboxymethyl)-1,4,7,10-tetraazacyclododecane-N',N'',N'''-triacetic acid tri-tert-butyl ester (5.6)

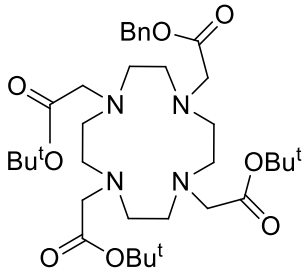

Compound **5.5** (2.38 g, 7.44 mmol) was added to a suspension of 60% NaH in DMF, after 2 hours stirring, benzylbromoacetate (2 g, 8.7 mmol) was added dropwise below 0 °C. The reaction mixture was stirred for 27 h at room temperature (r.t.), then a solution of 5% citric acid was added and the mixture extracted with chloroform. The product obtained was purified by flash chromatography with 8/1= CH_2Cl_2/MeOH as eluent to give **5** in 67% yield.

^{1}H NMR (200 MHz , DMSO-*d6)* δ 1.40 (bs, 18H), 1.44 (s, 9H), 2.43-1.94 (bs, 6H), 3.29-2.71 (bs, 7H), 3.31 (s, 2H), 3.46–3.39 (m, 2H), 5.13 (s, 2H), 7.35 (s, 5H).

^{13}C NMR (50 MHz, DMSO-d6) δ 31.2, 50.5, 52.3, 52.6, 53.8, 57.1, 58.3, 75.3, 85.7, 85.7, 128.7, 129.8, 144.7, 172.9, 174.3.

Synthesis of 2-(4,7,10-tris(2-tert-butoxy-2-oxoethyl)-1,4,7,10-tetraazacyclododecan-1-yl)acetic acid (5.2)

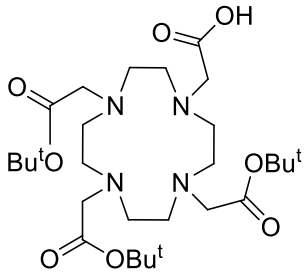

A mixture of **5.6** (0.83 g, 1.25 mmol) and 10% Pd/C (0.11 g) was hydrogenated in methanol under a positive H_2 atmosphere for 6 h. The catalyst was removed by filtration, and the filtrate was evaporated to yield the modified DOTA macrocycle **1** in 50% yield without further purification.

^{1}H NMR (200 MHz, $CDCl_3$) δ 1.40 (s, 9H), 1.41 (s, 18H), 2.64 (bs, 4H), 2.72 (bs, 4H), 2.87 (bs, 4H), 3.33 (bs, 4H), 3.36 (s, 6H), 3.46 (m, 2H) ppm.

^{13}C NMR (50 MHz, DMSO) δ 36.83, 36.88, 56.09, 58.59, 60.78, 61.88, 64.61, 65.63, 89.53, 179.30 ppm.

MALDI-MS (m/z): 572.6. $[M+H]^+$

ESI-MS (m/z): 573.4. $[M+H]^+$

Synthesis of 5-(benzyloxy)-2-bromo-5-oxopentanoic acid (5.8)

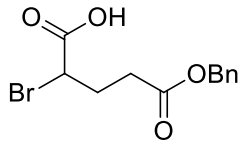

To a suspension of L-glutamic acid-5-benzylester (1.50 g, 6.48 mmol) and sodium bromide (2.27 g, 22.08 mmol) in a 1N solution of bromidric acid, cooled at 0°C, sodium nitrite (0.79 g, 11.45 mmol) was added portionwise. The yellow solution was stirred at this temperature for 2 h and finally 560 µL of 98% sulfuric acid was added, followed by diethylether. The water phase was extracted several times with Et_2O and the combined organic layers washed with brine. The crude product was purified by flash chromatography with 1/1=EtOAc/EtP, to obtain bromo-derivative **5.8** in 82% yield.

^{1}H NMR (200 MHz, $(CD_3)_2SO$) δ 2.00-2.40 (m, 4H, CH_2), 4.38-4.50 (m, 1H, CH-Br), 5.08 (s, 2H, CH_2), 5.74 (s, 1H, OH), 7.35 (m, 5H, H_{arom}).

^{13}C NMR (50 MHz, $CDCl_3$) δ 29.3 (1C, CH_2), 31.4 (1C, CH_2), 44.3 (1C, C-Br), 66.6 (1C, CH_2), 128.0 (1C, C_{arom}),128.2, 128.4 (2C, CH_{arom}), 135.3 (1C, C_{arom}), 172.0, 173.3 (1C, CO).

Synthesis of 5-benzyl 1-tert-butyl 2-bromopentanedioate (5.9)

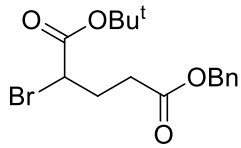

A solution of *tert*-butyltrichloroacetimidate (TBTA) (2.20 mL, 12.05 mmol) in 8 mL of cyclohexane was added dropwise to another solution of **5.8** (1.70 g, 5.63 mmol) in 7 mL of CHCl3. During the addition a white precipitate formed, which was dissolved by the addition of DMA followed by boron trifluoridiethyl etherate (120 µL, 0.56 mmol) as a catalyst. The reaction mixture was stirred for three days at r.t. then concentrated and the remaining DMA phase was extracted with hexane (3x10mL). The hexane phase was evaporated and the crude product product was purified by flash chromatography with 20/1=EtOAc/EtP followed by 10/1, to give But ester **5.9** in 50% yield.

^{1}H NMR (200 MHz, (CD3)2SO) δ 1.47 (s, 9H, CH3); 2.20-2.50 (m, 2H, CH2); 2.52-2.60 (m, 2H, CH2); 4.24 (dd, 1H, *J1* = 6.0 Hz, *J2* = 8.2 Hz, CH-Br); 5.13 (s, 2H, CH2); 7.36 (m, 5H, Harom).

Synthesis of 5-benzyl 1-tert-butyl 2-(4,7,10-tris(2-tert-butoxy-2-oxoethyl)-1,4,7,10-tetraaza cyclododecan-1-yl)pentanedioate (5.10)

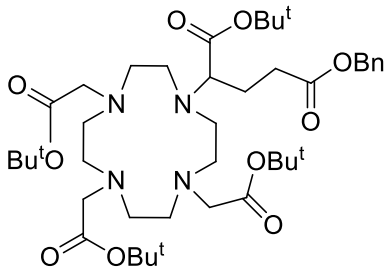

To a solution of **5.5** (918 mg, 1.79 mmol) in 31 mL of dry CH3CN, K2CO3 (740 mg, 5.36 mmol) was added. The reaction mixture was stirred at 60 °C for 10 min before adding dropwise, over a period of 40 min, a solution of **5.9** (1.14 g, 3.58 mmol) in 15 mL of dry CH3CN. After 42 h under stirring at 60° C the yellow solution was filtered throw celite and concentrated. The residue was purified by flash column chromatography using 20/1=CH2Cl2/MeOH followed by 8/1 as eluent, to obtain **5.10** in 59% yield. Melting point: 145°C.
^{1}H NMR (200 MHz, CDCl3) δ 1.45 (s, 36H, CH3); 1.90-3.60 (m, 27H); 5.07 (s, 2H, CH2); 7.33 (m, 5H).

Synthesis of 5-tert-butoxy-5-oxo-4-(4,7,10-tris(2-tert-butoxy-2-oxoethyl)-1,4,7,10-tetraazacyclododecan-1-yl)pentanoic acid (5.3)

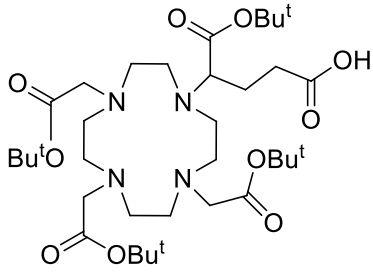

5-benzyl 1-tert-butyl 2-(4,7,10-tris(2-tert-butoxy-2-oxoethyl)-1,4,7,10-tetraaza cyclododecan-1-yl)pentanedioate **5.10** (100 mg, 0.127 mmol) was dissolved in 2.8 mL of

absolute ethanol and to this solution 37 mg of 10% Pd (C) were added. The reaction mixture was hydrogenated for two days, filtered over cotton wool pad and the filtrate concentrated to give **5.3** in 79% yield without purification.
^{1}H NMR (400 MHz, CD_3OD) δ 1.49 (s, 9H, CH3); 1.50 (s, 18H, CH3); 1.53 (s, 9H, CH3); 1.98-2.30 (m, 8H); 2.46-2.88 (m, 11H); 2.90-3.20 (m, 4H); 3.42-3.6 (m, 4H).
^{13}C NMR (100 MHz, CD_3OD) δ 28.3 (6C, CH3); 28.1 (6C, CH3); 33.3 (1C, CH2); 45.2, 53.9, 54.0, 56.6, 56.9 (12C, CH2); 61.3 (1C, CH); 82.9 (2C, C(CH3)3), 83.0, 83.6 (1C, C(CH3)3); 174.6, 174.7, 176.5, 176.7 (1C, CO).
FT-IR : 3422, 2974, 2929, 2840, 1726, 1362, 1223, 1166 cm^{-1}.
ESI-MS M+=701, 723 (100%); CI, 56(100%), 157, 600.

Synthesis of Synthesis of Taxol-2′-hemisuccinate (6.3)

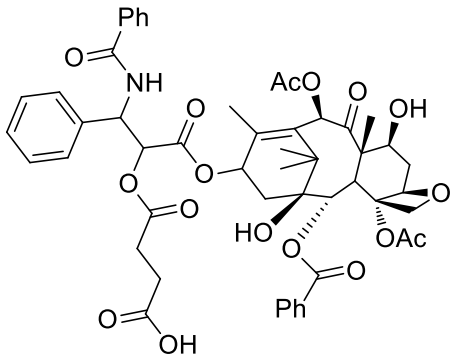

To a solution of taxol (0.1 g, 0.12 mmol) in 4 mL of dry pyridine, succinic anhydride (0.014 g, 0.14 mmol) and DMAP (0.003 g, 0.02 mmol) WEre added. The obtained solution was stirred for 3 h, at r.t, under a N_2 atmosphere, and then the solvent was evaporated under vacuum to obtain a colorless oil. The crude was dissolved in 20 mL of DCM and washed with a saturated solution of NH_4Cl (3 x 40 mL), followed by water (3 x 40 mL), to get rid of residual pyridine. The organic layer was dried over Na_2SO_4, filtered and evaporated to obtain a white solid as pure final compound (**6.3**) in 38% yield. ^{1}H NMR and ^{13}C NMR spectra are described in literature.[38]

ESI-MS: *m/z* = 852.17 $[M\text{-succ}]^-$, 952.17 $[M\text{-H}]^-$, 1906.00 $[2M\text{-H}]^-$; 976.17 $[M+Na]^+$**.**

Synthesis of *N*-succinimidyl diphenylphosphate (SDPP) (6.6)

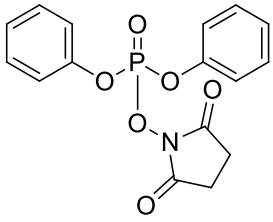

To a solution of N-hydroxysuccinimide (115 mg, 1 mmol) in dry DCM (4 mL) diphenyl chlorophosphate(268.6 mg, 1 mmol) and trimethylamine (101.19, 1 mmol) were added and the mixture was stirred at r.t. for 2 hours. The solvent was evaporated under vacuum and the crude product was dissolved in 10 mL of ethyl acetate and washed with a saturated aqueous solution of NaCl (3x10 mL). The organic layer was dried over Na_2SO_4, filtered and evaporated to obtain a white solid (350 mg) in quantitative yield. The product was used without purification and was stored in a freezer under nitrogen.

^{1}H-NMR (400 MHz, CDCl3) δ 7.50-7.22 (m, 10H), 2.81 (s, 4H) ppm.

Synthesis of 1-benzamido-3-(((2aR,4S,4aS,6R,11S,12S,12bS)-6,12b-diacetoxy-12-(benzoyloxy)-4,11-dihydroxy-4a,8,13,13-tetramethyl-5-oxo-2a,3,4,4a,5,6,9,10,11,12,12a,12b-dodecahydro-1H-7,11-methanocyclodeca[3,4]benzo[1,2-b]oxet-9-yl)oxy)-3-oxo-1-phenylpropan-2-yl (2,5-dioxo-2,5-dihydro-1H-pyrrol-1-yl) succinate (6.7)

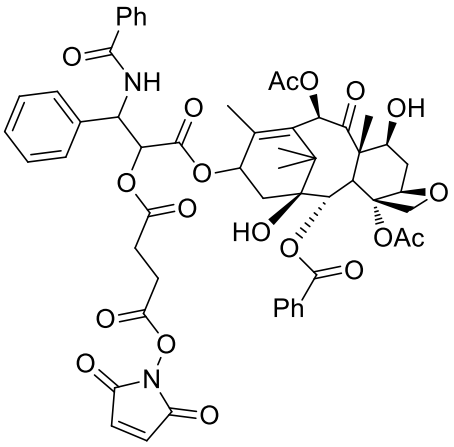

To a solution of taxol-2'-hemisuccinate **6.3** (40 mg, 0.035 mmol) in acetonitrile (1.2 mL) SDPP **6.6** (18 mg, 0.053 mmol) and trimethylamine (14 mg, 0.14 mmol)were added. The mixture was stirred under nitrogen for 6 hours, and then the solvent was evaporated under vacuum. The crude product was purified by flash column chromatography to afford the final product as a white solid in a 51% yield over two steps.
Spectroscopic data were previously reported. [156]
^{1}HNMR (300 MHz, CDCl3) δ 8.14 (d, *J* = 6.9, 2H), 7.71 (d, *J* = 6.9, 2H), 7.61 (t, *J* = 7.5 Hz, 1H), 7.54-7.33 (m, 10H), 6.30 (s, 1H), 6.28 (t, *J* = 8.4, 1H), 5.98 (dd, *J* = 9.3, 3.0, 1H), 5.69 (d, *J* = 7.5, 1H), 5.48 (d, *J* = 3.0, 1H), 4.99 (d, *J* = 8.4, 1H), 4.45 (dd, *J* = 10.7, 6.2 1H), 4.32 (d, *J* = 7.8, 1H), 4.21 (d, *J* = 8.7, 1H), 3.82 (d, *J* = 7.2, 1H), 2.91-2.51 (m, 8H), 2.49 (s, 3H), 2.38 (t, *J* = 7.5 Hz, 2H), 2.23 (s, 3H), 2.21-2.02 (m, 3H), 1.95 (s, 3H), 1.86 (m, 1H), 1.68(s, 3H), 1.24 (s, 3H), 1.14 (s, 3H) ppm.
ESI - MS: *m/z* = 1073.25 $[M+Na]^+$.

Bibliography

(1) Devita, V. T.; Chu, E. *Cancer Res* **2008**, *68* (21), 8643–8653.
(2) Chabner, B. A.; Roberts, T. G. *Nat. Rev. Cancer* **2005**, *5* (1), 65–72.
(3) Bos, J. L. *Mutat. Res. Genet. Toxicol.* **1988**, *195* (3), 255–271.
(4) National Toxicology Program. *Rep. Carcinog. Carcinog. profiles* **2011**, *12*, iii-499.
(5) Nardi, V.; Azam, M.; Daley, G. Q. *Curr. Opin. Hematol.* **2004**, *11* (1), 35–43.
(6) Yildirimer, L.; Thanh, N. T. K.; Loizidou, M.; Seifalian, A. M. *Nano Today* **2011**, *6* (6), 585–607.
(7) Shin, S. W. *Korean J. Radiol.* **2009**, *10* (5), 425–434.
(8) Torchilin, V. P. *Nat. Rev. Drug Discov.* **2005**, 145–160.
(9) ZHANG, J.; Q.LAN, C.; POST, M.; SIMARD, B.; DESLANDES, Y.; HAN, T. *CANCER GENOMICS AND PROTEOMICS* **2006**, 147–158.
(10) Rehlaender, B. .; Cho, M. *J. Pharm. Res* **1998**, *15* (11), 1652–1656.
(11) Carter, P. *Nat. Rev. Cancer* **2001**, *1*, 118–129.
(12) Chames, P.; Regenmortel, M. Van; Weiss, E.; Baty, D. *Br. J. Pharmacol.* **2009**, *157*, 220–233.
(13) Reubi, J. C. *Endocr. Rev.* **2003**, 389–427.
(14) Reubi, J. C.; Maecke, H.; Krenning, E. *J. Nucl. Med.* **2005**, No. 46, 67–75.
(15) van der Lely, A. J.; de Herder, W. W.; Krenning, E. P.; Kwekkeboom, D. J. *Endocrine* **2003**, *20* (3), 307–311.
(16) Falciani, C.; Fabbrini, M.; Pini, A.; Lozzi, L.; Lelli, B.; Pileri, S.; Brunetti, J.; Bindi, S.; Scali, S.; Bracci, L. *Mol. Cancer Ther.* **2007**, *6* (9), 2441–2448.
(17) Carraway~, R.; Leeman, S. E. *J. Biol. Chem.* **1973**, *2486861* (19).
(18) Binder, E.; Kinkead, B.; Owens, M. *Pharmacol. Rev.* **2001**, *53*, 453–486.
(19) Association for Research in Vision and Ophthalmology., J. R.; Zhou, J.; Ben-Shabat, S.; Vollmer, H.; Itagaki, Y.; Nakanishi, K. *Investigative ophthalmology & visual science.*; C.V. Mosby Co, 1977; Vol. 43.
(20) Cusack, B.; Groshan, K.; Mccormick, D. J.; Pangţ, Y.-P.; Perry, R.; Phung, C.-T.; Souder, T.; Richelson, E. *J. Biol. Chem.* **1996**, *271*, 15054–15059.
(21) White, J. F.; Noinaj, N.; Shibata, Y.; Love, J.; Kloss, B.; Xu, F.; Gvozdenovic-Jeremic, J.; Shah, P.; Shiloach, J.; Tate, C. G.; Grisshammer, R. *Nature* **2012**, *490* (7421), 508–513.
(22) Gui, X.; Liu, S.; Meng, Z.; Gao, Z.-H. *J. Cancer Ther.* **2013**, *4*, 12–17.
(23) Bracci, L.; Falciani, C.; Lelli, B.; Lozzi, L.; Runci, Y.; Pini, A.; De Montis, M. G.; Tagliamonte, A.; Neri, P. *J. Biol. Chem.* **2003**, *278* (47), 46590–46595.
(24) Brunetti, J.; Falciani, C.; Lelli, B.; Minervini, A.; Ravenni, N.; Depau, L.; Siena, G.; Tenori, E.; Menichetti, S.; Pini, A.; Carini, M.; Bracci, L. *Biomed Res. Int.* **2015**, 1–7.
(25) Brunetti, J.; Pillozzi, S.; Falciani, C.; Depau, L.; Tenori, E.; Scali, S.; Lozzi, L.; Pini, A.; Arcangeli, A.; Menichetti, S.; Bracci, L. *Sci. Rep.* **2015**, *5* (1), 17736.
(26) Wani, M. C.; Taylor, H. L.; Wall, M. E.; Coggon, P.; McPhail, A. T. *J. Am. Chem. Soc.* **1971**, *93* (9), 2325–2327.
(27) Fauzee1, N. J. S.; , Zhi Dong2, Y. W. *Asian Pacific J. Cancer Prev.* **2011**, *12*, 837–850.
(28) Schiff, P.B., Fant, J., Horwitz, S. B. *Nature* **1979**, *277*, 665–667.

(29) Jordan, M. A.; Wendell, K.; Gardiner, S.; Derry, W. B.; Copp, H.; Wilson, L. *Cancer Res.* **1996**, *56* (4), 816–825.
(30) Klauber, N.; Parangi, S.; Flynn, E.; Hamel, E.; D'Amato, R. J. *Cancer Res.* **1997**, *57* (1), 81–86.
(31) Spandidos, D.; Ethnikon Hidryma Ereunōn (Greece), D.; Kimura, M.; Yamashita, Y.; Kawakami, M.; Ishiguro, Y.; Nishimura, G.; Matsuda, H.; Tsukuda, M. *Oncology reports.*; [National Hellenic Research Foundation], 1994; Vol. 18.
(32) Singla, A. K.; Garg, A.; Aggarwal, D. *Int. J. Pharm.* **2002**, *235*, 179–192.
(33) du Bois, A.; Lück, H.-J.; Meier, W.; Adams, H.-P.; Möbus, V.; Costa, S.; Bauknecht, T.; Richter, B.; Warm, M.; Schröder, W.; Olbricht, S.; Nitz, U.; Jackisch, C.; Emons, G.; Wagner, U.; Kuhn, W.; Pfisterer, J.; Arbeitsgemeinschaft Gynäkologische Onkologie Ovarian Cancer Study Group. *J. Natl. Cancer Inst.* **2003**, *95* (17), 1320–1329.
(34) Piccart-Gebhart, M. J.; Burzykowski, T.; Buyse, M.; Sledge, G.; Carmichael, J.; Lück, H.-J.; Mackey, J. R.; Nabholtz, J.-M.; Paridaens, R.; Biganzoli, L.; Jassem, J.; Bontenbal, M.; Bonneterre, J.; Chan, S.; Basaran, G. A.; Therasse, P. *J. Clin. Oncol.* **2008**, *26* (12), 1980–1986.
(35) Lilley, L. L.; Scott, H. B. *Am. J. Nurs.* **1993**, *93* (12), 46–50.
(36) Williams, H.J., Scott, A.I., Dieden, R.A., Swindell, C.S., Chirlian, L.E., Francl, M.M., Heerding, J.M., Krauss, N. E. *Tetrahedron* **1993**, *49*, 6545.
(37) Greenwald, R. B.; Gilbert, C. W.; Pendri, A.; Conover, C. D.; Xia, J.; Martinez, A. *J. Med. Chem.* **1996**, *39*, 424–431.
(38) Liu, D.-Z.; Sinchaikul, S.; Vasu, P.; Reddy, G.; Chang, M.-Y.; Chen, S.-T. *Bioorganic Med. Chem. Lett.* **2007**, 617–620.
(39) Pankhurst, Q. a; Connolly, J.; Jones, S. K.; Dobson, J. *J. Phys. D. Appl. Phys.* **2003**, *36* (13), R167–R181.
(40) Kang, Y. S.; Risbud, S.; Rabolt, J. F.; Stroeve, P. *Chem. Mater.* **1996**, *8* (9), 2209–2211.
(41) Dobson, J. *Gene Ther.* **2006**, *13* (4), 283–287.
(42) Rudge, S.; Peterson, C.; Vessely, C.; Koda, J.; Stevens, S.; Catterall, L. *J. Control. Release* **2001**, *74* (1–3), 335–340.
(43) APPENZELLER, T. *Science (80-.).* **1991**, *254* (5036), 1300–1300.
(44) Knop, K.; Hoogenboom, R.; Fischer, D.; Schubert, U. S. *Angew. Chemie Int. Ed.* **2010**, *49* (36), 6288–6308.
(45) Talelli, M.; Rijcken, C. J. F.; Lammers, T.; Seevinck, P. R.; Storm, G.; Van Nostrum, C. F.; Hennink, W. E. *Langmuir* **2009**, *25*, 2060–2067.
(46) Buschow, K. H. J. *Encycl. Mater. Sci. Technol.* **2001**, elsevier.
(47) Zhang, L.; Gu, F.; Chan, J.; Wang, A.; Langer, R.; Farokhzad, O. *Clin. Pharmacol. Ther.* **2008**, *83* (5), 761–769.
(48) rif.pdf.
(49) Nabha, S.M., Wall, N.R., Mohammad, R.M., Pettit, G.R., Al-Katib, A. M. *Anticancer Drugs.* **2000**, *11* (5), 385–392.
(50) Essig M; J, D.; HP, S.; H, H.; M, W.; G, van K. *Strahlenther Onkol* **2000**, No. 176, 84–94.
(51) Hainfeld, J. F.; Slatkin, D. N.; Focella, T. M.; Smilowitz, H. M. *Br. J. Radiol.* **2006**, *79* (939), 248–253.
(52) Harisinghani, M. G.; Barentsz, J.; Hahn, P. F.; Deserno, W. M.; Tabatabaei, S.;

Hulsbergen van de Kaa, C.; de la Rosette, J.; Weissleder, R. *n engl j med* **2003**, *34825348*, 2491–2499.
(53) Debouttière, P.-J.; Roux, S.; Vocanson, F.; Billotey, C.; Beuf, O.; Favre-Réguillon, A.; Lin, Y.; Pellet-Rostaing, S.; Lamartine, R.; Perriat, P.; Tillement, O. *Adv. Funct. Mater.* **2006**, *16* (18), 2330–2339.
(54) *J. Adv. Res.* **2010**, *1* (1), 13–28.
(55) Cherukuri, P.; Curley, S. *Methods Mol Biol* **2010**, No. 624, 359 – 367.
(56) Hauck, T. S.; Jennings, T. L.; Yatsenko, T.; Kumaradas, J. C.; Chan, W. C. W. *Adv. Mater.* **2008**, *20* (20), 3832–3838.
(57) Huff, T. B.; Tong, L.; Zhao, Y.; Hansen, M. N.; Cheng, J.-X.; Wei, A. *Nanomedicine (Lond).* **2007**, *2* (1), 125–132.
(58) Turkevitch, J.; Stevenson, P. C.; Hillier, J. *Disc. Faraday Soc.* **1951**, No. 11, 55–75.
(59) Frans, G. *Nat. Phys. Sci.* **1973**, No. 241, 20–22.
(60) Grabar, K. C.; Freeman, R. G.; Hommer, M. B.; Natan, M. *J. Anal. Chem.* **1995**, No. 67, 735–743.
(61) Dobrowolska, P.; Krajewska, A.; Gajda-Rączka, M.; Bartosewicz, B.; Nyga, P.; Jankiewicz, B. J. *Materials (Basel).* **2015**, *8*, 2849–2862.
(62) Kimling, J.; Maier, M.; Okenve, B.; Kotaidis, V.; Ballot, H.; Plech, A. *J. Phys. Chem* **2006**, No. 110, 15700–15707.
(63) Brust, M.; Walker, M.; Bethell, D.; Schiffrin, D. J.; Whyman, R. *J. Chem. Soc. , Chem. Commun.* **1994**, 801–802.
(64) Waters, C. A.; Mills, A. J.; Johnson, K. A.; Schiffrin, D. J. *J. Chem. Commun.* **2003**, 540–541.
(65) Park, J. S.; Vo, A. N.; Barriet, D.; Shon, Y. S.; Lee, T. R. *Langmuir* **2005**, *21* (7), 2902–2911.
(66) Park, J. S.; Smith, A. C.; Lee, T. R. *Langmuir* **2004**, *20* (14), 5829–5836.
(67) Wojczykowski, K.; Meissner, D.; Jutzi, P.; Ennen, I.; Hütten, A.; Fricke, M.; Volkmer, D. *Chem. Commun. (Camb).* **2006**, No. 35, 3693–3695.
(68) Sharma, J.; Chhabra, R.; Andersen, C. S.; Gothelf, K. V.; Yan, H.; Liu, Y. *J. Am. Chem. Soc.* **2008**, *130* (25), 7820–7821.
(69) Turcu, I.; Zarafu, I.; Popa, M.; Chifiriuc, M.; Bleotu, C.; Culita, D.; Ghica, C.; Ionita, P. *Nanomaterials* **2017**, *7* (2), 43.
(70) Koufaki, M.; Detsi, A.; Theodorou, E.; Kiziridi, C.; Calogeropoulou, T.; Vassilopoulos, A.; Kourounakis, A. P.; Rekka, E.; Kourounakis, P. N.; Gaitanaki, C.; Papazafiri, P. *Bioorganic Med. Chem.* **2004**, *12* (18), 4835–4841.
(71) Kim, J.-H.; Sim, G.-S.; Bae, J.-T.; Oh, J.-Y.; Lee, G.-S.; Lee, D.-H.; Lee, B.-C.; Pyo, H.-B. *J. Pharm. Pharmacol.* **2008**, *60*, 863–870.
(72) Roux, S.; Garcia, B.; Bridot, J.-L.; Salome, M.; Marquette, C.; Lemelle, L.; Gillet, P.; Blum, L.; Perriat, P.; Tillement Olivier. *Langmuir* **2005**, *3* (6), 2526–2536.
(73) Abad, J. M.; Mertens, S. F. L.; Pita, M.; Fernández, V. M.; Schiffrin, D. J. *J. Am. Chem. Soc.* **2005**, *127* (15), 5689–5694.
(74) Beer, P. D.; Cormode, D. P.; Davis, J. J. *Chem. Commun.* **2004**, *44* (0), 414–415.
(75) Leff, D. V; Brandt, L.; Heath, J. R. *Langmuir* **1996**, No. 12, 4723–4730.
(76) Hostetler, M. J.; Wingate, J. E.; Zhong, C.-J.; Harris, J. E.; Vachet, R. W.; Clark, M. R.; Londono, J. D.; Green, S. J.; Stokes, J. J.; Wignall, G. D.; Glish, G. L.; Porter, M. D.; Evans, N. D.; Murray, R. W. *Langmuir* **1998**, *14* (1), 17–30.
(77) Leff, D. V; Ohara, P. C.; Heath, J. R.; Gelbart, W. M. *J. Phys. Chem* **1995**, *99*,

7036–7041.
(78) Ingram, R. S.; Hostetler, M. J.; Murray, R. W. *J. Am. Chem. Soc* **1997**, No. 119, 9175–9178.
(79) Hostetler, M. J.; Templeton, A. C.; Murray, R. W. *Langmuir* **1999**, *15* (11), 3782–3789.
(80) Song, Y.; Huang, T.; Murray, R. W. *J. Am. Chem. Soc* **2003**, No. 125, 11694–11701.
(81) Issa, F.; Fischer, J.; Turner, P.; Coster, M. J. *J. Org. Chem.* **2006**, *71* (12), 4703–4705.
(82) Hostetler, M. J.; Green, S. J.; Stokes, J. J.; Murray, R. W. *J. Am. Chem. Soc* **1996**, No. 118, 4212–4213.
(83) Kanaras, A. G.; Kamounah, F. S.; Schaumburg, K.; Kiely, C. J.; Brust, M. *Chem. Commun. (Camb).* **2002**, No. 20, 2294–2295.
(84) Templeton, A. C.; Hostetler, M. J.; Kraft, C. T.; Murray, R. W. *J. Am. Chem. Soc* **1998**, No. 120, 1906–1911.
(85) Templeton, A. C.; Hostetler, M. J.; Warmoth, E. K.; Chen, S.; Hartshorn, C. M.; Krishnamurthy, V. M.; Forbes, M. D. E.; Murray, R. W. *J. Am. Chem. Soc* **1998**, No. 120, 4845–4849.
(86) Templeton, A. C.; Cliffel, D. E.; Murray, R. W. *J. Am. Chem. Soc* **1999**, No. 121, 7081–7089.
(87) Demko, Z. P.; Sharpless, K. B. *Angew. Chemie - Int. Ed.* **2002**, *41* (12), 2113–2116.
(88) Oh, E.; Susumu, K.; Blanco-Canosa, J. B.; Medintz, I. L.; Dawson, P. E.; Mattoussi, H. *Small* **2010**, *6* (12), 1273–1278.
(89) Lowe, A. B. *Polym. Chem.* **2010**, *1*, 17–36.
(90) Gorges, J.; Kazmaier, U. *European J. Org. Chem.* **2015**, *2015* (36), 8011–8017.
(91) O'Mahony, G. *Synlett* **2004**, No. 3, 572–573.
(92) Ranu, B. C.; Mandal, T. *Synlett* **2007**, *3* (6), 925–928.
(93) Silveira, C.; Mendes, S.; Líbero, F. *Synlett* **2010**, *2010* (5), 790–792.
(94) Yee, A. M. *wellesley Coll. Digit. Sch. Arch.* **2012**.
(95) Zhou, Y.; Wang, S.; Zhang, K.; Jiang, X. *Angew. Chemie - Int. Ed.* **2008**, *47*, 1–4.
(96) Finetti, C.; Sola, L.; Pezzullo, M.; Prosperi, D.; Colombo, M.; Riva, B.; Avvakumova, S.; Morasso, C.; Picciolini, S.; Chiari, M. *Langmuir* **2016**, *32*, 7435–7441.
(97) Hoogenboom, R. *Angew. Chemie - Int. Ed.* **2010**, *49* (20), 3415–3417.
(98) Horstmann, B.; Korbus, M.; Friedmann, T.; Wolff, C.; Thiele, C. M.; Meyer-Almes, F. J. *Bioorg. Chem.* **2014**, *57*, 155–161.
(99) Liu, Y.; Shipton, M. K.; Ryan, J.; Kaufman, E. D.; Franzen, S.; Feldheim, D. L. *Anal. Chem.* **2007**, *79* (6), 2221–2229.
(100) Mei, B. C.; Susumu, K.; Medintz, I. L.; Delehanty, J. B.; Mountziaris, T. J.; Mattoussi, H. *J. Mater. Chem.* **2008**, *18* (41), 4949.
(101) Oh, E.; Susumu, K.; Goswami, R.; Mattoussi, H. *Langmuir* **2010**, *26* (10), 7604–7613.
(102) Jokerst, J. V; Lobovkina, T.; Zare, R. N.; Gambhir, S. S. *Nanomedicine* **2011**, *6* (4), 715–728.
(103) Balasubramanian, S. K.; Yang, L.; Yung, L.-Y. L.; Ong, C.-N.; Ong, W.-Y.; Yu, L. E. *Biomaterials* **2010**, *31*, 9023–9030.

(104) AL-Kazazz, F. F.; F AL-Imarah, K. A.; AL-Hasnawi, I.; Abbas Abdul-Majeed, D. *J. Eng. Res. Appl.* **2013**, *3* (6), 21–30.
(105) Sweeney, S. F.; Woehrle, G. H.; Hutchison, J. E. *J. Am. Chem. Soc* **2006**, *128*, 3190–3197.
(106) Ma, N.; Wang, Y.; Zhao, B.-X.; Ye, W.-C.; Jiang, S. *Drug Des. Devel. Ther.* **2015**, No. 9, 1585–1599.
(107) Yamakoshi, H.; Dodo, K.; Palonpon, A.; Ando, J.; Fujita, K.; Kawata, S.; Sodeoka, M. *J. Am. Chem. Soc* **2012**, *134* (20681–20689).
(108) Zhang, S.; Zou, J.; Elsabahy, M.; Karwa, A.; Li, A.; Moore, D. A.; Dorshow, R. B.; Wooley, K. L. *Chem. Sci.* **2013**, *4* (5), 2122–2126.
(109) Haldar, J.; Kondaiah, P.; Bhattacharya, S. *J. Med. Chem.* **2005**, *48* (11), 3823–3831.
(110) Cheon, Y. R.; Kim, Y. J.; Ha, J. J.; Kim, M. J.; Park, C. E.; Kim, Y. H. *Macromolecules* **2014**, *47* (24), 8570–8577.
(111) Gheorghe, A.; Chinnusamy, T.; Cuevas-Yañez, E.; Hilgers, P.; Reiser, O. *Org. Lett.* **2008**, *10* (19), 4171–4174.
(112) Soai, K.; Ookawa, A.; Kato, K. *Bulletin of the Chemical Society of Japan*. 1982, pp 1671–1672.
(113) Han, J.; Sun, L.; Chu, Y.; Li, Z.; Huang, D.; Zhu, X.; Qian, H.; Huang, W. *J. Med. Chem.* **2013**, *56* (24), 9955–9968.
(114) Meldal, M.; Tomøe, C. W. *Chem. Rev.* **2008**, *108* (8), 2952–3015.
(115) Kashmery, H. A.; Clark, A. W.; Dondi, R.; Fallows, A. J.; Cullis, P. M.; Burley, G. A. *Eur. J. Inorg. Chem.* **2014**, *2014* (28), 4886–4895.
(116) Parhi, P.; Mohanty, C.; Sahoo, S. K. *Drug Discov. Today* **2012**, *17* (17), 1044–1052.
(117) Mokhtari, R. B.; Homayouni, T. S.; Baluch, N.; Morgatskaya, E.; Kumar, S.; Das, B.; Yeger, H.; Mokhtari, R. B.; Homayouni, T. S.; Baluch, N.; Morgatskaya, E.; Kumar, S.; Das, B.; Yeger, H. *Oncotarget* **2015**, *8* (23), 38022–38043.
(118) Gudena, V.; Montero, A. J.; Glück, S. *Ther. Clin. Risk Manag.* **2008**, *4* (6), 1157–1164.
(119) Rau, K.-M.; Li, S.-H.; Chen, S.-M. S.; Tang, Y.; Huang, C.-H.; Wu, S.-C.; Chen, Y.-Y. *Jpn. J. Clin. Oncol.* **2011**, *41* (4), 455–461.
(120) Plunkett, W.; Huang, P.; Xu, Y. Z.; Heinemann, V.; Grunewald, R.; Gandhi, V. *Semin. Oncol.* **1995**, *22* (4 Suppl 11), 3–10.
(121) Sendai Fukusokan Kagaku Kenkyūjo., K.; Nihon Fukusokan Kagaku Kenkyūjo., A.; KAN, T.; FUKUYAMA, T. *Heterocycles.*; Sendai Institute of Heterocyclic Chemistry; Vol. 73.
(122) Weaver, L. G.; Singh, Y.; Burn, P. L.; Blanchfield, J. T. *RSC Adv.* **2016**, *6* (37), 31256–31264.
(123) Kamimura, A.; Matsu, H.; Suzukawa, H.; Sato, E.; Sumimoto, M.; Uno, H. *Chem. Lett.* **2012**, *41* (Entry 6), 984–986.
(124) Milenic, D. E.; Brady, E. D.; Brechbiel, M. W. *Nat. Rev. Drug Discov.* **2004**, *3* (6), 488–499.
(125) Liu, S.; Edwards, D. S. *Bioconjug. Chem.* **2001**, *12* (1), 7–34.
(126) Aime, S.; Botta, M.; Fasano, M.; Terreno, E. *Acc. Chem. Res.* **1999**, *32* (11), 941–949.
(127) Aime, S.; Botta, M.; Fasano, M.; Terreno, E. *Chem. Soc. Rev.* **1998**, *27* (1), 19–29.

(128) Meade, T. J.; Taylor, A. K.; Bull, S. R. *Curr. Opin. Neurobiol.* **2003**, *13* (5), 597–602.
(129) Jacobs, R. E.; Cherry, S. R. *Curr. Opin. Neurobiol.* **2001**, *11* (5), 621–629.
(130) Caravan, P.; Ellison, J. J.; Mcmurry, T. J.; Lauffer, R. B. *Chem. Rev.* **1999**, 2293–2352.
(131) Fichna, J.; Janecka, A. *Bioconjug. Chem.* **2003**, *14* (1), 3–17.
(132) Kovacs, Z.; De Leon-Rodriguez, L. *Mini. Rev. Org. Chem.* **2007**, *4* (4), 281–291.
(133) Li, M.; Meares, C. F. *Bioconjug. Chem.* **1993**, *4* (4), 275–283.
(134) Allen, M. J.; Meade, T. J. *J. Biol. Inorg. Chem.* **2003**, *8* (7), 746–750.
(135) Eisenwiener, K. P.; Powell, P.; Mäcke, H. R. *Bioorg. Med. Chem. Lett.* **2000**, *10* (18), 2133–2135.
(136) Holmberg, C. *Chem. Ber.* **1927**, *60*, 2197.
(137) Eisenwiener, K.-P.; Powell, P.; Mäcke, H. R. *Bioorg. Med. Chem. Lett.* **2000**, *10* (18), 2133–2135.
(138) Medintz, I. L.; Tetsuo Uyeda, H.; Goldman, E. R.; Mattoussi, H. *Nat. Mater.* **2005**, 435–446.
(139) Michalet, X.; Pinaud, F. F.; Bentolila, L. A.; Tsay, J. M.; Doose, S.; Li, J. J.; Sundaresan, G.; Wu, A. M.; Gambhir, S. S.; Weiss, S. *Science (80-.).* **2005**, *538* (2005), 538–544.
(140) Jamieson, T.; Bakhshi, R.; Petrova, D.; Pocock, R.; Imani, M.; Seifalian, A. M. *Biomaterials* **2007**, *28*, 4717–4732.
(141) Jaiswal, J. K.; Simon, S. M. *Trends Cell Biol.* **2004**, 497–504.
(142) Alivisatos, A. P.; Gu, W.; Larabell, C. *Annu. Rev. Biomed. Eng.* **2005**, *7* (1), 55–76.
(143) Samir, T. M.; Mansour, M. M. H.; Kazmierczak, S. C.; Azzazy, H. M. E. *Nanomedicine (Lond).* **2012**, *7* (11), 1755–1769.
(144) Farkhani, S. M.; Valizadeh, A. IEEE Xplore Full-Text PDF: http://ieeexplore.ieee.org/stamp/stamp.jsp?arnumber=6819331 (accessed Sep 27, 2017).
(145) Bernardin, A.; Cazet, A.; Guyon, L.; Delannoy, P.; Vinet, F.; Bonnaffé, D.; Texier, I. *Bioconjugate Chem.* **2010**, No. 21, 583–588.
(146) Wegner, K. D.; Hildebrandt, N. *Chem. Soc. Rev.* **2015**, *44* (14), 4792–4834.
(147) Li, S.; Gray, B. P.; Mcguire, M. J.; Brown, K. C. *Bioorg. Med. Chem.* **2011**, *19*, 5480–5489.
(148) Newkome, G. R.; Yao, Z.; Baker, G. R.; Gupta, V. K. *J. Org. Chem.* **1985**, *50* (11), 2003–2004.
(149) Wojczykowski, K.; Jutzi, P. *Synlett* **2006**, No. 1, 39–40.
(150) Ghosh, B.; Amado-Sierra, M. D. R. I.; Holmes, D.; Maleczka, R. E. *Org. Lett.* **2014**, *16* (9), 2318–2321.
(151) Benito-Alifonso, D.; Tremel, S.; Hou, B.; Lockyear, H.; Mantell, J.; Fermin, D. J.; Verkade, P.; Berry, M.; Galan, M. C. *Angew. Chemie - Int. Ed.* **2014**, *53* (3), 810–814.
(152) Dardonville, C.; Fernandez-Fernandez, C.; Gibbons, S. L.; Ryan, G. J.; Jagerovic, N.; Gabilondo, A. M.; Meana, J. J.; Callado, L. F. *Bioorganic Med. Chem.* **2006**, *14* (19), 6570–6580.
(153) Eising, S.; Lelivelt, F.; Bonger, K. M. *Angew. Chemie - Int. Ed.* **2016**, *55* (40), 12243–12247.
(154) Zhou, B.; Hu, Y.; Wang, C. *Angew. Chemie - Int. Ed.* **2015**, *54* (46), 13659–13663.

(155) De Figueiredo, R. M.; Oczipka, P.; Fröhlich, R.; Christmann, M. *Synthesis (Stuttg).* **2008**, No. 8, 1316–1318.
(156) Lim, J.; Simanek, E. E. *Org. Lett.* **2008**, *10* (2), 201–204.